NASA CONTRACTOR REPORT

NASA CR-1782

DYNAMICS AND STABILITY OF MECHANICAL SYSTEMS WITH FOLLOWER FORCES

by George Herrmann

Prepared by
STANFORD UNIVERSITY
Stanford, Calif.
for

NATIONAL AERONAUTICS AND SPACE ADMINISTRATION • WASHINGTON, D. C. • NOVEMBER 1971

1. Report No.	2. Government Accession No.	3. Recipient's Catalog No.
NASA CR-1782		

4. Title and Subtitle	5. Report Date
DYNAMICS AND STABILITY OF MECHANICAL SYSTEMS WITH FOLLOWER FORCES	November 1971
	6. Performing Organization Code
7. Author(s)	8. Performing Organization Report No.
George Herrmann	
9. Performing Organization Name and Address	10. Work Unit No.
Stanford University Stanford, California 94305	136-14-02-02
	11. Contract or Grant No. NGL 05-020-397 NGR 14-007-067
12. Sponsoring Agency Name and Address	13. Type of Report and Period Covered
National Aeronautics and Space Administration Washington, DC 20546	Contractor Report
	14. Sponsoring Agency Code

15. Supplementary Notes

16. Abstract

The monograph centers on problems of stability of equilibrium of mechanical systems with follower forces. Concepts of stability and criteria of stability are reviewed briefly, together with means of analytical specification of follower forces. Nondissipative systems with two degrees of freedom are discussed, and destabilizing effects due to various types of dissipative forces both in discrete and continuous systems, are treated. The analyses are accompanied by some quantative experiments and observations on demonstrational laboratory models.

17. Key Words (Suggested by Author(s))	18. Distribution Statement
Follower forces Stability Damping Critical loads	Unclassified - Unlimited

19. Security Classif. (of this report)	20. Security Classif. (of this page)	21. No. of Pages	22. Price*
Unclassified	Unclassified	240	$3.00

*For sale by the National Technical Information Service, Springfield, Virginia 22151

PREFACE

The principal aim of this monograph is to present a coherent and fairly comprehensive account of recent progress in the area of dynamics and stability of mechanical systems with follower forces. By "recent," quite specifically, is meant the period after 1963, the year of publication of the English translation of the first book (by V. V. Bolotin) devoted in its entirety to nonconservative problems of the theory of elastic stability, i.e., problems with follower forces.

The last decade has witnessed a considerable expansion of interest in this problem area, but the progress has been reported piecemeal by a variety of investigators in different countries and scattered in numerous journals. Even though advances are being continually made, it still appears to be justified to attempt to present an account of recent developments and to place them into a relative perspective. In this attempt, the author's own work and that of his collaborators has received, quite naturally, particular emphasis.

It is hoped that the monograph may prove useful as a source of information on the current state-of-the-art for the research worker and practicing engineer.

TABLE OF CONTENTS

CHAPTER I

INTRODUCTION

1.1 Structural Stability: Column Buckling

The structural engineer and the applied mechanician are usually becoming acquainted with the area of structural stability through Euler's problem of elastic column buckling.

There are several different ways in which the problem of column buckling can be presented to the beginner, but one of the most instructive ones is through an eccentrically loaded cantilevered column (Fig. 1.1) as was done recently by Ziegler [1].*

It is assumed that the column is homogeneous, obeys linear elastic Hooke's law (Young's modulus E) and is of constant cross-section. Let ℓ be the length of the column, EI the flexural rigidity, e the eccentricity of the (compressive) load P and f the deflection at the free end. The load P is assumed to be of the "dead" type, i.e., a weight which does not change in magnitude and direction as a possible consequence of the deformation of the column. If the slope of the deflected column axis w(x) is assumed to be small as compared to unity, the bending moment at section x is

$$M = P(e + f - w) \tag{1.1}$$

On the other hand in elementary theory of beam bending the bending moment M is known to be proportional to the curvature, i.e.,

$$M = EI\, w'' \tag{1.2}$$

Elimination of M in the above two relations leads to the differential equation of the deflection curve

$$EI\, w'' = P(e + f - w) \tag{1.3}$$

or

$$w'' + \frac{P}{EI} w = \frac{P}{EI} (e + f) \tag{1.4}$$

---

* Numbers in brackets indicate references compiled in a listing beginning on page 143.

The general solution of this equation can be written in the form, with the abbreviation $P/(EI) = \varkappa^2$

$$w = A \cos \varkappa x + B \sin \varkappa x + e + f \tag{1.5}$$

The unknown constants A, B and f are to be determined from the boundary conditions

$$w(0) = w'(0) = 0 \quad \text{and} \quad w(\ell) = f \tag{1.6}$$

which leads to the solution

$$w = \frac{e}{\cos \varkappa \ell} (1 - \cos \varkappa x) \tag{1.7}$$

and the end deflection

$$f = e \left(\frac{1}{\cos \varkappa \ell} - 1 \right) \tag{1.8}$$

It is seen from this last expression that if

$$\cos \varkappa \ell = 1 \; ; \quad \text{i.e.} \quad \varkappa = \frac{\pi}{2\ell} \; ; \quad P = \frac{\pi^2 EI}{4\ell^2} \tag{1.9}$$

the deflections at the free end f become infinite, regardless how small the eccentricity e. The column is said to buckle under the critical load (buckling load)

$$P_1 = \frac{\pi^2 EI}{4\ell^2} \tag{1.10}$$

Due to the assumptions introduced, the above relations are obviously valid only for small deflections. If a centrally loaded column is considered and if the analysis is based on a more exact (nonlinear) differential equation of the deflection curve, which allows for large slopes of this curve, the dependence of P on the end deflection f can be established, with the result illustrated in Fig. 1.2.

In the range of the load $0 < P < P_1$ there is only one equilibrium position possible, namely, that of the straight column (f = 0). This equilibrium position is stable in the sense that small disturbances or imperfections of various sorts are not followed by large deviations from this position. In the range $P > P_1$, by contrast, the perfectly straight column (f = 0) is still

in equilibrium, but this equilibrium is unstable since small disturbances will cause the column to move away from this position ($f \neq 0$). The stable equilibrium positions in this range, $P > P_1$, are located on a symmetric curve which branches from the straight line $f = 0$ at the point $P = P_1$.

It is thus seen that buckling of a column is associated with the phenomenon of bifurcation of equilibrium paths, a concept intimately associated with Euler's notion of stability and instability.

This concept of Euler in analyzing stability served technology well, particularly in the area of structural engineering and structural mechanics, as applied to buckling of beams, frames, plates, etc., and various combinations of structural elements, subjected to dead loads.

It was found, however, that this concept cannot be applied indiscriminately to the stability problem of any mechanical system. Specifically, systems which are not subjected to dead loads but rather to forces due to an interacting medium have often to be analyzed differently with regard to stability. Examples of such mechanical systems include airfoils placed in an airstream, turbine blades interacting with water, flexible pipes conveying fluid, elastic systems subjected to impinging fluid jets, as well as certain types of electro-mechanical interactions.

A common feature of such mechanical systems, or rather of forces acting on them, is that these forces are not derivable from a potential (by contrast to dead loads) and as a result a stability analysis based on Euler's concept of bifurcation of equilibrium may break down.

For such problems a more fundamental approach to problems of stability has to be followed, one which is, for instance, based on the dynamic method of investigating small motions induced as a result of perturbations of the positions of equilibrium. One finds then that stability of a mechanical system subjected to forces which are not derivable from a potential may, generally, be lost either through oscillations with increasing amplitude or through a nonoscillatory motion away from the equilibrium position. In the former case no bifurcation of equilibrium exists and therefore Euler's method breaks down. In the latter case the dynamic method leads essentially to the same results as Euler's static method of analyzing stability.

A significant property of forces which are not derivable from a potential is their dependence on the instantaneous position or configuration of the system upon which they are acting. That is these forces follow in some a priori prescribed manner the motion of the system. For this reason they have been termed not only nonconservative forces, but also circulatory forces, configuration-dependent forces or simply follower forces.

1.2 Aim and Scope of the Monograph

The present monograph centers on problems of stability of equilibrium of mechanical systems with follower forces. Follower forces, as acting on mechanical systems, may be of aerodynamic, hydrodynamic, electromagnetic or thermal origin. Furthermore, they occur frequently in automatic control systems.

The beginnings of analyses of stability of mechanical systems with follower forces go back to the late nineteen-twenties and are associated with the name of Nikolai [2,3] in Russia. Comprehensive, fundamental studies were carried out by Ziegler [4-7] in the fifties in Switzerland. The book by Bolotin [8], devoted in its entirety to nonconservative problems of the theory of elastic stability, presents a well-rounded state of knowledge as of a decade ago.

Several areas of stability problems of mechanical systems with follower forces, such as the highly developed area of aeroelasticity (cf. Garrick [9]) and stability of rotating shafts, will not be considered in the present monograph since these areas have already received considerable attention.

The primary purpose of the present monograph is limited in the sense that attention is confined to the developments of the last decade, i.e., after the publication of [8], and narrowed down further by emphasizing the analytical and experimental investigations in which the author and his coworkers were involved during the period of the last seven years. A review of the work, including numerous references, through the year 1966, is contained in reference [10].

Concepts of stability in mathematical terms, as well as criteria of stability are reviewed briefly in the still introductory Chapter II, together with means of analytical specification of follower forces. Chapter III is devoted to a discussion of nondissipative (i.e., purely elastic) systems with two degrees of freedom. An illustrative example is considered first and a general linear system next. A remarkable feature of systems with follower forces is that even small damping forces and certain other velocity-dependent forces may have a strong destabilizing effect. Such destabilizing effects, both in discrete and continuous systems, are treated in detail in Chapter IV. The special considerations which must be introduced in the analysis of continuous systems are discussed in Chapter V. Mechanical systems with follower forces may require particular procedures in their stability analysis. Such methods, including energy considerations, are dealt with in Chapter VI.

The analytical work on systems with follower forces is sometimes being criticized as being purely mathematical and as having no relevance to actual mechanical devices and structures. To counter this argument, several possibilities of physical realization of mechanical systems with follower forces are examined in Chapter VII. Qualitative observations on demonstrational laboratory models and quantitative experiments are reported in Chapter VIII.

CHAPTER II

CONCEPTS OF STABILITY AND FOLLOWER FORCES

The term "stability" assigns a quality to a state of a system which signifies that possible disturbances of the system will not essentially change the state. This qualitative description is necessarily vague and precise mathematical meaning is to be assigned to the terms "state," "disturbances" and "essential change."

The required mathematical apparatus has been supplied by Liapunov [11]. Let us consider a discrete system with r degrees of freedom described by r generalized coordinates q_i, and let us examine the special case of the state of equilibrium

$$q_i = 0 \qquad (i = 1,2,\ldots,r) \tag{2.1}$$

If the system is disturbed at a time $t = t_o$, at any instant t its state will be characterized by (generally nonvanishing) coordinates q_i and by generalized velocities $\dot{q}_i = \frac{dq_i}{dt}$ and can be thought of as a point in a 2r-dimensional Euclidean space with coordinates z_k

$$z_k = z_k(t) \qquad (k = 1,2,\ldots 2r) \tag{2.2}$$

The state of equilibrium (2.1), according to Liapunov, is said to be stable if for any $\epsilon > 0$ we can find a $\delta > 0$, depending on ϵ only (and possibly on t_o) such that

$$\sum_{k=1}^{2r} z_k^2 < \delta \quad \text{at} \quad t = t_o \tag{2.3}$$

implies

$$\sum_{k=1}^{2r} z_k^2 < \epsilon \quad \text{for } t_o \le t < \infty \tag{2.4}$$

In the opposite case the state (2.1) is called unstable.

The state is called asymptotically stable if it is stable and in addition

$$\lim_{t\to\infty} \sum_{k=1}^{2r} z_n^2 = 0 \tag{2.5}$$

This fundamental definition of stability by Liapunov has been refined and supplemented in various ways and reference should be made to the comprehensive texts by Minorsky [12], Krasovskii [13], LaSalle and Lefschetz [14], and Hahn [15]. A host of "fine" definitions has been introduced, e.g., uniform stability, quasi-equiasymptotic stability, total stability, stability in the whole, etc., [15] in order to classify possible effects of disturbances.

For the purposes of the present monograph it appears to be sufficient to employ just three terms, namely,

1) Asymptotic stability
2) Marginal stability
3) Instability

Types 1) and 3) have been defined above. Type 2) characterizes a state which is stable, again as defined above, but not asymptotically stable.

Expressed verbally, one can say that a state of equilibrium is asymptotically stable if small disturbances, inflicted upon the system at a certain time, decrease with time. The state is marginally stable if the disturbances do neither decrease nor increase with time, and it is unstable if the disturbances increase with time.

Side by side with Liapunov's concept of stability, it is possible and meaningful to introduce alternate definitions. The two other most current ones are due to Poincaré (orbital stability) and to Lagrange (boundedness of motions and orbits), but the distinction vanishes for the special case of equilibrium states. Further, it would be of interest to examine the behavior of the system under continuous disturbances and under arbitrarily large disturbances. For a discussion of the interrelation of various concepts of stability of dynamical systems, reference is made to Magiros [16]. Generalization of these concepts to continuous systems is not readily accomplished, because the notion of a metric has to be introduced, cf. Chapter V.

Having accepted a definition of stability, the first step in the analysis of the state of equilibrium of a system involves the consideration of criteria which would permit to decide whether a given state is asymptotically stable, marginally stable or unstable. In dynamical, discrete systems two categories of criteria have been evolved, one being based on the construction of the so-called Liapunov's function (Liapunov's direct method), the other being based on the examination of solutions of equations of motion and, in continuous systems, modal expansions. In problems of stability of equilibrium the former is related to the energy criterion which in turn, for certain systems, is equivalent to the static criterion (Euler method). The latter is usually referred to as the kinetic criterion or the vibration criterion. For a detailed discussion of stability criteria reference is made to [5-7,14].

The applicability of stability criteria, as emphasized by Ziegler [1,5-7, 17], strongly depends on the forces present in the mechanical system. If the forces depend explicitly on time, they are called instationary, if they do not, they are called stationary. The stationary forces generally depend on

both the generalized coordinates and generalized velocities. If velocity-dependent forces do no work in any elementary change of position, they are called gyroscopic forces (e.g. Coriolis forces); if they do negative work, they are referred to as dissipative (e.g. viscous damping, drag). Among the velocity-independent forces, i.e., forces which depend on generalized coordinates only, one encounters those which are derivable from a single-valued potential. These, such as for example, gravitational forces, are termed noncirculatory (or conservative). All other velocity-independent forces are referred to as circulatory, or nonconservative, or follower forces. Strictly speaking, dissipative, instationary and follower forces are all nonconservative forces, but the terms circulatory forces, follower forces and nonconservative forces are used in the literature with the same meaning and will be employed interchangeably in this work.

The bulk of the present monograph is concerned with various classes of mechanical systems whose common feature it is that follower (or circulatory, or "nonconservative") forces are always present. To investigate the state of equilibrium of such systems, the analysis can be based on linearized equations of motion (or equilibrium, in certain cases) in the vicinity of the state to be characterized. Since follower forces are stationary, the system of equations obtained is autonomous (no explicit time dependence) and homogeneous (no forcing terms). In discrete systems the circulatory nature of the follower forces manifests itself in that the force matrix is not symmetric, while in continuous systems the boundary value problem is nonself-adjoint.

In this monograph both, extensions of Liapunov's direct method and the "solution" method are employed, with emphasis on the latter. In discrete systems one is then concerned with a study of solutions of the type

$$q_i = A_1 e^{\lambda t} \quad \text{or}$$

$$q_i = A_i e^{i\omega t}$$

which leads to a study of the roots λ_k (or ω_k) of the associated characteristic equation [18]. If the real parts of all the characteristic roots λ_k are negative (or the imaginary parts of all the characteristic roots ω_k are positive), the system is asymptotically stable. By contrast, if at least one of the characteristic roots λ_k is positive (or ω_k is negative), the system is unstable. If all the roots λ_k are pure imaginary (or ω_k pure real), the system is marginally stable (critical case). Liapunov's theorems assert that linearized analysis is appropriate for asymptotically stable and unstable systems. In case of marginal stability of a linearized system, no statement can be made regarding the behavior of the actual nonlinear system.

The nature of the roots λ_k (or ω_k) can be determined without calculating the roots themselves. A variety of methods have been developed for this purpose [18], one of the most widely used being associated with the names of Routh and

Hurwitz.* Various definitions of follower forces as applied to continuous bodies have been discussed by Sewell [19], Nemat-Nasser [20], and Shieh and Masur [21].

For additional references, relating in particular the two areas of stability and control, the reader is referred to the recent bibliography by Wang [108].

* It has been called recently to the author's attention by P. C. Parks [106] that it was Hermite [107] who has established considerably earlier the conditions generally known as the "Routh-Hurwitz criterion."

CHAPTER III

NONDISSIPATIVE SYSTEMS WITH TWO DEGREES OF FREEDOM

3.1 An Illustrative Example

To illustrate some characteristic types of dynamic behavior, in the vicinity of an equilibrium configuration, of a mechanical system subjected to a follower force, let us consider a double pendulum, Fig. 3.1, composed of two rigid bars of equal lengths ℓ, which carry concentrated masses $m_1 = 2m$, $m_2 = m$. The position of equilibrium $\varphi_1 = \varphi_2 = 0$ is to be investigated when the system is subjected to a force P acting along the bars (positive when compressive). For this purpose a perturbed configuration ($\varphi_1 \neq 0$, $\varphi_2 \neq 0$, but both small) is investigated. In this position elastic restoring moments $c\varphi_1$ and $c(\varphi_2 - \varphi_1)$ are induced at the joints and the direction of the load P is specified to form an angle $\alpha\varphi_2$ with respect to the direction of the bar in the equilibrium position.

This system has been investigated by Ziegler [5] for the special case $\alpha = 1$, which may be termed the case of purely tangential loading. In Ref. [22] the full range $-\infty < \alpha < \infty$ has been examined. As can be easily verified, the load P (and thus the system) is conservative only for $\alpha = 0$. The system may be considered a two-degree-of-freedom model of a continuous cantilever.

The analysis, restricted to a linearized formulation, consists in the determination of the two natural frequencies of free vibration as a function of the loading. For sufficiently small loads both frequencies are real and the system is thus stable under an arbitrary small disturbance, exhibiting bounded harmonic oscillations. As the load is increased, instability may occur by either one frequency becoming zero (static buckling) at the critical loading and then in general purely imaginary, or the two frequencies becoming complex, having passed a common real value at the critical loading (marginal stability). The ensuing motion under a supercritical force in the first case is nonoscillatory with the amplitude increasing exponentially (divergent motion), and the critical load can be determined statically by the Euler method. In the second case the ensuing motion is an oscillation with a definite period but with an exponentially increasing amplitude, and the critical load cannot be found by the Euler method because no associated adjacent equilibrium exists. The first case could be called "static instability" in view of the behavior at the critical load, and the second "dynamic instability." In aeroelasticity, however, analogous phenomena have been termed "divergence" and "flutter," respectively, [23,24], and we propose to employ this terminology in the sequel.

Lagrange's equations in the form

$$\frac{d}{dt}\left(\frac{\partial L}{\partial \dot{\varphi}_k}\right) - \frac{\partial L}{\partial \varphi_k} = Q_k \qquad (L = T-V,\ k = 1,2) \tag{3.1}$$

are used to establish the linear equations of motion, in which the kinetic energy T is

$$T = \frac{1}{2} m\ell^2 \left[3\dot{\varphi}_1^{\,2} + 2\dot{\varphi}_1\dot{\varphi}_2 + \dot{\varphi}_2^{\,2}\right] \tag{3.2}$$

the potential energy V of the restoring moments is

$$V = \frac{1}{2} c \left[2\varphi_1^{\,2} - 2\varphi_1\varphi_2 + \varphi_2^{\,2}\right] \tag{3.3}$$

and the generalized forces Q_k (due to applied loading) are

$$\begin{aligned} Q_1 &= P\ell[\varphi_1 - \alpha\varphi_2] \\ Q_2 &= P\ell[(1-\alpha)\varphi_2] \end{aligned} \tag{3.4}$$

These forms lead to the equations of motion

$$\begin{aligned} &3m\ell^2\ddot{\varphi}_1 + m\ell^2\ddot{\varphi}_2 + (2c-P\ell)\varphi_1 + (\alpha P\ell - c)\varphi_2 = 0 \\ &m\ell^2\ddot{\varphi}_1 + m\ell^2\ddot{\varphi}_2 - c\varphi_1 + [c - (1-\alpha)P\ell]\,\varphi_2 = 0 \end{aligned} \tag{3.5}$$

which, in turn, stipulating exponential solutions of the form

$$\varphi_k = A_k e^{i\omega t} \qquad (k = 1,2) \tag{3.6}$$

yield the frequency equation

$$p_o\omega^4 - p_2\omega^2 + p_4 = 0 \tag{3.7}$$

where

$$\begin{aligned} p_o &= 2m^2\ell^4 \\ p_2 &= m\ell^2[7c - 2(2-\alpha)P\ell] \\ p_4 &= c^2 - (1-\alpha)[3cP\ell - (P\ell)^2] \end{aligned} \tag{3.8}$$

The four characteristic roots will occur in pairs, the positive and negative roots of the two values of ω^2 obtainable directly from the frequency equation. For a negative ω^2 one root describes an exponentially divergent motion; $\omega^2 = 0$ corresponds to neutral equilibrium, the appearance of an adjacent equilibrium configuration (static buckling, divergence). A complex value of ω^2 yields one root describing an oscillation with increasing amplitude (flutter). The system is thus stable only as long as both values of ω^2 are real and positive. We are interested in the manner in which ω^2 varies with P for different values of α. This is accomplished by investigating the curves of P versus real values of ω^2.

Expanding the frequency equation we find that it is a general quadratic equation in ω^2 and $P\ell$, of the form

$$A(\omega^2)^2 + B(\omega^2 P\ell) + C(P\ell)^2 + D(\omega^2) + E(P\ell) + F = 0 \tag{3.9}$$

where the discriminant, $B^2 - 4AC$, is

$$4m^2\ell^4 \left[2(1-\alpha) + \alpha^2\right] \tag{3.10}$$

Since this expression is always positive, the frequency curves (P versus ω^2; P, ω^2, real) are all of the hyperbolic type.

Except for degenerate cases, which shall be noted, there are but two general types of hyperbolas, with regard to orientation in the real ω^2, $P\ell$ plane, that may be encountered. These two types, qualitatively, are of "conjugate" orientations.

In the first type, each of the two branches of the hyperbola yields a single (real) value of ω^2 for every load and the two values never coincide. Instability may occur only in the form of divergence or divergent motions.

In the second general type of hyperbola, the two values of ω^2, for any load producing real values of ω^2, lie on the same branch of the curve. For each branch there is one critical load at which the two values coincide. Regardless of the behavior indicated by the real values of ω^2 on the branches, these two critical loads always bracket a single, limited range of the load "between" the two branches of the hyperbola, for which the values of ω^2 are complex and the free motions are of the flutter type. Since the system must be stable for sufficiently small loads, these critical loads must be of the same sign for any given value of α.

The solution of the frequency equation is

$$\omega_{1,2}^2 = \frac{7c - 2(2-\alpha)P\ell \mp \{4(P\ell)^2[2(1-\alpha) + \alpha^2] - 4cP\ell(8-\alpha) + 41c^2\}^{1/2}}{4m\ell^2} \tag{3.11}$$

from which P versus $\omega_{1,2}^2$ can be plotted for any α. We determine, first, the critical loads corresponding to coincidence of frequencies (occurring in the second type of hyperbola) by setting the discriminant equal to zero in the equation for $\omega_{1,2}^2$. This yields, for the critical loads, in nondimensional form, the equation

$$\frac{P\ell}{c} = \frac{(8-\alpha) \mp \{(8-\alpha)^2 - 41[2(1-\alpha) + \alpha^2]\}^{1/2}}{2[2(1-\alpha) + \alpha^2]} \tag{3.12}$$

Real values of these critical loads are associated with the second type of hyperbola, complex values with the first. We wish to determine the transitional values of α. Thus, setting this discriminant equal to zero,

$$(8-\alpha)^2 - 41\,[2(1-\alpha) + \alpha^2] = 0 \tag{3.13}$$

yields the roots $\alpha_{tr} = 0.345,\ 1.305$.

Substituting this equation into that for $\omega_{1,2}^2$ yields

$$[\omega_{1,2}^2]_{\alpha_{tr}} = \frac{7c - 2P\ell(2-\alpha) \mp \frac{1}{\sqrt{41}}[2P\ell(8-\alpha) - 41c]}{4m\ell^2} \tag{3.14}$$

with $\alpha = \alpha_{tr} = 0.345,\ 1.305$.

Thus two transitional values of α are obtained, at each of which the hyperbolas degenerate into two intersecting straight lines. Between these values of α the second type of hyperbola is found to occur, and the phenomenon of flutter is thus limited to this range of α. The corresponding critical loads are all positive (compressive).

Consider next the constant term p_4 in the frequency equation. The Euler method is equivalent to setting $p_4 = 0 (\omega^2 = 0)$, corresponding to intercepts of the hyperbolas on the P-axis. Setting $p_4 = 0$ we obtain for the Euler buckling loads, in nondimensional form

$$\frac{P\ell}{c} = \frac{1}{2}\left[3 \mp \left(\frac{5-9\alpha}{1-\alpha}\right)^{1/2}\right] \tag{3.15}$$

For real values of the load we must have $\alpha \leq \frac{5}{9}$ or $\alpha > 1$. Thus there are critical values of $\alpha(\alpha_{cr} = \frac{5}{9}, 1)$, marking the limits of a range in which no adjacent equilibrium position occurs in the system for any value of the load.

We note from the form of p_4 that the lower critical value of α is a function of the elastic and geometric parameters of the system, and under a variation of these parameters might increase indefinitely, approaching one as a limit. Thus, for $\alpha < 1$ there is a class of systems or loadings wherein the absence of an adjacent equilibrium configuration for any value of the load is a function of the elastic and geometric parameters. However, for $\alpha = 1$, the terms in p_4 involving P drop out entirely, leaving a positive definite expression which contains the elastic parameter alone. Therefore, in this special case alone, we may say that it is the specification of the loading itself which results in the absence of any possible adjacent equilibrium configuration. We note here that in the case of a uniform continuous cantilever subjected to a load characterized by the same type of parameter, the Euler method reveals a similar critical value of the parameter, which in that case is one half.

A third set of values of α of interest is denoted by α', and is associated with a coincidence of an Euler load with a critical load for flutter. This occurs when a value of ω^2, at which $\omega_1^2 = \omega_2^2$, is zero. Thus we set $\omega_{1,2}^2 = 0$, which is equivalent to setting $p_2 = 0$, $p_4 = 0$, simultaneously; i.e.,

$$[7c - 2(2-\alpha)P\ell] = 0 \tag{3.16}$$

and

$$c^2 - (1-\alpha)[3cP\ell - (P\ell)^2] = 0 \tag{3.17}$$

Solving the first equation for $P\ell$ and substituting into the second yields a quadratic equation in α, the roots of which are found to be $\alpha' = 0.423, 1.182$.

In the sequel we restrict our detailed attention to $0 \leq \alpha \leq 1$, as this range is somewhat more meaningful physically and is sufficient to demonstrate a connection between the various instability phenomena. Figure 3.2 shows the frequency curves for the various values of α of particular interest in this range. From these curves, in which both branches of the hyperbolas and their asymptotes are shown for completeness, we can determine by inspection the particular character of the frequency curve for any α in the range $0 \leq \alpha \leq 1$, and we proceed now to a discussion of the behavior of the individual curves in this range and the various stability phenomena that they illustrate.

For $0 \leq \alpha < \alpha_{tr}$ the hyperbolas are all of the first type, and the behavior is as previously discussed. The frequency curves and the characteristic behavior of the nonconservative systems are qualitatively indistinguishable from the conservative case. Obviously, the Euler method would yield the lowest buckling load, which here marks the boundary between the single stable and

unstable ranges of the loading. A kinetic analysis would yield nothing additional. With increasing values of α in this range, the hyperbolas draw closer to their asymptotes and finally degenerate into two straight lines at $\alpha = \alpha_{tr}$, as previously noted. This case marks the first occurrence of a coincidence of the characteristic roots.

For values of α greater than α_{tr} in this range, hyperbolas of the second type, with the conjugate orientation, occur and pull away from their asymptotes with increasing α. The upper branch lies entirely in the second quadrant, corresponding to divergent motion, and such an instability follows flutter with increasing load.

In this range, for $\alpha_{tr} < \alpha < \alpha'$ the coincidence of frequencies on the lower branch occurs at negative values of ω^2, with divergent motion already characterizing both modes. Thus in this class of systems the boundary between the single stable and unstable ranges of the loading parameter is marked solely by the appearance of an adjacent equilibrium configuration in the first mode, and is obtainable by the equilibrium approach. The system is unstable for all higher loads. The critical loads corresponding to coincidence of frequencies do not mark any bound between stability and instability.

Thus, for such systems, the Euler method would yield the critical load with regard to stability, even though the phenomenon of flutter is possible at some higher loadings. Conversely, the sole use of the kinetic method, if employed so as to determine merely the critical loads corresponding to the coincidence of frequencies, would lead to erroneous conclusions.

For $\alpha = \alpha'$, ω^2 at the coincidence of the frequencies on the lower branch is zero. The sequence of instabilities with increasing load is the same as in the preceding range of α.

For $\alpha > \alpha'$ the coincidence of frequencies occurs at positive values of ω^2 and this critical point now marks the bound between a stable and unstable range of the load. However, for $\alpha' < \alpha < \alpha_{cr}$ the lower branch still intersects the load axis, and the two corresponding critical loads, both occurring in the first mode, now bracket a separate range of instability through divergent motion. Such a system is rather remarkable in that it displays, for different loads, losses of stability by both divergence and flutter.

Thus for $\alpha' < \alpha < \alpha_{cr}$ we have a rather interesting sequence of free motions with increasing load, resulting in multiple regions of stability and instability. This is illustrated in Fig. 3.3 by the frequency curve for the arbitrary value of $\alpha = 0.5$. Such a system has characteristic free motions which include successively stable oscillations, divergent motion, stable oscillations, flutter, and then divergent motion again for all higher loads. In such a situation the lowest critical load marking the appearance of an instability would still be a buckling load, obtainable by the Euler method. However, the existence of the second range of stability, above the second "buckling" load, as well as its upper limit, would be revealed only by a detailed kinetic analysis.

For $\alpha = \alpha_{cr}$ the two buckling loads, bracketing the lower region of instability, coincide and the frequency curve is tangent to the load axis. Thus in this case there is a divergence instability at that isolated load, with no associated divergent motion for neighboring loads. The sequence of instabilities is otherwise the same as for $\alpha' < \alpha < \alpha_{cr}$.

For $\alpha \leq \alpha_{cr}$ the lowest critical load was always a buckling load, obtainable by the equilibrium approach, and varied continuously with α. Above α_{cr} no adjacent equilibrium configurations occur and the lowest critical load is that corresponding to the coincidence of the frequencies. There is thus a discontinuity (jump) in the magnitude of the lowest critical load, at $\alpha = \alpha_{cr}$. Systems in the class $\alpha_{cr} < \alpha \leq 1$ possess a single range of stability and of instability, with a sequence of characteristic free motions of stable oscillations, flutter, and finally divergence for all higher loads.

The foregoing discussion could be extended to the values of α outside the range $0 \leq \alpha \leq 1$, but is omitted here for the sake of brevity. However, a plot showing the variation in all the critical loads for a wider range of α, including the entire region of flutter instability, and with the asymptotic behavior of the critical loads for divergence clearly indicated for extreme values of α, is given in Fig. 3.4.

Considering systems corresponding to given values of α, this plot illustrates that in systems displaying multiple regions (and types) of instability under compressive loading, the lowest critical load may correspond to either divergence or flutter. Also illustrated is the existence of systems displaying instability by divergence for both compressive and tensile loads.

With the aid of the parameter α in the simple model analyzed here, we have attempted to show a connection between instability phenomena of divergence and flutter by demonstrating a generic relationship between such disparate frequency curves as those characterizing $\alpha = 0$ and $\alpha = 1$. Thus, such curves (and systems characterized by them) may be seen to be not of a singular or isolated nature, but part of a continuous "spectrum" of frequency curves.

The justification for considering the entire range of $-\infty < \alpha < +\infty$ may be made clearer through the following observation. The type of loading specified may be considered as the result of a superposition of two component loads, corresponding to constant-directional vertical loading ($\alpha = 0$) and tangential loading ($\alpha = 1$), the two being kept in a constant ratio as the loading is varied. In such a perspective, $0 < \alpha < 1$ corresponds to these component loads having the same sense. Then, $\alpha < 0$ and $\alpha > 1$ corresponds to these component loads having opposite senses, with their relative magnitudes determined by the magnitude and sign of α, and with positive load always corresponding to a resultant compressive loading.

The effect of weights of the masses has not been included here, but our investigations indicate that for small such constant loads the principal effect consists in shifting the frequency curves in the positive (negative) direction

of the abscissa for a suspended (inverted, Fig. 3.1) model. Referring to the frequency curve in Fig. 3.2 for $\alpha = 1$, we can see that the shift caused by stabilizing constant forces would result in an intercept of the upper branch of the hyperbola on the $\omega^2 = 0$ coordinate axis. This is, in fact, the case analyzed by Ziegler [5], in which the Euler method yielded a higher critical load than the kinetic method, and which has contributed to the general discrediting of the applicability of the static approach in nonconservative problems. This particular case is somewhat equivalent to the situation occurring herein for $1 < \alpha < \alpha_{tr}$, in which, under compressive loading, the system becomes unstable through flutter, with the higher critical load, for divergence, of no consequence.

3.2 General System with Two Degrees of Freedom

3.2.1 Governing Equations

Let us now generalize the specific results obtained in the previous section and consider a general system with two degrees of freedom. Let q_1, q_2 be the principal coordinates of the system and the equilibrium configuration $q_1 = q_2 = 0$ is to be investigated with regard to stability. The system is characterized by inertia (masses m_1 and m_2) and by restoring spring constants k_1 and k_2. Further, it is subjected to follower forces whose magnitude is dependent on a single parameter. The linear equations of motion may be then written as

$$\begin{aligned} m_1\ddot{q}_1 + k_1 q_1 + \alpha_{11}^* P q_1 + \alpha_{12}^* P q_2 &= 0 \\ m_2\ddot{q}_2 + k_2 q_2 + \alpha_{21}^* P q_1 + \alpha_{22}^* P q_2 &= 0 \end{aligned} \tag{3.18}$$

where α_{ij}^* are assumed to be given.

With the abbreviations

$$\begin{aligned} \omega_i^2 &= k_i/m_i \\ \alpha_{ij} &= \alpha_{ij}^*/m_i \end{aligned} \tag{3.19}$$

the equations of motion take on the form

$$\begin{aligned} \ddot{q}_1 + \omega_1^2 q_1 + \alpha_{11} P q_1 + \alpha_{12} P q_2 &= 0 \\ \ddot{q}_2 + \omega_2^2 q_2 + \alpha_{21} P q_1 + \alpha_{22} P q_2 &= 0 \end{aligned} \tag{3.20}$$

We wish to characterize the position of equilibrium for various ranges of P and for various ranges of the system parameters. For this purpose we investigate solutions of the type

$$q_k = A_k e^{i\omega t} , \qquad k = 1,2 \tag{3.21}$$

which lead to the homogeneous set

$$\begin{aligned} (-\omega^2+\omega_1{}^2+\alpha_{11}P)\ A_1 + \alpha_{12}PA_2 &= 0 \\ \alpha_{21}PA_1 + (-\omega^2+\omega_2{}^2+\alpha_{22}P)\ A_2 &= 0 \end{aligned} \tag{3.22}$$

and finally to the characteristic equation

$$F = \xi^2 - \left[(\xi_1+\xi_2) + (\alpha_{11}+\alpha_{22})P\right]\xi + (\xi_1+\alpha_{11}P)(\xi_2+\alpha_{22}P) - \alpha_{12}\alpha_{21}P^2 = 0 \tag{3.23}$$

where

$$\xi = \omega^2 , \qquad \xi_i = \omega_i{}^2 \qquad i = 1,2 \tag{3.24}$$

This equation represents a curve of second degree (a conic section) and may be written in the normal form

$$F = a\xi^2 + 2b\xi P + cP^2 + 2d\xi + 2eP + f = 0 \tag{3.25}$$

where the coefficients are given by

$$\begin{aligned} &a = 1; \qquad b = -(\alpha_{11}+\alpha_{22})/2; \qquad c = \alpha_{11}\alpha_{22} - \alpha_{12}\alpha_{21} \\ &d = -(\xi_1+\xi_2)/2; \qquad e = (\alpha_{11}\xi_2+\alpha_{22}\xi_1)/2; \qquad f = \xi_1\xi_2 \end{aligned} \tag{3.26}$$

The invariants of the characteristic curve are

$$\Delta = \begin{vmatrix} a & b & d \\ b & c & e \\ d & e & f \end{vmatrix} = \alpha_{12}\alpha_{21}(\xi_2-\xi_1)^2/4 \tag{3.27}$$

and

$$\delta = \begin{vmatrix} a & b \\ b & c \end{vmatrix} = -\left[(\alpha_{11}-\alpha_{22})^2 + 4\alpha_{12}\alpha_{21}\right]/4 \tag{3.28}$$

If $\Delta \neq 0$, equation (3.25) represents a regular second degree curve, namely,

an ellipse for $\delta > 0$

a parabola for $\delta = 0$

a hyperbola for $\delta < 0$

while, if $\Delta = 0$, the curve degenerates into two real or imaginary straight lines.

The system may lose stability, as we have seen, either by oscillating with increasing amplitudes (flutter) or by moving to another position of equilibrium (divergence). The critical values of P are associated with stationary points of the characteristic curve for $\xi > 0$ (flutter) and with points of intersection with the P-axis (divergence). The ranges of system parameters α_{ij} and ω_i will be determined in which either flutter or divergence or both flutter and divergence may occur.

3.2.2 Parameter Ranges

A. $\alpha_{12}\alpha_{21} > 0$

It will be shown that in this case no flutter can occur. First we determine the points of intersection of the characteristic curve (which is a hyperbola) with the P-axis which are

$$P = -\left(e \pm \sqrt{e^2-cf}\right)/c \qquad \text{for } c \neq 0 \tag{3.29}$$

$$P = -f/2e \qquad \text{for } c = 0 \tag{3.30}$$

The discriminant

$$D = e^2 - cf = \left[(\alpha_{11}\xi_2-\alpha_{22}\xi_1)^2 + 4\alpha_{12}\alpha_{21}\xi_1\xi_2\right]/4 \tag{3.31}$$

is positive and therefore there exists at least one real point of intersection.

To find stationary points of the characteristic curve $F(\xi,P) = 0$, we have to calculate

$$dF/dP = -(\partial F/\partial \xi)/(\partial F/\partial P) \tag{3.32}$$

and set this derivative equal to zero. If $\partial F/\partial P \neq 0$, it will be sufficient to examine

$$\partial F/\partial \xi = 2\xi + 2bP + 2d = 0 \tag{3.33}$$

This equation is to be solved for ξ and a substitution made into the equation for the characteristic curve which in turn, solved for P, yields

$$P = -\left[(e-bd) \pm \sqrt{(e-bd)^2-(c-b)^2(f-d^2)}\right]/(c-b^2) \tag{3.34}$$

In terms of system parameters the discriminant is

$$(e-bd)^2 - (c-b^2)(f-d^2) = -\alpha_{12}\alpha_{21}(\xi_2-\xi_1)^2/4 \qquad (3.35)$$

Let us assume first that the two natural frequencies ω_1 of the system are distinct. (The special case $\omega_1 = \omega_2$ will be discussed separately.) This implies that the discriminant in Eq. (3.34) is negative and thus no real points with a horizontal tangent exist, indicating impossibility of occurrence of flutter.

For $c \geq 0$ and $e < 0$, the solutions P of the characteristic equation are positive. The system is marginally stable for all values of P in the range $-\infty < P < P_1$, where P_1 is the smaller value of P from Eq. (3.29) and unstable for $P \geq P_1$ (see Fig. 3.5a). Similarly, for $c > 0$ and $e > 0$, both solutions of Eq. (3.29) are negative. Hence, the system is marginally stable for $P_1 < P < \infty$ (where $|P_1| < |P_2|$) and unstable for $P \leq P_1$ (see Fig. 3.5c). If $c < 0$, the two roots of Eq. (3.29) have different signs. In this case the region of marginal stability is given by $P_2 < P < P_1$, while the system is unstable for $P \geq P_1$ and for $P \leq P_2$ (see Fig. 3.5b).

B. $\alpha_{12}\alpha_{21} = 0$

If α_{12} and/or $\alpha_{21} = 0$, the characteristic equation takes on the form

$$F \equiv [\alpha_{11}P - (\xi-\xi_1)][\alpha_{22}P - (\xi-\xi_2)] = 0 \qquad (3.36)$$

which represents two straight lines which may be considered as the limiting case of the hyperbolas of the previous section approaching their asymptotes. Again flutter cannot occur and stability can be lost by divergence only. The regions of marginal stability and instability are given in Fig. 3.6.

In the special case $\alpha_{11} = \alpha_{22} = 0$ the eigenvalue curve degenerates into two straight lines parallel to the P-axis. Thus no instability can occur for any value of P.

C. $\alpha_{12}\alpha_{21} > 0$

a) Existence of Flutter

In this subsection the ranges will be established in which flutter may occur or cannot occur. We solve Eq. (3.33) for P

$$P = -(\xi+d)/b \qquad b \neq 0 \qquad (3.37)$$

and substitute into the characteristic equation with the result

$$A\xi^2 - 2B\xi + C = 0 \qquad (3.38)$$

which has the solutions

$$\xi_{I,II} = \left(B \pm \sqrt{B^2-AC}\right)/A \qquad \text{for } A \neq 0 \tag{3.39}$$

$$\xi = C/2B \qquad \text{for } A = 0 \tag{3.40}$$

where

$$\begin{aligned} A &= c - b^2 = -[(\alpha_{11}-\alpha_{22})^2 + 4\alpha_{12}\alpha_{21}]/4 \\ B &= Be - cd = -[(\alpha_{11}-\alpha_{22})(\alpha_{11}\xi_2-\alpha_{22}\xi_1) + 2\alpha_{12}\alpha_{21}(\xi_1+\xi_2)]/4 \\ C &= cd^2 - 2bed + b^2 f \end{aligned} \tag{3.41}$$

and

$$\sqrt{B^2-AC} = (\alpha_{11}+\alpha_{22})(\xi_2-\xi_1)\sqrt{-\alpha_{12}\alpha_{21}}\,/4 \tag{3.42}$$

We first consider the case $A \neq 0$. With the notation

$$\alpha_{11} = x, \quad \alpha_{22} = y, \quad \alpha_{12}\alpha_{21} = -p^2, \quad v = \xi_2/\xi_1 \tag{3.43}$$

we obtain

$$N_{I,II} \equiv B \pm \sqrt{B^2-AC} = -\xi_1\,[(x-y)(vx-y) - 2p^2(1+v) \pm (x+y)(1-v)p]/4 \tag{3.44}$$

which may conveniently be written in the form

$$N_{I,II} = -\xi_1 g_1 g_2/4 \tag{3.45}$$

where

$$\begin{aligned} g_1^{I,II} &= y - x \pm 2p \\ g_2^{I,II} &= y - vx \mp (v+1)p \end{aligned} \tag{3.46}$$

Similarly we write A in the form

$$A = -h_1 h_2/4 \tag{3.47}$$

where

$$\begin{aligned} h_1 &= y - x - 2p \\ h_2 &= y - x + 2p \end{aligned} \tag{3.48}$$

Thus we find

$$\xi_{I,II} = \xi_1 g_1^{I,II} g_2^{I,II} / h_1 h_2 \tag{3.49}$$

Since g_i and h_i are linear functions of x and y, it is easy to specify conditions for which ξ_I or ξ_{II}, respectively, are positive or negative. The result is given in Fig. 3.7 in which the shaded area indicates that both solutions ξ_i are negative and flutter cannot occur, while in the remaining area at least one ξ_i is positive and flutter may occur.

In the case A = 0 we had $\xi = c/2B$ which may be written as

$$\xi = g_2^{I} g_2^{II} / [(x+y)(x-y)(v-1)] \tag{3.50}$$

The solid lines in Fig. 3.8 show the region where $\xi > 0$, while the broken lines indicate $\xi < 0$.

It remains to investigate what happens if b = 0. The characteristic equations degenerate in this case to

$$F \equiv \xi^2 + cP^2 + 2d\xi + 2eP + f = 0 \tag{3.51}$$

and

$$\partial F/\partial \xi = 2\xi + 2d = 0 \tag{3.52}$$

It follows that

$$\xi = - d > 0 \tag{3.53}$$

and the equation for P is now

$$cP^2 + 2eP + f - d^2 = 0 \tag{3.54}$$

whose solutions are

$$P = - \left[e \pm \sqrt{e^2 - c(f-d^2)} \right] / c \qquad \text{for } c \neq 0 \tag{3.55}$$

$$P = - (f-d^2)/2e \qquad \text{for } c = 0 \tag{3.56}$$

Since

$$e^2 - c(f-d^2) = - \alpha_{12}\alpha_{21}(\xi_2-\xi_1)^2/4 > 0 \tag{3.57}$$

there is always a real solution for P which means that flutter may occur for b = 0.

b) Existence of Divergence

The discriminant D of equation (3.29) may be written as

$$D = \xi_1^2 t_1 t_2/4 \tag{3.58}$$

where

$$t_1 = y - vx + 2p\sqrt{v}$$
$$t_2 = y - vx - 2p\sqrt{v} \tag{3.59}$$

It can be shown that $t_i = 0$ are equations of the tangents to the hyperbola $c \equiv xy + p^2 = 0$.

Real points of intersection with the P-axis exist if $D \geq 0$. The plain area in Fig. 3.9 indicates the region where $D > 0$, i.e., where divergence is possible, while the shaded area indicates that $D < 0$, where divergence is not possible.

For the case $c = 0$ we have to use equation (3.30) and find that the solution P is finite except for the points T and T' at which the tangents $t_i = 0$ touch the hyperbola $c = 0$ (see Fig. 3.9). Fig. 3.10 combines Figs. 3.7 and 3.9 and shows a complete plot of the regions in which flutter or divergence, respectively, may occur or cannot occur. Fig. 3.10 can easily be constructed if $p = -\alpha_{12}\alpha_{21}$ and $v = \xi_2/\xi_1$ are given.

3.2.3 Summary of Results

If the loading parameter P is increased or decreased from its initial value (which need not be zero), the system may either remain stable, or it may lose stability by flutter or divergence. The results of the corresponding analysis are summarized in Fig. 3.11. Fig. 3.12 indicates qualitatively the ranges of stability for the loading parameter P for the various regions of the system parameters given in Fig. 3.11. Since substituting $-\alpha_{11}$ for α_{11} and $-\alpha_{22}$ for α_{22} only reverses the orientation of the P-axis, the ranges of stability for the regions of system parameters indicated with a prime are obtained by substituting -P for P. Thus, Figs. 3.11 and 3.12 give a complete plot for the ranges of stability of the system for the case $\alpha_{12}\alpha_{21} < 0$.

In many problems the initial value of the force P is zero, and one is only interested in how stability is lost first if a positive (or negative) force P is applied and increased. Fig. 3.13 shows whether stability is lost by flutter or divergence, respectively.

3.2.4 Special Case $\omega_1 = \omega_2$

If the two natural frequencies of the system coincide, the characteristic curve degenerates into two real or imaginary straight lines. The characteristic equation (3.23) may then be written as

$$F \equiv \left[cP + b\left(b+\sqrt{b^2-c}\right)\left(\xi-\xi_o\right)\right]\left[cP + \left(b-\sqrt{b^2-c}\right)\left(\xi-\xi_o\right)\right] = 0 \qquad \text{for } c \neq 0 \tag{3.60}$$

$$F \equiv (2bP + \xi - \xi_o)(\xi - \xi_o) = 0 \qquad \text{for } c = 0 \tag{3.61}$$

where

$$\xi_o = \xi_1 = \xi_2 \tag{3.62}$$

It is easily seen that for $\alpha_{12}\alpha_{21} > 0$ and for $\alpha_{12}\alpha_{21} = 0$ the results given in Figs. 3.5 and 3.6 hold if one sets $\xi_1 = \xi_2$. The results for $\alpha_{12}\alpha_{21} < 0$ are illustrated in Fig. 3.14. If the system parameters fall into the regions II, III or IV, only divergence may occur. For system parameters in region I, flutter will occur for each nonvanishing value of P, while for system parameters corresponding to point Q no instability will occur for any value of P.

CHAPTER IV

DESTABILIZING EFFECTS

4.1 Introduction

It has been discovered by Ziegler [5] not quite two decades ago that internal damping may have a destabilizing effect in a nonconservative elastic system. He considered a double pendulum with viscoelastic joints as a model of an elastic bar with internal damping and let a tangential force act at the free end. The critical loading obtained in complete absence of damping was found to be considerably higher than by including damping at the outset of the analysis and then letting the damping coefficients approach zero (vanishing damping) in the expression for the critical force.

This rather surprising and seemingly paradoxical finding was ascribed in later studies by Ziegler [6,7] to the possibility that internal damping is inadequately represented by linear damping forces which are linear combinations of the generalized velocities and that the hysteresis effect should be taken into account.

The destabilizing effect of damping was further elaborated upon by Bolotin [8] who considered a general two-degree-of-freedom system not related to any particular mechanical model and who found additionally that the destabilizing effect in the presence of slight and vanishing damping is highly dependent on the relative magnitude of damping coefficients in the two degrees freedom.

Additional insight into the destabilizing effects of linear viscous damping in systems with follower forces may be gained by not merely applying stability criteria but by studying also the roots of the characteristic equation (cf. Ref. [25]). Further, the results of the mathematical stability investigations may be interpreted in physical terms by introducing the concept of degree of instability. It becomes then possible to carry out a gradual transition from the case of small damping to the case of vanishing damping and relate both of these cases to that of no damping.

4.2 Illustrative Examples of Systems with Two Degrees of Freedom

4.2.1 A Model

For this purpose again a two-degree-of-freedom model is considered, Fig. 4.1, composed of two rigid weightless bars of equal length ℓ, which carry concentrated masses $m_1 = 2m$, $m_2 = m$. The generalized coordinates φ_1, φ_2 are again taken to be small. A load P applied at the free end is assumed to be acting at an angle φ_2 (pure follower force). At the joints the restoring moments $c\varphi_1 + b_1\dot{\varphi}_1$ and $c(\varphi_2-\varphi_1) + b_2(\dot{\varphi}_2-\dot{\varphi}_1)$ are induced.

The kinetic energy T, the dissipation function D, the potential energy V, and the generalized forces Q_1 and Q_2 are

$$T = \frac{1}{2} m\ell^2(3\dot{\varphi}_1^2 + 2\dot{\varphi}_1\dot{\varphi}_2 + \dot{\varphi}_2^2)$$

$$D = \frac{1}{2} b_1\dot{\varphi}_1^2 + \frac{1}{2} b_2(\dot{\varphi}_1^2 - 2\dot{\varphi}_1\dot{\varphi}_2 + \dot{\varphi}_2^2)$$

$$V = \frac{1}{2} c(2\varphi_1^2 - 2\varphi_1\varphi_2 + \varphi_2^2) \tag{4.1}$$

$$Q_1 = P\ell(\varphi_1 - \varphi_2)$$

$$Q_2 = 0$$

Lagrange's equations in the form

$$\frac{d}{dt}\left(\frac{\partial T}{\partial \dot{\varphi}_i}\right) + \frac{\partial D}{\partial \dot{\varphi}_i} - \frac{\partial T}{\partial \varphi_i} + \frac{\partial V}{\partial \varphi_i} = Q_i \qquad (i = 1,2) \tag{4.2}$$

are employed to establish the linear equations of motion

$$\begin{aligned} &3m\ell^2\ddot{\varphi}_1 + (b_1+b_2)\dot{\varphi}_1 - (P\ell-2c)\varphi_1 + m\ell^2\ddot{\varphi}_2 - b_2\dot{\varphi}_2 + (P\ell-c)\varphi_2 = 0 \\ &m\ell^2\ddot{\varphi}_1 - b_2\dot{\varphi}_1 - c\varphi_1 + m\ell^2\ddot{\varphi}_2 + b_2\dot{\varphi}_2 + c\varphi_2 = 0 \end{aligned} \tag{4.3}$$

which, upon stipulating solutions of the form

$$\varphi_i = A_i e^{\omega t} \qquad (i = 1,2) \tag{4.4}$$

yield the characteristic equation

$$p_o\Omega^4 + p_1\Omega^3 + p_2\Omega^2 + p_3\Omega + p_4 = 0 \tag{4.5}$$

with the coefficients

$$\begin{aligned} p_o &= 2 \\ p_1 &= B_1 + 6B_2 \\ p_2 &= 7 - 2F + B_1B_2 \\ p_3 &= B_1 + B_2 \\ p_4 &= 1 \end{aligned} \tag{4.6}$$

and the dimensionless quantities

$$\Omega = \ell \left(\frac{m}{c}\right)^{1/2} \omega$$

$$B_i = \frac{b_i}{\ell (cm)^{1/2}} \qquad (i = 1,2) \qquad (4.7)$$

$$F = \frac{P\ell}{c}$$

In the absence of damping ($B_1 = B_2 = 0$), the characteristic equation is a biquadratic

$$2\Omega^4 + (7-2F)\Omega^2 + 1 = 0 \qquad (4.8)$$

4.2.2 Critical Loads

From the assumed form of the time-dependence for the coordinates φ_i and on the basis of the kinetic stability criterion, it is evident that if all four roots of the characteristic equation are distinct, the necessary and sufficient conditions for stability are that the real roots and the real parts of the complex roots should be all negative or zero. In case of equal roots the general solution of φ_i will have terms which contain powers of t as a factor. If the real parts of equal roots are negative, the system will be stable (vibration with decreasing amplitude), but if these real parts are zero or positive, stability will not exist (vibration with increasing amplitude).

Let us turn our attention first to the case of an initially undamped system. The four roots of the biquadratic equation as a function of F are (a special case, $\alpha = 1$, of the problem treated in Section 3.1)

$$\Omega_{1,2,3,4} = \frac{1}{2}\left\{\pm\left[F - \left(\frac{7}{2} - \sqrt{2}\right)\right]^{1/2} \pm \left[F - \left(\frac{7}{2} + \sqrt{2}\right)\right]^{1/2}\right\} \qquad (4.9)$$

which, depending on the values of F, may turn out to be pure imaginary roots, complex roots, or pure real roots. The nature of these four roots as F varies is graphically illustrated in Fig. 4.2 in which the values of the roots are given by the intersection points of the root curves and the horizontal plane which is perpendicular to the F-axis and passes through the given value of F. The illustrations in Fig. 4.2 include a perspective of the root curves, and also the orthographic projections on the real plane (Im $\Omega = 0$), the imaginary plane (Re $\Omega = 0$) and the complex plane ($F = 0$).

It is found that there will always be two roots with positive real part if $F > \frac{7}{2} - \sqrt{2} = 2.086 = F_e$. For $F = F_e$ there exist two pairs of equal roots

whose real parts are all zero. Thus the system is unstable for $F \geq F_e$. For $F < F_e$ all roots are distinct and pure imaginary and thus the system is marginally stable.

We consider next a slightly damped system, assuming $B_1 = B_2 = 0.01$. No simple expressions for the four roots of the quartic equation exist; the numerical results obtained are illustrated in Fig. 4.3, where a perspective view is supplemented by three projections of the same three planes as in Fig. 4.2. Two roots will have a positive real part for $F > 1.464 = F_d$.

Stability can be investigated directly without determining the roots of the characteristic equation by applying the Routh-Hurwitz criteria, which require that all coefficients $p_j (j = 0, \ldots, 4)$ of the characteristic equation and the quantity

$$X = p_1 p_2 p_3 - p_0 p_3^2 - p_1^2 p_4 \tag{4.10}$$

be positive. For positive damping these stability conditions are satisfied, provided

$$\begin{aligned} p_2 &= 2\left[- F + \tfrac{1}{2}\,(7+B_1B_2)\right] > 0 \\ X &= 2(B_1^2+7B_1B_2+ 6B_2^2)\left\{- F + \left[\frac{4B_1^2+ 33B_1B_2+ 4B_2^2}{2(B_1^2+7B_1B_2+6B_2^2)} + \tfrac{1}{2}\,B_1B_2\right]\right\} > 0 \end{aligned} \tag{4.11}$$

For the system to be stable F must satisfy the following two inequalities, where $\beta = B_1/B_2$, $0 \leq \beta \leq \infty$:

$$\begin{aligned} F &< \tfrac{7}{2} + \tfrac{1}{2}\,B_1B_2 \\ F &< \frac{4\beta^2+ 33\beta + 4}{2(\beta^2+7\beta+6)} + \tfrac{1}{2}\,B_1B_2 \end{aligned} \tag{4.12}$$

Since

$$\frac{4\beta^2+ 33\beta + 4}{2(\beta^2+7\beta+6)} < \frac{7}{2} \tag{4.13}$$

for whatever β in its range, it is evident that the critical load will be governed by the second inequality, i.e.,

$$\bar{F}_d = \frac{4\beta^2+ 33\beta + 4}{2(\beta^2+7\beta + 6)} + \tfrac{1}{2}\,B_1B_2 \tag{4.14}$$

which depends on the ratio as well as the magnitudes of the damping coefficients.

For $B_i \ll 1$, as well as in the limit of vanishing damping, $\bar{F}_d$ becomes

$$F_d = \frac{4\beta^2 + 33\beta + 4}{2(\beta^2+7\beta+6)} \tag{4.15}$$

which is highly dependent on β and is in general smaller but never larger than F_e. The ratio of F_d to F_e versus β is plotted in Fig. 4.4. It is noted that when $\beta = 4 + 5\sqrt{2} = 11.07$, F_d/F_e reaches its maximum value 1. The destabilizing effect is thus eliminated in this particular case, similar to that found by Bolotin [8]. For $\beta = 0$, F_d/F_e reaches its minimum value 0.16; i.e., the maximum destabilizing effect is about 84 percent in the present two-degree-of-freedom system.

4.2.3 Case of Vanishing Damping

The two disparate values of the critical load for no damping ($B_i = 0$) and vanishing damping ($B_i \to 0$) justify a more detailed investigation of the limiting process as the damping coefficients approach zero.

Let us examine first the limiting process for the roots of the characteristic equation. It can be shown with the aid of the theory of equations [26] that if $B_i \ll 1$ and $F < 4.914$ this equation will have four complex roots. Let these roots be

$$\Omega = \begin{cases} \gamma_1 \pm i\gamma_2 \\ \lambda_1 \pm i\lambda_2 \end{cases} \tag{4.16}$$

Then one can write [26]

$$\begin{aligned} 2(\gamma_1 + \lambda_1) &= -\frac{p_1}{p_o} \\ 4\gamma_1\lambda_1[(\gamma_1+\lambda_1)^2 + (\gamma_2+\lambda_2)^2][(\gamma_1+\lambda_1)^2 + (\gamma_2-\lambda_2)^2] &= \frac{X}{p_o^3} \end{aligned} \tag{4.17}$$

where p_o, p_1, and X are as defined earlier. For vanishing damping

$$\begin{cases} \gamma_1 + \lambda_1 = 0 \\ \gamma_1\lambda_1[(\gamma_1+\lambda_1)^2 + (\gamma_2+\lambda_2)^2][(\gamma_1+\lambda_1)^2 + (\gamma_2-\lambda_2)^2] = 0 \end{cases} \tag{4.18}$$

Hence

$$\gamma_1 = -\lambda_1, \qquad \gamma_2 = \lambda_2$$

or

$$\gamma_1 = \lambda_1 = 0 \tag{4.19}$$

Thus

$$\Omega = \begin{cases} \pm i\gamma_2 \\ \pm i\lambda_2 \end{cases} \qquad \text{or} \qquad \Omega = \begin{cases} \gamma_1 \pm \gamma_2 \\ -\gamma_1 \pm i\gamma_2 \end{cases} \tag{4.20}$$

and a substitution of these four roots into the characteristic equation will show that they are the same as in the case of no damping.

In the case of $F \geq 4.914$, the four roots will all be real for small B_i. Let

$$\Omega = \begin{cases} u_1 \pm u_2 \\ v_1 \pm v_2 \end{cases} \tag{4.21}$$

In the limit of vanishing damping one can show similarly that either $u_1 = v_1 = 0$ or $u_1 = -v_1$ and $u_2 = v_2$. For either alternative, substitution into the characteristic equation reveals that the roots are the same as in the case of no damping.

Thus the conclusion is reached that whatever F the roots of the characteristic equation for no initial damping ($B_i = 0$) are identical to those of vanishing damping ($B_i \to 0$). This implies that the motions of the system, for some given initial conditions, and whatever F, will be identical in the case of no damping ($B_i = 0$) and vanishing damping ($B_i \to 0$).

We focus attention next on the loading F in the two cases and before passing to the limit consider small damping ($B_i \ll 1$). The positive real part of the roots of the characteristic equation in the range $F_d < F < F_e$ for several small values of B_2 and, as an example, $B_1 = 0$ (i.e., $\beta = 0$) have been calculated and the results are displayed in Fig. 4.5, where F is plotted as a function of Re Ω for nine values of B_2. This figure illustrates that for the larger values of B_2, F_d represents the critical load because for $F > F_d$ some roots will have a nonvanishing positive real part. A small increase of the load above F_d will result in a large increase of this real part. For small values of B_2, however, even though F_d is still strictly speaking the critical load, its significance is lessened, because a small increase of the load above

F_d will not result any longer in a large increase of Re Ω. Large increase of Re Ω will now be associated with small increase of a load which is slightly lower than F_e. For vanishing damping Re $\Omega = 0$ for any $F < F_e$. We thus conclude that during the limiting process the significance of F_d as a critical load is gradually transferred to F_e, and at the limit of vanishing damping ($B_i \to 0$) F_e has to be considered as the critical load. It is apparent now that this conclusion could only be reached by considering the roots of the characteristic equation and not by merely applying the stability criteria of Routh-Hurwitz. Further, the reasons for the stability criteria yielding different critical loads for no damping and for vanishing damping can be better understood by having considered small damping.

4.2.4 Degree of Instability

It was established in the preceding section that for vanishing damping ($B_i \to 0$) the four roots of the characteristic equation become identical to those of no damping ($B_i = 0$) while the stability criteria alone would in general yield disparate critical loads in these two cases.

To establish a further connection between the mathematically derived critical loads for no damping ($B_i = 0$) and vanishing damping ($B_i \to 0$) it appears helpful to introduce into the discussion a concept which might be called "degree of instability" and which embodies a relaxation of the concept of instability as used when applying the kinetic stability criterion. According to this latter criterion a system is stable if a suitable disturbance results in a bounded motion in the vicinity of the equilibrium configuration; e.g., the system is unstable if a disturbance leads to oscillations with increasing amplitude (flutter instability). For this type of loss of stability one can state that from a practical point of view it will certainly matter how fast the amplitudes increase.

For example, should a suitable initial disturbance be merely doubled in a time interval which is large as compared to, say, some reference period, while the duration of the system being subjected to a nonconservative force is by comparison relatively short, the system may be considered practically stable, while, mathematically, of course, one would have to conclude that it is unstable.

In order to weaken the kinetic stability criterion, one could prescribe arbitrarily the allowable increase of the disturbance and would then obtain for a given value of the load a critical time, not unlike in the case of creep buckling. As an alternative, one could introduce another measure of the rate of amplitude increase. By analogy to decaying oscillations, where the logarithmic decrement serves the purpose of quantitatively assessing the rate of decay, we can use the same quantity also as a measure of the rate of amplitude increase. Thus

$$\delta = \log \frac{A_n}{A_{n+1}} \tag{4.22}$$

where A_n is the amplitude of the oscillation at a certain time t and A_{n+1} is the amplitude at t + T, where T is the period. In the present problem, neglecting the terms of decaying magnitude in the general solution of φ_i, δ generally will be time-independent for flutter motions, except when the characteristic equation has equal pure imaginary roots.

The kinetic stability criterion requires $\delta \geq 0$; i.e., $A_n \geq A_{n+1}$. A negative δ properly could be called the logarithmic increment and in a real system it is conceivable that δ may attain a certain value δ_c in a certain interval of time without the system losing its stability in any practical sense.

For $\beta = B_1/B_2 = 1$ the critical load F is displayed as a function of $B_1 = B_2 = B$ in Figs. 4.6 and 4.7. For however small but finite negative value of δ, the critical load for vanishing damping ($B \to 0$) will always be that for no damping ($B = 0$), namely, F_e. However, the critical load for small damping ($B < 1$) may be smaller than F_e but for finite δ, however small, is always larger than F_d. For given δ the value of (small) damping B which is associated with the minimum value of the critical load can be determined.

For vanishing logarithmic increment ($\delta \to 0$) the function F(B) approaches a limiting curve which will contain the point F_d on the ordinate. For $\delta = 0$ the stability region is closed; i.e., points on the curve $\delta = 0$ in Fig. 4.7 are stable, including the point F_d on the ordinate. For $B = 0$ it is the point F_e which separates stability from instability, but belongs itself to the instability region. This limiting process provides thus additional insight into the generation of the critical load F_d.

4.2.5 A More General Model

Further interesting types of behavior may be discussed if the follower force is generalized by means of the parameter α as discussed in Section 3.1 without damping. The system to be analyzed is that of Fig. 4.8 (cf. Ref. [27]). The kinetic energy T, the dissipation function D and the potential energy V are the same as in Section 4.2.1, while the generalized forces Q_i are the same as those in Section 3.1. The associated equations of motion are

$$\begin{aligned} 3m\ell^2\ddot{\varphi}_1 + (b_1+b_2)\dot{\varphi}_1 - (P\ell-2c)\varphi_1 + m\ell^2\ddot{\varphi}_2 - b_2\dot{\varphi}_2 + (\alpha P\ell-c)\varphi_2 &= 0 \\ m\ell^2\ddot{\varphi}_1 - b_2\dot{\varphi}_1 - c\varphi_1 + m\ell^2\ddot{\varphi}_2 + b_2\dot{\varphi}_2 - [(1-\alpha)P\ell - c]\varphi_2 &= 0 \end{aligned} \tag{4.23}$$

which, upon stipulating solutions of the form (4.4) yield the characteristic equation

$$p_o\Omega^4 + p_1\Omega^3 + p_2\Omega^2 + p_3\Omega + p_4 = 0 \tag{4.24}$$

with the coefficients

$$p_o = 2$$

$$p_1 = B_1 + 6B_2$$

$$p_2 = 2(2-\alpha)\left[-F + \frac{7+B_1B_2}{2(2-\alpha)}\right] \tag{4.25}$$

$$p_3 = (1-\alpha)(B_1+2B_2)\left[-F + \frac{\beta+1}{(1-\alpha)(\beta+2)}\right]$$

$$p_4 = (1-\alpha)\left\{F - \frac{3}{2}\left[1 + \left(\frac{5/9-\alpha}{1-\alpha}\right)^{1/2}\right]\right\}\left\{F - \frac{3}{2}\left[1 - \left(\frac{5/9-\alpha}{1-\alpha}\right)^{1/2}\right]\right\}$$

The dimensionless quantities Ω, B_i, and F have been defined in Eqs. (4.7) and β is again $\beta = B_1/B_2$.

4.2.6 Root Domains of Characteristic Equation

It was found that small damping rather than vanishing or large damping is the cause of the destabilizing effect, and thus only small damping ($B_i \ll 1$) will be considered in the sequel.

Let us introduce first the following quantities:

$$H = \frac{1}{6}p_o p_2 - \frac{1}{16}p_1^2$$

$$\cong \frac{2}{3}(\alpha-2)\left[F - \frac{7}{2(2-\alpha)}\right]$$

$$I = p_o p_4 - \frac{1}{4}p_1 p_3 + \frac{1}{12}p_2^2$$

$$\cong \frac{1}{12}[4(\alpha^2-10\alpha+10)F^2 + 4(25\alpha-32)F + 73]$$

$$J = \frac{1}{6}p_o p_2 p_4 + \frac{1}{48}p_1 p_2 p_3 - \frac{1}{16}p_o p_3^2 - \frac{1}{16}p_1^2 p_4 - \frac{1}{216}p_2^3$$

$$\cong -\frac{1}{216}[(8\alpha^3+96\alpha^2-336\alpha+224)F^3 - (348\alpha^2-1464\alpha+1032)F^2 - (1362\alpha-1212)F - 161] \tag{4.26 cont.}$$

$$K = p_o^2 I - 12H^2$$

$$\cong -4[(\alpha-1)^2+1]\left\{F - \frac{1}{2[(\alpha-1)^2+1]} \times \{(8-\alpha) + 6.325\,[-(\alpha-0.345)(\alpha-1.305)]^{1/2}\}\right\}$$

$$\times \left\{F - \frac{1}{2[(\alpha-1)^2+1]}\{(8-\alpha) - 6.325\,[-(\alpha-0.345)(\alpha-1.305)]\}^{1/2}\right\}$$

$$\Delta = I^3 - 27J^2 \cong \frac{1}{8} p_4 K^2$$

$$X = p_1 p_2 p_3 - p_o p_3^2 - p_1^2 p_4$$

$$= B_2^2\{(1-\alpha)[\beta^2 + 12\beta + 4 - 8\alpha(\beta+2)]F^2$$

$$- [2(\beta^2+7\beta+6) + 2(1-\alpha)(\beta^2+11\beta-10)$$

$$+ (1-\alpha)(\beta^2+8\beta+12)B_1B_2]F + [4\beta^2+33\beta+4+(\beta^2+7\beta+6)B_1B_2]\}$$

$$\cong B_2^2\{(1-\alpha)[\beta^2 + 12\beta + 4 - 8\alpha(\beta+2)]F^2$$

$$- 2[\beta^2 + 7\beta + 6 + (1-\alpha)(\beta^2+11\beta-10)]F + (4\beta^2+33\beta+4)\} \qquad (4.26)$$

where $p_o,\ldots,p_4$ and other symbols have been defined previously.

It is known from the theory of equations [26] that:

(a) When $\Delta < 0$, the characteristic equation has two real and two complex roots.

(b) When $\Delta > 0$ and both H and K are negative, the four roots are all real.

(c) When $\Delta > 0$ and at least one of H and K is positive or zero, the four roots are all complex.

These criteria lead to the different root domains shown in Fig. 4.9. The domain marked by crosses indicates the existence of four real roots; that marked by dots corresponds to two real and two complex roots; and that marked by horizontal dashes or by diagonal lines indicates the existence of four complex roots. The more detailed nature of the roots and the related stable and unstable behavior of the system may be deduced from the following.

Domain $\Delta > 0$, $H < 0$, $K < 0$

This domain is marked by crosses in Fig. 4.9. In it, p_o, p_1, and p_4 are always positive; p_2 is always negative. Applying the well-known Descartes'

rule of signs, regardless of the sign of p_3, it is seen that in this domain the four real roots of the characteristic equation are always pairs of two positive and two negative ones. Consequently, this is throughout a region of instability by divergent motion.

Domains $\Delta < 0$

These domains are marked by dots in Fig. 4.9. Let the two real and two complex roots in these domains be represented by

$$\Omega = \begin{cases} \rho_1 \pm i\rho_2 \\ r_1 \pm r_2 \end{cases} \tag{4.27}$$

From the relations between roots and coefficients in the theory of equations [26] and the definition of the expression X in the Routh-Hurwitz criterion, the following relationships hold:

$$\begin{aligned} 2(\rho_1+r_1) &= -\frac{p_1}{p_o} = -\frac{1}{2}(B_1+6B_2) < 0 \\ 2[\rho_1(r_1^2-r_2^2) + r_1(\rho_1^2+\rho_2^2)] &= -\frac{p_3}{p_o} = -\frac{1}{2}p_3 \\ (\rho_1^2+\rho_2^2)(r_1^2-r_2^2) &= \frac{p_4}{p_o} = \frac{1}{2}p_4 \\ 4\rho_1 r_1\left\{\left[(\rho_1+r_1)^2 + \rho_2^2 - r_2^2\right]^2 + 4\rho_2^2 r_2^2\right\} &= \frac{X}{p_o^3} = \frac{1}{8}X \end{aligned} \tag{4.28}$$

As p_4 is always negative in these three domains, the third of the foregoing equations indicates that

$$r_2^2 > r_1^2 \tag{4.29}$$

which, in turn, shows that the two real roots are of opposite sign. Hence these three domains are also regions of instability. Again, recalling that $p_4 < 0$, it is seen from the foregoing four equations that the real part of the conjugate complex roots will be negative if $X > 0$ or if $X < 0$ and $p_3 < 0$, but will be positive if $X < 0$ and $p_3 > 0$. Whence it follows that divergent motion will prevail in this region, of the type as sketched in Fig. 4.10(a) if $X > 0$ or if $X < 0$ and $p_3 < 0$, or as in Fig. 4.10(b) if $X < 0$ and $p_3 > 0$. It is noted that, if the system is undamped ($B_1 = 0$), ρ_1 and r_1 will vanish identically. The undamped system will therefore undergo divergent motion of

the type as sketched in Fig. 4.10(c). By definition, in all these cases, the system is unstable.

Domain $K > 0$

This domain is marked by horizontal dashes in Fig. 4.9. Let us denote the four complex roots in this domain by

$$\Omega = \begin{cases} \gamma_1 \pm i\gamma_2 \\ \delta_1 \pm i\delta_2 \end{cases} \tag{4.30}$$

Then, as before, the following relationships are obtained:

$$\begin{aligned} 2(\gamma_1+\delta_1) &= -\frac{p_1}{p_o} = -\frac{1}{2}(B_1+6B_2) < 0 \\ 4\gamma_1\delta_1[(\gamma_1+\delta_1)^2 + (\gamma_2+\delta_2)^2][(\gamma_1+\delta_1)^2 + (\gamma_2-\delta_2)^2] &= \frac{X}{p_o^3} = \frac{1}{8}X \end{aligned} \tag{4.31}$$

which indicate that γ_1 and δ_1 (the real parts of the two pairs of conjugate complex roots) both will be negative if $X > 0$ but of opposite sign if $X < 0$.

Now, within this domain, we have

$$K \cong 8p_4 - p_2^2 > 0 \tag{4.32}$$

or

$$p_4 > \frac{1}{8} p_2^2 \tag{4.33}$$

which, in turn, leads to

$$X < -\frac{1}{8}(4p_3 - p_1p_2)^2 \leq 0 \tag{4.34}$$

Therefore, the real parts of the two pairs of conjugate complex roots are of opposite sign. The nature of these four roots indicates that in this domain the system will flutter.

Domain $\Delta > 0$, $H > 0$, $K < 0$

This domain is marked by diagonal lines in Fig. 4.9. As the four roots are all complex, the signs of the real parts of the roots will also be governed by the signs of X as asserted in the foregoing. Thus the system will vibrate with decreasing amplitude (asymptotic stability) if the values of α and F are in those parts of this domain where $X > 0$. However, the system will flutter if the values of α and F are in those parts where $X < 0$.

Further separation of stability from instability in the present domain is governed solely by the sign of X. This is illustrated for the four cases of $\beta = 0$, 1, 11.071, and ∞, as shown in Figs. 4.11, 4.12, 4.13, and 4.14, where the regions shaded by diagonal lines are regions of stability; those shaded by horizontal dashes are regions of flutter; those shaded by small triangles are regions of divergent motion of the type shown in Fig. 4.10(a); those shaded by dots are regions of divergent motion of the type shown in Fig. 4.10(b); and those shaded by crosses are regions of divergent motion in which the time increase of the generalized coordinates is of the exponential type.

It is to be noted that, in the present domain ($\Delta > 0$, $H > 0$, and $K < 0$), if the damping effects vanish, the four complex roots of the characteristic equation will all be pure imaginary and distinct. Thus the undamped system executes steady-state vibrations and is marginally stable throughout the domain, as found in [22].

4.2.7 Nature of Boundaries Separating Different Root Domains

In this section, the boundaries given by $X = 0$, $p_4 = 0$, and $K = 0$ will be examined. For the sake of convenience, the term "boundaries given by $X = 0$" will be restricted to mean only those parts of the curves given by $X = 0$ which lie in the domain $\Delta > 0$, $H > 0$, and $K < 0$.

Boundaries $X(\alpha,F,\beta) = 0$

On these boundaries, the characteristic equation has, by definition of X, two roots equal in magnitude but opposite in sign. These two roots are

$$\Omega_{1,2} = \pm \left(-\frac{p_3}{p_1}\right)^{1/2} \tag{4.35}$$

where p_1 is positive for positive damping. It is found that the curves $p_3 = 0$, $p_4 = 0$, and $X = 0$ have a common point of intersection which is given by

$$\alpha = \alpha' = \frac{\beta^2 + 3\beta + 1}{2\beta^2 + 5\beta + 2}$$

$$F = F' = \frac{2\beta + 1}{\beta + 1} \tag{4.36}$$

Further, as $p_3 = 0$ and $X = 0$ have only one point of intersection at (α', F') on $p_4 = 0$, it is evident that, along the boundaries given by $X = 0$, p_3 is always positive. This can be seen from Figs. 4.11, 4.12, 4.13 and 4.14. Consequently, $\Omega_{1,2}$ are two distinct pure imaginary roots. The sum of the other two conjugate complex roots is $-p_1/p_o = -\frac{1}{2} p_1$, which is negative (for positive damping). Hence, along the boundaries given by $X = 0$, the characteristic equation has two pure imaginary roots equal in magnitude but opposite in sign and two conjugate complex roots with negative real part. Thus the

system will execute steady-state vibrations as a result of some initial disturbance. It is only in this case that the damped, nonconservative system can undergo such motions.

Point of Intersection of $X = 0$, $p_3 = 0$, $p_4 = 0$

At this common intersection point denoted by (α', F'), the characteristic equation has two zero roots. The other two roots, being given by

$$p_o\Omega^2 + p_1\Omega + p_2 = 0 \tag{4.37}$$

are two conjugate complex roots with negative real part. The two zero roots will induce two terms of the form $c_1 + c_2 t$ in the general solution of φ_i. Thus the system will execute divergent motion in which the increase of φ_i is linear with respect to time. This point (α', F') is the only one at which the stability region for the damped, nonconservative system is open.

Points of Intersection of $p_4 = 0$, $X = 0$, $S = 0$

Let us introduce the quantity

$$S = p_1p_2 - p_op_3 \tag{4.38}$$

such that

$$X = p_3S - p_1^2p_4 \tag{4.39}$$

It can be shown that the curves $p_4 = 0$, $S = 0$, and $X = 0$ have two points of common intersection, denoted by (α'', F'') and (α''', F'''), where

$$\left.\begin{matrix}\alpha'' \\ \alpha'''\end{matrix}\right\} = \frac{(5\beta^2+228\beta+1440) \mp [(5\beta^2+180\beta+800)^2 - 6400\beta(\beta+6)]^{1/2}}{16(15\beta+112)}$$

$$F'' = \frac{5(\beta+8)}{2(\beta+10-4\alpha'')} \tag{4.40}$$

$$F''' = \frac{5(\beta+8)}{2(\beta+10-4\alpha''')}$$

These two points usually exist when β is finite, but the point (α''', F''') approaches infinity as $\beta \to \infty$. At the point (α'', F''), the characteristic equation has one zero root, one positive real root equal to $(-p_3/p_o)^{1/2}$, and two negative real roots equal to $-(-p_3/p_o)^{1/2}$ and $-p_1/p_o$; therefore, the system will execute divergent motions. At the point (α''', F'''), the four roots are

one zero root, two pure imaginary roots equal to $\pm (-p_3/p_1)^{1/2}$, and one negative real root equal to $-p_1/p_o$; hence, after the initial disturbance, the system will execute steady-state vibrations about a certain position which in general is not the position whose stability is being studied.

Boundaries $p_4 = 0$, Excluding Points (α', F'), (α'', F''), and (α''', F''')

Along these boundaries, the characteristic equation has one zero root and three other roots given by

$$p_o\Omega^3 + p_1\Omega^2 + p_2\Omega + p_3 = 0 \tag{4.41}$$

where, by the theory of equations and for small damping ($B_i \ll 1$), the three roots all will be real if $p_2 < 0$, but one real and two complex if $p_2 \geq 0$. In the range of either $F < F'$ or $\alpha > \alpha'''$ along $p_4 = 0$, the four roots are found to be one zero root, one negative real root, and two conjugate complex roots with negative real part. The nature of these four roots indicates that, after the initial disturbance, the system may execute transient vibrations and then come to rest at a position which in general is not the position whose stability is being studied. This phenomenon can be interpreted as a stabilizing effect of viscous damping because the same system with no damping would execute divergent motion.

The curves $p_2 = 0$ (i.e., $H = 0$), $p_4 = 0$, and $K = 0$ have two common intersection points at (0.423, 2.219) and (1.182, 4.281). In the range of $F' < F \leq 2.2.9$ along $p_4 = 0$, the four roots are one zero root, one positive real root, and two conjugate complex roots with negative real part. In the range $2.219 < F < 3$ along $p_4 = 0$, the four roots are one zero root, one positive real root, and two negative real roots. Thus, in the range of $F' \leq F < 3$ along $p_4 = 0$, the system will execute divergent motions.

In the range $F''' < F \leq 4.281$ along $p_4 = 0$, the four roots are one zero root, one negative real root, and two conjugate complex roots with positive real part; and thus flutter will occur. In the range $F > 4.281$ along $p_4 = 0$, the four roots are one zero root, one negative real root, and two positive real roots; hence the system will undergo divergent motions.

Boundary $K \cong 8p_4 - p_2^2 = 0$

The exact curve of $K = 0$ is

$$K = 8p_4 - p_2^2 - \left(p_1p_3 - \frac{1}{2}p_1^2p_2 + \frac{3}{64}p_1^4\right) = 0 \tag{4.42}$$

As B_i and, hence, p_1 and p_3 are assumed small, of the order of 10^{-3}, the last three terms in parentheses are higher-order terms and may be neglected. Thus

$$K \cong 8p_4 - p_2^2 = 0 \tag{4.43}$$

is a boundary curve which is close to the exact curve $K = 0$. Substituting $\frac{1}{8} p_2^2$ for p_4 in X, we have

$$X = -\frac{1}{8}(p_1 p_2 - 4p_3)^2 \leq 0 \tag{4.44}$$

which indicates that the system will be unstable when α and F are on the boundary curve given by $K = 8p_4 - p_2^2 = 0$, except at the point where X vanishes and p_3 is positive (steady-state vibrations). The instability mechanism, on the whole, will be of the flutter type, except at the points where the exact espressions of K and H are all negative (divergence).

4.2.8 Influence of Damping Ratio on Instability Mechanisms

In the preceding sections, it was established that stability is possible only in the region ($\Delta > 0$, $H > 0$, and $K < 0$), which is marked by diagonal lines in Fig. 4.9. In this region, the sign of X governs the type of motion, i.e., the system is stable if $X \geq 0$ and unstable if $X < 0$.

Critical loads for divergence, if any, are given by $p_4 = 0$; i.e., they are

$$F_{div} = \frac{3}{2}\left[1 \pm \left(\frac{5/9-\alpha}{1-\alpha}\right)^{1/2}\right] \tag{4.45}$$

On the other hand, critical loads for flutter, if any, are always given by $X = 0$, i.e., they are

$$F_{flu} = \frac{2(\beta^2+9\beta-2) - \alpha(\beta^2+11\beta-10) \pm (\beta+6)\left[(\beta^2-22\beta+1)\alpha^2 + 33\beta\alpha - 9\beta\right]^{1/2}}{8(\beta+2)(\alpha-1)(\alpha-\alpha_o)} \tag{4.46}$$

where $1 \neq \alpha \neq \alpha_o$, and

$$\alpha_o = \frac{\beta^2 + 12\beta + 4}{8(\beta+2)} \tag{4.47}$$

The two vertical lines $\alpha = 1$ and $\alpha = \alpha_o$ (Figs. 4.11 to 4.14) are asymptotes of $X = 0$. For $\alpha = 1$, the critical load is given by

$$F_{flu}\big|_{\alpha=1} = \frac{4\beta^2 + 33\beta + 4}{2(\beta^2 + 7\beta + 6)} \tag{4.48}$$

which was studied in Sect. 4.2.2. For $\alpha = \alpha_o$, the critical load for flutter, if any, becomes

$$F_{flu|\alpha=\alpha_o} = \frac{4(\beta + 2)(4\beta^2 + 33\beta + 4)}{\beta^4 + 7\beta^3 - 50\beta^2 - 332\beta + 24} \tag{4.49}$$

The curves of critical loads for $\beta = 0$, 1, 11.071, and ∞ are illustrated in Figs. 4.11, 4.12, 4.13, and 4.14.

For $\alpha = 0$ (conservative case) in Fig. 4.11, the point (0, -1), which is an intersection point of two branches of the curves given by $X = 0$, is itself on the boundary given by $X = 0$; therefore, this point corresponds to steady-state vibrations of the system. The point (0, -1) is thus also a point representing stability rather than a point which indicates an isolated critical load for the conservative system ($\alpha = 0$) with damping. However, depending on the ratio of damping coefficients, a nonconservative system ($\alpha \neq 0$) may have multiple critical loads for flutter, in addition to those for divergence, at the same value of α anywhere in the range $\alpha \lesseqgtr 0$, except for $5/9 < \alpha \leq 1$ where critical loads for flutter only will occur. Fig. 4.11 illustrates that, for $\beta = 0$, flutter will occur for any α, except $\alpha = 0$, while Fig. 4.12 shows that the smallest range of α in which flutter is possible becomes minimum ($5/9 < \alpha < 1.305$) when the damping coefficients are identical (i.e., $\beta = 1$).

It was found in Sect. 3.1 that the presence or absence of neighboring equilibrium positions was strongly influenced by the behavior of the nonconservative loading and also by the constraints of the system. A further result of this study is that the ratio of the damping coefficients may exert an analogous influence and may thus render the static criterion inapplicable for systems in which, without damping, the critical load could be determined statically. For instance, it is seen that, in the range $1/2 < \alpha < 5/9$, the static stability criterion is applicable if $\beta = \infty$ (see Fig. 4.14) but breaks down if $\beta = 0$ (see Fig. 4.11).

Similarly to applicability, the sufficiency of the static stability criterion (in the sense of supplying all critical loads) also depends on the ratio of damping coefficients. To exemplify this feature, let us examine again Figs. 4.11 and 4.14. In the range $\alpha < 1/2$, we note that the static stability criterion is sufficient if $\beta = \infty$ but proves to be insufficient if $\beta = 0$. The equation $p_4 = 0$ expresses, in fact, the static stability criterion, i.e., the condition of the static equilibrium of the system in the vicinity of its neutral configuration. Thus the static stability criterion is implied in the kinetic stability criterion, which is usually sufficient in determining all critical loads for the nonconservative system.

It is possible to identify the range of α in which flutter cannot occur, and thus the application of the kinetic criterion is not required. However, this range will depend on the ratio of the damping coefficients. To determine this range, we consider the expression F_{flu} derived in this section. Flutter cannot occur if the quantity $(\beta^2 - 22\beta + 1)\alpha^2 + 33\beta\alpha - 9\beta$ appearing under the

square root in that expression is negative. Thus flutter may occur in the following ranges:

$$\alpha \geq \alpha_1 \quad \text{and} \quad \alpha \leq \alpha_2 \quad \text{if} \quad \beta > a_1 \quad \text{or} \quad \beta < a_2 \tag{4.50}$$

or

$$\alpha_1 > \alpha > \alpha_2 \quad \text{if} \quad a_1 > \beta > a_2 \tag{4.51}$$

where

$$a_{1,2} = 11 \pm \sqrt{120} = \begin{cases} 21.954 \\ 0.046 \end{cases} \tag{4.52}$$

and

$$\alpha_{1,2} = \frac{-33\beta \pm [\beta(36\beta^2 + 297\beta + 36)]^{1/2}}{2(\beta - a_1)(\beta - a_2)}, \qquad (a_1 \neq \beta \neq a_2) \tag{4.53}$$

If $\beta = a_1$ or $\beta = a_2$, the range in which the kinetic stability criterion must be considered will be only $\alpha \geq 3/11$. Consequently, if there exists any range of α which is outside the foregoing specified ranges, the static stability criterion alone will be sufficient to determine all the critical loads, despite the nonconservativeness of the loading. However, according to the preceding section, if $\alpha < \alpha'$ or $\alpha > \alpha'''$, the static stability criterion definitely will be applicable but not necessarily sufficient in determining all critical loads.

4.2.9 Possibility of Elimination of Destabilizing Effects

Critical loads for flutter in the undamped system analyzed in Sect. 3.1 are given by the equation $K(\alpha, F, B_i) = 0$ with the terms due to small damping neglected; i.e., by the equation

$$K(\alpha,F) = -[4(\alpha^2 - 2\alpha + 2)F^2 + 4(\alpha - 8)F + 41] = 0 \tag{4.54}$$

Critical loads for flutter in the damped system analyzed here are given by

$$X(\alpha,F,\beta) = 0 \tag{4.55}$$

whose loci constitute, in fact, a family of curves in the α - F plane with β as the parametric constant. Different curves of the critical load for flutter will be obtained if different values are assigned to β in $X(\alpha,F,\beta) = 0$.

To study the interrelation between the curves of critical loads given by $K(\alpha,F) = 0$ and $X(\alpha,F,\beta) = 0$, let us examine the envelope of the family of curves defined by $X(\alpha,F,\beta) = 0$. It is known that, if an envelope exists, it must satisfy

$$X(\alpha,F,\beta) = 0 \tag{4.56}$$

and

$$\frac{\partial}{\partial\beta} X(\alpha,F,\beta) = 0 \tag{4.57}$$

Elimination of β in these two equations yields

$$(F-2)[(1-\alpha)F-2][4(1-\alpha)F-5]^2 \cdot K(\alpha,F) = 0 \tag{4.58}$$

where $K(\alpha,F)$ is as defined before. However, this equation may contain some curves which are other than the envelope. Deleting these, the true envelope is found as given by

$$[(1-\alpha)F - 2] \cdot K(\alpha,F) = 0 \tag{4.59}$$

Thus the curve for critical flutter loads of the system with no damping is a branch of the envelope of the family of curves of the critical flutter loads of the same system with damping. This remarkable relation shows a significant connection between the two governing equations of the critical loads for flutter of the undamped and the damped systems.

In consequence of the foregoing relation, it appears possible to eliminate the destabilizing effect of damping on the critical loads for flutter in the damped system if we choose the value of β which defines a curve of the family $X(\alpha,F,\beta) = 0$ tangent to $K(\alpha,F) = 0$ (the envelope) at the given value of α. Eliminating F in $X(\alpha,F,\beta) = 0$ and $(\partial/\partial\beta)X(\alpha,F,\beta) = 0$, we find that this value of β is given by the positive, real root of the quintic

$$\begin{aligned}(8\alpha - 3)(7\alpha - 3)(4\alpha - 3)\beta^5 &- (896\alpha^4 - 5{,}936\alpha^3 + 8{,}196\alpha^2 \\ &- 3{,}870\alpha + 594)\beta^4 - (12{,}800\alpha^4 - 60{,}928\alpha^3 + 82{,}680\alpha^2 \\ &- 38{,}664\alpha + 5832)\beta^3 - (80{,}128\alpha^4 - 365{,}280\alpha^3 + 502{,}416\alpha^2 \\ &- 234{,}576\alpha + 34{,}992)\beta^2 - (353{,}280\alpha^4 - 1{,}480{,}320\alpha^3 \\ &+ 1{,}925{,}856\alpha^2 - 874{,}800\alpha + 128{,}304)\beta - (838{,}656\alpha^4 \\ &- 2{,}941{,}056\alpha^3 + 3{,}411{,}072\alpha^2 - 1{,}469{,}664\alpha + 209{,}952) = 0\end{aligned} \tag{4.60}$$

and the critical load for flutter in this case is given by

$$F = \frac{(15-32\alpha)\beta^2 + (24-128\alpha)\beta + (84-496\alpha)}{2[(6-17\alpha+8\alpha^2)\beta^2 + (24-92\alpha+32\alpha^2)\beta + (120-484\alpha+256\alpha^2)]} \tag{4.61}$$

which will be identical to the critical loads for flutter of the same system with no damping.

For example, if the elimination of the destabilizing effect of damping for the case $\alpha = 1$ is desired, β must be equal to the positive, real root of

the quintic

$$\beta^5 + 6\beta^4 - 86\beta^3 - 884\beta^2 - 2612\beta - 2448 = 0 \tag{4.62}$$

i.e.,

$$\beta = 4 + 5\sqrt{2} = 11.071 \tag{4.63}$$

which, together with $\alpha = 1$, yields

$$F = \frac{7}{2} - \sqrt{2} = 2.086 \tag{4.64}$$

The critical load for $\alpha = 1$ in the undamped system determined in [5,22,25] is identical to the value we obtained in the foregoing. The complete elimination of the destabilizing effect for this case is thus attained, as is illustrated in Fig. 4.13. For $\alpha = 3/4$, a similar procedure will show that the destabilizing effect is completely removed when $\beta = \infty$. This is illustrated in Fig. 4.14.

The possibility of a complete elimination of the destabilizing effect depends on the existence of a positive, real root in the foregoing quintic. The range of α where the elimination of the destabilizing effect is of interest to us is, of course, $0.423 \leq \alpha \leq 1.305$. However, it is found that in the range

$$3/7 < \alpha < 3/4 \tag{4.65}$$

the quintic has no positive, real root. Thus, in this range, the system will always experience some destabilization for whatever value of β in its range $0 \leq \beta \leq \infty$.

For instance, let us consider the case $\alpha = 0.6$, where the critical load for the system with no damping is

$$F_e = \frac{5}{58}(37 - 6\sqrt{5}) = 2.033 \tag{4.66}$$

while the critical load for the system with damping is given by

$$F_d = \frac{1.4\beta^2 + 11.4\beta + 2 - (\beta+6)[0.36\beta^2 + 2.88\beta + 0.36]^{1/2}}{(3.2\beta + 6.4)(\alpha_o - 0.6)} \tag{4.67}$$

where

$$\alpha_o = \frac{\beta^2 + 12\beta + 4}{8(\beta + 2)} \tag{4.68}$$

The ratio of F_d to F_e versus β is plotted in Fig. 4.15. It is noted that the value of F_d/F_e increases as β increases and approaches $29/5(37-6\sqrt{5}) = 0.984$, instead of 1, as the upper limit when β approaches infinity; i.e., the destabilizing effect of damping is at least 1.6 percent if the value of α is kept at 0.6.

In the range $1.182 < \alpha < 1.305$, the undamped system has multiple critical loads for flutter given by $K(\alpha,F) = 0$. However, an investigation of the roots of the quintic shows that, for any α in the range $1.182 \leq \alpha \leq 1.285$, there is only one positive, real root which defines a curve of the family $X(\alpha,F,\beta) = 0$ tangent to the lower part of $K(\alpha,F) = 0$. Thus, in the range $1.182 \leq \alpha \leq 1.285$, the damped system has no critical load which is given by the upper part of $K(\alpha,F) = 0$.

As an alternative, the possibility of eliminating the effects of damping could also be studied by equating the frequencies first and then the critical forces, obtained with and without damping. The frequency of the undamped system is given by

$$\text{Im } \Omega = \frac{1}{2}\left[7 - 2(2-\alpha)F\right]^{1/2} \tag{4.69}$$

while the frequency of the system with damping is given by

$$\text{Im } \Omega = \left(\frac{P_3}{P_1}\right)^{1/2} = \left[\frac{(B_1+B_2) - (1-\alpha)(B_1+2B_2)F}{B_1 + 6B_2}\right]^{1/2} \tag{4.70}$$

Equating the two expressions and eliminating F in $K(\alpha,F) = 0$ leads to

$$28\left(\alpha - \frac{3}{7}\right)\left(\alpha - \frac{3}{4}\right)\beta^2 + 4(16\alpha^2 - 33\alpha + 9)\beta + 4(182\alpha^2 - 297\alpha + 81) = 0 \tag{4.71}$$

which, in turn, gives the range of Eq. (4.65) in which elimination of the damping effect is not possible for positive damping.

Fig. 4.16 illustrates the function $\beta(\alpha)$ which insures elimination of damping effects. For completeness, the required values of negative β in the range $3/7 < \alpha < 3/4$ have also been indicated.

4.3 Damping and Gyroscopic Forces in Systems with Two Degrees of Freedom

The joint effects of follower forces, linear viscous damping, and gyroscopic forces (i.e., velocity-dependent forces which do no work) have been studied in Ref. [28]. Considered was the system with two degrees of freedom

$$\begin{aligned} \ddot{q}_1 + a_{11}q_1 + a_{12}q_2 + b_{11}\dot{q}_1 + b_{12}\dot{q}_2 &= 0 \\ \ddot{q}_2 + a_{21}q_1 + a_{22}q_2 + b_{21}\dot{q}_1 + b_{22}\dot{q}_2 &= 0 \end{aligned} \tag{4.72}$$

The matrices a_{ij} and b_{ij} can be resolved uniquely into a symmetrical and antisymmetrical part:

$$\begin{Bmatrix} a_{11} & a_{12} \\ a_{21} & a_{22} \end{Bmatrix} = \begin{Bmatrix} a_{11} & a_{12}^* \\ a_{21}^* & a_{22} \end{Bmatrix} + \begin{Bmatrix} 0 & p \\ -p & 0 \end{Bmatrix} \tag{4.73}$$

where

$$a_{12}^* = a_{21}^* = (a_{12}+a_{21})/2, \qquad p = (a_{12}-a_{21})/2 \tag{4.74}$$

and

$$\begin{Bmatrix} b_{11} & b_{12} \\ b_{21} & b_{22} \end{Bmatrix} = \begin{Bmatrix} b_{11} & b_{12}^* \\ b_{21}^* & b_{22} \end{Bmatrix} + \begin{Bmatrix} 0 & \omega \\ -\omega & 0 \end{Bmatrix} \tag{4.75}$$

where

$$b_{12}^* = b_{21}^* = (b_{12}+b_{21})/2, \qquad \omega = (b_{12}-b_{21})/2 \tag{4.76}$$

By a suitable transformation of the form

$$\begin{aligned} q_1 &= \bar{q}_1 \cos\varphi - \bar{q}_2 \sin\varphi \\ q_2 &= \bar{q}_1 \sin\varphi - \bar{q}_2 \cos\varphi \end{aligned} \tag{4.77}$$

it is possible to make either a_{12}^* or b_{12}^* to vanish. Choosing the first possibility and writing again q_1, q_2, b_{12} ... for $\bar{q}_1$, $\bar{q}_2$, b_{12}^*, the following system of equations is obtained:

$$\begin{aligned} \ddot{q}_1 + a_{11}q_1 + pq_2 + b_{11}\dot{q}_1 + (b_{12}+\omega)\dot{q}_2 &= 0 \\ \ddot{q}_2 - pq_1 + a_{22}q_2 + (b_{12}-\omega)\dot{q}_1 + b_{22}\dot{q}_2 &= 0 \end{aligned} \tag{4.78}$$

The system has a potential energy function (is noncirculatory) if $p = 0$, it is purely circulatory for $a_{11} = a_{22} = 0$, it is nongyroscopic for $\omega = 0$, and is undamped if $b_{11} = b_{12} = b_{22} = 0$.

Solutions are sought in the form

$$q_i = A_i e^{\lambda t} \tag{4.79}$$

which lead to the characteristic equation

$$c_o\lambda^4 + c_1\lambda^3 + c_2\lambda^2 + c_3\lambda + c_4 = 0 \tag{4.80}$$

where

$$\begin{aligned} c_o &= 1 \\ c_1 &= b_{11} + b_{22} \end{aligned} \tag{4.81 cont.}$$

$$c_2 = a_{11} + a_{22} + (b_{11}b_{12} - b_{12}^2) + \omega^2$$

$$c_3 = a_{11}b_{22} + a_{22}b_{11} + 2p\omega$$

$$c_4 = a_{11}a_{22} + p^2 \tag{4.81}$$

For stability it is required that $c_i \geq 0$ $(i = 1,2,3,4)$ and that in addition

$$X = c_1c_2c_3 - c_oc_3^2 - c_1^2c_4 > 0 \tag{4.82}$$

If $c_1 = c_3 = 0$ this additional condition takes on the form

$$c_2^2 - 4c_oc_4 > 0 \tag{4.83}$$

It is to be noted that if $c_1 = 0$ but $c_3 \neq 0$ (or $c_1 \neq 0$ but $c_3 = 0$) the first inequality cannot be satisfied and thus the equilibrium is always unstable regardless of the actual values of the nonvanishing c_i.

Let us now examine the special case of an undamped system, $b_{ij} = 0$. The coefficients c_i are then

$$c_1 = 0, \quad c_2 = a_{11} + a_{22} + \omega^2, \quad c_3 = 2p\omega, \quad c_4 = a_{11}a_{22} + p^2 \tag{4.84}$$

Since $c_1 = 0$ and $c_3 \neq 0$ the system is unstable regardless how small the follower (circulatory) forces and the gyroscopic forces are.

Another special case of interest in which explicit results can be obtained is

$$a_{11} = a_{22} = a > 0, \quad b_{11} = b_{22} = b > 0, \quad b_{12} = 0 \tag{4.85}$$

Then we have

$$c_1 = 2b, \quad c_2 = 2a + b^2 + \omega^2, \quad c_3 = 2(ab + p\omega), \quad c_4 = a^2 + p^2 \tag{4.86}$$

For stability we must require

$$\begin{aligned} ab^2 + p\omega > 0 \qquad & (c_3 > 0) \\ ab^2 + p\omega b - p^2 > 0 \qquad & (X > 0) \end{aligned} \tag{4.87}$$

It is again seen from the second inequality that no stability is possible for $b = 0$ or for small b. The damping coefficient b has to be sufficiently large, namely

$$b > \left(- p\omega + \sqrt{p^2(\omega^2+4a)} \right) / (2a) \tag{4.88}$$

to insure stability. In the absence of purely gyroscopic forces, $\omega = 0$, the stability condition is

$$b > p/\sqrt{a} \tag{4.89}$$

4.4 Discrete Systems with Many Degrees of Freedom

Generalizing the findings concerning destabilizing effects found with specific examples of systems with two degrees of freedom, it is possible to state a number of theorems which are applicable to a rather broad class of systems with N degrees of freedom, (Ref. [29]). In particular, it can be shown that not only slight viscous damping, but all sufficiently small velocity-dependent forces may induce a destabilizing effect.

The system considered is assumed to be holonomic and autonomous, and is subjected to a set of generalized forces, $Q_j = Q_j(F)$; $j = 1,2,\ldots,N$, which are defined as linear functions of a real, finite parameter F. This parameter, $(0 \leq F < \infty)$, is associated with the magnitude of the externally applied forces, $Q_j = 0$ for $F = 0$.

Let

$$q_j = \dot{q}_j = 0, \qquad \left(j = 1,2,\ldots,N \; ; \quad \dot{q}_j \equiv \frac{dq_j}{dt} \right) \tag{4.90}$$

be the equilibrium state of the system. With $M = [M_{jk}]$ the generalized mass matrix, and

$$V = \frac{1}{2} \sum_{j,k=1}^{N} \bar{K}_{jk} q_j q_k \tag{4.91}$$

the strain energy function, assumed to be positive definite, the equations of motion of the undamped system may be written as

$$M_{jk}\ddot{q}_k + \bar{K}_{jk} q_k = Q_j \qquad j,k = 1,2,\ldots,N \tag{4.92}$$

where the summation convention on all repeated indices is implied and will be employed in the sequel.

Let us assume that the generalized forces, Q_j, are given as linear functions of the generalized coordinates

$$Q_j = FK_{jk} q_k \qquad j,k = 1,2,\ldots,N \tag{4.93}$$

where $K = [K_{jk}]$ is a nonsymmetric matrix, and F a real, finite parameter.

For $F = 0$, (4.92) represent the equations of free oscillation of the undamped system which we assume to possess N distinct, non-zero frequencies.

In conjunction with (4.92) we shall consider the following linear system

$$M_{jk}\ddot{q}_k + \epsilon G_{jk}\dot{q}_k + \bar{K}_{jk}q_k = Q_j \qquad j = 1,2,\ldots,N \tag{4.94}$$

where ϵ is an infinitesimal quantity, $G = [G_{jk}]$ a generally non-symmetric matrix with prescribed constant elements. For $\epsilon = 0$, Eqs. (4.94) reduce to Eqs. (4.92).

In the following sections we shall prove that the critical load of system (4.92) is an upper bound for the critical load of system (4.94) when $0(\epsilon^2)$ can be neglected in comparison with $0(\epsilon)$. Only the effect of velocity-dependent forces on the critical load of the system for flutter will be considered. The effect of these forces on the critical load for divergence is discussed in Refs. [6,7].

In the present context, therefore, the theorems proved in the sequel are applicable only when a linear system loses stability by flutter.

It is also of importance to note that an autonomous, linear, dynamic system can lose stability by flutter if and only if a solution of the form $q_k = A_k e^{i\omega t}$; $k = 1,2,\ldots N$, admits, at least, one ω with negative imaginary part. Further, we will employ the well-known property of linear autonomous dynamic systems of the type (4.92) that the roots of the characteristic equation are either real or pairs of complex conjugate numbers.

Let us first consider the effect of slight viscous damping. Thus we assume that $G = [G_{jk}]$ is a symmetric, non-negative matrix.

We take solutions of (4.92) and (4.94) in the form $q_k = A_k e^{i\omega t}$; $i = \sqrt{-1}$, and obtain

$$-\omega^2 M_{jk}A_k + (\bar{K}_{jk} - FK_{jk})A_k = 0 \tag{4.95}$$

$$-\omega^2 M_{jk}A_k + \epsilon i\omega G_{jk}A_k + (\bar{K}_{jk} - FK_{jk})A_k = 0 \qquad j,k = 1,2,\ldots,N \tag{4.96}$$

Systems (4.95) and (4.96) are each a set of linear, homogeneous equations in A_k. They have, therefore, nontrivial solutions if and only if the determinant of the coefficients of A_k, in each set, is equal to zero. These conditions yield

$$\det |a_{jk}| = 0 \tag{4.97}$$

$$\det |a_{jk} + \epsilon i\omega G_{jk}| = 0 \tag{4.98}$$

where $a_{jk} = -\omega^2 M_{jk} + (\bar{K}_{jk} - FK_{jk})$, and det $|a_{jk}|$ denotes the determinant of the matrix $[a_{jk}]$.

For F = 0, Eq. (4.97) yields the natural frequencies of the free vibration of the undamped system. We assume that these frequencies

$$(\omega_1^2 < \omega_2^2 < \ldots < \omega_N^2)$$

are distinct and non-zero. We now increase F and assume that for a certain value of F, say F_e, Eq. (4.97) yields, at least, a double non-zero frequency. Let us suppose that, for $F = F_e$, ω_1^2 is equal to ω_2^2 (see Fig. 4.17(a)), while all other (N-2) frequencies of the system are distinct and non-zero. If F is now increased beyond this critical value F_e, Eq. (4.97) will yield a pair of complex conjugate roots and, consequently, the system will oscillate with an exponentially increasing amplitude (flutter). We shall refer to F_e again as the critical load for the system without damping.

Let us now consider Eq. (4.98). For F = 0, the roots of this equation are all located on the left-hand side of the imaginary axis in the complex $i\omega$ plane. As we increase F, at least, one of these roots approaches the imaginary axis, and for a certain value of F, say F_d, Eq. (4.98) yields, at least, a real value for ω (see Fig. 4.17(b)). If F is now increased beyond this critical value F_d, at least, one of the roots of (4.98) becomes complex with negative imaginary part. The system, therefore, loses stability by flutter. We shall refer to F_d as the critical load for the system with damping.

In the sequel we will first study a system with two degrees of freedom and then extend our results to more general systems.

We expand the frequency equation of the damped system as follows

$$\det |a_{jk} + \epsilon i\omega G_{jk}| = \det |a_{jk}| + \epsilon i\omega G_{jk} a^{kj} - \epsilon^2 \omega^2 \det |G_{jk}|; \quad j,k = 1,2, \qquad (4.99)$$

where a^{kj} is the cofactor of the element a_{jk} in the det $|a_{jk}|$. Moreover, we assume that det $|G_{jk}| \neq 0$ (the case of det $|G_{jk}| = 0$ will be discussed later). Then, for det $|G_{jk}|$ finite and ϵ of infinitesimal order, we may neglect the last term on the right-hand side of Eq. (4.99) and obtain

$$\det |a_{jk}| + \epsilon i\omega G_{jk} a^{kj} = 0 \qquad j,k = 1,2 \qquad (4.100)$$

Theorem 1. The critical load, F_e, is an upper bound for the critical load, F_d, when $0(\epsilon^2)$ can be neglected in comparison with $0(\epsilon)$.

Proof. For $F = F_d$, Eq. (4.100) has, at least, one real root, $\omega = \bar{\omega}$, and the other roots are either real or complex with positive imaginary parts (the possibility of complex root with negative imaginary part is excluded, as it contradicts the assumption that F_d is the critical load). Therefore, for $F = F_d$ and ω real, det $|a_{jk}|$ and $G_{jk}a^{kj}$ are both real and we must have

$$\det |a_{jk}| = 0 \tag{4.101}$$

$$G_{jk}a^{kj} = 0 \qquad j,k = 1,2 \tag{4.102}$$

However, det $|a_{jk}| = 0$ cannot admit real roots if $F > F_e$. Therefore $F_d \leq F_e$.

Let us note that F_d can equal F_e if and only if the real root of (4.102) can be made equal to the double root of (4.101) for $F = F_e$. This, of course, depends on the other parameters of the system and may not always be achieved, as exemplified in Sect. 4.2.

We now retract to Eq. (4.99) and consider the case when det $|G_{jk}| = 0$. The frequency equation of the damped system with two degrees of freedom is now given by Eq. (4.100), independently of the order of magnitude of ϵ. Following the line of reasoning similar to that used in the proof of Theorem 1, we conclude that the critical load of the system without damping is an upper bound for that of the system with damping, no matter what the order of magnitude of ϵ may be. Therefore, we state the following theorem.

Theorem 2. The critical load, F_e, of the system without damping with two degrees of freedom is an upper bound for the critical load, F_d, of the system with damping for all finite values of ϵ when det $|G_{jk}| = 0$.

The proof of Theorem 1 was an immediate consequence of a property of the frequency equation of the system with damping and with two degrees of freedom. The problem becomes more complicated if the system has more than two degrees of freedom. However, one may still use a similar line of reasoning.

We expand Eq. (4.98), collect the terms of like power in ϵ, and obtain

$$\det |a_{jk} + \epsilon i\omega\, G_{jk}| = \det |a_{jk}| + \epsilon i\omega\, G_{jk}a^{kj} + 0(\epsilon^2) + \ldots, \quad j,k = 1,2,..N \tag{4.103}$$

The first term on the right-hand side of this equation is a polynomial of degree N in ω^2 and may be written as

$$\det |\, a_{jk}| \equiv P(\omega^2) \equiv P_N\omega^{2N} + P_{N-1}\omega^{2(N-1)} + \ldots + P_o \tag{4.104}$$

Similarly, the term $G_{jk}a^{kj}$, which is a polynomial of degree (N-1) in ω^2, can be written as

$$G_{jk}a^{kj} \equiv R(\omega^2) \equiv R_{N-1}\omega^{2(N-1)} + R_{N-2}\omega^{2(N-2)} + \ldots + R_o \tag{4.105}$$

Therefore, Eq. (4.103) becomes

$$\det \left|a_{jk} + \epsilon i\omega\, G_{jk}\right| = P(\omega^2) + i\epsilon\omega\, R(\omega^2) + 0(\epsilon^2) + \ldots \tag{4.106}$$

We neglect $0(\epsilon^2)$ and higher in Eq. (4.106) and obtain

$$P(\omega^2) + i\epsilon\omega\, R(\omega^2) = 0 \tag{4.107}$$

for the frequency equation of system (4.94). We now set $\omega = \lambda + i\epsilon\gamma$ and substitute into $P(\omega^2)$ and $R(\omega^2)$ to obtain

$$\begin{aligned} P(\lambda+i\epsilon\gamma) &= P(\lambda^2) + i\epsilon\gamma\left[2\lambda\,\frac{dP(\lambda^2)}{d(\lambda^2)}\right] + 0(\epsilon^2) + \ldots \\ R(\lambda+i\epsilon\gamma) &= R(\lambda^2) + 0(\epsilon) + \ldots \end{aligned} \tag{4.108}$$

Therefore, Eq. (4.107) becomes

$$P(\lambda^2) + i\epsilon\lambda\left[2\gamma\,\frac{dP(\lambda^2)}{d(\lambda^2)} + R(\lambda^2)\right] + 0(\epsilon^2) + \ldots = 0 \tag{4.109}$$

Neglecting terms of order higher than ϵ, we must have

$$P(\lambda^2) = 0, \quad \gamma = -\frac{R(\lambda^2)}{2P'(\lambda^2)}, \quad P'(\lambda^2) = \frac{dP(\lambda^2)}{d(\lambda^2)} \neq 0 \tag{4.110}$$

The first equation in (4.110) is the frequency equation of the system without damping and the second equation defines, to the first order of approximation in ϵ, the effect of slight damping on the frequencies of the system. The constraint given by $P'(\lambda^2) \neq 0$ indicates that the perturbation method breaks down when $P(\lambda^2) = 0$ admits double roots. For F = 0, the roots of equation $P(\lambda^2) = 0$ are all real and distinct. Thus in this case, to the first order of approximation in ϵ, the roots of Eq. (4.107) are

$$\pm\,\omega_k = \pm\,\lambda_k + i\epsilon\gamma_k, \quad \gamma_k = -\frac{R(\lambda_k^2)}{2P'(\lambda_k^2)}; \quad k = 1,2,\ldots,N \tag{4.111}$$

where λ_k^2 are real, positive roots of $P(\lambda^2) = 0$. The system can perform

oscillations only with an exponentially decaying amplitude and, therefore, all γ_k; $k = 1,2,\ldots,N$ are positive, real numbers.

We shall now assume that the system with damping is stable for all $F < F_d$ and consider the following cases:

$$\begin{aligned} &\text{(a)} \quad F < F_d < F_e \\ &\text{(b)} \quad F_e < F < F_d; \quad F_e < F_d \end{aligned} \tag{4.112}$$

For case (a), $P(\lambda^2) = 0$ yields N distinct roots. From Eq. (4.111) we then obtain γ_k; $k = 1,2,\ldots,N$, which are, by our assumption, all positive, real numbers.

For case (b), $P(\lambda)^2 = 0$ has, at least, one pair of complex conjugate roots. We denote these roots by $\overline{\lambda}_{1,2} = (\alpha \pm i\beta)$ and from (4.111) obtain

$$\pm \omega_{1,2} = \pm (\alpha \pm i\beta) - i\epsilon \frac{R[(\alpha \pm i\beta)^2]}{2P'[(\alpha \pm i\beta)^2]} \tag{4.113}$$

which indicates that, for $F > F_e$, the system with damping admits, at least, one complex frequency with negative imaginary part. This, therefore, contradicts the assumption that the system is stable for $F_d > F_e$. We are thus forced to take $F_d \leq F_e$ in order to remove the contradiction.

Let us note that, for $F = F_d = F_e$, Eqs. (4.111) can be used only for the distinct roots of $P(\lambda^2) = 0$. The perturbation method, which was introduced here breaks down if $P'(\lambda^2) = 0(\epsilon)$ while $R(\lambda^2)$ is non-zero. We shall not, however, concern ourselves with a detailed study of this case here and simply admit the possibility of $F_d = F_e$. In fact, as $F_d > F_e$ renders the system unstable, we can only conclude that $F_d \leq F_e$. Therefore, we may state the following theorem.

Theorem 3. The critical load, F_e, of system (4.92) is an upper bound for the critical load, F_d, of the system with slight damping when ϵ is sufficiently small.

For an arbitrary specified matrix $G = [G_{jk}]$ due to any type of velocity-dependent forces (including gyroscopic forces), system (4.94) may become self-exciting. That is, for an infinitely small value of F, the frequency equation of this system may possess complex roots with negative imaginary parts. In these cases we shall agree to define $F_d = 0$ as the critical load of this system.

On the other hand, the frequency equation of system (4.94) may yield roots with only positive imaginary parts for $F = 0(\epsilon)$. This indicates that this

system is stable for small values of the load parameter F. However, as we increase F, one of these roots may move toward the imaginary axis in the $i\omega$ plane. Therefore, for a certain value of F, say F_d, the frequency equation of system (4.94) may yield a non-zero, real root. In this case, if we then increase F beyond this critical value F_d, the frequency equation will have a root with negative imaginary part and the system will flutter. We shall refer to F_d as the critical load of system (4.94). On the basis of the above preliminaries it is now possible to follow the same chain of arguments outlined previously and establish the following more general theorems.

Theorem 4. The critical load, F_e, of system (4.92) is an upper bound for the critical load, F_d, of system (4.94) when ϵ is sufficiently small. $G = [G_{jk}]$ need not be a symmetric, positive definite matrix.

Theorem 5. The critical load, F_e, of system (4.92) with $N = 2$ is an upper bound for the critical load, F_d, of system (4.94) for all finite values of ϵ when $\det |G_{jk}| = 0$. $G = [G_{jk}]$ need not be a symmetric, positive definite matrix.

From the above results we immediately conclude that, in a linear system with N degrees of freedom, subjected to nonconservative (i.e. circulatory) forces, not only slight viscous damping but all sufficiently small velocity-dependent forces have, in general, a destabilizing effect. Moreover, the critical load, F_d, is highly dependent upon the structure of the matrix $G = [G_{jk}]$ but is always bounded from above by the critical load F_e. This indicates that, even at the limit as $\epsilon \to 0$, F_d is in general less than F_e. Let us explore this point in more detail for a system with two degrees of freedom.

For ϵ finite, the steady state motion of the system is possible if the frequency of the oscillation satisfies the following equations (see Eq. (4.99)):

$$\det |a_{jk}| - \epsilon^2\omega^2 \det |G_{jk}| = 0, \quad G_{jk}a^{kj} = 0; \qquad j,k = 1,2 \qquad (4.114)$$

In this case, one may solve the second equation in (4.114) for ω as a function of F and then substitute the result into the first equation to obtain a relationship between F and ϵ. In this manner a stability curve, in the F-ϵ plane, may be constructed (see Fig. 4.18). However, from Theorem 1 we immediately conclude that, in general, this curve suffers a finite discontinuity at $\epsilon = 0$. This means that, although for $\epsilon = 0$ the critical load is F_e, for $\epsilon = 0^+$ the critical load is given by F_d which is, in general, less than F_e. Therefore, the point F_e is, in general, an isolated point in the F-ϵ plane (Fig. 4.18). This phenomenon was interpreted physically in Sect. 4.2.

4.5 Destabilizing Effects in Continuous Systems

4.5.1 Introduction

It was shown in Sect. 4.4 that in a general circulatory system with N degrees of freedom not only slight viscous damping, but all sufficiently small velocity-dependent forces, such as Coriolis forces in vibrating pipes conveying fluid, or other gyroscopic forces, may have a destabilizing effect.

For a continuous system, however, which possesses an infinite number of degrees of freedom, no such theorems are as yet established. To study the effect of viscous damping forces in such systems most investigators, in general, reduce first the continuous system to a discrete one by means of, for example, the Galerkin method, and then study the reduced, discrete system [8,30,31]. But, as was shown in Sect. 4.4, a discrete system does, in fact, always have this property, except in very particular cases. Therefore, by this approach one does not know whether the original continuous system also exhibits the same behavior or whether it is produced only through the reduction procedure.

Let us show that the presence of sufficiently small velocity-dependent forces in a continuous elastic system subjected to follower forces does, indeed, have a destabilizing effect (cf. Ref. [32]). To this end, a cantilevered, continuous pipe conveying fluid at a constant velocity is considered. The internal and external viscous damping forces are also included, and then it is proved that the critical flutter load of the system may be reduced by almost 50% for some combinations of these velocity-dependent forces. The method of analysis effectively reduces a complicated nonself-adjoint boundary value problem (without discretization) to a simple frequency analysis by utilizing fully the fact that the velocity-dependent forces are sufficiently small.

It is of obvious interest to test the accuracy of the widely used Galerkin method with a two-term approximation. It is to be noted that such an analysis of this approximate method, for the case when the equations of motion of the system also contain mixed time and space derivatives, has been carried out in Ref. [32] for the first time.

Critical flutter loads of the system, for small velocity-dependent forces, and also for large values of Coriolis forces, were obtained by using the Galerkin method with a two-term approximation. The results are then compared with the exact solution. It is then shown that the two-term approximation yields sufficiently accurate values for the critical flutter load only if the velocity-dependent forces are small. Thus, for large values of Coriolis forces the critical load obtained by the Galerkin method with a two-term approximation may be greatly in error.

4.5.2 Cantilevered Pipe Conveying Fluid

We consider a cantilevered, uniform pipe of length L and internal cross-sectional area A, conveying fluid at a constant velocity U. A nozzle whose opening is n times smaller than A is placed at the free end of the system, as is shown in Fig. 4.19.

We shall assume that the material of the pipe obeys a stress-strain relationship of the Kelvin type, i.e.,

$$\sigma = E\epsilon + \eta\dot{\epsilon} \tag{4.115}$$

where E is the modulus of elasticity and η is the coefficient of viscosity. Under the assumption of plane sections remaining plane, the moment-curvature relationship, for small deformations, is

$$\frac{M}{EI} = -\left[\frac{\partial^2 y}{\partial x^2} + \frac{\eta}{E}\,\frac{\partial^3 y}{\partial x^2 \partial t}\right] \tag{4.116}$$

where M is the resultant moment at section x and at time t, I the moment of inertia, and y the transverse deflection of the pipe. With u denoting the displacement in the x direction, and z the distance of each fiber from the neutral axis, we also have

$$\sigma = \frac{Mz}{I}\,, \qquad \epsilon = \frac{\partial u}{\partial x}\,, \qquad u = -\,z\,\frac{\partial y}{\partial x} \tag{4.117}$$

The equation of motion may now be stated as

$$\frac{\partial^2 M}{\partial x^2} = p \tag{4.118}$$

where p is the resultant lateral force exerted on the pipe. This lateral force may be decomposed into three parts. The first part is due to the inertia forces and is given by $+ (m + m_1)\,\frac{\partial^2 y}{\partial t^2}$, where m is the mass of the pipe per unit of length, and m_1 the mass of the fluid contained within the pipe. The second part is due to Coriolis acceleration and is given by $+ 2m_1 U\,\frac{\partial^2 y}{\partial x \partial t}$, and finally, the third part, which is due to equivalent compressive force induced by the flux of momentum out of the pipe, and is given by $+ m_1 U^2 n\,\frac{\partial^2 y}{\partial x^2}$. Therefore, the equation of motion becomes

$$\frac{\partial^2 M}{\partial x^2} = (m+m_1)\,\frac{\partial^2 y}{\partial t^2} + 2m_1 U\,\frac{\partial^2 y}{\partial x \partial t} + m_1 U^2 n\,\frac{\partial^2 y}{\partial x^2} \tag{4.119}$$

and substitution from (4.115), (4.116), and (4.117) into (4.119) finally yields

$$EI\,\frac{\partial^4 y}{\partial x^4} + \eta I\,\frac{\partial^5 y}{\partial x^4 \partial t} + m_1 U^2 n\,\frac{\partial^2 y}{\partial x^2} + 2m_1 U\,\frac{\partial^2 y}{\partial x \partial t} + (m+m_1)\,\frac{\partial^2 y}{\partial t^2} = 0 \tag{4.120}$$

If we include also the effect of external damping in the form $K\frac{\partial y}{\partial t}$, where K is a constant, and introduce the following dimensionless quantities:

$$\xi = \frac{x}{L}, \qquad t = \tau\sqrt{\frac{(m+m_1)L^4}{EI}}, \qquad \frac{m_1}{m+m_1} = \beta',$$

$$\frac{m_1U^2nL^2}{EI} = F^2, \qquad \sqrt{\frac{\eta^2 I}{E(m+m_1)L^4}} = \delta', \qquad \sqrt{\frac{K^2L^4}{EI(m+m_1)}} = \gamma' \tag{4.121}$$

then we obtain

$$\frac{\partial^4 y}{\partial\xi^4} + \delta'\frac{\partial^5 y}{\partial\xi^4\partial\tau} + F^2\frac{\partial^2 y}{\partial\xi^2} + 2\sqrt{\frac{\beta'}{n}}F\frac{\partial^2 y}{\partial\xi\partial\tau} + \gamma'\frac{\partial y}{\partial\tau} + \frac{\partial^2 y}{\partial\tau^2} = 0 \tag{4.122}$$

To study the effect of small viscous damping forces and Coriolis forces, we now let

$$\delta' = \nu\delta, \qquad \gamma' = 2\nu\gamma, \quad \text{and} \quad \sqrt{\frac{\beta'}{n}} = \nu\beta \tag{4.123}$$

where ν is a small parameter. The equation of motion, (4.122), and the boundary conditions at $\xi = 0, 1$, may then be written as

$$\frac{\partial^4 y}{\partial\xi^4} + F^2\frac{\partial^2 y}{\partial\xi^2} + \frac{\partial^2 y}{\partial\tau^2} + \nu\left[\delta\frac{\partial^5 y}{\partial\xi^4\partial\tau} + 2\beta F\frac{\partial^2 y}{\partial\xi\partial\tau} + 2\gamma\frac{\partial y}{\partial\tau}\right] = 0$$

$$y = \frac{\partial y}{\partial\xi} = 0; \qquad \text{at} \quad \xi = 0 \tag{4.124}$$

$$\frac{\partial^2 y}{\partial\xi^2} = \frac{\partial^3 y}{\partial\xi^3} = 0; \quad \text{at} \quad \xi = 1$$

We wish to study the stability of system (4.124) when ν is sufficiently small.

We let $y = \psi(\xi)e^{i\omega\tau}$, and reduce (4.124) to the following boundary value problem

$$\frac{d^4\psi}{d\xi^4} + F^2\frac{d^2\psi}{d\xi^2} - \omega^2\psi + i\omega\nu\left[\delta\frac{d^4\psi}{d\xi^4} + 2\beta F\frac{d\psi}{d\xi} + 2\gamma\psi\right] = 0$$

$$\psi = \psi' = 0; \quad \text{at } \xi = 0 \tag{4.125}$$

$$\psi'' = \psi''' = 0; \quad \text{at } \xi = 1$$

where prime denotes differentiation with respect to ξ.

We then set $\psi = e^{\bar{\lambda}\xi}$; $\bar{\lambda} = \lambda + i\nu a$, and obtain

$$(\lambda+i\nu a)^4 + F^2(\lambda+i\nu a)^2 - \omega^2 + i\nu\omega\left[\delta(\lambda+i\nu a)^4 + 2\beta F(\lambda+i\nu a) + 2\gamma\right] = 0 \qquad (4.126)$$

which is the characteristic equation of system (4.125). Expanding (4.126) in a series of powers of ν, we are led to

$$\left\{\lambda^4 + F^2\lambda^2 - \omega^2\right\} + (i\nu)\left\{4a\lambda^3 + 2F^2\lambda a + \omega(\delta\lambda^4 + 2\beta F\lambda + 2\gamma)\right\} +$$
$$+ (i\nu)^2\left\{6a^2\lambda^2 + F^2a^2 + \omega(4\delta a\lambda^3 + 2\beta Fa)\right\} + (i\nu)^3\left\{4\lambda a^3 + 6\delta\omega a^2\lambda^2\right\} +$$
$$+ (i\nu)^4\left\{a^4 + 4\omega a^3\lambda\right\} + (i\nu)^5(\omega a^4) = 0 \qquad (4.127)$$

Next, we equate terms of like powers in ν, neglecting $0(\nu^2)$ and higher, and finally arrive at

$$\lambda^2 = -\frac{F^2}{2} \pm \sqrt{\left(\frac{F^2}{2}\right)^2 + \omega^2}$$

$$a = -\omega\,\frac{\delta\lambda^4 + 2\beta F\lambda + 2\gamma}{2\lambda(2\lambda^2 + F^2)}\,; \qquad \bar{\lambda} = \lambda + i\nu a \qquad (4.128)$$

The solution to system (4.125) may now be written as $\psi(\xi) = \sum_{j=1}^{4} A_j e^{\bar{\lambda}_j\xi}$, where A_j; $j = 1,2,3,4$, are constants which can be obtained from the boundary conditions at $\xi = 0,1$. That is, they must satisfy the following four linear, homogeneous equations:

$$\sum_{j=1}^{4} A_j = 0$$

$$\sum_{j=1}^{4} \bar{\lambda}_j A_j = 0$$

$$\sum_{j=1}^{4} \bar{\lambda}_j^2 A_j e^{\bar{\lambda}_j} = 0 \qquad (4.129)$$

$$\sum_{j=1}^{4} \bar{\lambda}_j^3 A_j e^{\bar{\lambda}_j} = 0$$

System (4.129) has non-trivial solutions if and only if the determinant of the coefficients is identically zero, i.e., the frequency equation is of the form (written out explicitly in [32])

$$\Delta_{\omega} \equiv \Delta\,(\bar{\lambda}_j) = 0 \tag{4.130}$$

This relation may be rewritten with the aid of (4.128) as follows, after expanding it in terms of powers of ν, and neglecting $0(\nu^2)$,

$$\begin{aligned}
\Delta \equiv\ & \left\{ F^4 + 2\omega^2 + 2\omega^2 \operatorname{ch}\lambda_1 \cos\lambda_3 + F^2\omega \operatorname{sh}\lambda_1 \sin\lambda_3 \right\} - \\
& - i\nu \left\{ \left(\frac{2\beta F\omega}{2\lambda_1^2+F^2}\right)\left[(\lambda_1^4 - \lambda_3^4) + (\lambda_3^3 - 3\lambda_1^2\lambda_3) \operatorname{ch}\lambda_1 \sin\lambda_3 + \right.\right. \\
& + (3\lambda_1\lambda_3^2 - \lambda_1^3) \operatorname{sh}\lambda_1 \cos\lambda_3\Big] + \left(\frac{\delta\lambda_1^4 + 2\gamma}{2\lambda_1(2\lambda_1^2+F^2)}\right)\Big[(\lambda_3^5 + 5\lambda_1^4\lambda_3) + \\
& + 6\lambda_1^2\lambda_3^3 \operatorname{ch}\lambda_1 \cos\lambda_3 - 4\lambda_1^3\lambda_3^2 \operatorname{sh}\lambda_1 \sin\lambda_3 + 2\lambda_1\lambda_3^4 \operatorname{sh}\lambda_1 \sin\lambda_3 + \\
& + 2\lambda_1^3\lambda_3^3 \operatorname{sh}\lambda_1 \cos\lambda_3 + \lambda_1^2\lambda_3^4 \operatorname{ch}\lambda_1 \sin\lambda_3 - \lambda_1^4\lambda_3^2 \operatorname{ch}\lambda_1 \sin\lambda_3\Big] + \\
& + \left(\frac{\delta\lambda_3^4 + 2\gamma}{2\lambda_3(2\lambda_1^2+F^2)}\right)\Big[(\lambda_1^5 + 5\lambda_1\lambda_3^4) + 6\lambda_1^3\lambda_3^2 \operatorname{ch}\lambda_1 \cos\lambda_3 + \\
& + 4\lambda_1^2\lambda_3^3 \operatorname{sh}\lambda_1 \sin\lambda_3 - 2\lambda_1^4\lambda_3 \operatorname{sh}\lambda_1 \sin\lambda_3 - 2\lambda_1^3\lambda_3^3 \operatorname{ch}\lambda_1 \sin\lambda_3 + \\
& \left. + \lambda_1^2\lambda_3^4 \operatorname{sh}\lambda_1 \cos\lambda_3 - \lambda_1^4\lambda_3^2 \operatorname{sh}\lambda_1 \cos\lambda_3\Big] \right\} = 0
\end{aligned} \tag{4.131}$$

where

$$\lambda_1^2 = -\frac{F^2}{2} + \sqrt{\left(\frac{F^2}{2}\right)^2 + \omega^2}\,, \qquad \lambda_3^2 = \frac{F^2}{2} + \sqrt{\left(\frac{F^2}{2}\right)^2 + \omega^2} \tag{4.132}$$

The first term in braces, in Eq. (4.131) is the frequency equation when $\nu = 0$, and the second term, to the first order of approximation in ν, indicates the effect of small viscous damping forces and Coriolis forces. For $\nu = 0$, we obtain the frequency equation of a purely elastic cantilevered beam subjected to a compressive force which stays tangent to the axis at the free end. The critical value of the load, in this case, is $F_e^2 = 20.05$, which was first computed by Beck [33].

For non-zero but sufficiently small values of ν and for small F, all the roots of equation (4.131) are located to the left of the imaginary axis in the complex $i\omega$ plane. As we increase F, at least one of these roots approaches the imaginary axis, and for a certain value of F, say F_d, Eq. (4.131) yields one purely imaginary root $i\omega = i\omega_c$. If we now increase F beyond this critical

value F_d, one of the roots of (4.131) becomes complex with negative imaginary part, and the system oscillates with an exponentially increasing amplitude. Therefore, for given values of δ, β and γ, we shall seek critical values of $\omega = \omega_c$ (real), and $F = F_d$ which identically satisfy (4.131). This is illustrated in Fig. 4.20 where, for $\delta = 1$, $\beta = 1$, and $\gamma = 0$, real (Δ_1) and imaginary ($-\Delta_2$) parts of Δ are plotted against the values of ω^2. Similar results may be obtained for other values of δ, β, and γ.

It may also be of interest to establish the destabilizing effect of Coriolis forces, internal viscous damping forces, and external viscous damping forces independently.

To this end, we let $\delta = \gamma = 0$, $\beta = 1$, and with $\gamma_d = \frac{F_d^2}{\pi^2}$ obtain, from Eq. (4.131), $\gamma_d = 1.78$. Similarly, for $\beta = \gamma = 0$ and $\delta = 1$, the critical load is obtained to be $\gamma_d = 1.107$. However, for $\beta = \delta = 0$ and $\gamma = 1$ we get $\gamma_d = 2.035$, which is equal to the critical load of the system when no velocity-dependent forces are present. That is, although sufficiently small Coriolis forces and internal viscous damping forces have a destabilizing effect in this continuous system, external viscous damping forces do not have the same effect.

The combined effect of velocity-dependent forces on the value of the critical parameter $\gamma_d = \frac{F_d^2}{\pi^2}$ is shown in Figs. 4.21 and 4.22. In these figures the parameter γ_d is plotted against β/δ for various values of γ. The horizontal dashed line in these figures represents the critical value of γ_d when no velocity-dependent forces exist and the cantilevered column is subjected to a compressive follower force at the free end (Beck's problem [33]).

It is important to note that the stability curves shown in Figs. 4.21 and 4.22 have a finite discontinuity at $\nu = 0$. That is, although for $\nu = 0$ we have $F^2 = F_e^2 = 20.05$, for $\nu = 0^+$, the critical value of F^2 is, in general, less than 20.05.

It may also be of interest to explore the order of magnitude of ν for which the destabilizing effect of velocity-dependent forces still exists. This may be accomplished by considering ν large and seeking values of ω and F for which Eq. (4.130) is identically satisfied. We note that, in Eq. (4.130), $\bar{\lambda}_j$; $j = 1,2,3,4$, are defined as functions of ω and the other parameters of the system through Eq. (4.126). In order to circumvent the difficulty of solving polynomials with complex coefficients, we let $\delta = \gamma = 0$ and put $\bar{\lambda} = i\eta$ in Eqs. (4.126) and (4.130).

The critical values of ω and F may now be evaluated by a computer. The computer may be instructed to obtain the roots of Eq. (4.126) for given parameters, and then calculate Δ, (Eq. (4.130)). These results are shown in Fig. 4.23, where $\gamma_d = \frac{F_d^2}{\pi^2}$ is plotted against values of $\sqrt{\frac{\beta'}{n}}$, by a solid line. The dashed line in this figure corresponds to the critical γ_d when the Galerkin method with a two-term approximation is employed for the analysis as follows.

We consider a set of orthonormal eigenfunctions, $\{\varphi_n(\xi)\}$, obtained by solving the following eigenvalue problem

$$\frac{d^4\varphi_n}{d\xi^4} - \omega_n^2\varphi_n = 0 \tag{4.133}$$

$$\varphi_n = \frac{d\varphi_n}{d\xi} = 0 \; ; \qquad \text{at} \quad \xi = 0 \tag{4.134}$$

$$\frac{d^2\varphi_n}{d\xi^2} = \frac{d^3\varphi_n}{d\xi^3} = 0 \; ; \qquad \text{at} \quad \xi = 1 \tag{4.135}$$

We then let $y = \sum_{n=1}^{\infty} q_n(\tau)\varphi_n(\xi)$, substitute it into the first equation in (4.124), multiply both sides of this equation by $\delta y = \sum_{m=1}^{\infty} \varphi_m(\xi)\delta q_m(\tau)$, and integrate the result from zero to 1 with respect to ξ to obtain

$$\frac{d^2q_n}{d\tau^2} + \sum_{m=1}^{\infty} (\omega_m^2\delta_{mn} + F^2 b_{mn})\, q_m +$$

$$+ \nu \sum_{m}^{\infty} (\delta\omega_m^2\delta_{mn} + 2\beta a_{mn} + 2\gamma\delta_{mn})\, q_m = 0, \qquad n = 1,2,\ldots,\infty \tag{4.136}$$

where

$$\varphi_m = \cosh \lambda_m\xi - \cos \lambda_m\xi - \sigma_m(\sinh \lambda_m\xi - \sin \lambda_m\xi)$$

$$\sigma_m = \frac{\sinh \lambda_m - \sin \lambda_m}{\cosh \lambda_m + \cos \lambda_m} \tag{4.137}$$

$$a_{mn} = \int_0^1 \frac{d\varphi_m}{d\xi}\,\varphi_n d\xi \tag{4.137}$$

$$\lambda_m^2 = \omega_m$$

$$b_{mn} = \int_0^1 \frac{d^2\varphi_m}{d\xi^2}\,\varphi_n d\xi$$

$$\delta_{mn} = \int_0^1 \varphi_m\varphi_n d\xi = \begin{cases} 1\ ; & \text{for } m = n \\ 0\ ; & \text{for } m \neq n \end{cases}$$

System (4.136) is a set of nonself-adjoint, linear, second order, homogeneous, ordinary differential equations which admit solutions of the form $q_m = A_m e^{i\omega\tau}$. To obtain the critical values of F^2, we seek conditions under which ω becomes complex with negative imaginary part. System (4.136), however, consists of infinite number of equations each with infinite number of terms. This, therefore, leads to a determinant which possesses an infinite number of rows and columns.

It is quite common to let $m,n = 1,2$ in Eqs. (4.136) and reduce this system to only two linear, homogeneous differential equations [8]. Hence, the characteristic equation becomes a polynomial of degree four, which can easily be solved. The values of F^2, which render at least one real root and all the other roots complex with positive imaginary parts, are then taken to be approximations to the critical flutter loads.

For sufficiently small values of ν, we may neglect terms associated with ν^2 in the characteristic equation, and using Routh-Hurwitz criteria, calculate approximate values of the critical load $F^2 = \gamma_d\pi^2$. In Table I these approximate flutter loads are compared with the exact values obtained in the previous section. From this table we observe that, for sufficiently small ν, the Galerkin method with a two-term approximation yields very accurate results. We note also that, for $\nu = 0$, this approximate method gives $F^2 = 20.15$ as compared with the exact critical load, $F^2 = 20.05$.

The above conclusion, however, does not imply that, for ν finite, the approximate method should necessarily give sufficiently accurate results. In fact, as is shown in Fig. 4.23 for $\delta = \gamma = 0$, the critical flutter load obtained by the approximate method (dashed line in Fig. 4.23) can be greatly in error for relatively large values of the Coriolis forces. We note that, for

$\sqrt{\frac{\beta'}{n}}$ smaller than 0.25, the resulting error, when the Galerkin method with a two-term approximation is used, is less than 5 percent and decreases as the value of ν decreases.

Among the other studies concerned with the destabilizing effects of velocity-dependent forces (and in particular linear viscous damping), mention should be made here of the papers by Leipholz [34] and Leonov and Zorii [35]. In Ref. [36] Bolotin and Zhinzher have used an expansion in fractional powers of the damping parameters and have established the conditions under which linear viscous damping has no effect on the critical load for flutter. By contrast, Zorii [37] was interested in determining the maximum effect which (small) linear viscous damping may have on the critical load.

4.6 Destabilizing Effects Due to Phenomena Other than Linear Viscosity

4.6.1 Thermoelastic and Hysteretic Damping

Not only linear viscous damping, but other types of dissipation mechanisms are associated with destabilizing effects. In Ref. [38] a general formulation of the stability analysis of elastic continuous systems subjected to follower forces in the presence of thermomechanical coupling was presented and applied to the problem of a cantilever under a tangential follower force at the free end. A pronounced destabilizing effect of thermoelastic dissipation was found to exist. Bilinear hysteretic damping was studied in Ref. [39] where it was shown that it may have a destabilizing effect similar to linear viscous damping, but that this effect disappears for a large class of hysteretic systems.

4.6.2 Magnetic Damping in a Discrete System

Damping in a system can be realized also through the interaction of a current carrying conductor with a magnetic field. Leibowitz and Ackerberg [40] have found that the motion of an electrically conducting, perfectly flexible wire placed in a transverse magnetic field will also be damped, but in a manner somewhat weaker than the familiar viscous damping.

It is of interest to examine the effect of such magnetic damping on the stability of equilibrium of some circulatory elastic systems, cf. Ref. [41], where additional details are given. A simple system with two degrees of freedom is considered first, and a destabilization is found to be caused by the magnetic field.

The system consists of two rigid weightless rods, each of length ℓ, carrying concentrated masses m and 2m and acted upon by a follower force P (Fig. 4.24). The rods OA and AB constitute portions of electrical circuits having resistances R_1 and R_2, respectively, and are constrained to undergo at most plane motion. A uniform magnetic field $\mathcal{B}_o$ acts in a direction perpendicular to the plane of possible motion.

A displacement from the equilibrium configuration ($\varphi_1 = \varphi_2 = 0$) will result in elastic restoring moments $c\varphi_1$ and $c(\varphi_2 - \varphi_1)$ at the hinges, and motion of the system in the magnetic field will induce a potential difference between any two points of the rods given by

$$\int \underset{\sim}{v} \times \mathcal{B}_o \cdot d\underset{\sim}{s} \tag{4.138}$$

where the integration is taken over the conducting path joining the points and $\underset{\sim}{v} = \underset{\sim}{v}(s)$ is the velocity of the conductor. The potential difference will result in the generation of a current, $\mathcal{I}$, according to

$$\mathcal{I} = \frac{1}{R}\int_o^{\ell} \underset{\sim}{v} \times \mathcal{B}_o \cdot d\underset{\sim}{s} \tag{4.139}$$

and therefore a force per unit length of conductor given by

$$\underset{\sim}{f} = \underset{\sim}{e} \times \mathcal{B}_o \tag{4.140}$$

where $\underset{\sim}{e}$ is a unit vector in the direction of the current. The force distribution (4.140) will of course be normal to the conductor and in a direction which opposes the motion.

For the system being considered the distributions f_1 and f_2 are

$$\begin{aligned} f_1 &= r_1\dot{\varphi}_1 \\ f_2 &= r_2(2\dot{\varphi}_1 + \dot{\varphi}_2) \end{aligned} \tag{4.141}$$

where

$$r_j = \mathcal{B}_o{}^2 \ell^2/2R_j \quad (j = 1,2) \tag{4.142}$$

and the dots indicate differentiation with respect to time t. Taking as generalized coordinates the (small) angles φ_1 and φ_2, the kinetic energy T and the generalized forces Q_1, Q_2 are found to be

$$\begin{aligned} T &= m\ell^2(3\dot{\varphi}_1{}^2 + 2\dot{\varphi}_1\dot{\varphi}_2 + \dot{\varphi}_2{}^2)/2 \\ Q_1 &= (P\ell - 2c)\varphi_1 - (P\ell - c)\varphi_2 - (r_1 + 4r_2)\ell^2\,\dot{\varphi}_1/2 \\ Q_2 &= c(\varphi_1 - \varphi_2) - r_2\ell^2(2\dot{\varphi}_1 + \dot{\varphi}_2)/2 \end{aligned} \tag{4.143}$$

These quantities are substituted into Lagrange's equations to obtain the linear equations of motion:

$$3m\ell^2\,\ddot{\varphi}_1 + (r_1+4r_2)\ell^2\,\dot{\varphi}_1/2 - (P\ell-2c)\varphi_1 + m\ell^2\,\ddot{\varphi}_2 + r_2\ell^2\,\dot{\varphi}_2 + (P\ell-c)\varphi_2 = 0$$

$$m\ell^2\,\ddot{\varphi}_1 + r_2\ell^2\,\dot{\varphi}_1 - c\varphi_1 + m\ell^2\,\ddot{\varphi}_2 + r_2\ell^2\,\dot{\varphi}_2/2 + c\varphi_2 = 0 \qquad (4.144)$$

The general solution of the system (4.144) is taken in the form

$$\varphi_j = \sum_{k=1}^{4} A_j^k\, e^{\omega_k t} \qquad (j = 1,2) \qquad (4.145)$$

and leads to the characteristic equation

$$q_o\omega^4 + q_1\omega^3 + q_2\omega^2 + q_3\omega + q_4 = 0 \qquad (4.146)$$

with the coefficients being given by

$$\begin{aligned} q_o &= 2m^2\ell^4/c^2 \\ q_1 &= (r_1+3r_2)m\ell^4/2c^2 \\ q_2 &= (7-2P\ell/c + r_1r_2\ell^2/4cm)\ell^2 m/c \\ q_3 &= (r_1+10r_2-3r_2P\ell/c)\ell^2/2c \\ q_4 &= 1 \end{aligned} \qquad (4.147)$$

Routh-Hurwitz criteria lead to the critical load

$$\hat{F}_{md} = 35/12 + \mu_1/6\mu_2 + \mu_2(1+\mu_1^2+3\mu_1\mu_2)4\mu_1 - \left\{\left[5/12 + \mu_1/6\mu_2 - \mu_2(1+\mu_1^2+3\mu_1\mu_2)/4\mu_1\right]^2 + (\mu_1+3\mu_2)^2/6\mu_1\mu_2\right\}^{1/2} \qquad (4.148)$$

where

$$F = P\ell/c$$

$$\mu_j = r_j \ell/(4cm)^{1/2} \qquad (j = 1,2) \tag{4.149}$$

A point of interest regarding (4.148) is that although $\hat{F}_{md} \to \infty$ as $\mu_1 \to \infty$ (i.e., the system can be made stable for arbitrarily large P), it remains finite for $\mu_1 \neq 0$ and $\mu_2 \to \infty$. In fact

$$\lim_{\mu_2 \to \infty} \hat{F}_{md} = \begin{cases} 10/3 & \text{if } \mu_1 \neq 0 \text{ is finite} \\ (10 + \lambda)/3 & \text{if } \mu_1 = \lambda\mu_2 \end{cases} \tag{4.150}$$

In the case of small damping, i.e., $\mu_j \ll 1$, $\hat{F}_{md}$ is written F_{md} and becomes

$$F_{md} = 35/12 + \varkappa/6 + 1/4\varkappa - \left[35/12 + \varkappa/6 + 1/4\varkappa)^2 - (4\varkappa + 1/\varkappa + 45)/6\right]^{1/2} \tag{4.151}$$

where

$$\varkappa = \mu_1/\mu_2$$

We note that the greatest destabilizing effect is realized as $\varkappa \to 0$. We further note that F_{md} is a monotone increasing function of $\varkappa$.

Comparison with the case of internal viscous damping (Eq. 4.14) reveals that $\overline{F}_d$ becomes unbounded as either B_1 or B_2 becomes large, provided the other parameter is non-zero. With magnetic damping, on the other hand, we have the result (4.150), and therefore magnetic damping can be said to be weaker than internal viscous damping. Furthermore, while it is possible to eliminate the destabilizing effect with a viscous damping coefficient ratio of 11.07, the critical load of the magnetically damped system is always smaller than $F_{e\ell}$.

It may be of interest to compare the effects of magnetic damping with those of linear external viscous damping. If in the double pendulum system of Fig. 4.24 external damping forces act which are proportional to the velocity with constants k_1 (along OA) and k_2 (along AB), then the damping force distributions are, for small angles, linear functions of distance along the rods (see Fig. 4.25). In this case, the equations of motion are

$$3m\ell^2 \ddot{\varphi}_1 + (k_1 + 3k_2)\dot{\varphi}_1\ell^3/3 - (P\ell - 2c)\varphi_1 + m\ell^2 \ddot{\varphi}_2 + k_2\dot{\varphi}_2\ell^3/2 + (P\ell - c)\varphi_2 = 0 \tag{4.153 cont.}$$

$$m\ell^2\,\ddot{\varphi}_1 + k_2\dot{\varphi}_1\ell^3/2 - c\varphi_1 + m\ell^2\,\ddot{\varphi}_2 + k_2\dot{\varphi}_2\ell^3/3 + c\varphi_2 = 0 \qquad (4.153)$$

A development parallel to that which led to Eq. (4.148) yields the following expression for the critical load parameter:

$$\hat{F}_{ev} = \left(L - \sqrt{L^2 + 4MN}\right)/N \qquad (4.154)$$

where

$$\begin{aligned} L &= 4(\eta_1 + 8\eta_2)(\eta_1 - 2\eta_2) + 5\eta_2(\eta_1 + 3\eta_2)(7 + 4\eta_1\eta_2 + 3\eta_2^2) \\ M &= 2(\eta_1 + 8\eta_2)^2 + (\eta_1 + 3\eta_2)^2 \\ &\quad - (\eta_1 + 8\eta_2)(\eta_1 + 3\eta_2)(7 + 4\eta_1\eta_2 + 3\eta_2^2) \\ N &= 10\eta_2(2\eta_1 + \eta_2) \end{aligned} \qquad (4.155)$$

and

$$\eta_j = k_j\ell^2/(36cm)^{1/2} \qquad (4.156)$$

Examination of (4.154) establishes the following results:

Just as in the two previous cases, the system can be made stable for arbitrarily large P by letting η_1 be arbitrarily large, i.e., as $\eta_1 \to \infty$ ($0 \neq \eta_2$ is finite) $\hat{F}_{ev} \to \infty$. The behavior of (4.154) as both η_1 and η_2 become large resembles that of $\hat{F}_{md}$ rather than $\hat{F}_{iv}$. In this case

$$\lim_{\eta_2 \to \infty} \hat{F}_{ev} = \begin{cases} 16/5 & \text{if } \eta_1 \text{ is finite} \\ (16 + 2\lambda)/5 & \text{if } \eta_1 = \lambda\eta_2 \end{cases} \qquad (4.157)$$

Thus the external viscous damping of the type being considered is also weaker than the internal damping. It is noted, however, that when both damping parameters become unbounded $\hat{F}_{md} < \hat{F}_{ev}$ for all $\lambda > 4$.

Another feature common to all three types of damping is that the critical load approaches the value 2 as $\mu_2(B_2, \eta_2)$ approaches zero, and this result is independent of $\mu_1(B_1, \eta_1)$. If, however, $\mu_1(B_1, \eta_1)$ approaches zero, both F_d and $\hat{F}_{iv}$ approach the value 1/3 (independently of μ_2, B_2) while the value of $\hat{F}_{ev}$ depends upon η_2:

$$\lim_{\eta_1 \to 0} \hat{F}_{ev} = 3(7 + 3\eta_2^2)/2 - 32/5 - \left\{ \left[3(7 + 3\eta_2^2)/2 - 32/5\right]^2 + 274/5 - 48(7 + 3\eta_2^2)/5\right\}^{1/2} \tag{4.158}$$

and

$$\lim_{\eta_2 \to 0} \left(\lim_{\eta_1 \to 0} \hat{F}_{ev}\right) = 2$$

$$\lim_{\eta_2 \to \infty} \left(\lim_{\eta_1 \to 0} \hat{F}_{ev}\right) = 16/5 \tag{4.159}$$

In the case of small damping, i.e., $\eta_j \ll 1$, (4.154) becomes

$$F_{ev} = [35(\varkappa + 3) + 4(\varkappa + 8)(\varkappa - 2)]/10(2\varkappa + 1) - \left\{ \left[7(\varkappa + 3)/2(2\varkappa + 1) + 2(\varkappa + 8)(\varkappa - 2)/5(2\varkappa + 1)\right]^2 - \left[8\varkappa^2 + 78\varkappa + 62\right]/5(2\varkappa + 1)\right\}^{1/2} \tag{4.160}$$

where

$$\varkappa = \eta_1/\eta_2 \tag{4.161}$$

This result differs markedly from the cases of internal viscous and magnetic damping in that F_{ev} does not depend upon $\varkappa$ but is equal to the constant value of 2. Therefore, the critical load parameter $\hat{F}_{ev}$ in the case of external viscous damping differs from the value of 2 at most by terms which are of second degree in η_j.

4.6.3 Magnetic Damping in a Continuous System

As a second example of the effect of magnetic damping, an elastic continuous cantilever acted upon by a follower force P will be considered (cf. Ref. [41]). According to the Bernoulli-Euler theory, the equation of motion which describes the system when EI is constant is

$$EI \frac{\partial^4 v}{\partial x^4} + P \frac{\partial^2 v}{\partial x^2} + \rho \frac{\partial^2 v}{\partial t^2} = w(x) \tag{4.162}$$

where EI is the flexural rigidity, ρ the lineal mass density, and w(x) is the force per unit length acting in the y-direction.

The displacement $v(x,t)$ must satisfy the boundary conditions

$$v(0,t) = \frac{\partial v}{\partial x}(0,t) = 0$$

$$\frac{\partial^2 v}{\partial x^2}(\ell,t) = \frac{\partial^3 v}{\partial x^3}(\ell,t) = 0 \tag{4.163}$$

Now, if the cantilever is a portion of an electrical circuit having resistance R and if the system undergoes motion in the presence of a uniform magnetic field $\mathcal{B}_o$ whose direction is normal to the x-y plane, then the induced current will provide the following damping force distribution:

$$w(x) = -\frac{\mathcal{B}_o^2}{R}\int_o^{\ell} \frac{\partial v}{\partial t}\, dx \tag{4.164}$$

With the substitution of (4.164) into (4.162) and the introduction of the dimensionless parameters

$$\xi = x/\ell$$

$$\tau = t(\rho\ell^4/EI)^{-1/2}$$

$$F = P\ell^2/EI \tag{4.165}$$

$$\nu = \mathcal{B}_o^2\ell^3/(\rho R^2 EI)^{1/2}$$

the equation of motion and boundary conditions appear as

$$\frac{\partial^4 v}{\partial \xi^4} + F\frac{\partial^2 v}{\partial \xi^2} + \nu\int_o^1 \frac{\partial v}{\partial \tau}\, d\xi + \frac{\partial^2 v}{\partial \tau^2} = 0$$

$$v = \frac{\partial v}{\partial \xi} = 0 \text{ at } \xi = 0 \tag{4.166}$$

$$\frac{\partial^2 v}{\partial \xi^2} = \frac{\partial^3 v}{\partial \xi^3} = 0 \text{ at } \xi = 1$$

In order to deduce stability criteria for this system, we consider modal solutions of (4.166), i.e., we set

$$v(\xi,\tau) = \Psi(\xi)e^{\Omega\tau} \tag{4.167}$$

Substitution of (4.167) into (4.166) results in the following boundary value problem for Ψ.

$$\frac{d^4\Psi}{d\xi^4} + F\frac{d^2\Psi}{d\xi^2} - \Omega^2(K-\Psi) = 0 \tag{4.168}$$

$$\Psi = \frac{d\Psi}{d\xi} = 0 \quad \text{at} \quad \xi = 0$$

$$\frac{d^2\Psi}{d\xi^2} = \frac{d^3\Psi}{d\xi^3} = 0 \quad \text{at} \quad \xi = 1 \tag{4.169}$$

where the functional K has been defined according to

$$\Omega\nu \int_0^1 \Psi d\xi = -\Omega^2 K \tag{4.170}$$

We proceed now in a purely formal manner to solve (4.168) subject to (4.169): The general solution of (4.168) is

$$\Psi = A_1 \sin \omega_1\xi + A_2 \cos \omega_1\xi + A_3 \sinh \omega_2\xi + A_4 \cosh \omega_2\xi + K \tag{4.171}$$

where

$$\begin{aligned} \omega_1^2 &= [(F^2 - 4\Omega^2)^{1/2} + F]/2 \\ \omega_2^2 &= [(F^2 - d\Omega^2)^{1/2} - F]/2 \end{aligned} \tag{4.172}$$

Substitution of the solution (4.171) into the boundary conditions leads to a system of four nonhomogeneous algebraic equations in the coefficients $A_j (j = 1,\ldots,4)$ whose solution is found to be

$$\begin{aligned} A_1 &= -K\omega_1^2\,\omega_2^3(\omega_1 \sin \omega_1 \cosh \omega_2 + \omega_2 \cos \omega_1 \sinh \omega_2)/\Delta \\ A_2 &= K\omega_1\,\omega_2^3(\omega_1\omega_2 \sin \omega_1 \sinh \omega_2 - \omega_1^2 \cos \omega_1 \cosh \omega_2 - \omega_2^2)/\Delta \\ A_3 &= K\omega_1^3\,\omega_2^2(\omega_1 \sin \omega_1 \cosh \omega_2 + \omega_2 \cos \omega_1 \sinh \omega_2)/\Delta \\ A_4 &= -K\omega_1^3\,\omega_2(\omega_1\omega_2 \sin \omega_1 \sinh \omega_2 + \omega_2^2 \cos \omega_1 \cosh \omega_2 + \omega_1^2)/\Delta \end{aligned} \tag{4.173}$$

where

$$\Delta = \omega_1\omega_2 \left[\omega_1^4 + \omega_2^4 + 2\omega_1^2\,\omega_2^2 \cos\omega_1 \cosh\omega_2 \right.$$

$$\left. + \omega_1\omega_2(\omega_1^2 - \omega_2^2)\sin\omega_1 \sinh\omega_2\right] \qquad (4.174)$$

The fact that the above solution is given in terms of the unknown functional $K(\Psi)$ is not a severe deficiency since primary interest in the present context is focused on the nature of the complex frequencies Ω. As long as the real part of Ω is negative, the rod will be asymptotically stable, i.e., will oscillate with exponentially decreasing amplitude. The characteristic equation, by which the nature of Ω may be examined, is obtained by requiring that (4.171) satisfy (4.170) nontrivially, the A_j being given by (4.173). This requirement leads to the following transcendental equation for Ω:

$$\Delta\Omega = \nu\left[\omega_1\omega_2^4(1-\cos\omega_1)\sinh\omega_2 - \omega_1^2\,\omega_2^3 \sin\omega_1 \cosh\omega_2\right.$$

$$- \omega_1^3\,\omega_2^2 \cos\omega_1 \sinh\omega_2 + \omega_1^4\,\omega_2 \sin\omega_1(1-\cosh\omega_2)$$

$$\left. - \omega_1^5 \sinh\omega_2 - \omega_2^5 \sin\omega_1\right] = \nu\Delta_2 \qquad (4.175)$$

For small values of F and for positive damping ($\nu > 0$), all the roots of (4.175) are located in the left half of the complex plane. As F is increased, one of the roots approaches the imaginary axis and subsequently takes on a positive real part. When this occurs then, by virtue of (4.167), oscillations with exponentially increasing amplitude will result. The value of F beyond which Ω has a positive real part will be designated as F_{md}. As $F \to F_{md}$, there must be one imaginary root of (4.175), and since ω_1, ω_2 are real whenever Ω is imaginary, both sides of (4.175) must approach zero simultaneously.

The critical load is found numerically to be $F_{md} = 12.84$, and the result is independent of the magnitude of the magnetic damping (provided it is nonzero). Comparing this value with the critical load in the absence of a magnetic field, $F_{e\ell} = 20.05$, we find that the magnetic damping has a destabilizing effect of 36 percent.

4.6.4 Retarded Follower Force

The system with two degrees of freedom discussed in Sect. 3.1 was subjected in Ref. [42] to a retarded follower force. It is remarkable that a destabilizing effect is associated also with retardation of a follower force with constant time lag τ, which was specified as

$$\theta(t) = \varphi_2(t-\tau) \qquad (4.176)$$

The linearized equations for small motions about the position of static equilibrium ($\varphi_1 = \varphi_2 = 0$) are

$$\begin{aligned} 3m\ell^2\,\ddot{\varphi}_1 + m\ell^2\,\ddot{\varphi}_2 + (2c-P\ell)\varphi_1 - c\varphi_2 + P\ell\theta = 0 \\ m\ell^2\,\ddot{\varphi}_1 + m\ell^2\,\ddot{\varphi}_2 - c\varphi_1 + (c-P\ell)\varphi_2 + P\ell\theta = 0 \end{aligned} \tag{4.177}$$

Solutions are sought again in the form (4.4) and lead to the frequency equation

$$\begin{vmatrix} 3m\ell^2\omega^2 + 2c - P\ell & m\ell^2\omega^2 - c + P\ell e^{-\omega\tau} \\ m\ell^2\omega^2 - c & m\ell^2\omega^2 + c - P\ell + P\ell e^{-\omega\tau} \end{vmatrix} = 0 \tag{4.178}$$

The presence of exponential terms suggests the application of Pontryagin's stability criteria rather than those of Routh-Hurwitz. After a comprehensive and rather elaborate analysis we arrive to the important result that a very small (vanishing) time lag renders the system unstable for all positive (compressive) values of the applied force P. Even under the most favorable time lag the critical load was found to be $F = P\ell/c = 0.177$, as compared to $F = 2.086$ for the same system without any retardation τ.

In supplementing the analysis of Ref. [42], it may be remarked here that for small time lag the stability investigation can be readily carried out employing the simpler Routh-Hurwitz criteria. If $\varphi_2(t-\tau)$ is expanded into a Taylor series about $\varphi_2(t)$ (see Ref. [18]) and if only the first two terms are retained, the equations of motion simplify to:

$$\begin{aligned} 3m\ell^2\,\ddot{\varphi}_1 + m\ell^2\,\ddot{\varphi}_2 + (2c-P\ell)\varphi_1 - c\varphi_2 + P\ell\varphi_2 - P\ell\tau\dot{\varphi}_2 = 0 \\ m\ell^2\,\ddot{\varphi}_1 + m\ell^2\,\ddot{\varphi}_2 - c\varphi_1 + (c-P\ell)\varphi_2 + P\ell\varphi_2 - P\ell\tau\dot{\varphi}_2 = 0 \end{aligned} \tag{4.179}$$

and lead to the frequency equation of the form

$$p_o\Omega^4 + p_1\Omega^3 + p_2\Omega^2 + p_3\Omega + p_4 = 0 \tag{4.180}$$

with

$$\begin{aligned} p_o &= 2; & p_1 &= -2FT; \\ p_2 &= 7 - 2F; & p_3 &= FT(F-3); & p_4 &= 1 \end{aligned} \tag{4.181}$$

where

$$\Omega^2 = m\ell^2\omega^2/c; \qquad F = P\ell/c;$$
$$T = \tau\omega/\Omega = \tau\sqrt{c}/\ell\sqrt{m} \tag{4.182}$$

One of the Routh-Hurwitz conditions for asymptotic stability is that p_o and p_1 be of the same sign which results in the critical value of $F_{cr} = 0$, that is for $F < 0$ the system is asymptotically stable and for $F > 0$ it is unstable, verifying thus the result of Ref. [42]. The remaining Routh-Hurwitz conditions do not supply more stringent requirements of F. It is noteworthy that F_{cr} does not depend on the value of T. The conclusion is reached that in the presence of even the slightest lag the system is unstable under a compressive follower force. Further, the Taylor series expansion introduced above clearly exhibits that small time lag is associated with the introduction of terms of odd power in the frequency equation, having this in common with linear viscous damping.

The destabilizing effect is in general introduced by any sufficiently small, velocity-dependent forces, such as, for example, Coriolis forces. Some types of such forces are realized by fluid jets; they have received considerable attention and have been referred to as "jet damping," [43]. Others are produced, e.g., by flow through pipes [44].

4.7 Uncertainties

The foregoing examples of various destabilizing effects amply illustrate the necessity of a firmer grasp of certain aspects in the analysis of stability problems as applied to systems subjected to follower forces, cf. [45]. What is needed in particular is additional insight into the experimental determination of system parameters, cf. Sect. 8.2. If very small, even vanishing quantities which induce a destabilizing effect have such a decisive influence on the critical loads calculated analytically, how should these quantities be measured with required accuracy? Further, how can one be sure that the "correct" or "right"parameters have been included? It is even conceivable that (vanishing) destabilizing effects exist which have never been thought of as yet, and which have perhaps an even stronger influence on the stability boundaries of a given system than any of those mentioned. Below some attempts are described to remedy this obviously unsatisfactory state of affairs.

If we are dealing with a man-made system, it would probably be desirable, if possible, to make it well-behaved by means of a suitable choice of system parameters and, in particular, by making it strongly asymptotically stable to begin with. This is done sometimes in control systems where the "doubtful," "critical" or "marginal" case of Liapunov (pure imaginary roots of the characteristic equation) is interpreted as describing an inherently unstable system. It is well known that if a system is asymptotically stable, small "destabilizing" quantities will have but a small effect on the critical loads; this effect will vanish with the vanishing of the "destabilizing" quantity.

In many man-made systems and in given natural systems the uncertainty cannot be circumvented in this manner. It may then be suggested that the analysis of stability be replaced (or supplemented) by an analysis of "patterns of behavior" of the disturbed system for various ranges of the controlling parameter (force). Since we are interested here only in oscillatory response to a disturbance, three types of behavior are qualitatively sketched in Fig. 4.26. Let it be our aim to classify the response in just two categories. Depending upon the specific performance requirements of the system at hand, it may be meaningful to place the response in Figs. 4.26a and 4.26b into one category and the response in Fig. 4.26c into the other. In the first category the disturbance remains small during a certain interval of time, while growing fairly large in the second category during the same interval.

As a measure of the rate of growth of the oscillations it is convenient to introduce the largest real part α of the relevant root of the characteristic equation. This is analogous to the introduction of the smallest negative part as the "absolute stability margin" [18].

The stability analysis corresponding to a given $\alpha > 0$ can be carried out by introducing the transformation (Fig. 4.27)

$$\Omega = \rho + \alpha \tag{4.183}$$

into the characteristic equation, e.g.,

$$p_o\Omega^4 + p_1\Omega^3 + p_2\Omega^2 + p_3\Omega + p_4 = 0$$

which yields the modified characteristic equation for ρ

$$a_o\rho^4 + a_1\rho^3 + a_2\rho^2 + a_3\rho + a_4 = 0 \tag{4.184}$$

where

$$a_o = p_o; \quad a_1 = p_1 + 4\alpha p_o; \quad a_2 = p_2 + 3\alpha p_1 + 6\alpha^2 p_o \tag{4.185}$$

$$a_3 = p_3 + 2\alpha p_2 + 3\alpha^2 p_1 + 4\alpha^3 p_o; \quad a_4 = p_4 + \alpha p_3 + \alpha^2 p_2 + \alpha^3 p_1 + \alpha^4 p_o$$

Applying the usual Routh-Hurwitz criteria to this modified equation, the critical force can be calculated. For the system of Fig. 4.1 the critical force F_c is to be calculated from

$$x \equiv a_1a_2a_3 - a_oa_3^2 - a_1^2a_4 \tag{4.186}$$

and is found to be

$$F_c = \left(B \overset{(+)}{-} \sqrt{B^2 - AC}\right)/A \tag{4.187}$$

where

$$A = 8\alpha(d_1 - 2\alpha d_o)$$

$$B = d_1 d_3 + 2\alpha d_1 d_2 - 4\alpha d_o d_3 - \alpha^2 d_1^2 \qquad (4.188)$$

$$C = d_1 d_2 d_3 - d_o d_3^2 - d_1^2 d_4$$

and

$$d_o = p_o; \quad d_1 = p_1 + 4\alpha p_o; \quad d_2 = 7 + B_1 B_2 + 3\alpha p_1 + 6\alpha^2 p_o$$

$$d_3 = p_3 + 2\alpha(7 + B_1 B_2) + 3\alpha^2 p_1 + 4\alpha^3 p_o \qquad (4.189)$$

$$d_4 = p_4 + \alpha p_3 + \alpha^2(7 + B_1 B_2) + \alpha^3 p_1 + \alpha^4 p_o$$

The results of the numerical calculations are displayed in Fig. 4.28. Thin solid lines represent the critical force F_c as function of the growth parameter α for given damping coefficients B_i. The thin curves in Fig. 4.28 are the same as those in Fig. 4.5, but they have been calculated in a different manner and their interpretation is also entirely different.

The critical force as defined with the aid of the growth parameter α is not entirely satisfactory because it does not separate the different types of behavior illustrated in Fig. 4.26. We seek now to define what we may call a "transition" force F_t below which α (whether positive or negative) would be relatively small and above which it would be relatively large. It appears to be reasonable to define the transition force F_t as the force for which the absolute value of the curvature of a given curve $F(\alpha) = 0$ attains a maximum. Corresponding calculations have been carried out and the values of the transition force F_t for various values of the damping coefficients have been joined by a thick solid line in Fig. 4.28. It is noted that for given damping coefficients B_i there exists an associated transition force F_t which in turn corresponds to a certain particular value of growth parameter α_t. The experimental determination of system parameters associated with F_t appears to be feasible. It should be also observed that as damping decreases F_t approaches F_e, while F_t approaches F_d as damping increases. The relationship between critical and transition forces is thus clarified.

It is rather evident that the two types of system behavior which are separated by F_t can be less or more different and thus it may be appropriate to introduce the notion of degree of separation σ associated with any particular value of F_t. This additional characteristic separating "patterns of

behavior" could be made to depend on the magnitudes of curvature and slope of the function $F(\alpha)$ at α_t.

The parameter α can be employed yet for another, purely mathematical purpose. For small α, B_1 and B_2 Eq. (4.186) may be written in the form

$$[\alpha^2 + \alpha(B_1+6B_2)/4](F-F_{e1})(F-F_{e2}) - (B_1+B_2)(B_1+6B_2)(F-F_d) = 0 \quad (4.190)$$

Here F_{e1} and F_{e2} are the critical loads obtained in the absence of damping, while F_d is the critical load for vanishing damping. It is observed that either critical load may be obtained by a limiting process in Eq. (4.190), which gives either α, F, B_1 or B_2 in terms of the remaining three quantities. If the growth parameter $\alpha \to 0$, it is seen that $F \to F_d$, which depends only on $\beta = B_1/B_2$ but not on B_1 and B_2 itself. By contrast, if the damping coefficients are made to vanish first, then $F \to F_{e1}$ or $F \to F_{e2}$, regardless of the value of the (small) value of α. Thus the introduction of the growth parameter α permits to approach the critical load for no damping F_{e1} even in the presence of vanishing damping, removing mathematically any destabilizing effects.

CHAPTER V

CONTINUOUS SYSTEMS

5.1 Introduction

In the preceding chapter one aspect of problems of continua was not elaborated upon, namely, that stability must necessarily be defined with respect to a metric (sometimes implied) which measures distance in an infinite-dimensional space. One has to define what is meant by "nearness" to the equilibrium configuration whose stability is being examined. This metric may be postulated in various suitable forms, depending upon the physical aspects and the requirements of the specific problem at hand. The equations of the boundary value problem of a continuum, together with an explicitly defined metric ρ form a functional metric space whose fundamental properties depend strongly on ρ and thus lead to different results of a stability analysis.

With reference to a conservative system, Koiter [46,47] has pointed out that a conventional generalization of Liapunov's definition of stability, which requires that the displacements and the velocities remain arbitrarily small at each point and for all positive time, provided the initial disturbances are sufficiently small, can hardly be considered satisfactory. A modified concept of stability was suggested which reduces to Liapunov's definition for the case of a discrete system.

In this Chapter, following the development of Ref. [48], a sufficient condition for the stability of a linearly viscoelastic continuum subjected to surface tractions which follow partially the deformation of the solid is established with respect to an average metric.

5.2 Definitions of Stability

We consider a finite isotropic, homogeneous, linearly viscoelastic solid, bounded by a regular surface S, contained in a volume V. At the time $t = 0$, the solid is in a state of initial stress σ_{ij}: $i,j = 1,2,3$, caused by a system of partial follower surface tractions p_i, applied at the boundary S. We shall refer to the state of initial stress of the solid as unperturbed (equilibrium) state and study its possible motions with reference to this state. Furthermore, we shall assume that the quantities describing the perturbed state are small (these quantities will, subsequently, be indicated by a bar) so that all terms of order higher than the second may be neglected. The equations of motion of the perturbed solid, referred to a fixed orthogonal Cartesian coordinate system, are [8]

$$\bar{\sigma}_{ij,j} + (\sigma_{jk}\bar{u}_{i,k})_{,j} - m\ddot{\bar{u}}_i = 0 \quad \text{in V}, \qquad \bar{\sigma}_{ij}n_j + \sigma_{jk}\bar{u}_{i,k}n_j = \tilde{p}_i \quad \text{on S}, \qquad (5.1)$$

$$i,j,k = 1,2,3$$

where m is the mass density, x_j are the coordinates, $\bar{u}_i$ the displacement components measured from the unperturbed state, n_j the components of the unit normal to S, $\tilde{p}_i$ the perturbations of the applied surface tractions. In these equations and in the sequel the repeated indices are summed over the range of their definition. A comma followed by indices k, j indicates differentiation with respect to x_j, x_k, and dots denote derivatives with respect to time. We shall assume here that

$$\tilde{p}_i = \alpha(\vec{x}) p_j \bar{u}_{i,j} \quad \text{on} \quad S \tag{5.2}$$

where $\alpha(\vec{x}) \equiv \alpha(x_1, x_2, x_3)$ is a parameter which serves to describe the manner in which the surface tractions follow the deformation. If $\alpha \equiv 0$ the system is conservative and for $\alpha \equiv 1$ we have the case of follower force introduced in [8]. The constitutive equations shall be taken in the form

$$\begin{aligned} &\bar{\sigma}_{ij} = C_{ijk\ell} \bar{u}_{(\ell,k)} + C'_{(ijk\ell)} \dot{\bar{u}}_{(\ell,k)}; \quad u_{(k,\ell)} = \tfrac{1}{2}(u_{k,\ell} + u_{\ell,k}) \\ &C_{ijk\ell} = \lambda \delta_{ij} \delta_{k\ell} + 2\mu \delta_{ik} \delta_{j\ell} \\ &C'_{ijk\ell} = \lambda' \delta_{ij} \delta_{k\ell} + 2\mu' \delta_{ik} \delta_{j\ell} \end{aligned} \tag{5.3}$$

where δ_{ij} is the Kronecker delta, λ and μ are Lamé constants, and λ' and μ' are viscous constants corresponding to Lamé constants.

A general solution to the nonself-adjoint mixed initial and boundary value problem (5.1) cannot, in general, be easily obtained. Therefore, in order to study the stability of this system, we have to resort to some other means and, consequently, we shall not expect to gain as much information concerning stability as we would if we were to construct and evaluate a general solution of the system. As we shall see, this is by no means a shortcoming. A strong stability criterion, that may be imposed on the system and which could be applied if we were to solve system (5.1) completely, would be of doubtful interest.

In this connection, we shall consider a certain functional (which, in effect, expresses the energy of the system) and explore the stability of (5.1) in some appropriate average sense. Furthermore, we shall show that the usual Galerkin method, which reduces the system of partial differential equations (5.1) to a set of ordinary differential equations, yields the same results as those obtained by a study of the functional mentioned, provided all the series expansions employed converge in an average sense.

To this end, we consider a complete set of normalized eigenvectors, obtained by solving the homogeneous, self-adjoint system deduced from (5.1) by setting $\sigma_{ij} = C'_{ijk\ell} = \tilde{p}_i = 0$, which has the same geometrical boundary

conditions as the original problem. Let this set of orthonormal eigenvectors be denoted by $\{\varphi_{in}(\vec{x})\}$; $i = 1,2,3$, $n = 1,2,\ldots,\infty$. We shall reduce our original system of partial to a system of ordinary differential equations by expanding $\bar{u}_i$ and its derivatives in terms of these eigenvectors, without any attempt to resolve the question of convergence. However, some comparison between the results obtained by applying this method to some simple problems and the exact solutions [8] certainly suggests that convergence may be assumed.* In our problem, we shall therefore state that if convergence exists (in an average sense at least) then the two methods yield identical results.

Let us now consider the fundamental question concerning stability of a solid, and review first the definitions of stability for a discrete system, mentioned in the Introduction.

We examine a system with r degrees of freedom described by generalized coordinates q_n and generalized velocities $\dot{q}_n$; $n = 1,2,\ldots,r$. For a holonomic and autonomous system, we write the equations of motion as

$$\dot{z}_n = f_n(z_1,z_2\ldots,z_{2r}); \quad n = 1,2,\ldots,2r \tag{5.4}$$

where

$$z_n = q_n$$

$$z_{r+n} = \dot{q}_n; \quad n = 1,2,\ldots,r$$

and $f_n(\vec{z})$ are bounded, continuous, real functions vanishing for $z_n = 0$. We assume f_n satisfy all the conditions required for the existence of a single-valued solution for $t > 0$ in the region of the definition of z_n. Furthermore, we represent the state of this dynamic system by a point in a 2r-dimensional Euclidean space, E_{2r}, with coordinates z_n; $n = 1,2,\ldots,2r$. The equilibrium state of the system at the origin is said to be stable if for any $\epsilon > 0$ we can find a $\delta > 0$ depending on ϵ only such that when $\sum_{n=1}^{2r} z_n^2 < \delta$ at $t = 0$, we have $\sum_{n=1}^{2r} z_n^2 < \epsilon$ for all $t > 0$. In the opposite case $z_n = 0$ is called unstable [14]. Furthermore, $z_n = 0$ is called asymptotically stable if it is stable and $\lim_{t \to \infty} \left[\sum_{n=1}^{2r} z_n^2 \right] = 0$.

---

* The paradox in the problem of flutter of a membrane, as was shown in [8], is not related to the fact that the system is nonself-adjoint.

The above definitions of stability are due to Liapunov [11,14]. He also supplied the proofs of necessity and sufficiency, employing the notion of distance in the finite-dimensional Euclidean space E_{2r}.

For systems with an infinite number of degrees of freedom (continuous systems) the notion of distance in an infinite dimensional space needs to be introduced, if one wishes to extend Liapunov's concepts to such systems. In this case, we have to be concerned with functionals rather than functions and must explicitly define a measure (metric ρ) of distance of two states of the system and then study the stability of the system with respect to this metric ρ. The metric ρ may be selected in any suitable manner (provided it satisfies three fundamental conditions [49] so as to fulfill some physical requirements of the problem at hand. It may be desirable, for example, to limit the displacements and the velocities at each point of the solid, in which case we define

$$\rho_1 = \bar{u}_i \bar{u}_i + \dot{\bar{u}}_i \dot{\bar{u}}_i \quad \text{everywhere in V and on S}$$

In some other cases, we may wish to restrict the strains as well as the displacements and the velocities at each point of the solid, such that

$$\rho_2 = \bar{u}_i \bar{u}_i + \dot{\bar{u}}_i \dot{\bar{u}}_i + \bar{u}_{i,j} \bar{u}_{i,j} \quad \text{everywhere in V and on S}$$

For most practical problems, however, it is usually preferable to define ρ in an average sense; for example,

$$\rho_3 = \int_V \left[\dot{\bar{u}}_i \dot{\bar{u}}_i + \bar{u}_{i,j} \bar{u}_{i,j} + \bar{u}_i \bar{u}_i \right] dv$$

We now state the definition of the stability of the initial state of a solid with respect to an explicitly defined metric ρ, by appropriately extending the corresponding definition for a finite system.

The initial state of the continuous solid is said to be stable if for a given $\epsilon > 0$ we can find a $\delta > 0$ depending on ϵ only such that when $\rho < \delta$ at $t = 0$ we have $\rho < \epsilon$ for all $t > 0$. In the opposite case, the initial state is called unstable. Furthermore, the unperturbed state is called asymptotically stable if it is stable and $\lim_{t \to \infty} \rho = 0$. The sufficiency theorem of stability may now be stated as follows:

Theorem. In order that the unperturbed state of system (5.1) be stable with respect to a metric ρ, it is sufficient that there exists, by virtue of the requirements of the boundary value problem (5.1), a finite, nonincreasing functional which is identically equal to zero for $\rho = 0$ and admits an infinitely small upper bound with respect to the metric ρ.

This theorem is an appropriate version of the theorem of stability given by Movchan [50]. In the sequel we shall use this theorem to establish a sufficiency criterion for the stability of system (5.1). But let us first discuss some aspects of the definition of stability.

It is seen that the stability criteria are highly dependent upon the specification of the metric ρ. We may not, therefore, expect to apply a criterion obtained, say, for ρ_3 to ρ_2 and get like results. The problem which was treated by Shield and Green [51] may exemplify this very point. An isotropic, homogeneous, linearly elastic sphere was perturbed by radially symmetric applied infinitesimal disturbances at $t = 0$ and it was shown that the strain at the center of the sphere can become finite for some $t > 0$. Let us show that although this system is unstable with respect to the metric ρ_2, it is stable with respect to ρ_3. To this end consider the following functional

$$H_1 = \frac{1}{2}\left[\int_V (m\dot{\bar{u}}_i\dot{\bar{u}}_i + C_{ijk\ell}\bar{u}_{i,j}\bar{u}_{k,\ell})\, dv\right]$$

whose time derivative is zero by virtue of the equation of motion, and which admits an infinitesimal upper bound with respect to the metric ρ_3. From the inequalities [52]

$$C_1 \int_V \bar{u}_i\bar{u}_i dv \le \int_V \bar{u}_{i,j}\bar{u}_{i,j} dv$$

$$C_2 \int_V \bar{u}_{i,j}\bar{u}_{i,j} dv \le \int_V C_{ijk\ell}\bar{u}_{i,j}\bar{u}_{k,\ell} dv$$

which are valid for all admissible motions of the solid, with C_1 and C_2 being fixed positive constants independent of $\bar{u}_i$, we immediately construct the inequality

$$H_1 \ge K\rho_3 \quad \text{for all } t \ge 0$$

where K is also a fixed positive number not dependent on $\bar{u}_i$. We let $H_1 < K\epsilon$ and obtain $\rho_3 < \epsilon$ at $t = 0$. But H_1 is a nonincreasing function of time. Therefore $K\epsilon$ is an upper bound of H_1 for all $t \ge 0$, which implies

$$\rho_3 < \epsilon \quad \text{for all } t \ge 0$$

In [51], the initial disturbances were taken to be

$$u = \frac{u}{r} = \frac{\partial u}{\partial r} = 0, \qquad \dot{u} = \frac{2c}{r}\left[\frac{1}{r} f'(r) - f''(r)\right] \qquad \text{at } t = 0$$

where r measures distances from the center of the sphere, $c = \frac{\lambda + 2\mu}{m}$, and f(r) is given by

$$f(r) = 0 \qquad 0 \le r \le a$$

$$f(r) = \frac{1}{\epsilon^5 a^5}(r-a)^4(r-a-2\epsilon a) \qquad a \le r \le a + 2\epsilon a$$

$$f(r) = 0 \qquad a + 2\epsilon a \le r$$

A simple calculation shows that $\rho_3 = 0(\epsilon)$ at $t = 0$. Furthermore, at $t = a/c$ we have, for $0 \le r \le 2\epsilon a$,

$$u = \frac{1}{\epsilon^5 a^5} r^2 (2\epsilon a - r)^3 (7r - 6\epsilon a)$$

which immediately yields $\rho_3 = 0(\epsilon)$ at $t = a/c$, while the strain at the center of the sphere at this instant is finite:

$$\left[\frac{u}{r}\right]_{r=\epsilon a} = 1, \qquad \left[\frac{\partial u}{\partial r}\right]_{r=\epsilon a} = 6$$

In this example, one is able to obtain an exact solution to the differential equations of the boundary value problem. Therefore, one is in the position of requiring as strong a stability criterion as one pleases. We see that the system is not stable with respect to ρ_2, although it is stable with respect to ρ_3. The important point to note in this connection is that the stability with respect to the metric ρ_3 could have been deduced without possessing an explicit solution of the problem.

In most practical problems, the system may well be stable for all practical purposes, while it may not satisfy the pointwise stability conditions with respect to the metrics ρ_1 and ρ_2. In those cases there may exist a finite number of points in V where an infinitesimal perturbation at $t = 0$ may cause finite, say, strains at these points for some $t > 0$. If the collection of these points forms a set with measure zero, then the stability may exist with respect to the metric ρ_3.

The metric ρ_3 seems to be more appealing also from a purely mathematical point of view. In this regard, let us note that the series expansion of a piecewise continuous function in a finite domain is an approximation in a mean square sense and not a pointwise representation. The following discussion will, therefore, be devoted to the stability of system (5.1) with respect to the metric ρ_3.

5.3 Analysis of Stability

We consider a functional H given by

$$H = \frac{1}{2}\left\{\int_V [m\dot{\bar{u}}_i\dot{\bar{u}}_i + C_{ijk\ell}\bar{u}_{i,j}\bar{u}_{k,\ell} + (1-\alpha)\sigma_{jk}\bar{u}_{i,k}\bar{u}_{i,j}]\, dv \right.$$
$$\left. + 2\int\int_V [C'_{ijk\ell}\dot{\bar{u}}_{i,j}\dot{\bar{u}}_{k,\ell} - \sigma_{jk}(\alpha\bar{u}_{i,j})_{,k}\dot{\bar{u}}_i]\, dv\, dt\right\} \qquad (5.5)$$

and note that, from the requirements of the boundary value problem (5.1), H is

a continuous functional which vanishes identically at the initial unperturbed state of the solid, $\rho_3 = 0$. The total time derivative of H is

$$\frac{dH}{dt} = \int_V [m\ddot{\bar{u}}_i\dot{\bar{u}}_i + C_{ijk\ell}\dot{\bar{u}}_{i,j}\bar{u}_{k,\ell} + (1-\alpha)\sigma_{jk}\bar{u}_{i,k}\dot{\bar{u}}_{i,j}$$

$$+ C'_{ijk\ell}\dot{\bar{u}}_{i,j}\dot{\bar{u}}_{k,\ell} - \sigma_{jk}(\alpha\bar{u}_{i,j})_{,k}\dot{\bar{u}}_i]\,dv \qquad (5.6)$$

But we have

$$\int_V [C_{ijk\ell}\bar{u}_{k,\ell} + C'_{ijk\ell}\dot{\bar{u}}_{k,\ell}]\,\dot{\bar{u}}_{i,j}dv = \int_S \bar{\sigma}_{ij}n_j\dot{\bar{u}}_i dS - \int_V \bar{\sigma}_{ij,j}\dot{\bar{u}}_i dv$$

and

$$\int_V \left\{(1-\alpha)\sigma_{jk}\bar{u}_{i,k}\dot{\bar{u}}_{i,j} - \sigma_{jk}(\alpha\bar{u}_{i,j})_{,k}\dot{\bar{u}}_i\right\} dv = -\int_V [\sigma_{jk}\bar{u}_{i,k}]_{,j}\dot{\bar{u}}_i dv$$

$$+ \int_S [\sigma_{jk}\bar{u}_{i,k}n_j - \alpha p_k\bar{u}_{i,k}]\,\dot{\bar{u}}_i dS$$

where in the last reduction we have used the fact that for the unperturbed state we have

$$\sigma_{ij,j} = 0 \quad \text{in} \quad V \qquad \text{and} \qquad \sigma_{jk}n_k = p_j \quad \text{on} \quad S$$

Equation (5.5) now becomes

$$\frac{dH}{dt} = \int_V \left\{m\ddot{\bar{u}}_i - \bar{\sigma}_{ij,j} - (\sigma_{jk}\bar{u}_{i,k})_{,j}\right\}\dot{\bar{u}}_i dv + \int_S [\bar{\sigma}_{ij}n_j + \sigma_{jk}\bar{u}_{i,k}n_j$$

$$- \alpha p_j\bar{u}_{i,j}]\,\dot{\bar{u}}_i dS \qquad (5.7)$$

which is identically equal to zero by virtue of Eqs. (5.1) for all actual perturbed motions of the solid. Moreover, if H is a positive definite functional, then it admits an infinitely small upper bound with respect to ρ_3. To show this we let $|\bar{u}_i| < \sqrt{\epsilon}$, $|\dot{\bar{u}}_i| < \sqrt{\epsilon}$ and $|\bar{u}_{i,j}| < \sqrt{\epsilon}$ at $t = 0$*, and obtain

$$\rho_3 < 15V\epsilon \quad \text{at } t = 0$$

Then, as $H > 0$, we have

$$H < K\epsilon = \delta \quad \text{at } t = 0$$

---

* The initial disturbances may also admit singularities at finite number of isolated points in V such that $\rho_3 = 0(\epsilon)$, and $H = 0(\epsilon)$ at $t = 0$.

where K is a positive constant. But δ is an upper bound of H for all $t > 0$, as H is a nonincreasing function of time. Therefore, if H is a positive definite functional, then all the requirements of the sufficiency theorem are fulfilled and we have the following theorem:

Theorem. For a linearly viscoelastic solid subjected to a set of partial follower forces to be stable with respect to the metric ρ_3, it is sufficient that the functional H given by Eq. (5.5) be a positive definite quantity for admissible perturbed motions of the solid about the state of initial stress.

Let us note that the requirement of H being a positive definite functional may imply a stronger stability condition than is given by ρ_3. This touches then upon the question of the necessary conditions which will not be dealt with here.

From the above discussion we may conclude that the commonly used energy methods yield stability criteria with respect to an average metric ρ_3. Therefore we may not, by any means, expect to retrieve any more information than is retained after this averaging process. This conclusion is also valid for most approximate methods such as the Ritz, the Galerkin, and other methods, where we use some averaging processes to reduce the system of partial to a set of ordinary differential equations. We shall explore this point further in the sequel, but let us make first another remark regarding system (5.1) and functional H. We let solution of (5.1) be of a form $\bar{u}_i = \psi_i(\vec{x})e^{pt}$ and obtain from (5.5)

$$H = e^{2pt}\left\{\frac{1}{2}\int_V [p^2 m\psi_i\psi_i + C_{ijk\ell}\psi_{i,j}\psi_{k,\ell} + (1-\alpha)\sigma_{jk}\psi_{i,k}\psi_{i,j}]\,dv\right.$$

$$\left. + \int_V [pC'_{ijk\ell}\psi_{i,j}\psi_{k,\ell} - \sigma_{jk}(\alpha\psi_{i,j})_{,k}\psi_i]\,dv\right\} \qquad (5.8)$$

If we substitute $\bar{u}_i = \psi_i e^{pt}$ into Eqs. (5.1), we obtain an eigenvalue problem with eigenvalues p. From Eq. (5.8) we may conclude that, for H to be a nonincreasing function of time, p must have a nonpositive real part.

We now reduce Eqs. (5.1) to a set of ordinary differential equations. We assume that $\bar{u}_i$ and its derivatives can be expanded in terms of the complete set of eigenvectors $\{\varphi_{in}(\vec{x})\}$ i = 1,2,3, n = 1,2,...,∞, such that

$$\int_V \left|\bar{u}_i\bar{u}_i - \sum_{n=1}^{N}\varphi_{in}\varphi_{in}q_n^2(t)\right| dv < \epsilon_1, \quad \int_V \left|\dot{\bar{u}}_i\dot{\bar{u}}_i - \sum_{n=1}^{N}\varphi_{in}\varphi_{in}\dot{q}_n^2(t)\right| dv < \epsilon_2 \qquad (5.9)\ \text{cont.}$$

$$\int_V \left| \bar{u}_{i,j}\bar{u}_{k,\ell} - \sum_{n=1}^{N}\sum_{m=1}^{N} \varphi_{in,j}\varphi_{km,\ell} q_n(t) q_m(t) \right| dv < \epsilon_3$$

$$\int_V \left| \bar{u}_{i,jk}\dot{\bar{u}}_i - \sum_{n=1}^{N}\sum_{m=1}^{N} \varphi_{in,jk}\varphi_{im} q_n(t)\dot{q}_m(t) \right| dv < \epsilon_4 \qquad (5.9)$$

and

$$\int_V \left| \dot{\bar{u}}_{i,j}\dot{\bar{u}}_{k,\ell} - \sum_{n=1}^{N}\sum_{m=1}^{N} \varphi_{in,j}\varphi_{km,\ell} \dot{q}_n(t)\dot{q}_m(t) \right| dv < \epsilon_5 \qquad i,j,k,\ell = 1,2,3$$

for some $N > M$, where M is a large positive number depending on ϵ_i; $i = 1,2,\ldots,5$ in the above inequalities and ϵ_i may be made as small as we please by selecting M sufficiently large. For such an M, Eq. (5.7) reduces to

$$\sum_{m=1}^{N} \left\{ \ddot{q}_m + \sum_{n=1}^{N} C_{mn}\dot{q}_n + \omega_m^2 \sum_{n=1}^{N} (\delta_{mn} + b_{mn}) q_n \right\} \dot{q}_m = 0$$

where

$$b_{mn} = \frac{1}{\omega_m^2} \left[\int_V (1-\alpha)\sigma_{jk}\varphi_{in,j}\varphi_{im,k} dv - \int_V \sigma_{jk}(\alpha\varphi_{in,j})_{,k}\varphi_{im} dv \right] \qquad (5.10)$$

and

$$C_{mn} = \int_V C'_{ijk\ell}\varphi_{kn,\ell}\varphi_{im,j} dv$$

In obtaining (5.10), in addition to the Gauss theorem we have also utilized the fact that $\{\varphi_{in}\}$ are solutions to

$$C_{ijk\ell}\varphi_{kn,\ell j} + m\omega_n^2\varphi_{in} = 0 \quad \text{in V}, \qquad C_{ijk\ell}\varphi_{kn,\ell} n_j = 0 \quad \text{on S}, \qquad \int_V m\varphi_{in}\varphi_{im} dv = \delta_{mn}$$

For $\dot{q}_m$; $m = 1,2,\ldots,N$ not identically zero, Eqs. (5.10) yield

$$\ddot{q}_m + \sum_{n=1}^{N} C_{mn}\dot{q}_n + \omega_m^2 \sum_{n=1}^{N} (\delta_{mn} + b_{mn}) q_n = 0, \qquad m = 1,2,\ldots,N \qquad (5.11)$$

which is a system of nonself-adjoint, ordinary differential equations.

Similarly, H reduces to

$$\bar{H} = \frac{1}{2} \sum_{m=1}^{N} \left\{ \left[\dot{q}_m^2 + \omega_m^2 q_m^2 \right] + \sum_{n=1}^{N} a_{mn} q_n q_m + 2 \int \sum_{n=1}^{N} \left[C_{mn} \dot{q}_n \dot{q}_m + \bar{b}_{mn} q_n \dot{q}_m \right] dt \right\}$$

where

$$a_{mn} = \int_V (1-\alpha) \sigma_{jk} \varphi_{in,j} \varphi_{im,k} dv, \qquad \bar{b}_{mn} = - \int_V \sigma_{jk} (\alpha \varphi_{in,j})_{,k} \varphi_{im} dv$$

and

$$b_{mn} = \frac{1}{\omega_m^2} (a_{mn} + \bar{b}_{mn}) \tag{5.12}$$

For a positive definite H in a region $\rho_3 < R$; $R > 0$, we can find an M such that $\bar{H}$ is also a positive definite quantity within a ring $\bar{R}_1 < \bar{\rho}_3 < \bar{R}$, where $\bar{\rho}_3$ is defined by

$$\bar{\rho}_3 = \sum_{n=1}^{N} (q_n^2 + \dot{q}_n^2)$$

in a 2 N-dimensional Euclidean space. Moreover, $\bar{R}_1$ is dependent only upon ϵ_i in inequalities (5.9) and may be made as small as we please by choosing M large enough. From the stability theorem we therefore conclude that, for system (5.1) to be stable with respect to the metric ρ_3, it is sufficient that $\bar{H}$ be a positive definite quantity. But $\bar{H}$ vanishes for $\bar{\rho}_3 = 0$ and $d\bar{H}/dt$ is identically equal to zero along any path satisfying equations (5.11). Therefore, by Liapunov's stability theorem [14], system (5.11) is stable when $\bar{H}$ is a positive definite quantity, and likewise when H is a positive definite quantity.

The study of stability of the system of linear homogeneous ordinary differential equations (5.10) is, however, a classical mathematical problem. For the stability of (5.11), it is necessary and sufficient that the roots of the characteristic equation of (5.11) have nonpositive real parts. However, the study of the functional $\bar{H}$, which in fact is a statement of the energy of the system, can provide us with a better insight into the physical behavior of the system. Divergent motion may occur if, for a virtual (static) displacement of the system, the work of the applied forces equals the change in the strain energy of the system, namely,

$$\delta \int_V \frac{1}{2} \left[C_{ijk\ell} \bar{u}_{i,j} \bar{u}_{k,\ell} + (1-\alpha) \sigma_{jk} \bar{u}_{i,k} \bar{u}_{i,j} \right] dv - \int_V \sigma_{jk} (\alpha \bar{u}_{i,j})_{,k} \delta \bar{u}_i dv = 0$$

or equivalently

$$\delta \int_V \frac{1}{2} \left[C_{ijk\ell} \bar{u}_{i,j} \bar{u}_{k,\ell} + \sigma_{jk} \bar{u}_{i,k} \bar{u}_{i,j}\right] dv - \int_S \alpha p_j \bar{u}_{i,j} \delta \bar{u}_i dS = 0 \qquad (5.13)$$

where δ is the variational symbol.

Let us now assume that α is function of a real parameter γ; $-\infty < \gamma < +\infty$, in addition to x_1, x_2, and x_3; $\alpha \equiv \alpha(x_1, x_2, x_3; \gamma)$. Moreover, we consider a proportional loading $\beta p_j(\vec{x})$, where β is a finite, dimensionless, real number; $0 \leq \beta < \infty$. In this way, the plane of β - γ is divided into regions of stability and instability by equation (5.13). The effect of the linear viscosity (Eq. 5.3), in this case, is to make the stability regions a closed set (except, possibly, for a set with measure zero; a finite number of isolated points in this plane).

The limiting condition for the flutter of system (5.1), by contrast, is obtained when

$$H_3 = \int_0^{\frac{2\pi}{\omega}} \int_V \left[C'_{ijk\ell} \dot{\bar{u}}_{i,j} \dot{\bar{u}}_{k,\ell} - \sigma_{jk} (\alpha \bar{u}_{i,j})_{,k} \dot{\bar{u}}_i\right] dv\, dt = 0$$

where ω is the frequency of steady state oscillation of the solid about its unperturbed state. The motion of the solid decays if $H_3 > 0$ and amplifies if $H_3 < 0$.

For continuous systems with slight damping, Nemat-Nasser [53] proved that the flutter load parameter of the undamped system is an upper bound for that of the system with slight damping. He also established the necessary and sufficient condition for stability with respect to flutter and sufficiency conditions for stability with respect to divergence and flutter. Based on energy considerations he further suggested in [53] an approximate method of stability analysis which reduces to the usual energy criterion for the case of conservative loading. A complex treatment of a class of one-dimensional continuous systems was suggested in [54].

For a further discussion of stability of continuous (not necessarily nonconservative) systems, reference should be made to the recent work by Hsu [55] and by Knops and Wilkes [56].

CHAPTER VI

METHODS OF ANALYSIS

6.1 Discrete Systems

6.1.1 Introduction

The mathematical analysis of stability of discrete systems is most readily carried out using Routh-Hurwitz criteria to determine the nature of eigenvalues, a subject amply explored in the literature, see, e.g., [18]. As an alternative, one could think of applying Liapunov's direct method, [14], with suitable modifications. In conservative systems this method is tantamount to the well-known energy method, but in systems with follower forces suitable generalizations are required. Such a generalization has been presented by Walker [57]. The approach has the advantage, over an eigenvalue analysis, that the manner, in which various parameter changes influence stability, becomes much more visible. Below the idea and examples presented in Ref. [57] are reproduced.

Let us examine first a conservative discrete dynamic system in vector form

$$M\ddot{q} + C\dot{q} + Kq = 0 \tag{6.1}$$

where q is an n-vector of displacement, M, C, K are n x n matrices, and M is positive definite and symmetric. Most early work is based on energy considerations, and considers the so-called "conservative" problem (K symmetric and positive definite) with "dissipation" forces (C symmetric and positive semidefinite) and/or "gyroscopic" forces (C skew symmetric) [58]. For this problem, the total energy

$$E = \frac{1}{2}\,\dot{q}^T M\dot{q} + \frac{1}{2}\,q^T Kq \tag{6.2}$$

is a positive-definite function, having the time derivative

$$\dot{E} = -\,\dot{q}^T C\dot{q} \tag{6.3}$$

Depending on whether C is definite, semidefinite, or zero, various exact statements can be made concerning stability or asymptotic stability of the equilibrium $q = \dot{q} = 0$ [58].

6.1.2 A "Generalized Energy" Function

The generalization in Ref. [57] starts by defining n-vectors $q_1 = q$, $q_2 = \dot{q}$ and placing the system in the form

$$\begin{aligned} \dot{q}_1 &= q_2 \\ \dot{q}_2 &= -\,M^{-1} Kq_1 - M^{-1} Cq_2 \end{aligned} \tag{6.4}$$

while assuming $M = M^T$, det $|M| \neq 0$, det $|K| \neq 0$. These assumptions are maintained throughout.

Consider now the general quadratic form

$$V = \underset{\sim}{q}_1^T F \underset{\sim}{q}_1 + \underset{\sim}{q}_2^T G \underset{\sim}{q}_2 + \underset{\sim}{q}_2^T H \underset{\sim}{q}_1 \tag{6.5}$$

where F, G, H, are n x n matrices, $F = F^T$, $G = G^T$. Taking the time derivative according to the equations of state, we have

$$\dot{V} = - \underset{\sim}{q}_1^T K^T M^{-1} H \underset{\sim}{q}_1 - \underset{\sim}{q}_2^T \left[2GM^{-1} C - H \right] \underset{\sim}{q}_2 \tag{6.6}$$

$$+ \underset{\sim}{q}_2^T \left[2F - 2GM^{-1} K - C^T M^{-1} H \right] \underset{\sim}{q}_1$$

The above function and its derivative are sufficiently general for a full attack on the stability problem by the methods of Liapunov, but are also too complicated to be of much practical value. It seems desirable to sacrifice some generality if a significant reduction in complexity would result. Keeping in mind that when the energy method works, it works very easily, suppose we now restrict the function V to have two of the properties which the energy function, when it is meaningful, normally has; namely: (1) If $C = 0$, then $\dot{V} \equiv 0$, (2) If $C \neq 0$, then $\dot{V}$ depends only upon $\underset{\sim}{q}_2$. These conditions imply

$$F = GM^{-1} K = \left[GM^{-1} K \right]^T$$

$$H = 0 \tag{6.7}$$

Thus, the restricted function is

$$V = \underset{\sim}{q}_1^T GM^{-1} K \underset{\sim}{q}_1 + \underset{\sim}{q}_2^T G \underset{\sim}{q}_2 \tag{6.8}$$

where G and $GM^{-1}K$ are symmetric, and its derivative is

$$\dot{V} = - 2 \underset{\sim}{q}_2^T GM^{-1} C \underset{\sim}{q}_2 \tag{6.9}$$

We note that $GM^{-1}C$ need not be symmetric, and that $\dot{V} \equiv 0$ if $GM^{-1}C$ is skew-symmetric. We also note that for symmetric K we may choose $G = M$ and produce the energy function, although we need not do so. Since the symmetry requirements on G and $GM^{-1}K$ result in (n^2-n) linear equations in the n^2 elements of G, there are normally n independent matrices G (producing n independent functions V) which satisfy these requirements.

We are now in a position to draw some conclusions:

Theorem 1. If there exists a matrix G such that $GM^{-1}C$ is positive definite, while G and $GM^{-1}K$ are symmetric and positive definite, the equilibrium is asymptotically stable.

Theorem 2. If there exists a matrix G such that $GM^{-1}C$ is positive semidefinite, while G and $GM^{-1}K$ are symmetric and positive definite, the equilibrium is stable.

Theorem 3. If there exists a matrix G such that $GM^{-1}C$ is positive definite, while G and $GM^{-1}K$ are symmetric but not both positive semidefinite,* the equilibrium is unstable.

Theorem 4. If there exists a matrix G such that $GM^{-1}C$ is skew-symmetric,** while G and $GM^{-1}K$ are symmetric and definite of the same sign, the equilibrium is stable but not asymptotically stable.

Theorem 5. If there exists a matrix G such that $GM^{-1}C$ is skew-symmetric, while G and $GM^{-1}K$ are symmetric, the function $V = \underset{\sim}{q}_1^T GM^{-1}K \underset{\sim}{q}_1 + \underset{\sim}{q}_2^T G\underset{\sim}{q}_2$ is an integral.

Although the conditions of Theorems 1-4 are only sufficient, not necessary, it seems that in the great majority of problems one of the first three theorems should prove applicable. A definiteness requirement on an n x n matrix results in n inequalities and, as previously noted, symmetry requirements on G and $GM^{-1}K$ result in only (n^2-n) equations in the n^2 elements of G. Theorems 4 and 5 are less generally applicable, particularly when $C \neq 0$, since their satisfaction may involve up to $\frac{1}{2}(3n^2-n)$ equations and, for Theorem 4, up to 2n inequalities. However, it may be noted that every result previously obtained by the energy method [58](K is then necessarily symmetric) is included here by letting G = M.

There are normally n independent matrices G which satisfy the symmetry requirements on G and $GM^{-1}K$. If the problem is specified in terms of parameters and is being attacked analytically, there is often an apparent choice for the n arbitrary elements of G which simplify the definiteness conditions on $GM^{-1}C$ or, if $GM^{-1}C$ is skew-symmetric, the definiteness conditions on G and $GM^{-1}K$. When M is diagonal, a usable result is sometimes found by setting diag [G] = diag [M], thus specifying n elements of G a priori. This choice is one which produces G = M in the absence of follower forces, and this may be desirable since the energy function usually works well in such problems.

---

* A definite matrix is also semidefinite, as is the zero matrix.

** The zero matrix is also skew-symmetric.

Two examples involving follower forces are presented to illustrate the use of these procedures.

Example 1. Consider the system

$$M\ddot{q} + C\dot{q} + Kq = 0 \tag{6.10}$$

where

$$M = \begin{bmatrix} m_1 & 0 \\ 0 & m_2 \end{bmatrix}, \quad C = \begin{bmatrix} 0 & 0 \\ 0 & 0 \end{bmatrix}, \quad K = \begin{bmatrix} k_1 & -k_3 \\ k_3 & k_2 \end{bmatrix} \tag{6.11}$$

If we choose diag [G] = diag [M], $G = G^T$,

$$G = \begin{bmatrix} m_1 & g \\ g & m_2 \end{bmatrix} \tag{6.12}$$

and

$$GM^{-1}K = \begin{bmatrix} k_1+k_3g/m_2 & -k_3+k_2g/m_2 \\ k_1g/m_1+k_3 & -k_3g/m_1+k_2 \end{bmatrix} \tag{6.13}$$

For $GM^{-1}K$ to be symmetric, we find

$$-k_3 + k_2\, g/m_2 = k_1\, g/m_1 + k_3 \tag{6.14}$$

which implies

$$g = \frac{2k_3m_1m_2}{k_2m_1-k_1m_2} \tag{6.15}$$

Since $GM^{-1}C = 0$, we will utilize Theorem 4. Conditions for positive definiteness of G and $GM^{-1}K$ are, assuming $m_1 > 0$, $m_2 > 0$,

$$\text{(a)} \quad m_1m_2 - g^2 > 0 \tag{6.16}$$

$$\text{(b)} \quad m_2k_1 + m_1k_2 > 0 \tag{6.17}$$

$$\text{(c)} \quad (k_3^2 + k_1k_2)(m_1m_2 - g^2) > 0 \tag{6.18}$$

By Theorem 4 these are sufficient conditions for stability, but they also happen to be the necessary and sufficient conditions for distinct purely imaginary eigenvalues.

A result which is immediately apparent from this analysis is that proportional damping always results in asymptotic stability when the preceding conditions are satisfied. That is, if

$$C = \alpha M + \beta K \quad (\alpha\beta \geq 0,\ \alpha + \beta > 0) \tag{6.19}$$

then

$$GM^{-1}C = \alpha G + \beta\, GM^{-1}K \tag{6.20}$$

and $GM^{-1}C$ is positive definite since G and $GM^{-1}K$ are positive definite. Theorem 1 thus implies asymptotic stability.

This is not to imply that C need be proportional, or even dissipative, for an answer to be obtained. Consider the general matrix

$$C = \begin{bmatrix} c_1 & c_4 \\ c_3 & c_2 \end{bmatrix} \tag{6.21}$$

for which, using the previous G, we have

$$GM^{-1}C = \begin{bmatrix} c_1 + c_3 g/m_2 & c_4 + c_2 g/m_2 \\ c_3 + c_1 g/m_1 & c_2 + c_4 g/m_1 \end{bmatrix} \tag{6.22}$$

Assuming conditions (a), (b), (c), are satisfied, Theorem 1 implies asymptotic stability provided

$$\text{(d)} \quad c_1 m_2 + c_3 g > 0 \tag{6.23}$$

$$\text{(e)} \quad (c_1 c_2 - c_3 c_4) \cdot (m_1 m_2 - g^2) > 0 \tag{6.24}$$

If (d) and (e) are satisfied, but one or more of (a), (b), (c), is strictly violated, Theorem 3 implies instability. Stability is assured by Theorem 2 when (a), (b), (c) are satisfied while (d) and (e) are weakly satisfied.

For certain values of the parameters, it is clear that a definitive result is not given by the preceding analysis. However, all of the preceding was based on one specific choice for diag [G]. Other choices can be made and results obtained which are applicable under different parameter restrictions.

It may be noted in general that for problems having C = 0, Theorem 4 is the only one of the first four theorems having a possibility of success, and

it can be satisfied only for systems which would be asymptotically stable with the addition of proportional damping.

Example 2. Let us consider the problem discussed in Sect. 3.1 which should serve as a fair demonstration of the operation of the proposed method. The equations of motion are

$$\underset{\sim}{M}\ddot{\underset{\sim}{q}} + \underset{\sim}{C}\dot{\underset{\sim}{q}} + \underset{\sim}{K}\underset{\sim}{q} = \underset{\sim}{0} \tag{6.25}$$

where

$$M = m\ell^2 \begin{bmatrix} 3 & 1 \\ 1 & 1 \end{bmatrix}, \quad C = \begin{bmatrix} 0 & 0 \\ 0 & 0 \end{bmatrix}, \quad K = k \begin{bmatrix} 2-\gamma & \alpha\gamma-1 \\ -1 & 1-(1-\alpha)\gamma \end{bmatrix} \tag{6.26}$$

where $m\ell^2 > 0$, $k > 0$, and $\gamma = P\ell/k$. The parameters of interest are γ and α, which relate to the magnitude and direction of the nonconservative load.

Choosing a general symmetric G,

$$G = \begin{bmatrix} \alpha_1 & g \\ g & \alpha_2 \end{bmatrix} \tag{6.27}$$

we find that the symmetry of $GM^{-1}K$ implies

$$g\,[1 - 2(1-\alpha)\gamma] = \alpha_2(\gamma-5) - \alpha_1(\gamma-2) \tag{6.28}$$

Since $GM^{-1}C = 0$, we hope to apply Theorem 4.

Looking ahead to possible algebraic difficulties in the definiteness conditions on G and $GM^{-1}K$, let us try the simplest choice for (α_1, α_2), i.e., one which produces $g = 0$:

$$\begin{aligned} \alpha_1 &= 5 - \gamma \\ \alpha_2 &= 2 - \gamma \end{aligned} \tag{6.29}$$

Thus,

$$G = \begin{bmatrix} 5-\gamma & 0 \\ 0 & 2-\gamma \end{bmatrix} \tag{6.30}$$

and

$$GM^{-1}K = \frac{km\ell^2}{2} \begin{bmatrix} (5-\gamma)(3-\gamma) & -(5-\gamma)(2-\gamma) \\ -(5-\gamma)(2-\gamma) & (2-\gamma)[4-(3-2\alpha)\gamma] \end{bmatrix} \tag{6.31}$$

We see that G is positive definite for $\gamma < 2$. Assuming this restriction, we find that $GM^{-1}K$ is positive definite provided

$$1 + (1-\alpha)(\gamma^2 - 3\gamma) > 0 \tag{6.32}$$

The bifurcation plot in the (γ,α) plane is shown in Fig. 6.1. We have just obtained the shaded region below $\gamma = 2$ as a region of stability by Theorem 4. However, eigenvalue analysis [22] shows the entire shaded region to be the exact region of stability. Since our theorems are only sufficient, not necessary, it may be worth-while to try another choice for G. We see that the previous choice for G fails at $\gamma = 2$ because $\alpha_2 = 2 - \gamma$ is required to be positive, a necessary condition for positive definiteness of our previous G. Let us simply reverse our definition of α_2 and choose

$$\begin{aligned} \alpha_1 &= 5 - \gamma \\ \alpha_2 &= \gamma - 2 \end{aligned} \tag{6.33}$$

for which

$$g = 2(\gamma-2)(\gamma-5)/[1 - 2(1-\alpha)\gamma] \tag{6.34}$$

Some tedious calculations show that the conditions for positive definiteness of G and $GM^{-1}K$ are now

$$\begin{aligned} &2 < \gamma < 5 \\ &41 - 32\gamma + 4\alpha\gamma(1+\alpha\gamma) + 8\gamma^2(1-\alpha) > 0 \\ &7 - 4\gamma + 2\alpha\gamma > 0 \\ &1 + (1-\alpha)(\gamma^2 - 3\gamma) > 0 \end{aligned} \tag{6.35}$$

These conditions define the shaded area above $\gamma = 2$ in Fig. 6.1. Thus, with the exception of the line $\gamma = 2$, we have determined the entire region of the parameter plane which produces a stable equilibrium.

We may perform a special investigation for $\gamma = 2$. We have then

$$G = \begin{bmatrix} \alpha_1 & g \\ g & \alpha_2 \end{bmatrix}, \qquad GM^{-1}K = \frac{km\ell^2}{2} \begin{bmatrix} \alpha_1 - 3g & g(4\alpha-2) \\ g-3\alpha_2 & \alpha_2(4\alpha-2) \end{bmatrix} \tag{6.36}$$

where the symmetry of $GM^{-1}K$ implies

$$g = \frac{3\alpha_2}{3-4\alpha} \tag{6.37}$$

Choosing $\alpha_1 = 1$, we find that the conditions for positive definiteness of G and $GM^{-1}K$ are now that there exist an $\alpha_2 > 0$ such that

$$(3-4\alpha)^2 - 9\alpha_2 > 0$$

$$(4\alpha-2)[(3-4\alpha)^2 - 9\alpha_2] > 0 \tag{6.38}$$

$$(3-4\alpha)^2 - 9\alpha_2(3-4\alpha) > 0$$

These can be satisfied by choosing $9\alpha_2 < (3-4\alpha)^2$, provided $\alpha > \frac{1}{2}, \neq \frac{3}{4}$. This completes the determination of the entire region of stability in the parameter plane. Again we note that the addition of any form of proportional damping

$$C = \eta M + \beta K (\eta\beta \leq 0,\ \eta + \beta > 0) \tag{6.39}$$

leads to asymptotic stability of the equilibrium by Theorem 1, provided (γ,α) is in the shaded region of Fig. 6.1. The difficulty of reaching this general conclusion by eigenvalue analysis need not be dwelt upon.

6.1.3 A General Approach

When problems are encountered for which there seems no apparent choice for the n arbitrary elements of G which produces a usable result, or in which the order is so great as to require the use of a computer, it may be desirable to apply the method in its fullest generality. A systematic approach might be as follows:

1) Define diag $[G_i] = \underset{\sim}{e}_i$, where $\underset{\sim}{e}_1 = (1,0,\ldots)$, $\underset{\sim}{e}_2 = (0,1,0,\ldots)$ etc.

2) Determine G_i by the symmetry of G_i and $G_iM^{-1}K$

3) Set $G = \sum_{i=1}^{n} \alpha_i G_i$

4) Note that $GM^{-1}K = \sum_{i=1}^{n} \alpha_i G_i M^{-1} K$

$$GM^{-1}C = \sum_{i=1}^{n} \alpha_i G_i M^{-1} C$$

5) Determine whether a vector $\underset{\sim}{\alpha}$ exists such that $GM^{-1}C$ is positive definite or semidefinite, if so, use Theorems 1, 2, or 3.

6) Determine whether a vector α exists such that $GM^{-1}C$ is skew-symmetric; if so, use Theorem 4 and/or 5.

6.1.4 Exceptional Cases

Although it is true that there are problems for which there exists no matrix G satisfying the conditions of any of the first four theorems, implying stability cannot be determined in this manner, it seems that there is often something quite unusual about such problems. One such is the following:

$$\underset{\sim}{M}\ddot{\underset{\sim}{q}} + \underset{\sim}{C}\dot{\underset{\sim}{q}} + \underset{\sim}{K}\underset{\sim}{q} = 0$$

$$M = \begin{bmatrix} m_1 & 0 \\ 0 & m_2 \end{bmatrix}, \qquad C = \begin{bmatrix} 0 & c \\ -c & 0 \end{bmatrix}, \qquad K = \begin{bmatrix} k_1 & 0 \\ 0 & k_2 \end{bmatrix} \tag{6.40}$$

where $m_1 > 0$, $m_2 > 0$, and $k_1 m_2 \neq k_2 m_1$.

Using the most general form for symmetric G, we have

$$G = \begin{bmatrix} \alpha_1 & g \\ g & \alpha_2 \end{bmatrix} \tag{6.41}$$

and

$$GM^{-1}K = \frac{1}{m_1 m_2} \begin{bmatrix} \alpha_1 k_1 m_2 & g k_2 m_1 \\ g k_1 m_2 & \alpha_2 k_2 m_1 \end{bmatrix} \tag{6.42}$$

Symmetry implies

$$g = 0 \tag{6.43}$$

and therefore

$$GM^{-1}C = \frac{c}{m_1 m_2} \begin{bmatrix} 0 & \alpha_1 m_2 \\ -\alpha_2 m_1 & 0 \end{bmatrix} \tag{6.44}$$

and it is impossible to satisfy Theorems 1 or 3 for any choice of (α_1, α_2).

Theorem 4 can be satisfied by choosing $\alpha_1 = m_1$, $\alpha_2 = m_2$, provided $GM^{-1}K$ is then positive definite. Since

$$G = \begin{bmatrix} m_1 & 0 \\ 0 & m_2 \end{bmatrix}, \qquad GM^{-1}K = \begin{bmatrix} k_1 & 0 \\ 0 & k_2 \end{bmatrix} \tag{6.45}$$

we see that Theorem 4 implies stability provided $k_1 > 0$, $k_2 > 0$. However, eigenvalue analysis assures stability provided only that

$$k_1 m_2 + k_2 m_2 > 0$$
$$k_1 k_2 > - c^2 \tag{6.46}$$

which allow the possibility of one of the k_i actually being negative. However, noting that our $GM^{-1} = I$, we see that Theorem 3 assures that instability will occur if C is increased by any positive definite matrix and either of the k_i is negative. That is, when the k_i are in the range for stability predicted by eigenvalue analysis, but not in the range for which any of our stability theorems apply, the addition of any complete dissipation leads to instability.* On the other hand, when the k_i are in our allowable range, $k_1 > 0$, $k_2 > 0$, the addition of any complete dissipation leads to asymptotic stability by Theorem 1, a much more natural result.

6.1.5 Remarks

Although each of the examples was begun under the assumption of no dissipation and we initially applied Theorem 4, this was only for the purpose of illustrating that we can make qualitative statements about the effects of various types of damping via Theorems 1 and 3. In practice, Theorem 4 is the most difficult to use and, in the real world, it is the least likely to apply. When the linear approximation indicates stability which is not asymptotic, the stability or instability of the physical system is determined by parameter errors and/or any slight nonlinearities [58,15]. Therefore, Theorem 4 is useful in problems which are primarily of academic interest.

These remarks do not generally apply to Theorem 2, although it too concludes only stability. If the conditions of Theorem 2 are satisfied and those of Theorem 1 are not, one can often still conclude asymptotic stability by use of an invariance principle due to LaSalle [59]. This usually requires a detailed analysis of the differential equations, however.**

Theorem 5 allows the rapid generation of up to n integrals, particularly when C = 0, and so permits a possible reduction in the order of the system

---

* This is a well known result concerning the phenomenon of gyroscopic stabilization [58].

** In particular, one must determine whether any invariant set other than $(\underset{\sim}{q}_1, \underset{\sim}{q}_2) = (\underset{\sim}{0}, \underset{\sim}{0})$, is contained in the set defined by $\underset{\sim}{q}_2^T GM^{-1} C \underset{\sim}{q}_2 = 0$. If not, the conditions of Theorem 2 imply asymptotic stability of the equilibrium [59].

from 2n to as low as n. However, the algebraic difficulties of such reduction may be considerable. The primary use of Theorem 5 is to determine "constants of the motion," in problems in which these are of some interest.

6.2 Continuous Systems

6.2.1 Introduction

The class of nonself-adjoint eigenvalue problems is not as extensively investigated as that of self-adjoint ones and special attention must be paid to the mathematical methods used in determining the eigenvalues. A justification of applying the Galerkin method to bars subjected to nonconservative loads was offered by Leipholz [60] and the convergence of this method, as applied to the same problems, was studied by him in Ref. [61]. Leipholz also used the method of finite differences in evaluating the eigenvalue of an elastic bar subjected to a uniformly distributed tangential load [62]. He extended the applicability of the Galerkin method to a broader class of linear nonself-adjoint eigenvalue problems [63] than those studied in Ref. [62]. This class contains all eigenvalue problems which arise from originally self-adjoint problems by addition of a linear differential expression which destroys the former self-adjointness. The convergence of the Galerkin method for nonconservative stability problems of plates and shells was studied by Leipholz in Ref. [64]. A discussion of the Galerkin method as applied to systems with damping is discussed by Leipholz in Ref. [65].

Levinson [66] has shown that for certain problems the Galerkin method converges for a broader class of trial functions than assumed by Leipholz. Further, Levinson extended Hamilton's principle and the Ritz method such as to make them applicable to nonconservative problems.

The Ritz method in nonvariational formulation was applied to nonconservative problems by Marchenko [67]. Both the Ritz and the Galerkin methods have been extended further by Leipholz [68]. In particular, the conditions to be fulfilled by the coordinate functions are weakened; these functions need not satisfy the dynamical boundary conditions and under certain circumstances not even the geometrical ones. This study includes also some considerations of convergence.

In treating dissipative dynamic systems of mathematical physics, which are governed by nonself-adjoint linear operators, it is often found convenient to introduce the adjoint system (or field) and to consider formally a conservative process [69], [70]. The original field contains an energy sink, and in the adjoint field an energy source of the same strength is incorporated in order to make the combined field conservative.

It is of interest to note that the notion of the adjoint field can be introduced also in treating nondissipative, nonconservative systems, i.e., dynamic systems subjected to circulatory forces. In particular, in structural systems subjected to follower forces, the consideration of adjoint force fields leads to interesting consequences. Indeed, for this class of nonconservative

systems, both the original field and its adjoint force field are associated with energy sources [71], and yet the combination of these two fields results in a conservative one.

As an example, consider the Beck problem [33], i.e., a cantilevered elastic bar subjected at its free end to a compressive follower force (see Fig. 6.2). The equation of motion and the boundary conditions are

$$\frac{\partial^4 y}{\partial x^4} + F\frac{\partial^2 y}{\partial x^2} + \frac{\partial^2 y}{\partial t^2} = 0$$

$$y = \frac{\partial y}{\partial x} = 0 \qquad \text{at} \quad x = 0 \tag{6.47}$$

$$\frac{\partial^2 y}{\partial x^2} = \frac{\partial^3 y}{\partial x^3} = 0 \qquad \text{at} \quad x = 1$$

where dimensionless quantities are employed. We now construct the adjoint boundary-value problem by considering a function $z = z(x,t)$, defined for $0 \le x \le 1$ and $t \ge 0$, such that the following equation of motion and boundary conditions at $x = 0$ are satisfied identically:

$$\frac{\partial^4 z}{\partial x^4} + F\frac{\partial^2 z}{\partial x^2} + \frac{\partial^2 z}{\partial t^2} = 0$$

$$z = \frac{\partial z}{\partial x} = 0 \qquad \text{at} \quad x = 0 \tag{6.48}$$

We then seek boundary conditions for z, at $x = 1$, such that

$$\int_0^1 z\left(\frac{\partial^4 y}{\partial x^4} + F\frac{\partial^2 y}{\partial x^2} + \frac{\partial^2 y}{\partial t^2}\right) dx = \int_0^1 y\left(\frac{\partial^4 z}{\partial x^4} + F\frac{\partial^2 z}{\partial x^2} + \frac{\partial^2 z}{\partial t^2}\right) dx \tag{6.49}$$

If we now integrate the right side of the preceding equation by parts and use boundary conditions in Eq. (6.47), we immediately obtain the following boundary conditions for z at $x = 1$:

$$\frac{\partial^2 z}{\partial x^2} + Fz = 0 \qquad \frac{\partial^3 z}{\partial x^3} + F\frac{\partial z}{\partial x} = 0 \qquad \text{at} \quad x = 1 \tag{6.50}$$

Equations (6.48) and (6.50) now define the system adjoint to the Beck problem. The inspection of Eqs. (6.48) and (6.50) readily reveals that they describe the Reut problem [8] sketched in Fig. 6.3.

It was shown in Refs. [8] and [33] that both systems depicted in Figs. 6.2 and 6.3 lose stability for the same value of the load, i.e., $F_{cr} = 20.05$. For $F > F_{cr}$, energy is transferred to the bar by the work of the applied force, which in turn increases the conservative energy of the system, making the response unbounded (flutter). Thus, both force fields are associated with source of energy. However, it can be readily seen, both on mathematical and physical grounds (see Fig. 6.4), that the combined system is conservative, and the bar shown in Fig. 6.4 is incapable of losing stability by flutter. Indeed, the loss of stability in the combined case will occur by divergence (buckling, attainment of another equilibrium configuration). In conclusion, it should be mentioned that adjoint systems can be constructed also for the nonconservative problems discussed in Refs. [8], [72] and [73].

Adjoint systems have been also examined in Ref. [74]. The possibility of constructing adjoint equations for the purpose of developing approximate methods in aeroelasticity similar to energy methods was indicated already in Ref. [75]. The usefulness of adjoint systems in solving stability problems of elastic continua with follower forces was exhibited in Ref. [76], as described below.

6.2.2 Stability of an Elastic Continuum

Let us consider an isotropic, homogeneous, elastic solid occupying a volume V bounded by a finite surface S. It will be assumed that on one part of the boundary of the solid S_o the displacements are prescribed so as to preclude a rigid body motion. The body is at rest and in a state of initial stress σ_{ij}, $i,j = 1,2,3$, due to the applied nonconservative (follower) forces on the surface $S - S_o$ of the solid. To study the stability of this rest position the system is slightly perturbed and the type of ensuing motion is studied. Referred to an orthogonal cartesian coordinate system x_j, Bolotin [8] has obtained the following equations for the ensuing motion:

$$\frac{\partial}{\partial x_j}\left(\lambda_{ijk\ell}\frac{\partial \bar{u}_k}{\partial x_\ell}\right) + \beta\frac{\partial}{\partial x_j}\left(\sigma_{jk}\frac{\partial \bar{u}_i}{\partial x_k}\right) - \rho\frac{\partial^2 \bar{u}_i}{\partial t^2} = 0 \quad \text{in } V \tag{6.51}$$

$$\lambda_{ijk\ell}\frac{\partial \bar{u}_k}{\partial x_\ell}n_j + \beta\sigma_{jk}\frac{\partial \bar{u}_i}{\partial x_k}n_j = \beta p_i \quad \text{on } S - S_o \tag{6.52}$$

$$\bar{u}_i = 0 \quad \text{on } S_o \tag{6.53}$$

$$\lambda_{ijk\ell} = \lambda\delta_{ij}\delta_{k\ell} + 2\mu\delta_{ik}\delta_{j\ell} \tag{6.54}$$

$$\delta_{ij} = \begin{cases} 0, & i \neq j \\ 1, & i = j \end{cases}$$

In Eqs. (6.51)-(6.54), ρ is the mass density, $\bar{u}_j$ is the displacement vector measured from the undisturbed state and n_j is the outward positive unit normal vector to S. No body forces are assumed to be present and β is a parameter associated with the magnitude of externally applied surface tractions. In Eq. (6.54), λ and μ are Lamé's constants of elasticity. The repeated indices are summed over the range of their definitions and p_j are the components of perturbations of the applied surface tractions and their forms will depend on the behavior of the nonconservative forces. They will generally be homogeneous functions of displacements and their derivatives with respect to both space and time. In the present study, however, it suffices to restrict p_i to the following expression:

$$p_i = a_{ij}\bar{u}_j + b_j \frac{\partial \bar{u}_i}{\partial x_j} \quad \text{on } S - S_o \tag{6.55}$$

where a_{ij} and b_j are coefficients which are independent of the vector $\bar{u}_j$ and its derivatives but in general are functions of spatial coordinates x_j.

We may assume a solution of the above boundary value problem in the form

$$\bar{u}_j(x_1,x_2,x_3,t) = u_j(x_1,x_2,x_3)e^{i\omega t}, \qquad i = (-1)^{1/2}$$

which results in the following eigenvalue problem:

$$\frac{\partial}{\partial x_j}\left(\lambda_{ijk\ell}\frac{\partial u_k}{\partial x_\ell}\right) + \beta\frac{\partial}{\partial x_j}\left(\sigma_{jk}\frac{\partial u_i}{\partial x_k}\right) - \Lambda u_i = 0 \quad \text{in } V \tag{6.56}$$

$$\lambda_{ijk\ell}\frac{\partial u_k}{\partial x_\ell}n_j + \beta\sigma_{jk}\frac{\partial u_i}{\partial x_k}n_j = \beta\left(a_{ij}u_j + b_j\frac{\partial u_i}{\partial x_j}\right) \quad \text{on } S - S_o \tag{6.57}$$

$$u_i = 0 \quad \text{on } S_o \tag{6.58}$$

$$\Lambda = -\omega^2 \tag{6.59}$$

Equations (6.56)-(6.58) constitute a nonself-adjoint homogeneous system and stability of the solid will be governed by the character of the eigenvalues Λ^m, $m = 1,2,\ldots\infty$, for nontrivial solutions. In view of the fact that the applied surface tractions are not derivable from a potential, it is not possible to express the eigenvalues Λ^m in the form of a ratio of two positive-definite integrals, and thus the usefulness of variational principles seems dubious in this case.

6.2.3 The Adjoint System

By constructing an adjoint system by means of certain mathematical relations analogous to the definitions in the theory of ordinary differential equations, Λ may be expressed in terms of the original and the adjoint variables, and as a consequence Λ will assume a stationary value. In the theory of ordinary differential equations, a system adjoint to one governed by a differential equation and boundary conditions may be constructed formally by repeated integration by parts [77]. Being guided by this observation we examine the problem

$$\frac{\partial}{\partial x_j}\left(\lambda_{ijk\ell}\frac{\partial u_k^*}{\partial x_\ell}\right) + \beta\frac{\partial}{\partial x_j}\left(\sigma_{jk}\frac{\partial u_i^*}{\partial x_k}\right) - \Lambda^* u_i^* = 0 \quad \text{in } V \tag{6.60}$$

$$\lambda_{ijk\ell}\frac{\partial u_k^*}{\partial x_\ell}n_j + \beta\sigma_{jk}\frac{\partial u_i^*}{\partial x_k}n_j = \beta a_{ij}u_j^* + \beta c_{ij}u_j^* \quad \text{on } S - S_o \tag{6.61}$$

$$u_i^* = 0 \quad \text{on } S_o \tag{6.62}$$

as being possibly adjoint to that given by Eqs. (6.56)-(6.58). Here, c_{ij} is a function of b_j, u_j and its derivatives. If an adjoint system is to be defined through equations (6.60)-(6.62), one must obtain c_{ij} by solving a certain homogeneous integral equation on the surface $S - S_o$. The above-mentioned integral equation reduces to satisfying the following:

$$b_j\frac{\partial u_i}{\partial x_j} - u_j c_{ji} = 0 \tag{6.63}$$

Expression (6.63) involves three independent equations in nine unknown quantities c_{ij} and thus an adjoint system is not uniquely defined [77]. As a consequence of Eq. (6.63) the following holds:

$$\int_V u_i^*\left[\frac{\partial}{\partial x_j}\left(\lambda_{ijk\ell}\frac{\partial u_k}{\partial x_\ell}\right) + \beta\frac{\partial}{\partial x_j}\left(\sigma_{jk}\frac{\partial u_i}{\partial x_k}\right)\right] dV$$

$$= \int_V u_i\left[\frac{\partial}{\partial x_j}\left(\lambda_{ijk\ell}\frac{\partial u_k^*}{\partial x_\ell}\right) + \beta\frac{\partial}{\partial x_j}\left(\sigma_{jk}\frac{\partial u_i^*}{\partial x_k}\right)\right] dV \tag{6.64}$$

This expression appears to be similar to Maxwell's reciprocity relations in conservative systems, in which case $u_i \equiv u_i^*$. The bracketed terms are recognized to be resultant forces associated with the original and the adjoint systems, respectively.

Now let Λ^m, $m = 1,2,\ldots\infty$, be the eigenvalues of equations (6.56)-(6.58), and Λ^{*m}, $m = 1,2,\ldots\infty$, those of equations (6.60)-(6.62), while the corresponding eigenfunctions are u_j^m and u_j^{*m}, respectively. From Eqs. (6.56), (6.60) and (6.64), we have

$$\Lambda^m \int_V u_i^m u_i^{*n} dV = \int_V u_i^{*n} \left[\frac{\partial}{\partial x_j}\left(\lambda_{ijk\ell} \frac{\partial u_k^m}{\partial x_\ell}\right) + \beta \frac{\partial}{\partial x_j}\left(\sigma_{jk} \frac{\partial u_i^m}{\partial x_k}\right)\right] dV$$

$$= \int_V u_i^m \left[\frac{\partial}{\partial x_j}\left(\lambda_{ijk\ell} \frac{\partial u_k^{*n}}{\partial x_\ell}\right) + \beta \frac{\partial}{\partial x_j}\left(\sigma_{jk} \frac{\partial u_i^{*n}}{\partial x_k}\right)\right] dV$$

$$= \Lambda^{*n} \int_V u_i^m u_i^{*n} dV \tag{6.65}$$

Therefore,

$$(\Lambda^m - \Lambda^{*n}) \int_V u_i^m u_i^{*n} dV = 0 \tag{6.66}$$

At this point we wish to apply the argument of Roberts [77] to prove that the sets of eigenvalues $\{\Lambda^m\}$ and $\{\Lambda^{*m}\}$ are identical. Let us suppose that $\{\Lambda^m\}$ and $\{\Lambda^{*n}\}$ are not identical sets, then

$$\int_V u_i^{*n} u_i^m dV = 0; \quad \int_V u_i^{*n} \left[\frac{\partial}{\partial x_j}\left(\lambda_{ijk\ell} \frac{\partial u_k^m}{\partial x_\ell}\right) + \beta \frac{\partial}{\partial x_j}\left(\sigma_{jk} \frac{\partial u_i^m}{\partial x_k}\right)\right] dV = 0 \tag{6.67a}$$

and for the special case when $m = n$,

$$\int_V u_i^{*m} u_i^m dV = 0 \tag{6.67b}$$

If the set of eigenvectors $\{u_i^m\}$ is complete, Eq. (6.67b), together with Eq. (6.67a), would imply that u_i^{*m} is identically zero, which is not nontrivial. Hence the two sets of eigenvalues are identical. Also, similarly to the property of orthogonality of principal modes in the theory of small vibrations, Eq. (6.67a) reveals that the two sets of eigenfunctions $\{u_i^m\}$ and $\{u_i^{*m}\}$ are bi-orthonormal, i.e., each function of either set is orthogonal to every member of the other set except those which belong to the same eigenvalue.

From (6.65) it also follows that

$$\Lambda^m = \frac{\int_V u_i^{*m} \left[\frac{\partial}{\partial x_j}\left(\lambda_{ijk\ell}\frac{\partial u_k^m}{\partial x_\ell}\right) + \beta\frac{\partial}{\partial x_j}\left(\sigma_{jk}\frac{\partial u_i^m}{\partial x_k}\right)\right] dV}{\int_V u_i^m u_i^{*m}\, dV} = \frac{I_1}{I_2} \quad \text{(say)} \qquad (6.68)$$

Let us consider now the effect on Λ^m due to infinitesimal variations δu_i^m and δu_i^{*m} which are arbitrary except that they satisfy the boundary conditions (6.57), (6.58) and (6.61), (6.62). Therefore,

$$\delta\Lambda^m = \frac{1}{I_2}(\delta I_1 - \Lambda^m \delta I_2)$$

$$= \frac{1}{\int_V u_i^m u_i^{*m}\, dV}\int_V \left\{\left[\frac{\partial}{\partial x_j}\left(\lambda_{ijk\ell}\frac{\partial u_k^m}{\partial x_\ell}\right) + \beta\frac{\partial}{\partial x_j}\left(\sigma_{jk}\frac{\partial u_i^m}{\partial x_k}\right)\right]\delta u_i^{*m}\right.$$

$$+ u_i^{*m}\left[\frac{\partial}{\partial x_j}\left(\lambda_{ijk\ell}\frac{\partial \delta u_k^m}{\partial x_\ell}\right) + \beta\frac{\partial}{\partial x_j}\left(\sigma_{jk}\frac{\partial \delta u_i^m}{\partial x_k}\right)\right]$$

$$\left. - \Lambda^m\left(u_i^m \delta u_i^{*m} + u_i^{*m}\delta u_i^m\right)\right\} dV \qquad (6.69)$$

Equation (6.69) reduces, after application of the divergence theorem and satisfaction of boundary conditions, to

$$\delta\Lambda^m = \frac{1}{\int_V u_i^{*m} u_i^m\, dV}\int_V \left\{\delta u_i^{*m}\left[\frac{\partial}{\partial x_j}\left(\lambda_{ijk\ell}\frac{\partial u_k^m}{\partial x_\ell}\right) + \beta\frac{\partial}{\partial x_j}\left(\sigma_{jk}\frac{\partial u_i^m}{\partial x_k}\right) - \lambda^m u_i^m\right]\right.$$

$$\left. + \delta u_i^m\left[\frac{\partial}{\partial x_j}\left(\lambda_{ijk\ell}\frac{\partial u_k^{*m}}{\partial x_\ell}\right) + \beta\frac{\partial}{\partial x_j}\left(\sigma_{jk}\frac{\partial u_i^{*m}}{\partial x_k}\right) - \lambda^m u_i^{*m}\right]\right\} dV \qquad (6.70)$$

Equation (6.70) is clearly a useful version of a variational principle and implies that if Eqs. (6.56) and (6.60) are obeyed, $\delta\Lambda^m$ is zero with an accuracy of first order for all small arbitrary variations δu_i^m and δu_i^{*m} that satisfy the boundary conditions (6.57), (6.58) and (6.61), (6.62),

respectively. Thus a definite statement can be made regarding the error involved in stipulating that the eigenvalues are stationary values.

6.2.4 An Approximate Method of Stability Analysis

The extremum property of the eigenvalues Λ^m, as expressed by Eq. (6.70), suggests an approximate procedure for their determination, in the spirit of approximate methods for self-adjoint systems based on variational principles. We may select two sets of trial functions $U_i^m(\alpha_1,\alpha_2,\ldots)$ and $U_i^{*m}(\alpha_1^*, \alpha_2^*,\ldots)$ which satisfy the appropriate boundary conditions and contain undetermined parameters α_j and α_j^*. An approximate expression of the eigenvalues Λ^m is obtained, by using Eq. (6.68), as a function of these parameters. A stationary value of Λ^m is then obtained by determining the parameters from equations of the type

$$\frac{\partial \Lambda^m}{\partial \alpha_j} = 0; \qquad \frac{\partial \Lambda^m}{\partial \alpha_j^*} = 0$$

which is reminiscent of the Rayleigh-Ritz procedure for conservative systems.

6.2.5 Illustrative Example

In this section we wish to apply the approximate method discussed above to investigate the stability of equilibrium of a cantilevered bar subjected to a follower load. The governing equations of motion may be expressed as [8]

$$\frac{d^4u}{dx^4} + F\frac{d^2u}{dx^2} - \omega^2 u = 0; \qquad 0 \le x \le 1 \tag{6.71}$$

$$u = \frac{du}{dx} = 0 \qquad \text{at } x = 0$$

$$\frac{d^2u}{dx^2} = \frac{d^3u}{dx^3} = 0 \qquad \text{at } x = 1 \tag{6.72}$$

In Eqs. (6.71) and (6.72), dimensionless quantities are employed and ω denotes the frequency of oscillation. The equations of an adjoint system of this problem, which was first discussed in Ref. [78], are as follows:

$$\frac{d^4u^*}{dx^4} + F\frac{d^2u^*}{dx^2} - \omega^2 u^* = 0 \tag{6.73}$$

$$u^* = \frac{du^*}{dx} = 0 \qquad \text{at } x = 0$$

$$\frac{d^2u^*}{dx^2} + Fu^* = \frac{d^3u^*}{dx^3} + F\frac{du^*}{dx} = 0 \qquad \text{at } x = 1 \tag{6.74}$$

The eigenvalue ω^2 in the two problems will be the same as established in general in the previous section, and we wish to determine it approximately. We assume, then, that u and u^* may be written in the form:

$$u = \sum_{n=1}^{N} \alpha_n u_n \tag{6.75}$$

$$u^* = \sum_{n=1}^{N} \alpha_n^* u_n^* \tag{6.76}$$

where u_n, u_n^* are certain assumed functions of x which satisfy the boundary conditions (6.72) and (6.74), respectively, and α_n, α_n^* are constants to be determined as discussed. We multiply (6.71) by u^* and integrate over the length. If we substitute the expansions (6.75) and (6.76), the following relation is obtained:

$$\omega^2 = \frac{\int_0^1 \sum_{m=1}^{N} \alpha_m^* u_m^* \left(\frac{d^4}{dx^4} + F\frac{d^2}{dx^2}\right) \sum_{n=1}^{N} \alpha_n u_n dx}{\int_0^1 \sum_{m=1}^{N} \alpha_m^* u_m^* \sum_{n=1}^{N} \alpha_n u_n dx} = \frac{\sum_{m,n=1}^{N} \alpha_m^* \alpha_n A_{mn}}{\sum_{m,n=1}^{N} \alpha_m^* \alpha_n B_{mn}} \tag{6.77}$$

where

$$A_{mn} = \int_0^1 u_m^* \left(\frac{d^4 u_n}{dx^4} + F\frac{d^2 u_n}{dx^2}\right) dx$$

$$B_{mn} = \int_0^1 u_m^* u_n dx$$

To obtain the best possible result, we must now seek an extremum of the expression for ω^2 considered as a function of the parameters α_n and α_n^*. A

simple and familiar way would be to treat ω^2 as a Lagrangian undetermined multiplier and seek directly the stationary value of the following:

$$I = \frac{1}{\omega^2} \sum_{m,n=1}^{N} \alpha_m^* \alpha_n A_{mn} - \sum_{m,n=1}^{N} \alpha_m^* \alpha_n B_{mn} \tag{6.78}$$

by requiring that

$$\frac{\partial I}{\partial \alpha_m^*} = \frac{\partial I}{\partial \alpha_n} = 0$$

Since u and u^* are functions that satisfy the adjoint relations in the sense discussed before, it is a simple matter to show that $\partial I/\partial \alpha_m^*$ and $\partial I/\partial \alpha_m$ would result in two matrix relations which are adjoint to each other and thus they would yield identical eigenvalues. Therefore, in the sequel only the following relation will be considered:

$$\frac{\partial I}{\partial \alpha_m^*} = 0 \tag{6.79}$$

Equation (6.79) is a homogeneous, linear, algebraic equation in α_n and, therefore, a nontrivial solution exists only if the determinant formed by the coefficients of α_n vanishes. This results in a polynomial equation for ω^2 which represents approximately the frequency equation of the system.

Let us consider the following specific trial functions with N = 2:

$$u = \alpha_1 \left(x^2 - \frac{2}{3} x^3 + \frac{x^4}{6} \right) + \alpha_2 \left(x^3 - x^4 + \frac{3}{10} x^5 \right) \tag{6.80}$$

$$u^* = \alpha_1^* \left\{ x^2 - \frac{2(F^2+4F+24)}{F^2+6F+72} x^3 + \frac{F^2+12}{F^2+6F+72} x^4 \right\}$$

$$+ \alpha_2^* \left\{ x^3 - \frac{2(F^2+12F+120)}{F^2+16F+240} x^4 + \frac{F^2+6F+72}{F^2+16F+240} x^5 \right\} \tag{6.81}$$

Functions (6.80) and (6.81) satisfy the boundary conditions (6.72) and (6.74), respectively. Following the procedure as discussed before, we obtain the frequency equation:

$$(\eta_{11}\eta_{22} - \eta_{12}\eta_{21})\omega^4 + (\theta_{11}\eta_{22} + \theta_{22}\eta_{11} - \theta_{12}\eta_{21} - \eta_{12}\theta_{21})\omega^2 + (\theta_{11}\theta_{22} - \theta_{12}\theta_{21}) = 0 \tag{6.82}$$

where

$$\theta_{11} = \frac{4}{3} - A + \frac{4}{5}B + \frac{FA}{70} - \frac{FB}{60}$$

$$\theta_{12} = 1 - \frac{6}{5}A + \frac{6}{5}B + \frac{F}{10} - \frac{2FA}{35} + \frac{FB}{28}$$

$$\theta_{21} = 1 - \frac{4}{5}A' + \frac{2}{3}B' + \frac{F}{30} - \frac{2}{105}A'F + \frac{1}{84}B'F$$

$$\theta_{22} = \frac{6}{5} - \frac{6}{5}A' + \frac{8}{7}B' + \frac{2}{35}F - \frac{1}{28}A'F + \frac{1}{42}B'F$$

$$\eta_{11} = -\frac{71}{630} + \frac{31}{336}A - \frac{59}{756}B$$

$$\eta_{12} = -\frac{103}{1680} + \frac{43}{840}A - \frac{79}{1800}B$$

$$\eta_{21} = -\frac{31}{336} + \frac{177}{(42)(54)}A' - \frac{73}{(18)(60)}B'$$

$$\eta_{22} = -\frac{43}{840} + \frac{79}{1800}A' - \frac{19}{495}B'$$

$$A = \frac{2(F^2 + 4F + 24)}{F^2 + 6F + 72}$$

$$B = \frac{F^2 + 12}{F^2 + 6F + 72}$$

$$A' = \frac{2(F^2 + 12F + 120)}{F^2 + 16F + 240}$$

$$B' = \frac{F^2 + 6F + 72}{F^2 + 16F + 240}$$

Equation (6.82) will yield distinct real roots for vanishing F, and when F is increased the two roots will coalesce at the critical value $F = F_{cr}$ beyond which (6.82) will yield complex roots. By trial and error F_{cr} is computed to be 19.45, whereas a more precise calculation by Beck [33] yields $F_{cr} = 20.05$. Incidentally, if one uses only the trial function (6.80), the method of Galerkin yields $F_{cr} = 20.6$. This result was first computed by Levinson [66].

A similar approximate method of stability analysis was worked out independently of the above by Ballio [79].

6.3 Energy Considerations

It appears appropriate to discuss energy considerations in the context of methods of analysis, because such considerations, as in the class of conservative systems, may lead to the establishment of approximate methods of analysis. In addition, energy considerations may be useful in deriving the differential equations of motion (as well as the boundary conditions) and to provide additional insight into certain aspects of instability phenomena.

As compared to the vast amount of literature concerned with stability of mechanical systems with follower forces, it is somewhat surprising to observe that only few studies contain energy considerations. While investigating the dynamics of articulated pipes, Benjamin [80] invoked Hamilton's principle and discussed the energy transfer to the system. In Ref. [71] an extension of the usual energy method was proposed, such as to make it applicable for the stability analysis of circulatory systems with and without velocity-dependent forces. Energy considerations formed the basis of deriving equations of motion in systems with follower forces in Ref. [81].

Energetic and thermodynamic considerations in stability of conservative and nonconservative systems were discussed in Ref. [82]. In Ref. [83] an approximate energy method for finding the relationship between the force parameter and the amplitude of steady-state oscillations of nonlinear, nonconservative, autonomous systems was suggested. Stability criteria on the basis of "equivalent energy" conditions were established in Ref. [21].

CHAPTER VII

POSSIBILITIES OF PHYSICAL REALIZATION

7.1 Introduction

It is a peculiar common feature of much published analytical work on the dynamics and stability of mechanical systems with follower forces, that the possible physical origin of such forces is not mentioned. The follower forces are introduced into the analysis either through a sketch, with forces being merely indicated by arrows, or through a specified functional dependence of the forces on generalized coordinates. Thus the problem is reduced immediately to a mathematical analysis and the relationship to mechanics (as a branch of physics or engineering) becomes most tenuous. The motivation for much of this type of work appears to have been sheer curiosity in determining the sometimes unexpected behavior of an imagined system, rather than an explanation of observed phenomena.

This clearly unsatisfactory state of imbalance in the development of an area of applied mechanics can be rectified by paying, as a first step, attention to the possible physical origin of the follower forces which are introduced into the analysis and building, as a second step, actual demonstration models, to be followed by a quantitative experimental program.

Let us discuss in this Chapter some possible origins of follower forces. If the mechanical system should be able to lose a position of equilibrium through oscillations with increasing amplitudes, a source of energy should be coupled, through the follower forces, to the system. In one category of problems involving rotating shafts this energy is supplied by the driving motor and stability is lost by lateral oscillations. This category of problems is deliberately not covered in this report.

In another category, the energy is supplied through a moving fluid to the mechanical system. If the fluid surrounds the mechanical system whose stability is being studied, the problem belongs to the broad and technically most significant area of aeroelasticity. The kinetic energy of a fluid can be transferred to the system also through internal flow in flexible pipes and by means of impinging jets. Some of these possibilities will be discussed presently.

It is conceivable that other forms of energy, such as, e.g., chemical and electro-magnetic energy, could constitute appropriate sources which, under suitable conditions of coupling, could induce flutter-type instabilities. Among all these possibilities, the author is aware only of some recent work on instability (including flutter) of bars induced by radiant heat, as mentioned in Sect. 7.4.

7.2 Instability Modes of Cantilevered Bars Induced by Fluid Flow Through Attached Pipes

7.2.1 General

Let us discuss, as an example, the problem stated in the above heading. This particular example has been chosen, because various types of instabilities occur in a richer variety than, e.g., in a single, axi-symmetric flexible pipe conducting fluid, a system discussed in Chapter VIII since some actual experiments have been reported. It will be shown that a cantilevered bar having two axes of symmetry may lose stability by either torsional divergence, torsional flutter or transverse flutter, but not transverse divergence. The Coriolis forces can have either a stabilizing or a destabilizing effect on both the torsional flutter and the transverse flutter, depending upon the parameters of the system [84]. Stability of a similar bar subjected to a single eccentric follower force was discussed in Ref. [85]. The treatment can be considered a special case of no Coriolis forces.

7.2.2 Derivation of Equation of Motion and Boundary Conditions

We consider a thin-walled, cantilevered, elastic beam with two pairs of flexible pipes, which are attached to the bar at a distance h/2 from the z-axis (so that the whole system deforms as a unit) and pump fluid at a constant velocity U through the pipes, as sketched in Fig. 7.1. We designate the length of the system by L, the torsional rigidity by $C = GJ$, and the warping rigidity by $C_1 = EC_w$, [86], and similar to the work of Benjamin [80] obtain the equation of torsional motion of the system, using Hamilton's principle. With $\varphi(z,t)$ denoting the angle of rotation at section z and at time t, the strain energy of the torsional deformation is [87]

$$V_1 = \frac{1}{2}\int_o^L [C_1(\varphi'')^2 + C(\varphi')^2]\, dz \tag{7.1}$$

where primes denote differentiation with respect to z. The kinetic energy is

$$T_1 = \frac{1}{2}\int_o^L mr^2(\dot{\varphi})^2\, dz \tag{7.2}$$

where a dot denotes differentiation with respect to time, m is the mass of the assembly per unit of length (exclusive of the mass of the fluid), and r is the polar radius of gyration of the cross-section of the system.

The total kinetic energy of the fluid may be obtained by adding to the kinetic energy of the fluid contained within the pipes, T_2, the change in the kinetic energy of the fluid entering and leaving the pipes during a very small interval of time Δt:

$$T' = T_2 + 2MU\left(\frac{1}{2}U_o^2 - \frac{1}{2}U_i^2\right)\Delta t \tag{7.3}$$

where T' is the total kinetic energy of the fluid, M the mass density of the fluid per unit length of each pair of pipes, $\vec{U}_o$ the outlet velocity vector, and $\vec{U}_i$ the inlet velocity vector. But $\vec{U}_i = U\hat{i}$, where $\hat{i}$ is the unit vector in the z-direction, and $\vec{U}_o = \dot{\vec{r}} + nU\hat{\tau}$ where $\hat{\tau}$ is the unit vector tangent to the top (bottom) pipe at $z = L$, $\vec{r}$ is the position vector of the top (bottom) pipe at $z = L$, and n is the ratio of the area of each pipe to that of the attached nozzle at the free end. Hence, $\delta T'$ becomes

$$\delta T' = \delta T_2 + 2MU(\dot{\vec{r}} + nU\hat{\tau}) \cdot \delta\vec{r} \tag{7.4}$$

The components of the absolute velocity of the fluid are $\dot{y} + U(\partial y/\partial z)$ in the y-direction, and $U\left[1 - \frac{1}{2}(y')^2\right] - \dot{w}$ in the z-direction, where $w(z,t)$ denotes the average displacement at section z and at time t in the z-direction. T_2 then becomes (within an additive constant)

$$T_2 = 2M\int_o^L \left(\frac{1}{2}\dot{y}^2 + U\dot{y}y' - U\dot{w}\right)dz$$

But $y = (h/2)\varphi$, which yields

$$T_2 = 2M\int_o^L \left[\frac{h^2}{8}\dot{\varphi}^2 + \frac{Uh^2}{4}\dot{\varphi}\varphi' - U\dot{w}\right]dz \tag{7.5}$$

With $\hat{j}$ being the unit vector along the y-axis, we have (see Fig. 7.1)

$$\hat{\tau} = \hat{j}\sin\theta + \hat{i}\cos\theta = \hat{j}(y')_{z=L} + \hat{i}$$

$$= \left[\frac{h}{2}\varphi'(L)\right]\hat{j} + \hat{i}$$

$$\vec{r} = \hat{j}(y)_{z=L} - \hat{i}(w)_{z=L} = \left[\frac{h}{2}\varphi(L)\right]\hat{j} - \left[w(L)\right]\hat{i}$$

Then

$$(\dot{\vec{r}} + nU\hat{\tau}) \cdot \delta\vec{r} \approx -nU\,\delta w(L) + \frac{h^2}{4}\left[\dot{\varphi}(L) + nU\,\varphi'(L)\right]\delta\varphi(L) \tag{7.6}$$

where $\dot{w}(L)\delta w(L)$ is neglected (being a term of higher order). The Lagrangian now becomes

$$L = T_1 + T_2 - V_1 + 2MnU^2 w(L) \tag{7.7}$$

and Hamilton's principle takes on the form

$$\delta \int_{t_1}^{t_2} L dt - \int_{t_1}^{t_2} MU \frac{h^2}{2} \left[\dot{\varphi}(L) + nU\, \varphi'(L)\right] \delta\varphi(L) dt = 0 \tag{7.8}$$

where

$$w(L) = \frac{1}{2} \int_o^L r^2 (\varphi')^2 dz$$

Carrying out the variations and using integration by parts, we obtain

$$C_1 \frac{\partial^4 \varphi}{\partial z^4} + \left[2MnU^2 r^2 - C\right] \frac{\partial^2 \varphi}{\partial z^2} + MUh^2 \frac{\partial^2 \varphi}{\partial z \partial t} + \left(mr^2 + M \frac{h^2}{2}\right) \frac{\partial^2 \varphi}{\partial t^2} = 0$$

$$\varphi = \frac{\partial \varphi}{\partial z} = 0; \qquad z = 0$$

$$\left.\begin{aligned} &\frac{\partial^2 \varphi}{\partial z^2} = 0 \\ &C_1 \frac{\partial^3 \varphi}{\partial z^3} \left[MnU^2 \left(2r^2 - \frac{h^2}{2}\right) - C\right] \frac{\partial \varphi}{\partial z} = 0 \end{aligned}\right\} \quad z = L \tag{7.9}$$

We now introduce the following dimensionless quantities:

$$\xi = \frac{z}{L}$$

$$\tau = t \sqrt{\left[\frac{C_1}{[mr^2 + (h^2/2)M] L^4}\right]}$$

$$\varkappa = \frac{CL^2}{C_1}$$

$$\alpha = \frac{h}{r}, \qquad \beta = \frac{M}{m}$$

$$\beta' = \frac{\beta}{1 + (\alpha^2/2)\beta}, \quad \text{and} \quad F = \frac{MnU^2 r^2 L^2}{C_1}$$

Equations (7.9) then become

$$\frac{\partial^4\varphi}{\partial\xi^4} + [2F-\varkappa]\frac{\partial^2\varphi}{\partial\xi^2} + \sqrt{\left(\beta'\frac{F}{n}\right)}\,\alpha^2\frac{\partial^2\varphi}{\partial\xi\partial\tau} + \frac{\partial^2\varphi}{\partial\tau^2} = 0$$

$$\varphi = \frac{\partial\varphi}{\partial\xi} = 0; \qquad \text{at } \xi = 0$$

$$\left.\begin{aligned} &\frac{\partial^2\varphi}{\partial\xi^2} = 0 \\ &\frac{\partial^3\varphi}{\partial\xi^3} + \left[F\left(2 - \frac{\alpha^2}{2}\right) - \varkappa\right]\frac{\partial\varphi}{\partial y} = 0 \end{aligned}\right\} \quad \xi = 1 \tag{7.10}$$

which are analogous to those obtained in Ref. [72] for cantilevered bars subjected at the free end to follower forces, except for the third term in the first equation, which is due to the Coriolis acceleration. As we shall see in the sequel, this term can have either a destabilizing or a stabilizing effect. That is, for sufficiently small Coriolis forces (n large and β' small) the system loses stability (by torsional or transverse flutter) under smaller F than obtained when $n = \infty$ (no Coriolis forces). On the other hand, for β'/n sufficiently large, the critical value of F can be increased by increasing β'/n.

We note here that, in torsional instability similar to transverse instability, the Coriolis forces have an effect similar to that of internal viscous damping [32]. That is, although damping (and also Coriolis forces) is a dissipating agency, when it is sufficiently small, it may act as a channel for the transfer of energy to the system from the source, which is always associated with the type of nonconservative forces considered here [71].

7.2.3 Stability Analysis

Frequency equation. We take the solution of system (7.10) as $\varphi(\xi,\tau) = \psi(\xi)e^{i\omega\tau}$ and obtain the following eigenvalue problem:

$$\frac{d^4\psi}{d\xi^4} + [2F-\varkappa]\frac{d^2\psi}{d\xi^2} + (i\omega)\sqrt{\left(\beta'\frac{F}{n}\right)}\,\alpha^2\frac{d\psi}{d\xi} - \omega^2\psi = 0$$

$$\psi = \frac{d\psi}{d\xi} = 0; \qquad \text{at } \xi = 0$$

$$\left.\begin{aligned} &\frac{d^2\psi}{d\xi^2} = 0 \\ &\frac{d^3\psi}{d\xi^3} + \left[F\left(2 - \frac{\alpha^2}{2}\right) - \varkappa\right]\frac{d\psi}{d\xi} = 0 \end{aligned}\right\} \quad \xi = 1 \tag{7.11}$$

We then let $\psi(\xi) = Ae^{i\lambda\xi}$ and obtain

$$\lambda^4 - (2F-\kappa)\lambda^2 - \omega\sqrt{\left(\beta'\frac{F}{n}\right)}\alpha^2\lambda - \omega^2 = 0 \tag{7.12}$$

Equation (7.12) is a polynomial of degree four in λ and therefore has, in general, four complex roots. Let these roots be designated by λ_j; $j = 1,2,\ldots,4$. Then,

$$\psi(\xi) = \sum_{j=1}^{4} A_j e^{i\lambda_j\xi}$$

which may now be substituted into the boundary conditions to yield four homogeneous equations for four constants A_j. These equations are

$$\begin{aligned}
&\sum_{j=1}^{4} A_j = 0 \\
&\sum_{j=1}^{4} \lambda_j A_j = 0 \\
&\sum_{j=1}^{4} \lambda_j^2 A_j e^{i\lambda_j} = 0 \\
&\sum_{j=1}^{4} (\lambda_j^2 - \eta)\lambda_j A_j e^{i\lambda_j} = 0
\end{aligned} \tag{7.13}$$

where $\eta = F(2-\alpha^2/2) - \kappa$. System (7.13) has nontrivial solutions if and only if the determinant of the coefficients of A_j; $j = 1,2,\ldots,4$ is identically zero, i.e., the frequency equation is

$$\begin{aligned}
\Delta \equiv\ & e^{i(\lambda_1+\lambda_2)}(\lambda_1^2\lambda_2^2+\eta\lambda_1\lambda_2)(\lambda_2-\lambda_1)(\lambda_4-\lambda_3) \\
& - e^{i(\lambda_1+\lambda_3)}(\lambda_1^2\lambda_3^2+\eta\lambda_1\lambda_3)(\lambda_3-\lambda_1)(\lambda_4-\lambda_2) \\
& + e^{i(\lambda_1+\lambda_4)}(\lambda_1^2\lambda_4^2+\eta\lambda_1\lambda_4)(\lambda_4-\lambda_1)(\lambda_3-\lambda_2)
\end{aligned} \tag{7.14}$$

cont.

$$+ e^{i(\lambda_2+\lambda_3)}(\lambda_2^2\lambda_3^2+\eta\lambda_2\lambda_3)(\lambda_3-\lambda_2)(\lambda_4-\lambda_1)$$

$$- e^{i(\lambda_2+\lambda_4)}(\lambda_2^2\lambda_4^2+\eta\lambda_2\lambda_4)(\lambda_4-\lambda_2)(\lambda_3-\lambda_1)$$

$$+ e^{i(\lambda_3+\lambda_4)}(\lambda_3^2\lambda_4^2+\eta\lambda_3\lambda_4)(\lambda_4-\lambda_3)(\lambda_2-\lambda_1) = 0 \qquad (7.14)$$

where λ_1, λ_2, λ_3, and λ_4 are defined as functions of ω through Eq. (7.12).

Torsional buckling. To obtain the condition for divergent torsional motion, we let $\omega = 0$ in Eq. (7.12) and obtain $\lambda_{1,2} = 0$, and $\lambda_{3,4} = \pm\sqrt{(2F-\varkappa)}$. Then, with $\varkappa = \delta\pi^2$ and $\bar{F} = 2F - \varkappa = \gamma\pi^2$, Eq. (7.14) reduces to

$$\alpha^2 = -\frac{4\gamma\cos\pi\sqrt{\gamma}}{(\gamma+\delta)(1-\cos\pi\sqrt{\gamma})} \qquad (7.15)$$

which is identical to the equation obtained for the torsional buckling of a cantilevered beam subjected at the free end to follower forces [72]. The first branch of the torsional buckling, corresponding to the first mode of instability, is shown by the solid line in Fig. 7.2.

Torsional flutter. For given α, β, n, δ and $\bar{F} = \gamma\pi^2$, Eqs. (7.12) and (7.14) yield the frequencies of torsional oscillations. When $\bar{F}$ is small, these frequencies are all located on the left hand side of the imaginary axis in the complex $i\omega$ plane and the system can perform only damped torsional oscillations.

As we increase $\bar{F}$, one of these frequencies approaches the imaginary axis, and for a certain value of $\bar{F}$, say $\bar{F}_{cr}$, Eqs. (7.12) and (7.14) yield a real value for ω. If we now increase $\bar{F}$ beyond this critical value, one of the roots of (7.14) becomes complex with negative imaginary part. The beam will oscillate with an exponentially increasing amplitude. Consequently, we shall seek, for given α, β, n, and δ, values of ω (real) and $\bar{F}$ which identically satisfy (7.12) and (7.14). This can be done directly with the aid of a computer. The computer can be instructed to find the roots of Eq. (7.12) for specified values of α, β, n, δ, ω, and γ, and then compute the value of Δ. By varying the value of ω and γ systematically, the critical ω and γ may easily be selected which make both real and imaginary parts of Δ identically zero. This is illustrated in Fig. 7.3 where for $\alpha = 1.50$, $\delta = 1.0$, $\beta = 1.0$, and $n = 1$, both real and imaginary parts of $\Delta = \Delta_1 + i\Delta_2$ are plotted against the values of ω^2. We see that for $\gamma = 3.40$, and $\omega^2 = 1.13\pi^4$, Δ is identically zero. Similar results may be obtained for other values of α, β, and n. In this manner torsional flutter curves may be constructed. The first branch

(the only practically significant one) of torsional flutter is shown in Fig. 7.2 by dashed lines, for $\delta = 1$, $n = 1$, and indicated values of β. The solid curve for torsional flutter in Fig. 7.2 is the limiting case when $n = \infty$ and corresponds to the torsional flutter of a cantilevered bar subjected at the free end to compressive follower forces [72].

It must be noted that, even for relatively large values of $\beta(n=1)$, the Coriolis forces may have a destabilizing effect for certain values of α. (For example, for $\beta = 0.1$ and $1.0 < \alpha < 1.35$, as is seen in Fig. 7.2.)

Transverse flutter. In addition to torsional buckling and torsional flutter, the bar may lose stability also by transverse flutter [87]. The equation of motion and the boundary conditions for this case have been derived by employing Hamilton's principle in [80] and D'Alembert's principle in [87]. Here, we may simply identify C_1 with EI, $\varphi(z,t)$ with $y(z,t)$ and write

$$EI \frac{\partial^4 y}{\partial z^4} + 2MnU^2 \frac{\partial^2 y}{\partial z^2} + 4MU \frac{\partial^2 y}{\partial z \partial t} + (2M + m) \frac{\partial^2 y}{\partial t^2} = 0$$

$$y = \frac{\partial y}{\partial z} = 0; \qquad \text{at } z = 0$$

$$\frac{\partial^2 y}{\partial z^2} = \frac{\partial^3 y}{\partial z^3} = 0; \qquad \text{at } z = 0$$

which, by introducing the following dimensionless quantities:

$$\xi = \frac{z}{L}, \qquad \tau = t \sqrt{\left[\frac{EI}{(2M+m)L^4}\right]}$$

$$F_1 = \frac{MnU^2L^2}{EI}, \qquad \beta = \frac{M}{m}, \qquad \beta'' = \frac{2\beta}{2\beta+1}$$

reduces to

$$\frac{\partial^4 y}{\partial \xi^4} + 2F_1 \frac{\partial^2 y}{\partial \xi^2} + \sqrt{\left(\frac{8\beta''}{n} F_1\right)} \frac{\partial^2 y}{\partial \xi \partial \tau} + \frac{\partial^2 y}{\partial \tau^2} = 0$$

$$y = \frac{\partial y}{\partial \xi} = 0; \qquad \xi = 0$$

$$\frac{\partial^2 y}{\partial \xi^2} = \frac{\partial^3 y}{\partial \xi^3} = 0; \qquad \xi = 1$$

Equation (7.12) now becomes

$$\lambda^4 - 2F_1\lambda^2 - \omega\sqrt{\left(\frac{8\beta''}{n}F_1\right)}\,\lambda - \omega^2 = 0 \qquad (7.12')$$

and equation (7.14) takes on the form

$$\begin{aligned}\Delta = {} & e^{i(\lambda_1+\lambda_2)}\lambda_1^2\lambda_2^2(\lambda_2-\lambda_1)(\lambda_4-\lambda_3) \\ & - e^{i(\lambda_1+\lambda_3)}\lambda_1^2\lambda_3^2(\lambda_3-\lambda_1)(\lambda_4-\lambda_3) \\ & + e^{i(\lambda_1+\lambda_4)}\lambda_1^2\lambda_4^2(\lambda_4-\lambda_1)(\lambda_4-\lambda_2) \\ & + e^{i(\lambda_2+\lambda_3)}\lambda_2^2\lambda_3^2(\lambda_3-\lambda_2)(\lambda_4-\lambda_1) \\ & - e^{i(\lambda_2+\lambda_4)}\lambda_2^2\lambda_4^2(\lambda_4-\lambda_2)(\lambda_3-\lambda_1) \\ & + e^{i(\lambda_3+\lambda_4)}\lambda_3^2\lambda_4^2(\lambda_4-\lambda_3)(\lambda_2-\lambda_1) = 0\end{aligned} \qquad (7.14')$$

For a given β and n, we now seek values of ω and F_1 which identically satisfy (7.12′) and (7.14′). In this manner we obtain the limit of transverse flutter, as shown by horizontal dashed lines in Fig. 7.2 for $EIr^2/C_1 = 1.5$ and $\beta = 0.1, 0.2$. In this figure, the horizontal solid line indicates the limit of transverse flutter for $n = \infty$ [72]. We note that for $\beta = 0.5, 1.0$, the transverse flutter occurs at $\gamma = 12.2$, and 15.8 respectively. These values are not shown in Fig. 7.2.

7.2.4 Analysis of Flutter by Indirect Method

The method used in the previous section for the analysis of flutter was a direct one. That is, for a given system we directly obtained the critical values of γ and ω. One may solve the same problem by an indirect method which was employed in [87].

To this end we let λ_j; $j = 1,2,\ldots,4$ denote the roots of Eq. (7.12). Then we have

$$\lambda_1 + \lambda_2 + \lambda_3 + \lambda_4 = 0$$

$$\lambda_1\lambda_2 + \lambda_1\lambda_3 + \lambda_1\lambda_4 + \lambda_2\lambda_3 + \lambda_2\lambda_4 + \lambda_3\lambda_4 = -(2F-\varkappa)$$

$$\lambda_1\lambda_2\lambda_3 + \lambda_1\lambda_2\lambda_4 + \lambda_1\lambda_3\lambda_4 + \lambda_2\lambda_3\lambda_4 = \sqrt{\left(\beta' \frac{F}{n}\right)}\,\alpha^2\omega \qquad (7.16a)$$

$$\lambda_1\lambda_2\lambda_3\lambda_4 = -\omega^2$$

The first equation in (7.16a) is identically satisfied if we let

$$\lambda_1 = a - b - c$$

$$\lambda_2 = -a + b - c \qquad (7.16b)$$

$$\lambda_3 = -a - b + c$$

$$\lambda_4 = a + b + c$$

and from the remaining equations we obtain

$$a^2 + b^2 + c^2 = \frac{2F-\varkappa}{2}$$

$$abc = \frac{1}{8}\sqrt{\left(\beta' \frac{F}{n}\right)}\,\alpha^2\omega \qquad (7.16c)$$

$$a^4 + b^4 - 2a^2b^2 - 2b^2c^2 - 2c^2a^2 = -\omega^2$$

We now let

$$a = \frac{1}{2}(p + iq)$$

$$b = \frac{1}{2}(p - iq) \qquad (7.16d)$$

and from (7.16c) obtain

$$p^2 - q^2 + 2c^2 = 2F - \varkappa$$

$$(p^2 + q^2)c = \frac{1}{2}\sqrt{\left(\beta' \frac{F}{n}\right)}\,\alpha^2\omega \qquad (7.16e)$$

$$(p^2 - c^2)(q^2 + c^2) = \omega^2$$

where p, q, and c are all real. Substituting from (7.16d) into (7.16b) and then into the frequency equation (7.14), we finally arrive at, after a series of tedious manipulations,

$$\Delta \equiv \Delta_1 + i\Delta_2 = 0$$

where:

$$\begin{aligned}
\Delta_1 &= cp \{2 [3p^2q^2 - q^4 - c^2(p^2 + q^2) + 4c^4] + (p^2 - 3q^2 - 4c^2)\eta \} \cos p \sinh q \\
&+ cq \{2 [p^4 - 3p^2q^2 - c^2(p^2 + q^2) - 4c^4] - (3p^2 - q^2 - 4c^2)\eta \} \sin p \cosh q \\
&+ pq \{[(p^2+q^2)(q^2 - p^2 + 2c^2)] + (p^2 + q^2)\eta \} \sin 2c \\
\Delta_2 &= \{[p^2q^2(q^2 - p^2) + c^2(p^4 + q^4 - 6p^2q^2) - 3c^4(p^2 - q^2) - 4c^6] \qquad (7.17) \\
&+ [2p^2q^2 - c^2(p^2 - q^2) + 4c^4]\eta \} \sin p \sinh q \\
&+ pq \{2 [-p^2q^2 + 3c^2(p^2 - q^2) - 7c^4] - [p^2 - q^2 - 2c^2]\eta \} \cos p \cosh q \\
&- pq \{[p^4 + q^4 + 2c^2(q^2 - p^2) + 2c^4] - [p^2 - q^2 - 2c^2]\eta \} \cos 2c
\end{aligned}$$

For an assumed value of c and given α and $\kappa = \delta\pi^2$, we may now find p and q such that $\Delta_1 = \Delta_2 = 0$. Then, from equations (7.16e) the corresponding values of F, β, and ω, for a given n, may be computed.

The above method is an indirect one, as we do not know, in advance, which particular problem is being investigated. Moreover, if a computer is being used to find values of p and q which satisfy $\Delta_1 = \Delta_2 = 0$, it is then just as easy to employ the direct method outlined in the previous section. However, for small values of Coriolis forces, that is for sufficiently small $\sqrt{(\beta'/n)}$, one may reduce Eqs. (7.17) by neglecting the higher order terms in c and study the effect of small Coriolis forces directly. This we shall discuss in the following section.

7.2.5 The Effect of Small Coriolis Forces

We consider equation (7.17) and by neglecting $O(c)^2$ and higher order terms obtain

$$\bar{\Delta}_1 = p\{2[3p^2q^2 - q^4] + [p^2 - 3q^2]\eta\}\cos p \sinh q$$
$$+ q\{2[p^4 - 3p^2q^2] + [q^2 - 3p^2]\eta\}\sin p \cosh q$$
$$+ 2pq\{(q^4 - p^4) + (p^2 + q^2)\eta\} = 0 \qquad (7.18)$$
$$\bar{\Delta}_2 = pq[(q^2 - p^2) + 2\eta]\sin p \sinh q$$
$$+ [-2p^2q^2 - (p^2 - q^2)\eta]\cos p \cosh q$$
$$- [p^4 + q^4 - (p^2 - q^2)\eta] = 0$$

where

$$p^2 = \sqrt{\left(\omega^2 + \bar{F}\frac{2}{4}\right)} + \frac{\bar{F}}{2}$$
$$q^2 = \sqrt{\left(\omega^2 + \bar{F}\frac{2}{4}\right)} - \frac{\bar{F}}{2} \qquad (7.19)$$

The second equation in (7.18) is the frequency equation for $n = \infty$, (no Coriolis forces [72]), and the first equation, to the first order of approximation in $\sqrt{(\beta'/n)} = O(c)$, presents the effect of sufficiently small Coriolis forces. We note that $\bar{\Delta}_1$ and $\bar{\Delta}_2$ are both independent of c and, therefore, we may directly seek values of ω and $\bar{F}$ which make them identically zero. This is illustrated in Fig. 7.4 for $\alpha = 1.5$, where the critical load is found to be $\gamma = 1.67$. In Fig. 7.5, the critical load γ is plotted against α for sufficiently small Coriolis forces (the dashed curve). The solid curve for torsional flutter in this figure is for the limiting case of $n = \infty$ [72]. We note that the existence of Coriolis forces does not alter the region of divergent motion, as is expected. However, it makes this region a closed set, that is, in the presence of Coriolis forces, the points on the divergent curve indicate neutrally stable states. The horizontal solid line in Fig. 7.5 denotes the limit of transverse flutter for $n = \infty$, and the horizontal dashed line indicates that limit for sufficiently small Coriolis forces [32], (for $EI_x r^2/C_1 = 1.5$).

It may be of interest to obtain the critical values of γ for $\beta = \infty$ and $n = 1$. This, of course, provides the upper limit of torsional and transverse flutter. The dotted curve in Fig. 7.5 represents this limiting case for $\delta = 1$. We note that transverse flutter, for $\beta = \infty$ and $n = 1$, occurs at $\gamma \approx 47$, which is not shown in Fig. 7.5.

7.3 Stability of a Bar in Parallel Fluid Flow, Taking into Consideration the Head Resistance

The problem of a cantilevered bar placed in a fluid flow was analyzed by Kordas [88]. The head resistance was assumed to be represented by pure follower force, which was not further related to any parameters of the bar or the fluid. Piston theory [89] was assumed to characterize lateral pressure on the bar. The continuous system was replaced by a system with two degrees of freedom and stability limits in terms of relevant parameters of the problem were calculated.

7.4 Stability of Bars Subjected to Radiant Heat

In a recent paper Augusti [90] has suggested a special construction of the links of an articulated bar, which would make it sensitive to radiant heat. The links are made up of cells; the heat absorbed by each cell causes thermal deformations which induce a relative rotation of the two adjacent bars. An interesting feature of the resulting equations, e.g., for a bar with two degrees of freedom, is that derivatives of generalized coordinates (angles of rotation) up to third order are introduced. Depending upon the combination of relevant parameters, stability can be lost by flutter or by divergence.

Thermally induced vibration and flutter of flexible booms were discussed by Yu [91] and commented on by Augusti [92], where further references to this phenomenon can be found.

CHAPTER VIII

LABORATORY EXPERIMENTS AND MODELS

8.1 Introduction

As already mentioned, it is the intent to discuss in this monograph only those problems involving follower forces which do not belong to the now almost classical areas of aeroelasticity and stability of rotating shafts. If we omit these two categories, the only two remaining areas of problems with follower forces which have been realized to date involve internal flow through flexible pipes and fluid jets impinging on a deformable structure.

As regards the former area, mention should be made above all of the pioneering work by Benjamin [80,93] on the dynamics of a system of articulated cantilevered pipes conveying fluid in which both divergence and flutter were observed and stability boundaries were determined analytically and also by means of quantitative experiments. Benjamin's work was continued by Gregory and Paidoussis [87,94] who studied theoretically and experimentally continuous tubular cantilevers conveying fluid. One should also recall the earlier work by Long [95] on vibration of a tube containing flowing fluid, who, however, did not observe any instabilities, being interested only in the influence of the fluid flow on frequencies of vibration. Divergence of a simply supported pipe conveying fluid was observed more recently by Dodds and Runyan [96]. Simply supported and cantilevered pipes conveying fluid were investigated also by Greenwald and Dugundji [97].

The dynamics and stability of slender cylinders surrounded by, rather than containing, flowing fluid was studied analytically and experimentally by Paidoussis [98-100]. He points out that, provided the flow direction coincides with the axis of the cylinder at rest, then, for small motions about the position of rest, the forces exerted by the fluid in the two cases of external and internal flow are closely similar. This becomes evident on considering that the forces exerted by the fluid, excepting those due to fluid friction, in both cases arise from lateral acceleration of the flowing fluid, caused by lateral motion of the cylinder. In external flow, this acceleration is suffered by the virtual or "associated" mass of fluid, which is dynamically equivalent to the contained mass of fluid in internal flow. Hawthorne [101], taking advantage of this similarity, investigated the stability of flexible tubes towed in water and demonstrated that divergence instability is possible in such systems.

In this context it is deemed appropriate to mention some related but considerably more complex hydro-elastic-pneumatic problems arising in structural dynamics of launch vehicles studied by Runyan, Pratt and Pierce [102], as well as the broad area of propeller-rotor whirl flutter, a comprehensive review of which was recently prepared by Reed [103].

The mechanics of impinging jets was studied to date from the point of view of fluid behavior, one of the goals being the determination of the pressure distribution at a rigid surface. By contrast, in a recent study [104] the interest centered on the behavior of a primarily elastic structure subjected to an impinging jet. Quantitative experiments were carried out and compared with theoretical predictions, as described in the following section.

8.2 Instability of a Mechanical System Induced by an Impinging Fluid Jet

8.2.1 General

The mathematical model of the physical system considered here may be called Reut's problem, mentioned already in Sect. 6.2. It consists of a cantilever with a rigid plate at its free end, which is normal to the axis. It is subjected to a force, acting on the plate, which is always collinear with the undeformed axis of the cantilever, Fig. 8.1. Bolotin [8] reports that this problem was first posed by Reut in 1939 and solved by Nikolai in the same year. In this context, Bolotin suggests that the force in Reut's problem may be realized by an impinging jet of absolutely inelastic particles, since the kinetic energy of the particles is completely absorbed upon impact. It appears, however, that no attempt was ever made to follow up these suggestions, or to realize Reut's problem in any other way. Bolotin also suggests that the pressure from a jet of liquid or gas may induce such a force when the inclination of the force, as the bar deforms, is neglected.*

In an attempt to construct models based on these ideas, it was discovered that by covering the plate with screens of certain mesh sizes a problem very close to the Reut's one may be realized. The resultant force, in this case, has an inclination which can be controlled by a suitable arrangement of screens of various mesh sizes; the point of application of the resultant force, however, always lies on the axis of the undeformed cantilever. When this force stays normal to the end plate, the system loses stability by divergence (attainment of another equilibrium state); the force is conservative. On the other hand, if the force stays collinear with the undeformed axis of the bar, the loss of stability occurs by flutter (oscillations with increasing amplitudes); the force is nonconservative. By controlling the inclination of the force, various degrees of nonconservativeness may be attained.

The experimental results are obtained using a system with two degrees of freedom, rather than a continuous cantilever. The applied force is induced by an impinging air jet. The degree of nonconservativeness is controlled by employing suitable end attachments, resulting in either divergent or flutter-type motions of the system. Also, the effect of viscous damping forces is investigated. It is found that the experimentally obtained flutter load corresponds rather closely to the theoretical prediction when small dissipative forces are

---

* This, of course, is not acceptable, since it is precisely the presence of the component of the force in the direction normal to the impinging fluid that, in this case, renders the system conservative.

included; this confirms the earlier findings that small damping forces may have a destabilizing effect.

8.2.2 Description of Model and Supporting Equipment

The model consists of two like rigid rods, Fig. 8.2. One rod is elastically hinged to the first rod and free at the other end. The system is constrained to move in a horizontal plane, being supported by long, light wires. Various rigid attachments can be placed at the free end of the second rod. The attachment consists basically of a rigid flat plate covered with a combination of screens of various mesh sizes. This attachment is rigidly fixed and mounted normal to the axis of the second rod. In the absence of any disturbance, the system is in equilibrium when the two rods are collinear (undisturbed configuration).

A fixed nozzle is placed along the equilibrium axis of the system, one inch away from the attachment, and an air jet is made to impinge upon the attachment. The flow rate can be varied by means of a valve. The dynamic pressure at the nozzle corresponding to a given flow rate can be read from a dial gage.

It is observed that as the flow rate, and hence the force on the attachment, is increased and passes a certain (critical) value, the system does not remain in the undisturbed configuration. Stability is lost by either flutter (oscillations with increasing amplitudes) or by divergence (buckling - the attainment of another equilibrium state), depending on the nature of the attachment used. If the attachment is a flat plate with a smooth surface (a flat sheet of aluminum) facing the air jet, then the loss of stability occurs by divergence. By contrast, flutter-type motion is observed if the attachment is a plate with screens of certain mesh sizes placed on the surface that faces the impinging fluid. The sequence of photographs in Fig. 8.3 illustrates the flutter-type motion, while Fig. 8.4 depicts a buckled state (divergence). Fig. 8.5 and Table 2 present the numerical values for all the relevant properties of the system.

The supporting equipment consists of a calibrating system which is used to correlate the dynamic pressure, hence the flow rate, with the actual force which acts on the system. Three square steel plates are placed horizontally one above the other, and are separated and supported by sets of steel leaf springs. The steel leaf springs connecting the two lower plates permit displacement in only one direction, while those connecting the upper two plates permit displacement only in the perpendicular direction. Two stages are thus formed. The displacement of each stage is, with a high degree of accuracy, proportional to the component of the force which acts along the direction of the displacement. With the aid of a pair of strain gages attached to the steel leaf springs, and using a compensating network, readings can be taken which are proportional to the respective displacements of each stage. In this manner, strain-gage readings can be related to the magnitude of the force acting on the system.

The supporting equipment just described is used to find the direction and the magnitude of the force on the attachment when the dynamic pressure of the impinging air jet at the nozzle is known. The attachment is mounted on the top plate of the supporting stages and then subjected to the air jet at a given angle of incidence, Fig. 8.6. The magnitude and the direction of the resultant force corresponding to a given angle of incidence and for a given dynamic pressure are thus obtained experimentally.

8.2.3 Theory

As already mentioned, the problem of a cantilever with a rigid cross plate at its free end and subjected to a force which is always directed along the initial, undeformed axis of the cantilever, was first posed by Reut in 1939. It is essential to note that the applied force in Reut's problem is not attached to a material point of the system, but rather to a line in space. In structural mechanics, boundary-value problems are commonly posed for surface tractions which are connected to the material points upon which they act. As a result, the difference between the displacements of the material points and of the points of application of the forces disappears.

In the present problem, the force is induced by the action of an air jet upon the end plate. It may be assumed that such an action is equivalent to a resultant force whose point of application lies always on the axis of the undeformed system; that is, along the direction of the flow. This force continuously disengages from the material point on which it is instantaneously acting. This force is conservative only if it stays normal to the end plate as the system deforms. In the subsequent analysis, we will denote this force by P and the angle by which it rotates, as the system deforms, by $\alpha\varphi_2$.

We consider small lateral motions of the system as shown in Fig. 8.5. The rigid bar, designated by I, is connected to the support by a rotational spring of stiffness K_1 and carries at its other end a rotational spring of stiffness K_2 to which is attached another rigid rod, designated as II. In addition, rods I and II are connected to two linear coil springs as shown in Fig. 8.5. Since the displacement of the spring connected to bar I is not coupled with the motion of bar II, the stiffness K_1 properly accounts for the effect of this spring. The spring connected to bar II is located at a distance d_2 from the center of the middle joint and has stiffness K_3.

The inertial properties are represented by seven masses m_j, $j = 1,2,\ldots 7$, and seven centroidal moments of inertia I_j, $j = 1,2,\ldots 7$. The mass of the end rotational spring is denoted by m_1, and that of the rod I is denoted by m_2. The central rotational spring has in effect two masses m_3 and m_4 which are attached to the rods I and II, respectively. The mass of the rod II is m_5, and m_6 is that of the collar which fits the attachment having mass m_7.

The distance between the centers of the end and the middle rotational springs is denoted by ℓ_1, while the mass m_7 is at a distance ℓ_2 from the center of the middle joint. The dimensions a_1, b_1, and c_1 are the distances from the center of the end joint to masses m_1, m_2, and m_3, respectively, while a_2, b_2, and c_2 designate the respective distances of m_4, m_5, and m_6 from the center of the middle joint.

The two rotational springs were made of high tempered spring steel with identical geometry and, therefore, they have small damping with, plausibly, the same damping constant ϵ_1. Since the attachment has a large surface area which moves relative to the impinging air jet, an external linear damping with constant ϵ_2 appears to be a reasonable representation of the corresponding damping mechanism.

The magnitude of the force due to the impinging air jet is P, the direction of which encloses an angle $\alpha\varphi_2$ with the undeformed axis. α is assumed to be a constant which will be determined experimentally with the help of the auxiliary equipment as described in Sect. 8.2.4. φ_1 and φ_2 are the respective rotations of bars I and II from the initial straight position.

The following equations of motion are obtained by employing D'Alembert's principle:

$$\begin{aligned} A_{11}\ddot{\varphi}_1 + A_{12}\ddot{\varphi}_2 + B_{11}\dot{\varphi}_1 + B_{12}\dot{\varphi}_2 + (C_{11} - P\ell_1)\varphi_1 + (C_{12} + P\ell_1\alpha)\varphi_2 &= 0 \\ A_{21}\ddot{\varphi}_1 + A_{22}\ddot{\varphi}_2 + B_{21}\dot{\varphi}_1 + B_{22}\dot{\varphi}_2 + (C_{21} + P\ell_1)\varphi_1 + (C_{22} + P\ell_2\alpha)\varphi_2 &= 0 \end{aligned} \tag{8.1}$$

where

$$\begin{aligned} A_{11} &= (m_4 + m_5 + m_6 + m_7)\ell_1^2 + m_1a_1^2 + m_2b_1^2 + m_3c_1^2 + I_1 + I_2 + I_3 \\ A_{12} &= A_{21} = (m_4a_2 + m_5b_2 + m_6c_2 + m_7\ell_2)\ell_1 \\ A_{22} &= m_4a_2^2 + m_5b_2^2 + m_6c_2^2 + m_7\ell_2^2 + I_4 + I_5 + I_6 + I_7 \\ B_{11} &= \epsilon_2\ell_1^2 + 2\epsilon_1 \\ B_{12} &= B_{21} = \epsilon_2\ell_1\ell_2 - \epsilon_1 \\ B_{22} &= \epsilon_2\ell_2^2 + \epsilon_1 \\ C_{11} &= K_1 + K_2 + K_3\ell_1^2 \end{aligned} \tag{8.2 cont.}$$

$$C_{12} = C_{21} = -K_2 + K_3 \ell_1 d_2$$

$$C_{22} = K_2 + K_3 d_2^2 \tag{8.2}$$

Undamped System - Flutter. Consider first the undamped case: i.e., let $\epsilon_1 = \epsilon_2 \equiv 0$. Then $B_{ij} = 0$. Assuming solutions of the form

$$\varphi_1 = \Phi_1 e^{i\omega t}$$

$$\varphi_2 = \Phi_2 e^{i\omega t} \tag{8.3}$$

where $i = \sqrt{-1}$, Φ_1 and Φ_2 are undetermined amplitudes, ω is an undetermined frequency and t is the time variable, the associated frequency equation is

$$a\omega^4 + b\omega^2 + c = 0 \tag{8.4}$$

where

$$a = A_{11}A_{22} - A_{12}^2$$

$$b = 2A_{12}C_{12} + A_{12}P\ell_1(1+\alpha) - A_{11}P\ell_2\alpha - A_{11}C_{22} - A_{22}C_{11} + A_{22}P\ell_1 \tag{8.5}$$

$$c = C_{11}P\ell_2\alpha - P^2\ell_1\alpha(\ell_1+\ell_2) - C_{12}P\ell_1\alpha - C_{12}P\ell_1 + C_{11}C_{22} - C_{12}^2 - C_{22}P\ell_1$$

Flutter occurs if ω is complex with a negative imaginary part. The threshold (critical) value of P, called P_*, is obtained by setting

$$b^2 - 4ac = 0 \tag{8.6}$$

and is

$$P_{*1,2} = \frac{2hk - fg}{f^2 - 4hj} \pm \frac{2}{f^2 - 4hj}\sqrt{h^2k^2 - hkfg - 4h^2jm + hjg^2 + hmf^2} \tag{8.7}$$

where

$$f = A_{12}\ell_1(1+\alpha) - A_{11}\ell_2\alpha + A_{22}\ell_1$$

$$g = 2A_{12}C_{12} - A_{11}C_{22} - A_{22}C_{11}$$

$$h = A_{11}A_{22} - A_{12}^2 \tag{8.8 cont.}$$

$$j = -\ell_1\alpha(\ell_1+\ell_2)$$

$$k = C_{11}\ell_2\alpha - C_{12}\ell_1\alpha - C_{12}\ell_1 - C_{22}\ell_1$$

$$m = C_{11}C_{22} - C_{12}^2 \tag{8.8}$$

As the value of P is increased, flutter will occur when P becomes equal to the lower value of P_*. Note that P_* is a function of α through equations (8.8). P_* exists only when the argument of the square root in Eq. (8.7) is nonnegative.

Damped System - Flutter. Using an assumed solution of the form (8.3) in Eqs. (8.1) results in the following determinant which is set equal to zero for a nontrivial solution:

$$\begin{vmatrix} -\omega^2A_{11} + C_{11} - P\ell_1 + i\omega B_{11} & -\omega^2A_{12} + P\ell_1\alpha + C_{12} + i\omega B_{12} \\ -\omega^2A_{12} + C_{12} + P\ell_1 + i\omega B_{12} & -\omega^2A_{22} + P\ell_2\alpha + C_{22} + i\omega B_{22} \end{vmatrix} = 0 \tag{8.9}$$

If we neglect the product of ϵ_1 and ϵ_2 in the expansion of (8.9), we obtain two equations by separating the real and imaginary parts. The first equation is the same as equation (8.4). The equation resulting from the imaginary part yields the following relation:

$$\omega^2 = \frac{B_{11}(P\ell_2\alpha+C_{22}) + B_{22}(C_{11}-P\ell_1) - B_{12}[P\ell_1(1+\alpha) + 2C_{12}]}{A_{22}B_{11} + A_{11}B_{22} - 2A_{12}B_{12}} \tag{8.10}$$

Substituting ω^2 from Eq. (8.10) into Eq. (8.4) and denoting by P_d the threshold values of P for this case, we obtain

$$P_{d_{1,2}} = -\frac{u}{2w} \pm \frac{1}{2w}\sqrt{u^2 - 4wv} \tag{8.11}$$

where

$$u = \frac{2hqr}{s^2} + \frac{qg + fr}{s} + k \tag{8.12}$$

cont.

$$v = \frac{hr^2}{s^2} + \frac{gr^2}{s} + m$$

$$w = \frac{hq^2}{s^2} + \frac{fq}{s} + j \tag{8.12}$$

and

$$q = \ell(3\epsilon\alpha - 2)$$

$$r = (1 + 2\epsilon)C_{22} + (1 + \epsilon)C_{11} - 2C_{12}(1 - \epsilon) \tag{8.13}$$

$$s = (1 + 2\epsilon)A_{22} + (1 + \epsilon)A_{11} - 2A_{12}(1 - \epsilon)$$

where

$$\epsilon \equiv \epsilon_1/\epsilon_2\ell^2 \quad \text{and} \quad \ell \equiv \ell_1 \approx \ell_2 \tag{8.14}$$

Thus, the critical force depends not only on α, but also on ϵ, essentially the ratio of the damping coefficients. The critical force is the lower of the two values of P_d and it exists only when the argument of the square root in Eq. (8.11) is nonnegative.

Divergence. For divergence, or buckling, ω is set equal to zero in Eq. (8.4). The condition is then

$$c = 0 \tag{8.15}$$

Denoting the value of P at which this occurs by P_b, we have

$$P_{b_{1,2}} = -\frac{k}{2j} \pm \frac{1}{2j}\sqrt{k^2 - 4jm} \tag{8.16}$$

where j, k, and m are defined by Eqs. (8.8).

As are P_* and P_d, P_b is also a function of α, but it is independent of the mass distribution. P_b exists only if $k^2 - 4jm \geq 0$.

Results. With the system parameters given, including the spring constants, which are determined experimentally (see Sect. 8.2.4), Eqs. (8.7), (8.11), and (8.16) must be solved for P for each specified value of α. This repetitious task was performed with the aid of a CDC 3400 computer.

As can be seen in Fig. 8.5, for $\alpha = 0$, the force P is always directed along the equilibrium line; i.e., the line defined by $\varphi_1 = \varphi_2 = 0$. When $\alpha = 1$,

the force is always perpendicular to the surface of the attachment. As discussed earlier, in the former case the force is nonconservative, while in the latter it is conservative. It turns out that with the present setup, experimentally realizable α are in the range $0.23 \leq \alpha \leq 0.91$.

Unfortunately, mechanical failure of the joints occurred during the advanced stage of experimental measurements and, consequently, when the model was reassembled, the spring constants K_1, K_2, and K_3 changed. Thus it became necessary to designate the previous model by system I and the reassembled model by system II. With due respect to the difference in system parameters, stability curves, P versus α, are shown in Figs. 8.12 and 8.13.

8.2.4 Experimental Procedure and Results

Correlation of Force With Air Pressure and Determination of α. To find the magnitude and the direction of the force acting on the attachment due to a given airflow rate, the supporting equipment described in Sect. 8.2.2 is used.

The nozzle assembly is detached from the model and mounted adjacent to the calibrating device, Fig. 8.6, parallel to the direction of motion of one of the stages. The rigid attachment is separated from the model and mounted on a special bracket on the top plate of the calibrating stages. This bracket may be rotated so that the angle between a normal to the attachment and the center line of the nozzle, namely φ_2, may be varied. Markings are provided for $\varphi_2 = 0, 5, 10, 15, 20, 25$, and 30 deg.

The first step is to find a relation between the displacement of the stages and the force applied to the top plate. This is done by applying known forces along the deflections of each stage and noting the strain-gage readings. If the direction parallel to the nozzle is designated by x and the perpendicular direction by y, relations of the form

$$P_x = S_1 \Delta e_x \qquad P_y = S_2 \Delta e_y \tag{8.17}$$

may be written. P_x and P_y are the forces, and Δe_x and Δe_y are the differences in strain-gage readings between no load and full load, for the x and y-directions, respectively. S_1 and S_2 are the proportionality constants.

The next step is to correlate the force, P, with the air pressure, p. From the free-body diagram of the attachment mounted on the calibrating system, Fig. 8.7, the following relations are obtained:

$$P_x(p) = P(p) \cos \alpha(p)\varphi_2 \qquad P_y(p) = P(p) \sin \alpha(p)\varphi_2 \tag{8.18}$$

where the force P has been split into its components P_x and P_y, which are functions of the pressure, p. The parameter α is assumed to be a function of p also. From Eqs. (8.18) we can write

$$\arctan\left[\frac{P_y}{P_x}(p)\right] = \alpha(p)\varphi_2 \tag{8.19}$$

For a given attachment and angle φ_2, strain-gage readings are taken for a set of pressures. These in turn yield the forces P_x and P_y corresponding to each pressure. The angle of incidence, φ_2, is then varied from 0-30 deg in 5-deg increments and for each value of φ_2 an average value for P_y/P_x is obtained over a range of pressures p. It turns out experimentally that P_x and P_y are linear functions of p, as one would expect, and thus the ratio P_y/P_x is independent of p. This means that α must be independent of p because of Eq. (8.19). If arctan P_y/P_x is plotted versus φ_2, the result is (very nearly) a straight line and, therefore, the slope may be interpreted as α in Eq. (8.19). α is a constant for a given attachment.

The critical force is read, or interpolated as the value of P_x at $\varphi_2 = 0$ corresponding to the critical value of pressure. For small φ_2, $P \approx P_x$; this is within the scope of the linearized theory.

In this manner, the value of α is obtained experimentally for each attachment.

Determination of Stiffnesses.

Dynamic Method. The spring constants K_1, K_2, and K_3 may be determined experimentally by a simple dynamic analysis of various motions of the system. The spring constant K_1 associated with the end joint and the linear spring attached to bar I may be evaluated by locking the middle joint so that the two bars move as a rigid unit, Fig. 8.8. After giving a small disturbance, the natural frequency is measured from which K_1 is determined. In a similar manner, the spring constant K_2 of the middle joint may be determined by locking the end joint, removing the linear spring attached to bar II and allowing the system to oscillate freely, Fig. 8.9.

Spring constant K_3 can be found if K_2 is known. The linear spring is attached to bar II in its original position and the natural frequency is measured. This gives an expression for the combined stiffness from which K_3 may be evaluated.

Static Method. An alternate procedure is to use a static method whereby forces are directly applied and the resulting deflection measured. The procedure is divided into three steps and is explained in Figs. 8.10 and 8.11.

Theoretically, these two methods should yield identical results. Experimentally, the results of the two methods differed slightly, Table 2. The static measurement is to be preferred because the dynamic method depends upon the square of experimentally measured frequencies which are not known with great accuracy.

Summary and Results. The basic steps in the experimental procedure are as follows: First, choose an attachment and mount it on the model. Raise the air pressure slowly from zero and note the critical pressure at which the system starts exhibiting amplified oscillations (flutter) or shows a static loss of stability (buckling). The supporting equipment is then used to find α and to find the force P corresponding to the critical pressure p. The spring constants are then determined experimentally for use in the theoretical analysis.

When choosing attachments, it is desirable that they all be of about the same weight and that a wide range of α be covered more or less uniformly. A wide variety of screens and sandpapers were weighed and combinations were chosen that met these requirements. The values of α which were experimentally realized lie in the range 0.238 to 0.913, the latter being for an attachment consisting of a smooth flat plate.

In Figs. 8.12 and 8.13, the experimental results are shown together with the theoretical curves. As was mentioned, two systems had to be considered because of a mechanical failure of the joints. For each experimental run a point of instability is drawn on the diagram at the corresponding α and P. A $\odot$ is used for a flutter point, while $\otimes$ is used to denote divergence. The measurements are labeled 1 through 8 for system I and 1 through 12 for system II.

Table 3 summarizes the experimental and theoretical results and provides a comparison between these results.

8.2.5 Discussion of Results, Conclusions and Recommendations

The results of this study are summarized in Figs. 8.12 and 8.13 and in Table 3. It is noted that the experimentally determined critical points lie somewhat below the theoretical stability curves for undamped flutter and divergence. In the discussion which follows, the possible reasons for this discrepancy are explored.

One of the primary reasons for the discrepancy between the theoretical stability curve for undamped flutter and the experimentally observed points of flutter appears to lie in the fact that damping is present in the physical system. The damping mechanism assumed in the analysis has already been discussed. Stability curves for flutter with small damping taken into account

are shown in Figs. 8.12 and 8.13 for several values of the damping ratio ϵ. It is seen from these figures that in the presence of damping the theoretical stability curves come to pass very near the experimental points. No attempt was made to determine ϵ with a high degree of accuracy since the assumed damping mechanism, while reasonable, was chosen mostly for its simplicity and it is doubtful that it represents completely the actual damping in the system. Supplementary experiments indicated that the assumed values of ϵ are realistic.

The results presented indicate that damping has a destabilizing effect on the system and that the presence of damping extends the flutter region to higher values of α. Also, the lower values of the damping ratio are associated with lower values of flutter loads and a wider flutter range. This confirms results shown previously in Chapter IV.

The theoretical curves bounding the regions of flutter (with and without damping) and divergence were found to be rather insensitive to small changes in system parameters, as indicated in Table 2, with the possible exception of the spring constants. The dynamic measurement of the spring constants provides another possible source for the discrepancy since the calculation depends on the square of a measured quantity; i.e., the frequency of free oscillations. But, the spring constants were determined also using the static method previously described. Difficulties may arise here, however, in measuring the applied force by means of hanging weights on a light string which passes over an air bearing.

Since the two methods of measuring the spring constants gave somewhat different results, Table 2, it was decided to investigate the effect of a 5 percent difference in either K_1, K_2, or K_3. A computer program was written in which each calculated spring constant was subjected to a $\pm$ 5 percent uncertainty. If an envelope is drawn about the nine curves thus obtained, the effect is roughly to give a maximum error of $\pm$ 6 gm (or $\pm$ 4 - 10 percent). No other system parameter, Table 2, is subject to an error approaching 5 percent, except possibly the moments of inertia, but these are insignificant when compared to the mass-times-distance-squared terms to which they are added.

The observed discrepancy between the theoretical curve for divergence and the experimental points may be due also, in part, to the uncertainty in the values of the spring constants, but the major cause of error seems to lie in the possibility of initial imperfections and nonlinear effects.

Since the physical model is not an ideal linear system free of imperfections, there is no single, sharply defined divergence load. An arbitrary criterion of the load required for a one-inch deflection of the middle joint was used as the condition for divergence. By this definition, the experimental points of divergence were somewhat below (15-25 percent) the divergence curves obtained from the linear analysis, Figs. 8.12, 8.13, and Table 3. In an attempt to explain this discrepancy it seems advisable to investigate the nonlinear divergence theory as well as the effects of initial imperfections. This is discussed in detail in the next section for $\alpha = 0.717$ (run 11).

The results of this investigation are shown in Fig. 8.14, with a detailed description of the curves given in Sect. 8.2.6. It is noted that the postulated criterion for divergence gives very nearly the same load for both the linear (curve A) and the nonlinear (curve B) cases, and thus the theoretical divergence curves given in Figs. 8.12 and 8.13 actually represent the divergence loads for the nonlinear theory in conjunction with the adopted criterion.

The strong effect of imperfections on the divergence load is discussed in Sect. 8.2.6. Initial imperfections in the amount $\varphi_{10} = 0.01$, $\varphi_{20} = -0.01$, as shown in curve D, are indeed reasonable for this model. This corresponds to a no-load deflection of about 0.1 inch at the middle joint. This small imperfection lowers the theoretical divergence load by about 15 percent.

Curve F is the experimental force-deflection curve for run 11. Note that the shape of the curve differs somewhat from the theoretical curves shown. It should be pointed out that the points used to draw this curve are rather difficult to obtain since holding the air pressure constant to obtain a deflection reading does not prevent the motion of the model. Since the run of the curve F is somewhat different from the other curves, the likelihood exists that other sources for the discrepancy may be present. It may be appropriate to mention here that it has been noted repeatedly in the past that structural systems buckle at loads below those theoretically expected.

To provide better insight into the discrepancy under discussion, the experimental procedure was also scrutinized. The method of correlating the air pressure as read on the dial gage, to the actual force on the attachment, was studied with the conclusion that no appreciable error could be introduced.

8.2.6 Nonlinear Divergence Analysis

The equations of motion, assuming φ_1 and φ_2 are not small, neglecting inertial effects, thereby restricting the equations to use for divergence analysis, and allowing for imperfections by assuming that the equilibrium configuration is not a straight line, are

$$\begin{aligned} &K_1\bar{\varphi}_1 - K_2(\bar{\varphi}_2 - \bar{\varphi}_1) - P\ell_1 \cos\alpha\varphi_2 \sin\varphi_1 \\ &\quad + K_3\ell_1(\ell_1 \sin\bar{\varphi}_1 + d_2 \sin\bar{\varphi}_2)\cos\bar{\varphi}_1 \\ &\quad + P\ell_1 \sin\alpha\varphi_2 \cos\varphi_1 = 0 \\ &K_2(\bar{\varphi}_2 - \bar{\varphi}_1) + P \sin\alpha\varphi_2 [\ell_2 \cos\varphi_2 \\ &\quad + \tan\varphi_2(\ell_1 \sin\varphi_1 + \ell_2 \sin\varphi_2)] + P\ell_1 \cos\alpha\varphi_2 \sin\varphi_1 \\ &\quad + K_3 d_2(\ell_1 \sin\bar{\varphi}_1 + d_2 \sin\bar{\varphi}_2) \cos\bar{\varphi}_2 = 0 \end{aligned} \tag{8.20}$$

where $\bar{\varphi}_1 = \varphi_1 - \varphi_{10}$, $\bar{\varphi}_2 = \varphi_2 - \varphi_{20}$, and φ_{10} and φ_{20} are the no-load values of φ_1 and φ_2, respectively.

Restricting the magnitude of φ_1 and φ_2 by setting

$$\sin \varphi_1 = \varphi_1 - \varphi_1^3/6$$
$$\cos \alpha\varphi_2 = 1 - (\alpha\varphi_2)^2/2 \tag{8.21}$$

the equations may be written as polynomials of the form

$$A_1\varphi_1^3 + A_2\varphi_2^3 + A_3\varphi_1\varphi_2^2 + A_4\varphi_1^2\varphi_2 + A_5\varphi_1^2 + A_6\varphi_2^2 + A_7\varphi_1\varphi_2 + A_8\varphi_1 + A_9\varphi_2 + A_{10} = 0$$
$$B_1\varphi_1^3 + B_2\varphi_2^3 + B_3\varphi_1\varphi_2^2 + B_4\varphi_1^2\varphi_2 + B_5\varphi_1^2 + B_6\varphi_2^2 + B_7\varphi_1\varphi_2 + B_8\varphi_1 + B_9\varphi_2 + B_{10} = 0 \tag{8.22}$$

A computer program was written to solve these two third-degree algebraic equations simultaneously for various values of P, φ_{10}, and φ_{20}. The results are given in Fig. 8.14 for $\alpha = 0.717$ (run 11) in the form P versus φ_1. The variation of φ_2 with P is essentially similar. The vertical dotted line represents the angle φ_1 corresponding to one-inch deflection of the middle joint, which is the buckling criterion used in this study.

Curve A represents the linear case for $\varphi_{10} = \varphi_{20} = 0$. No deflection occurs until the buckling load is reached. Curve B represents the imperfection-free nonlinear case where the approximations (8.21) are used. The buckling loads predicted by curves A and B are rather close.

Curves C, D, and E are drawn for the values of φ_{10} and φ_{20} indicated. Note that the buckling loads, as determined by the intersection of the response curves with the dotted vertical line, depend significantly on the magnitude of φ_{10} and φ_{20}.

Curve F is the experimental response curve for the model with the attachment used for run 11 ($\alpha = 0.717$) in place.

8.3 Demonstrational Models

Considerable insight into the possible types of dynamic behavior of mechanical systems subjected to nonconservative forces may be gained not only through quantitative experiments, but also by qualitative observations of demonstrational models. A set of such models has been recently designed and constructed at the Structural Mechanics Laboratory of Northwestern University [105], and it is intended to develop this set further at the Applied Mechanics Laboratory of Stanford University. A brief description of the models follows.

Model A

The model consists of two like rigid pipe-segments (Fig. 8.15a). The first is elastically hinged to a fixed base, while the other is elastically hinged to the first and carries a nozzle at the free end. In addition to the elastic hinges, the stiffness of the system can be varied by means of lateral, spiral springs. The system is constrained to move in a horizontal plane, being suspended by long, light strings. A fluid can be conveyed through the pipes, entering at the fixed end and leaving through the nozzle. In the absence of the fluid, or for small rate of discharge, the pipes are at rest and colinear, defining the equilibrium configuration. Two symmetrically placed strings in the horizontal plane are attached to the free end of the pipe and pulled toward the fixed base at a small angle relative to the pipe axis.

It is observed that as the flow rate is increased, and passes a certain (critical) value, the pipe system does not remain in the undisturbed configuration. The loss of stability occurs either by divergence or by flutter, depending upon the stiffness of the auxiliary coil springs at the free end and the tension in the wires. If the coil spring at the free end is sufficiently soft, or is removed, and the tension in the wires small, then the loss of stability occurs by flutter-type motion. By contrast, for sufficiently stiff coil springs, or for large enough tension in the wires, the system loses stability by divergence (Fig. 8.15b).

In experimenting with this system, it was found that the system can admit two distinct critical flutter flow rates. One is associated with relatively large initial disturbances and the other corresponds to small initial perturbations. That is, for a certain range of flow rates, the system is asymptotically stable when disturbed by sufficiently small initial input of energy, while it oscillates with increasing amplitude about the undeformed axis for sufficiently large initial perturbations (loss of stability in the large). Above this range the system loses stability by flutter for any initial disturbances (loss of stability in the small).

A thorough and systematic investigation (both analytical and experimental) of articulated pipes conveying fluid was presented by Benjamin [80,93]. The model described here represents a generalization of Benjamin's system by including a nozzle to control Coriolis forces, lateral springs to control effective constraints, and tension wires to control the direction of the resultant forces acting at the free end. It appears that the existence of loss of stability in the large was not observed before in such systems.

Model B

This model consists essentially of a piece of a rubber tube, fixed at one end and elastically restrained in the axial direction at the other end, at which rotation is prevented, Fig. 8.16. The tube is confined to move in the horizontal plane, being suspended by means of long, light strings. A fluid can be conveyed through the tube, entering at the fixed end. The other end being closed, the fluid is ejected through two nozzles, placed at a certain distance from the fixed end symmetrically with respect to the tube in the direction parallel to the tangent to the tube at that section. The nozzles are mounted in a fixture which is made to slide on an air cushion. The sleeve providing the sliding support at the elastically constrained end is also supported by an air bearing. In Fig. 8.16 the tubes supplying air for the bearings are seen on the left part of the photograph.

It is observed that the straight equilibrium configuration may be lost if the flow rate of the air passing through the tube exceeds a certain critical value. Loss of stability can occur by either flutter or divergence, depending upon the distance between the nozzles and the fixed end. It may be remarked that by attaching a series of pairs of nozzles along the tube, the problem of a bar subjected to disturbed tangential follower forces may be realized.

Model C

This model consists of a cantilevered thin elastic strip at whose free end a circular rigid plate is attached in a plane normal to the axis, Fig. 8.17. The surface of the plate can be varied by placing screens of different mesh sizes. A nozzle whose axis is parallel to the axis of the strip can be made to discharge fluid at a constant rate which impinges upon the plate.

It is observed that as a certain critical flow rate is exceeded, the cantilever may lose stability by either flutter or divergence, depending upon the mesh size of the screen attached to the plate. Both torsional and bending deformation are observed to occur for both types of loss of stability, with torsional deformations becoming more pronounced with increased eccentricity.

Model D

This model consists of a cantilevered thin elastic strip at whose two longitudinal edges flexible tubes are attached through one of which fluid at constant rate can be conveyed, entering at the fixed end and leaving through the open end, Fig. 8.18a. The other tube does not convey any fluid and is provided solely to decrease the asymmetry of the cross-section.

It is observed that as the flow rate exceeds a certain critical value, the cantilever loses stability by bending-torsional flutter, Fig. 8.18b. It is also observed that a certain range of flow rates restores the original undeformed equilibrium configuration which may have been lost by lateral

buckling caused by attaching a given weight at the free end. Fig. 8.18c shows the buckled configuration at zero flow rate and Fig. 8.18d shows the restored original equilibrium position, achieved with a certain flow rate. As the flow rate is increased further beyond a certain value, stability is lost by flutter.

Model E

This model consists, as in the previous two cases, of a cantilevered elastic strip at whose two longitudinal edges flexible tubes are attached. A rigid pipe is placed along the transverse free edge and connected to the longitudinal tubes, Fig. 8.19. Fluid is conveyed at a constant rate through the longitudinal tubes, entering at the fixed end of the cantilever, and is discharged through an end opening in the rigid pipe, whose other end is closed.

It is observed that as the flow rate is increased beyond a certain critical value, stability is lost by bending-torsional flutter. The system may be considered as model of an aircraft wing with a jet engine at the free end.

Model F

This model consists of a rigid closed cylinder which can roll on a horizontal plane. A piece of a rigid pipe is attached to the cylinder by means of an elastic hinge, which carries a nozzle at the free end, Fig. 8.20a. Fluid can be conveyed into the cylinder by means of a flexible tube, which then enters the pipe and is discharged through the nozzle.

It is observed that as the rate of discharge is increased beyond a certain value, the system acquires a (stable) equilibrium position such that the pipe is vertical and its axis passes through the center of the cylinder, Fig. 8.20b. As the rate of discharge is increased further, another definite (critical) value is reached, beyond which the system begins to execute oscillations with increasing amplitudes about the preceding equilibrium state (flutter).

Model G

This model consists of a rigid cylinder, as in the previous model, which can roll on a convex rigid cylindrical segment which in turn is fixed in a concave rigid cylindrical segment, this latter being free to roll on a horizontal plane, Fig. 8.21a. The rigid cylinder is closed at the end planes and is provided with an opening and a nozzle on the lateral surface, the axis of the nozzle passing through the center of the cylinder. Fluid can be conveyed through a flexible tube to the cylinder and is discharged through the nozzle.

It is observed that as the rate of discharge is increased beyond a certain value, the system acquires a (stable) equilibrium configuration such that the axis of the nozzle is vertical, Fig. 8.21b. As the rate of discharge is increased further, another definite (critical) value is reached, beyond which the system begins to oscillate with increasing amplitudes about the preceding equilibrium state (flutter), Fig. 8.21c. If the convex cylinder segment on which the cylinder rolls is replaced by a flat plate, Fig. 8.21d, no flutter is observed.

Model H

This model consists of a rigid pipe segment suspended by means of a flexible tube and hanging in the vertical position, Fig. 8.22. The lower end of the rigid pipe carries an attachment, the essential part of which consists of two nozzles placed in a plane normal to the axis of the pipe segment, parallel to each other. The flexible tube is connected to a fixed base. Fluid can be conveyed through the flexible tube, entering the rigid pipe segment and discharging through the nozzles in opposite directions.

It is observed that for any constant flow rate above a certain minimum value, the rigid pipe begins to move like a spherical pendulum with monotonically increasing amplitude, which will approach a limiting value for a sufficiently small flow rate. The minimum value of the constant flow rate which produces the onset of the pipe motion is not sharply defined. It is further observed that the same motion is initiated if the rigid pipe segment is made very short as compared to the flexible tube, and vice versa.

The problem of a cantilevered bar subjected at the free end to a twisting moment which rotates with the end cross-section of the bar was first considered by Nikolai [2]. He found that the undeformed rectilinear equilibrium configuration is unstable for any nonvanishing magnitude of the twisting moment.

REFERENCES

1. Ziegler, H.: Principles of Structural Stability. Blaisdell Publishing Company (Waltham, Mass.), 1968.

2. Nikolai, E. L.: "On the Stability of the Rectilinear Form of a Compressed and Twisted Bar" (in Russian), Izvest. Leningr. Politekhn. in-ta, vol. 31, 1928. (Reprinted in Selected Studies in Mechanics. Gos. Izdat. Techniko-Teoretischeskoi Literatury, Moscow, 1955, pp. 357-387.)

3. Nikolai, E. L.: "On the Problem of Stability of a Twisted Bar" (in Russian), Vestnik prikl. mat. i mekh., vol. 1, 1929. (Reprinted in Selected Studies in Mechanics. Gos. Izdat. Techniko-Teoreticheskoi Literatury, Moscow, 1955, pp. 388-406.)

4. Ziegler, H.: "Stabilitätsprobleme bei geraden Stäben und Wellen." ZAMP, vol. 2, no. 4, 1951, pp. 265-289.

5. Ziegler, H.: "Die Stabilitätskriterien der Elastomechanik." Ingr.-Arch., vol. 20, no. 1, 1952, pp. 49-56.

6. Ziegler, H.: "Linear Elastic Stability." ZAMP, vol. 4, 1953, pp. 89-184.

7. Ziegler, H.: "On the Concept of Elastic Stability." Advances in Applied Mechanics, vol. 4. Academic Press, 1956, pp. 351-403.

8. Bolotin, V. V.: Nonconservative Problems of the Theory of Elastic Stability (English translation). G. Herrmann, ed., Pergamon Press, 1963.

9. Garrick, I. E.: Aerodynamic Flutter. AIAA Reprint Series, 1969.

10. Herrmann, G.: "Stability of Equilibrium of Elastic Systems Subjected to Nonconservative Forces." Appl. Mech. Reviews, vol. 20, 1967, pp. 103-108.

11. Liapunov, A. M.: "Problème général de la stabilité du mouvement." Ann. Fac. Sci. Toulouse, vol. 9, 1907, pp. 203-474 (French translation; reprinted by Princeton University Press, 1952. Original paper published in Comm. Soc. Math., Kharkov, 1893.)

12. Minorsky, N.: Nonlinear Oscillations. Van Nostrand Co., 1962.

13. Krasovskii, N. N.: Stability of Motion. Stanford University Press, 1963.

14. LaSalle, J.; and Lefschetz, S.: Stability by Liapunov's Direct Method with Applications. Academic Press, 1961.

15. Hahn, W.: Theory and Applications of Liapunov's Direct Method. Prentice-Hall (Englewood Cliffs, N. J.), 1963.

16. Magiros, D. G.: "Stability Concepts of Dynamical Systems." Information and Control, vol. 9, 1966, pp. 531-548.

17. Ziegler, H.: "Some Developments in the Theory of Stability." Proc. Canadian Congr. of Appl. Mech., vol. 3, 1967, pp. 233-250.

18. Porter, B.: Stability Criteria for Linear Dynamical Systems. Academic Press, 1968.

19. Sewell, M. J.: "On Configuration-Dependent Loading." Arch. Rat. Mech. Anal., vol. 23, 1967, 327-351.

20. Nemat-Nasser, S.: "On Local Stability of a Finitely Deformed Solid Subjected to Follower Type Loads." Quart. Appl. Math., vol. 26, 1968, pp. 119-129.

21. Shieh, R. C.; and Masur, E. F.: "Some General Principles of Dynamic Instability of Solid Bodies." ZAMP, vol. 19, 1968, pp. 927-941.

22. Herrmann, G.; and Bungay, R. W.: "On the Stability of Elastic Systems Subjected to Nonconservative Forces." J. Appl. Mech., vol. 31, no. 3, 1964, pp. 435-440.

23. Bisplinghoff, R. L.; Ashley, H.; and Halfman, R. L.: Aeroelasticity. Addison-Wesley Publishing Company, Inc. (Cambridge, Mass.), 1955.

24. Fung, Y. C.: An Introduction to the Theory of Aeroelasticity. John Wiley and Sons, Inc. (New York), 1955.

25. Herrmann, G.; and Jong, I.-C.: "On the Destabilizing Effect of Damping in Nonconservative Elastic Systems." J. Appl. Mech., vol. 32, no. 3, 1965, pp. 592-597.

26. Burnside, W. S.; and Panton, A. W.: The Theory of Equations. Tenth ed., Dublin, Hodges, Figgis and Company (New York), 1935.

27. Herrmann, G.; and Jong, I.-C.: "On Nonconservative Stability Problems of Elastic Systems with Slight Damping." J. Appl. Mech., vol. 33, no. 1, 1966, pp. 125-133.

28. Bottema, O.: "On the Stability of the Equilibrium of a Linear Mechanical System." ZAMP, vol. 6, no. 2, 1955, pp. 97-104.

29. Nemat-Nasser, S.; and Herrmann, G.: "Some General Considerations Concerning the Destabilizing Effect in Nonconservative Systems." ZAMP, vol. 17, no. 2, 1966, pp. 305-313.

30. Hedgepeth, J. M.; Budiansky, B.; and Leonard, R. W.: "Analysis of Flutter in Compressible Flow of a Panel on Many Supports." J. Aeron. Sci., vol. 21, no. 7, 1954, pp. 475-486.

31. Johns, D. J.; and Parks, P. C.: "Effect of Structural Damping on Panel Flutter." Aircraft Eng., Oct. 1960, pp. 304-308.

32. Nemat-Nasser, S.; Prasad, S. N.; and Herrmann, G.: "Destabilizing Effect of Velocity-Dependent Forces in Nonconservative Continuous Systems." AIAA J., vol. 4, no. 7, 1966, pp. 1276-1280.

33. Beck, M.: "Die Knicklast des einseitig eingespannten, tangential gedrückten Stabes." ZAMP, vol. 3, 1952, pp. 225-228.

34. Leipholz, H.: "Über den Einfluss der Dämpfung bei nichtkonservativen Stabilitätsproblemen elastischer Stäbe." Ingr.-Arch., vol. 33, no. 5, 1964, pp. 308-321.

35. Leonov, M. Ya.; and Zorii, L. M.: "Effect of Friction on the Critical Load of a Compressed Rod." Soviet Physics-Doklady, vol. 7, no. 7, 1963, pp. 611-613. (Translated from Doklady Akad. Nauk SSSR, vol. 145, July 1962, pp. 295-297.)

36. Bolotin, V. V.; and Zhinzher, N. I.: "Effects of Damping on Stability of Elastic Systems Subjected to Nonconservative Forces." Int. J. Solids and Structures, vol. 5, no. 9, 1969, pp. 965-989.

37. Zorii, L. M.: "On the Stability of a Bar Under a Nonconservative Load" (in Russian). Inst. of Machine Science and Automation Sci. Notes, vol. 4, 1964, pp. 23-34.

38. Huang, N. C.; and Shieh, R. C.: "Thermomechanical Coupling Effect on the Stability of Nonconservative Elastic Continuous Systems." Int. J. Mech. Sci., vol. 12, 1970, pp. 39-49.

39. Jong, I.-C.: "On Stability of a Circulatory System with Bilinear Hysteresis Damping." J. Appl. Mech., vol. 36, 1969, pp. 76-82.

40. Leibowitz, M. A.; and Ackerberg, R. C.: "The Vibration of a Conducting Wire in a Magnetic Field." Quart. J. Mech. Appl. Math., vol. 16, 1963, pp. 507-519.

41. Smith, T. E.; and Herrmann, G.: "Stability of Circulatory Elastic Systems in the Presence of Magnetic Damping." Acta Mechanica, in print.

42. Kiusalaas, J.; and Davis, H. E.: "On the Stability of Elastic Systems under Retarded Follower Forces." Int. J. Solids and Structures, vol. 6, 1970, pp. 399-409.

43. Thomson, W. T.; and Reiter, G. S.: "Jet Damping of a Solid Rocket: Theory and Flight Results." AIAA J., vol. 3, 1965, pp. 413-417.

44. Herrmann, G.; and Nemat-Nasser, S.: "Instability Modes of Cantilevered Bars Induced by Fluid Flow Through Attached Pipes." Int. J. Solids and Structures, vol. 3, 1967, pp. 39-52.

45. Herrmann, G.: "Determinism and Uncertainty in Stability." Proc. IUTAM-Symp. on Instability of Continuous Systems (Karlsruhe), Sept. 1969, Springer-Verlag, in press.

46. Koiter, W. T.: "The Concept of Stability of Equilibrium for Continuous Bodies." Proc. Koninkl. Nederl. Akademie van Wetenschappen, Ser. B, vol. 66, no. 4, 1963, pp. 173-177.

47. Koiter, W. T.: "The Energy Criterion of Stability for Continuous Elastic Bodies." Proc. Koninkl. Nederl. Akademie van Wetenschappen, Ser. B. vol. 68, 1965, pp. 178 and 190.

48. Nemat-Nasser, S.; and Herrmann, G.: "On the Stability of Equilibrium of Continuous Systems." Ingr.-Arch., vol. 35, no. 1, 1966, pp. 17-24.

49. Vulikh, B. Z.: Functional Analysis for Scientists and Technologists (English translation). I. N. Sneddon, ed., Pergamon Press, 1963.

50. Movchan, A. A.: "The Direct Method of Liapunov in Stability Problems of Elastic Systems" (English translation). J. Appl. Math. Mech., vol. 23, 1959, pp. 686-700.

51. Shield, R. T.; and Green, A. E.: "On Certain Methods in the Stability Theory of Continuous Systems." Arch. Rat. Mech. Anal., vol. 12, 1963, pp. 354-360.

52. Mikhlin, S. G.: The Problem of the Minimum of a Quadratic Functional. GTTI (Moscow), 1952.

53. Nemat-Nasser, S.: "On the Stability of the Equilibrium of Nonconservative Continuous Systems with Slight Damping." J. Appl. Mech., vol. 34, no. 2, June 1967, pp. 344-348.

54. Prasad, S. N.; and Herrmann, G.: "Complex Treatment of a Class of Non-conservative Stability Problems." Developments in Theoretical and Applied Mechanics (Proc. Fourth Southeastern Conf. on Theor. and Appl. Mech., New Orleans, La.), vol. 8, D. Frederick, ed., Pergamon Press, 1970, pp. 305-318.

55. Hsu, C. S.: "Dynamic Stability of Autonomous and Continuous Elastic Systems." Rept. No. AM-66-3. Div. Appl. Mech., Univ. of California, Berkeley, 1966.

56. Knops, R. J.; and Wilkes, E. W.: "On Movchan's Theorems for Stability of Continuous Systems." Int. J. Eng. Sci., vol. 4, 1966, pp. 303-329.

57. Walker, J. A.: "On the Stability of Linear Discrete Dynamic Systems." J. Appl. Mech., vol. 37, no. 2, June 1970, pp. 271-275.

58. Chetaev, N. G.: The Stability of Motion. Pergamon Press, 1961.

59. LaSalle, J. P.: "Some Extensions of Liapunov's Second Method." IRE Trans. on Circuit Theory, Dec. 1960, pp. 520-527.

60. Leipholz, H.: "Anwendung des Galerkinschen Verfahrens auf nichtkonservative Stabilitätsprobleme des elastischen Stabes." ZAMP, vol. 13, 1962, pp. 359-372.

61. Leipholz, H.: "Über die Konvergenz des Galerkinschen Verfahrens bei nichtselbstadjungierten und nichtkonservativen Eigenwertsproblemen." ZAMP, vol. 14, 1963, pp. 70-79.

62. Leipholz, H.: "Die Knicklast des einseitig eingespannten Stabes mit gleichmässig verteilter, tangentialer Längsbelastung." ZAMP, vol. 13, 1962, pp. 581-589.

63. Leipholz, H.: "Über die Zulässigkeit des Verfahrens von Galerkin bei linearen, nichtselbstadjungierten Eigenwertsproblemen." ZAMP, vol. 16, 1965, pp. 837-843.

64. Leipholz, H.: "Über die Konvergenz des Galerkinschen Verfahrens bei nichtkonservativen Stabilitätsproblemen von Platten und Stäben." ZAMM, vol. 45, (GAMM-Tagung), 1965, pp. 127-129.

65. Leipholz, H.: "Grundzüge einer Stabilitätstheorie für elastische Systeme unter nichtkonservativer Belastung." Ingr.-Arch., vol. 34, no. 1, 1965, pp. 56-68.

66. Levinson, M.: "Application of the Galerkin and Ritz Methods to Nonconservative Problems of Elastic Stability." ZAMP, vol. 17, 1966, pp. 431-442.

67. Marchenko, G. A.: "Ritz Method in Nonconservative Problems of Elastic Stability Theory" (in Russian). Aviatsionnaia tekhnika, vol. 3, 1966, pp. 62-68.

68. Leipholz, H.: "Über die Befreiung der Ansatzfunktionen des Ritzschen und Galerkinschen Verfahrens von den Randbedingungen." Ingr.-Arch., vol. 36, no. 4, 1967, pp. 251-261.

69. Morse, P. M.; and Feshbach, H.: Methods of Theoretical Physics. Pt. I. McGraw-Hill Book Co., Inc., 1953, pp. 298-299.

70. Tasi, J.; and Herrmann, G.: "Thermoelastic Dissipation in High-Frequency Vibrations of Crystal Plates." J. Acoust. Soc. Am., vol. 36, 1964, pp. 100-110.

71. Herrmann, G.; and Nemat-Nasser, S.: "Energy Considerations in the Analysis of Stability of Nonconservative Structural Systems." Dynamic Stability of Structures (Proc. Int. Conf., Evanston, Ill.), G. Herrmann, ed., Pergamon Press, 1967, pp. 299-308.

72. Nemat-Nasser, S.; and Herrmann, G.: "Torsional Instability of Cantilevered Bars Subjected to Nonconservative Loading." J. Appl. Mech., vol. 33, 1966, pp. 102-104.

73. Como, M.: "Lateral Buckling of a Cantilever Subjected to a Transverse Follower Force." Int. J. Solids and Structures, vol. 2, 1966, pp. 515-523.

74. Ballio, G.: "Sistemi aggiunti in problemi di stabilità elastica in campo non conservativo." Rendiconti dell'Istituto Lombardo di Scienze e Lettere, vol. 101, 1967, pp. 331-360.

75. Flax, A. H.: "Aeroelastic Problems at Supersonic Speed." Proc. Second Int. Aeronautical Conf. (New York), sponsored by the Inst. Aeron. Sci. and Royal Aeron. Soc., 1949, pp. 322-360.

76. Prasad, S. N.; and Herrmann, G.: "The Usefulness of Adjoint Systems in Solving Nonconservative Stability Problems of Elastic Continua." Int. J. Solids and Structures, vol. 5, no. 7, 1969, pp. 727-735.

77. Roberts, P. H.: "Characteristic Value Problems Posed by Differential Equations Arising in Hydrodynamics and Hydromagnetics." J. Math. Anal. Applic., vol. 1, 1960, pp. 195-214.

78. Nemat-Nasser, S.; and Herrmann, G.: "Adjoint Systems in Nonconservative Problems of Elastic Stability." AIAA J., vol. 4, 1966, pp. 2221-2222.

79. Ballio, G.: "Formulazione variazionale del problema dell'asta caricata in punta da forze non conservative." Costruzioni Metalliche (Milano), no. 4, 1967, pp. 258-264.

80. Benjamin, T. B.: "Dynamics of a System of Articulated Pipes Conveying Fluid. Part I." Proc. Roy. Soc. A, (London), vol. 261, 1961, pp. 457-486.

81. Como, M.: "Del metodo dell'energia nella stabilità dei sistemi elastici soggetti a forze posizionali conservative e non conservative." No. 226, Università degli studi di Napoli,Quaderni di Teoria e Tecnica delle Strutture, Aug. 1966.

82. Nemat-Nasser, S.; and Roorda, J.: "On the Energy Concepts in the Theory of Elastic Stability." Acta Mechanica, vol. 4, no. 3, 1967, pp. 296-307.

83. Roorda, J.; and Nemat-Nasser, S.: "An Energy Method for Stability Analysis of Nonlinear Nonconservative Systems." AIAA J., vol. 5, no. 7, 1967, pp. 1262-1268.

84. Herrmann, G.; and Nemat-Nasser, S.: "Instability Modes of Cantilevered Bars Induced by Fluid Flow Through Attached Pipes." Int. J. Solids and Structures, vol. 3, 1967, pp. 39-52.

85. Lin, K. H.; Nemat-Nasser, S.; and Herrmann, G.: "Stability of a Bar under Eccentric Follower Force." J. Eng. Mech. Div., ASCE, vol. 93, no. EM4, Aug. 1967, pp. 105-115.

86. Timoshenko, S.; and Gere, J.: Theory of Elastic Stability. McGraw-Hill Book Co., Inc., 1961.

87. Gregory, R. W.; and Paidoussis, M. P.: "Unstable Oscillation of Tubular Cantilevers Conveying Fluid. Part I." Proc. Roy. Soc. A, (London), vol. 293, 1966, pp. 512-527.

88. Kordas, Z.: "The Stability Problem of a Bar in Parallel Fluid Flow, Taking into Consideration the Head Resistance." Polska Akad. Nauk, Nauk Technicznych Bull., vol. 13, no. 5, 1965, pp. 267-276.

89. Ashley, H.; and Zartarian, G.: "Piston Theory - A New Aerodynamic Tool for the Aeroelastician." J. Aeron. Sci., vol. 23, no. 12, 1956, pp. 1109-1118.

90. Augusti, G.: "Instability of Struts Subject to Radiant Heat." Meccanica, vol. 3, no. 3, 1968, pp. 1-10.

91. Yu, Y. Y.: "Thermally Induced Vibration and Flutter of a Flexible Boom." J. Spacecraft, vol. 6, no. 8, 1969, pp. 902-910.

92. Augusti, G.: "Technical Comment on 'Thermally Induced Vibration and Flutter of Flexible Booms.'" J. Spacecraft Rockets, to be published.

93. Benjamin, T. B.: "Dynamics of a System of Articulated Pipes Conveying Fluid. Part II." Proc. Roy. Soc. A, (London), vol. 261, 1961, pp. 487-499.

94. Gregory, R. W.; and Paidoussis, M. P.: "Unstable Oscillation of Tubular Cantilevers Conveying Fluid. Part II." Proc. Roy. Soc. A, (London), vol. 293, 1966, pp. 528-542.

95. Long, Jr., R. H.: "Experimental and Theoretical Study of Transverse Vibration of a Tube Containing Flowing Fluid." J. Appl. Mech., vol. 22, no. 1, 1955, pp. 65-68.

96. Dodds, Jr., H. L.; and Runyan, H. L.: "Effect of High-Velocity Fluid Flow on the Bending Vibrations and Static Divergence of a Simply Supported Pipe." NASA TN D-2870, 1965.

97. Greenwald, A. S.; and Dugundji, J.: "Static and Dynamic Instabilities of a Propellant Line." ASRL, Tech. Rept. 134-3, Massachusetts Inst. of Technology, May 1967.

98. Paidoussis, M. P.: "Vibration of Flexible Cylinders with Supported Ends, Induced by Axial Flow." Proc. Thermodynamics and Fluid Mechanics Conv. (Liverpool). The Institution of Mechanical Engineers (London), 1966, pp. 268-279.

99. Paidoussis, M. P.: "Dynamics of Flexible Slender Cylinders in Axial Flow. Part I. Theory." J. Fluid Mech., vol. 26, pt. 4, 1966, pp. 717-736.

100. Paidoussis, M. P.: "Dynamics of Flexible Slender Cylinders in Axial Flow. Part II. Experiments." J. Fluid Mech., vol. 26, pt. 4, 1966, pp. 737-751.

101. Hawthorne, W. R.: "The Early Development of the Dracone Flexible Barge." Proc. Inst. Mech. Engrs. (London), vol. 175, 1961, p. 52.

102. Runyan, H. L.; Pratt, K. G.; and Pierce, H. B.: "Some Hydro-Elastic-Pneumatic Problems Arising in the Structural Dynamics of Launch Vehicles." [Preprint] 65-AV-27, Nat. Conf. of the Aviation and Space Div., ASME (Los Angeles, Calif.), May 1965.

103. Reed III, W. H.: "Review of Propeller-Rotor Whirl Flutter." NASA TR R-264, 1967.

104. Feldt, W. T.; Nemat-Nasser, S.; Prasad, S. N.; and Herrmann, G.: "Instability of a Mechanical System Induced by an Impinging Fluid Jet." J. Appl. Mech., vol. 36, no. 4, 1969, pp. 693-701.

105. Herrmann, G.; Nemat-Nasser, S.; and Prasad, S. N.: "Models Demonstrating Instability of Nonconservative Mechanical Systems." Tech. Rept. No. 66-4, Str. Mech. Lab., Northwestern Univ., June 1966.

106. Parks, P. C.: " A New Look at the Routh-Hurwitz Problem using Liapunov's Second Method." Bull. de l'Académie Polonaise des Sciences, vol. 12, no. 6, 1964, pp. 19-21.

107. Hermite, C.: "Sur le nombre des racines d'une équation algébrique comprise entre des limites données." J. reine angew. Math., vol. 52, 1854, pp. 39-51.

108. Wang, P. K. C.: "Theory of Stability and Control for Distributed Parameter Systems - a Bibliography." Int. J. Control, vol. 7, 1968, pp. 101-116.

TABLE 1

COMPARISON BETWEEN THE EXACT SOLUTION AND THE TWO-TERM GALERKIN APPROXIMATION: SMALL VELOCITY-DEPENDENT FORCES

β	γ	δ	$\gamma_d = F^2/\pi^2$	
			Exact	Galerkin Method
0.0	1.0	0.0	2.035	2.035
1.0	0.0	0.0	1.780	1.768
0.0	0.0	1.0	1.107	1.082
1.0	0.0	1.0	1.462	1.447
2.5	0.0	1.0	1.73	1.729
5.0	0.0	1.0	1.92	1.924
0.0	1.0	1.0	1.155	1.133
1.0	1.0	1.0	1.483	1.469
2.5	1.0	1.0	1.735	1.738
5.0	1.0	1.0	1.925	1.926
0.0	10.0	1.0	1.426	1.414
1.0	10.0	1.0	1.618	1.611
2.5	10.0	1.0	1.795	1.794
5.0	10.0	1.0	1.935	1.940
0.0	100.0	1.0	1.895	1.902
1.0	100.0	1.0	1.926	1.930
2.5	100.0	1.0	1.960	1.964
5.0	100.0	1.0	1.996	2.000

TABLE 2

SYSTEM DATA

Dimensions (cm)	Part	Mass (gm)	Centroidal moment of inertia ($gm \cdot cm^2$)
$a_1 = 0.692$	1	10.20	~ 0
$b_1 = 16.3$	2	22.0	1655
$c_1 = 31.9$	3	42.1	~ 0
$a_2 = 0.692$	4	10.20	~ 0
$b_2 = 16.3$	5	22.0	1655
$c_2 = 32.3$	6	3.2	~ 0
$d_2 = 25.3$	7	43.5	771
$\ell_1 = 32.4$			
$\ell_2 = 32.6$			

Spring constants		Dynamic method	Static method
System I	K_1	5.70×10^6 dyne·cm	...
	K_2	9.12×10^5 dyne·cm	...
	K_3	3.50×10^2 dyne/cm	...
System II	K_1	5.34×10^6 dyne·cm	5.45×10^6 gm·cm
	K_2	9.02×10^5 dyne·cm	9.41×10^6 gm·cm
	K_3	3.35×10^2 dyne/cm	3.53×10^2 gm/cm

TABLE 3

SUMMARY OF NUMERICAL RESULTS

		SYSTEM I						SYSTEM II					
		Experimental		Theoretical			% error	Experimental		Theoretical			% error
Run #	α	*	P_{crit} (gm)	1 (gm)	2 (gm)	3 (gm)		*	P_{crit} (gm)	1 (gm)	2 (gm)	3 (gm)	
1	0.343	F	56.4	72	55	...	+ 2.5	F	70.2	89	62	...	+12.9
2	0.327	F	55.2	70	55	...	+ 0.3	F	69.7	88	62	...	+11.1
3	0.560	B	94.9	..	..	124	-23.4	B	118.3	..	..	140	-15.1
4	0.368	F	57.2	73	55	...	+ 3.8	F	75.7	90	63	...	+19.2
5	0.548	B	99.9	..	..	125	-20.1	B	116.0	..	..	140	-17.0
6	0.913	B	95.9	..	..	117	-18.0	B	111.9	..	..	130	-13.8
7	0.533	B	97.9	..	..	125	-21.7	B	110.2	..	..	140	-21.3
8	0.346	F	58.8	77	55	...	+ 6.9	F	69.8	89	62	...	+11.4
9	0.454							F	77.0	..	66	...	+16.7
10	0.320							F	70.2	87	62	...	+12.9
11	0.717							B	105.0	..	..	135	-14.8
12	0.238							F	69.7	83	62	...	+12.4

* Observed loss of stability: F = flutter, B = buckling.

1 Undamped flutter.

2 Damped flutter, $\varepsilon = 5.0$.

3 Buckling.

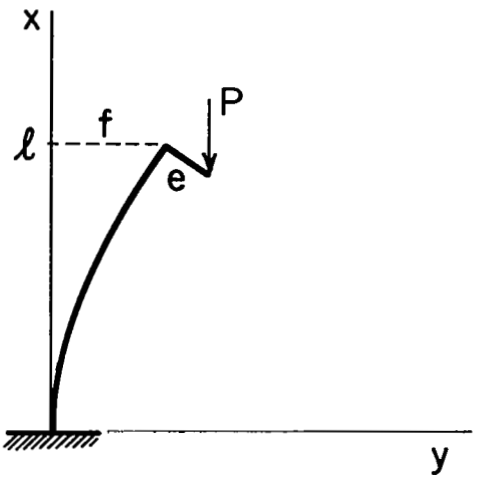

Fig. 1.1 Column under compressive eccentric load

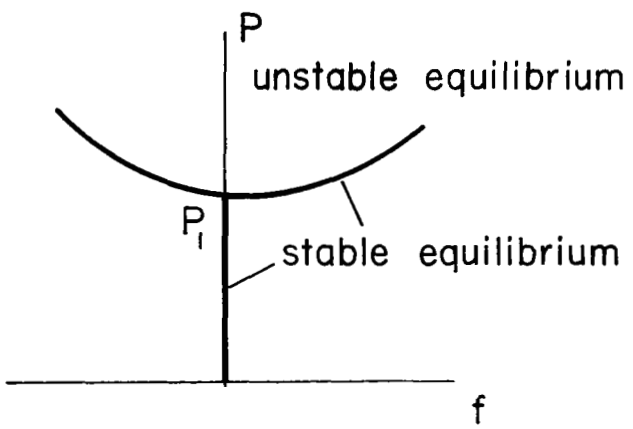

Fig. 1.2 Equilibrium curves of a centrally loaded column

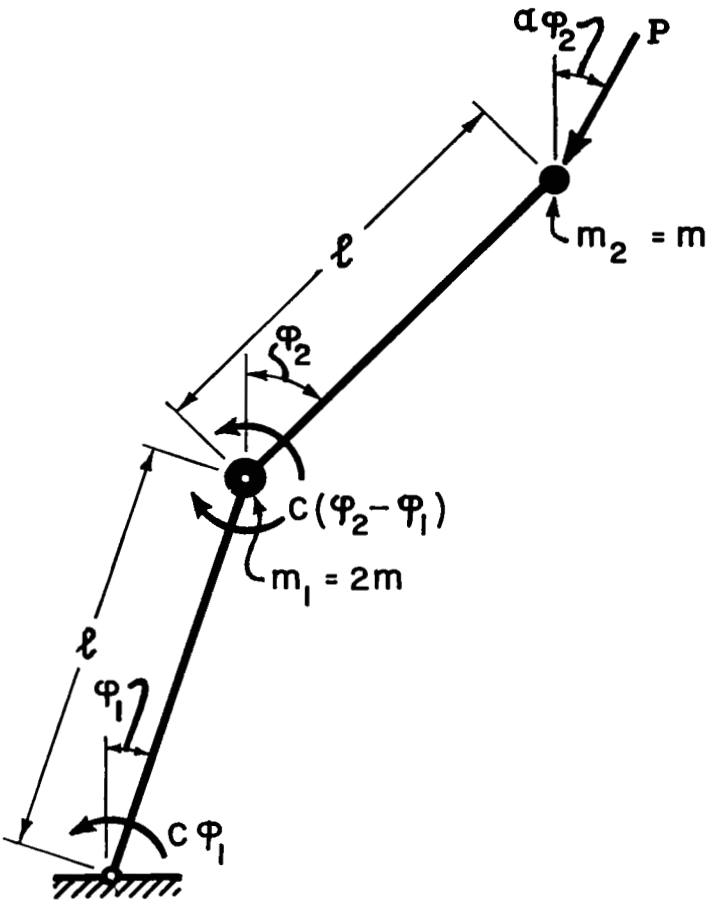

Fig. 3.1 Two-degree-of-freedom model

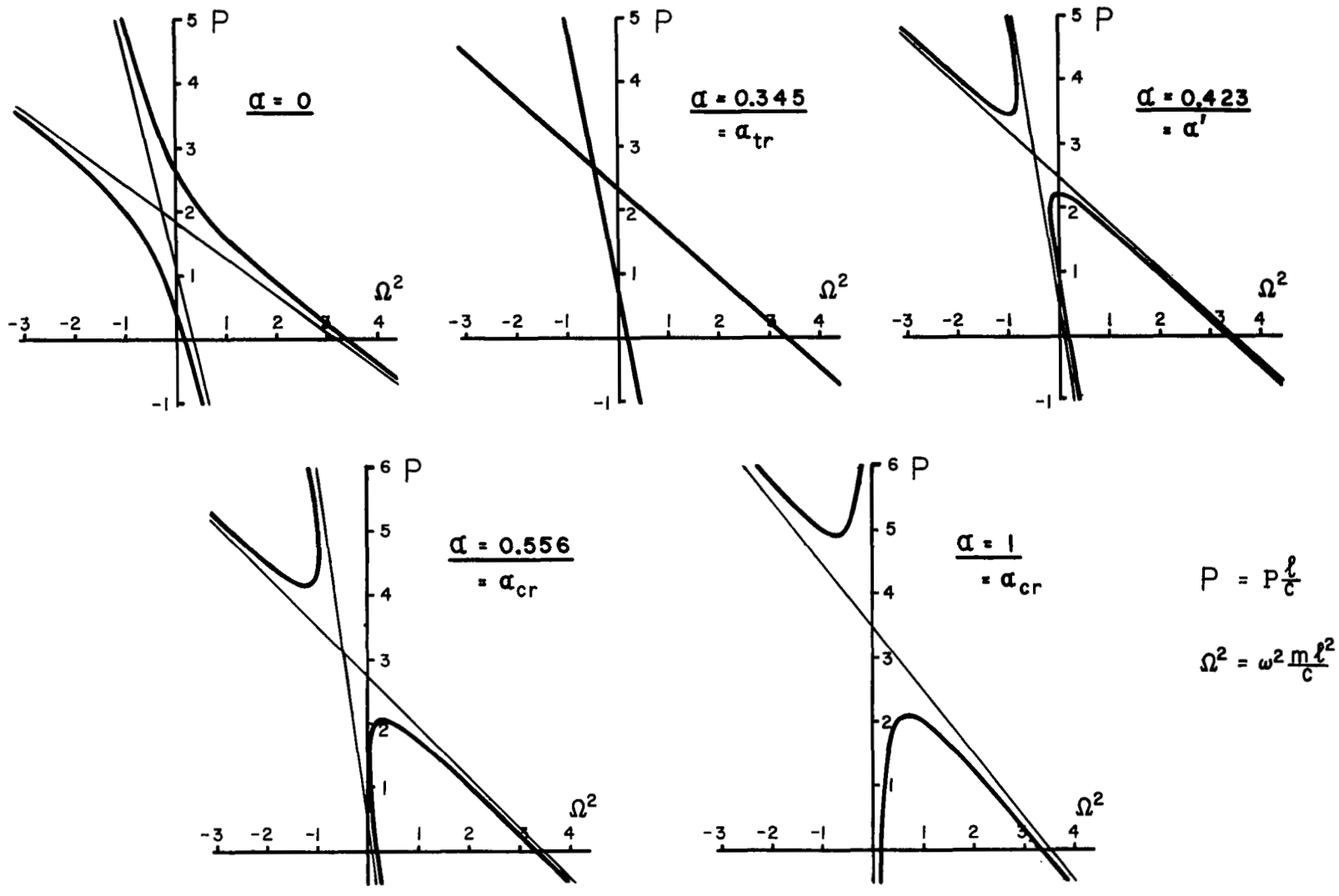

Fig. 3.2 Load versus frequency curves for particular values of parameter α in the range $0 \leq \alpha \leq 1$

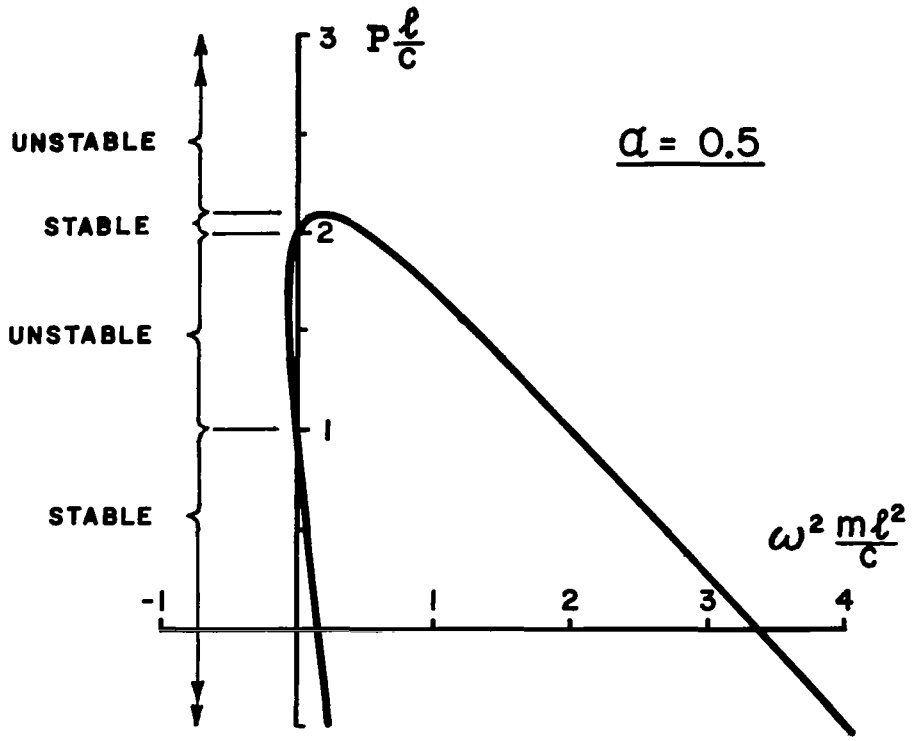

Fig. 3.3 Detail of load versus frequency curve for $\alpha = 0.5$, illustrating multiple ranges of stability and instability

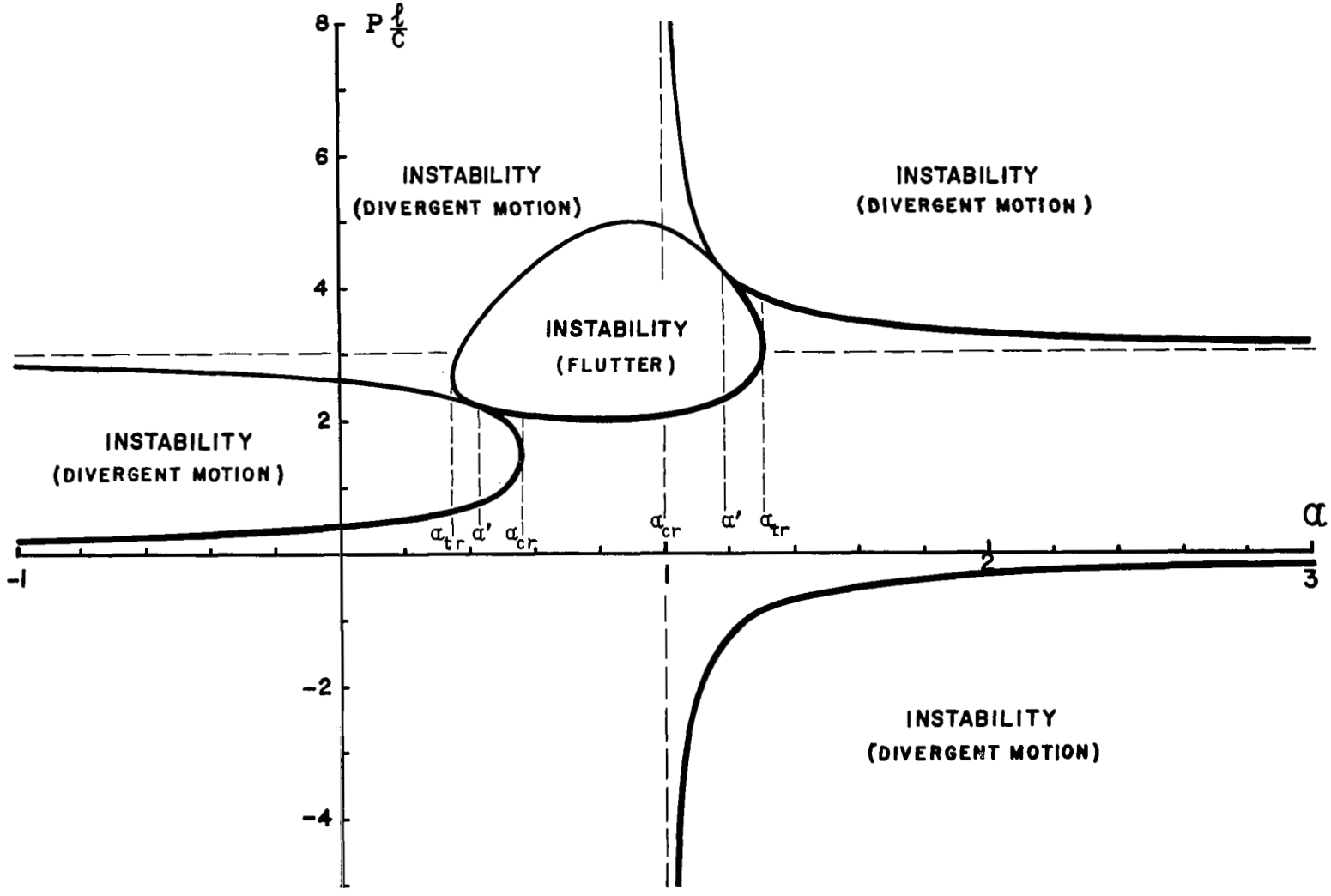

Fig. 3.4 Critical loads versus parameter α

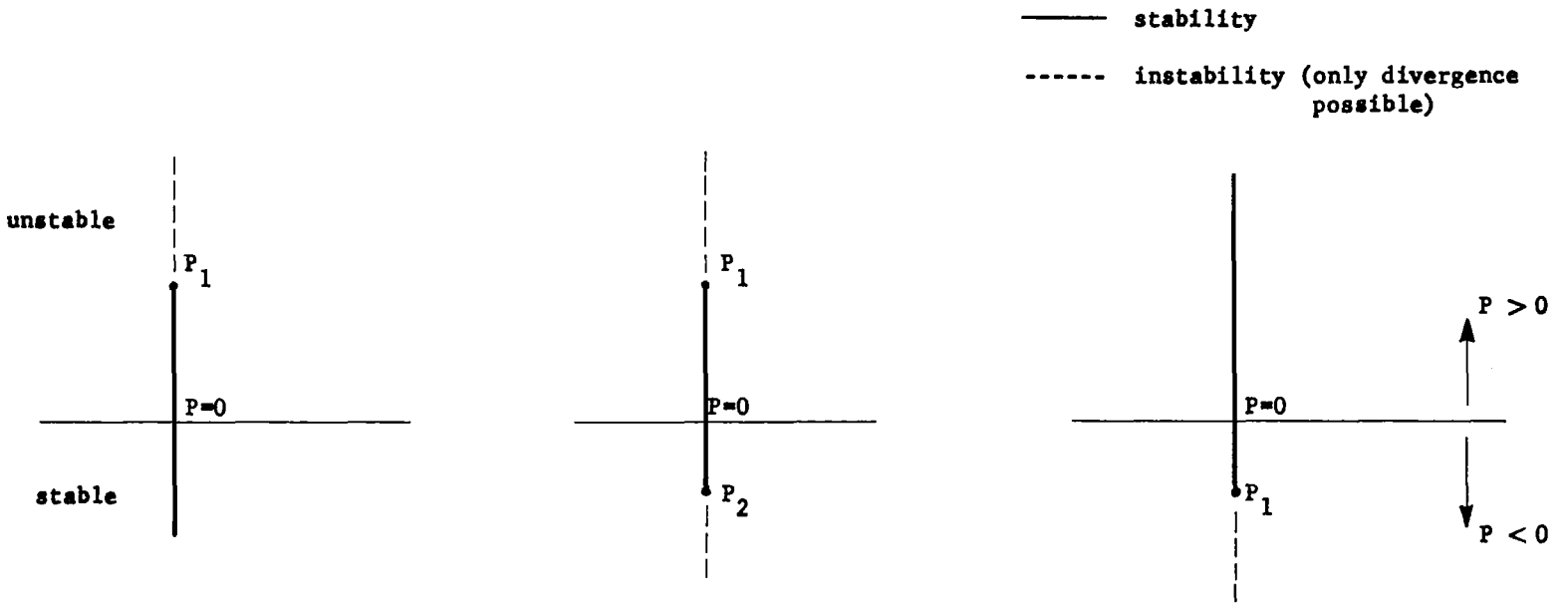

Fig. 3.5 Regions of stability for $\alpha_{12}\alpha_{21} > 0$

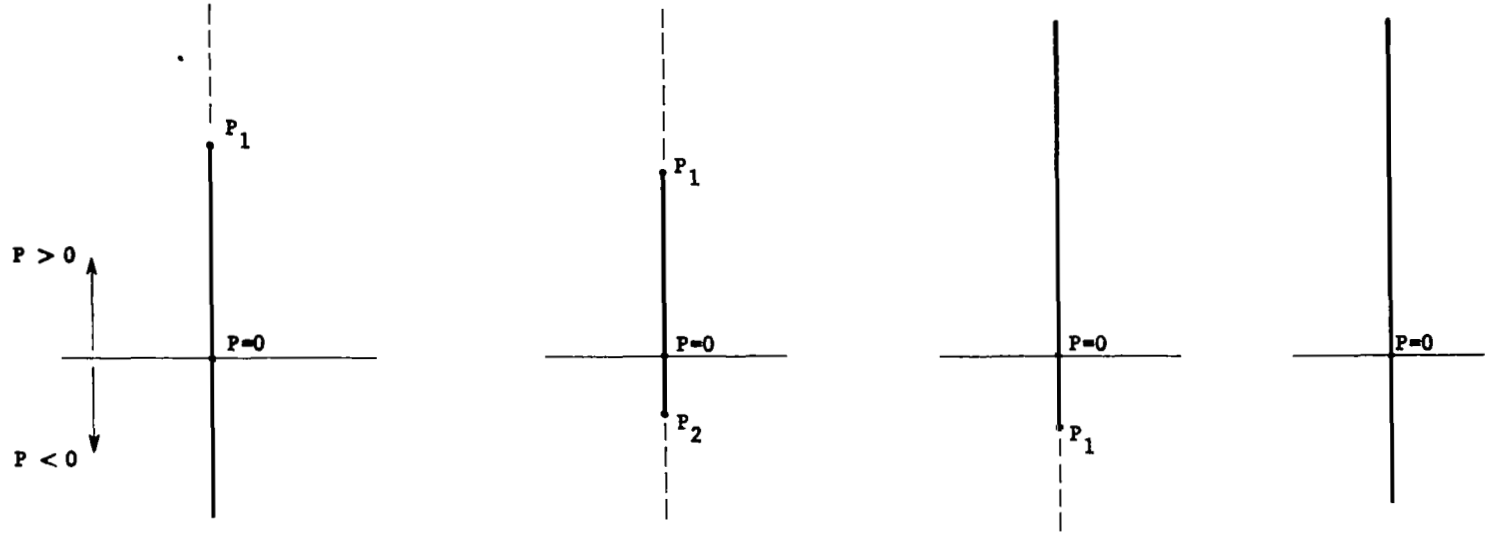

$c = \alpha_{11}\alpha_{22} \geq 0$

$2e = \alpha_{11}\xi_2 + \alpha_{22}\xi_1 < 0$

(a)

$c = \alpha_{11}\alpha_{22} < 0$

(b)

$c = \alpha_{11}\alpha_{22} \geq 0$

$2e = \alpha_{11}\xi_2 + \alpha_{22}\xi_1 > 0$

(c)

$\alpha_{11} = \alpha_{22} = 0$

——— stability

------ instability (only divergence possible)

Fig. 3.6 Regions of stability for $\alpha_{12}\alpha_{21} = 0$

Plain area: flutter may occur

Shaded area: no flutter possible

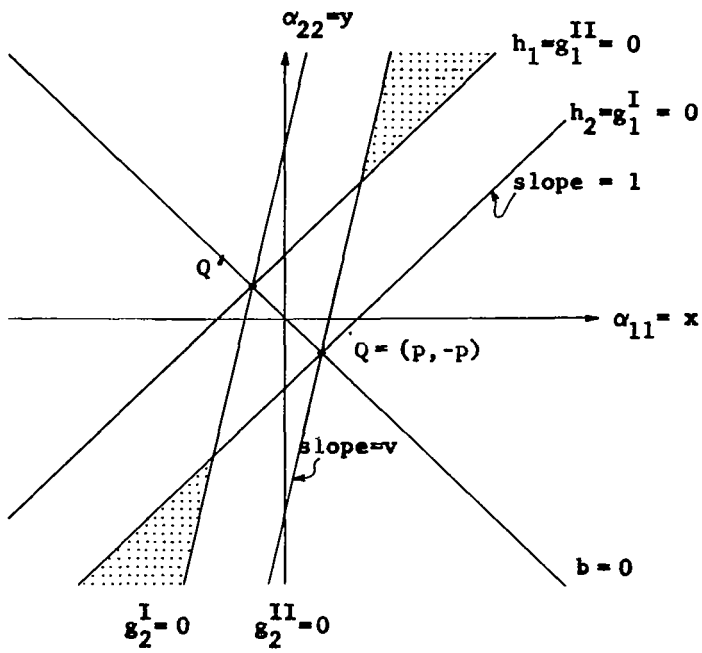

Note: straight lines $g_2^i = 0$ have slope v; v and p are defined

Fig. 3.7 Existence of flutter

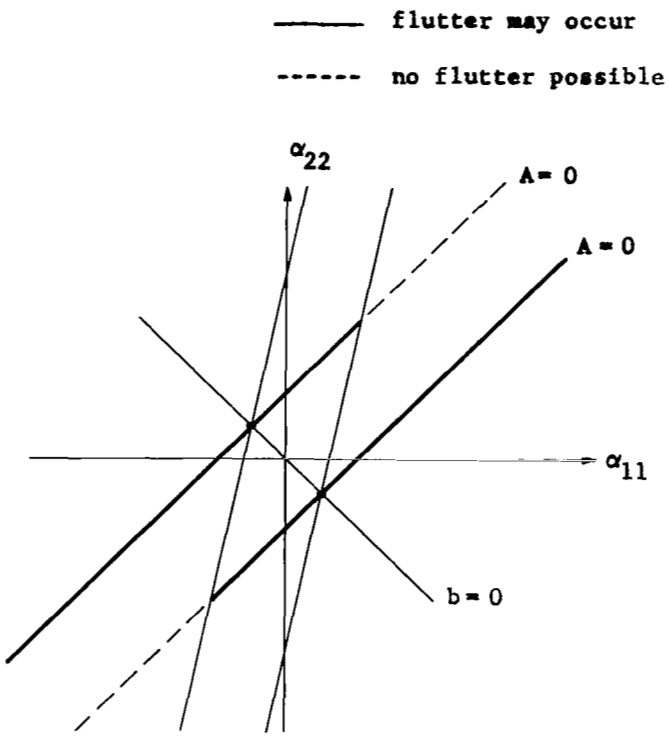

Fig. 3.8 Existence of flutter for A = 0

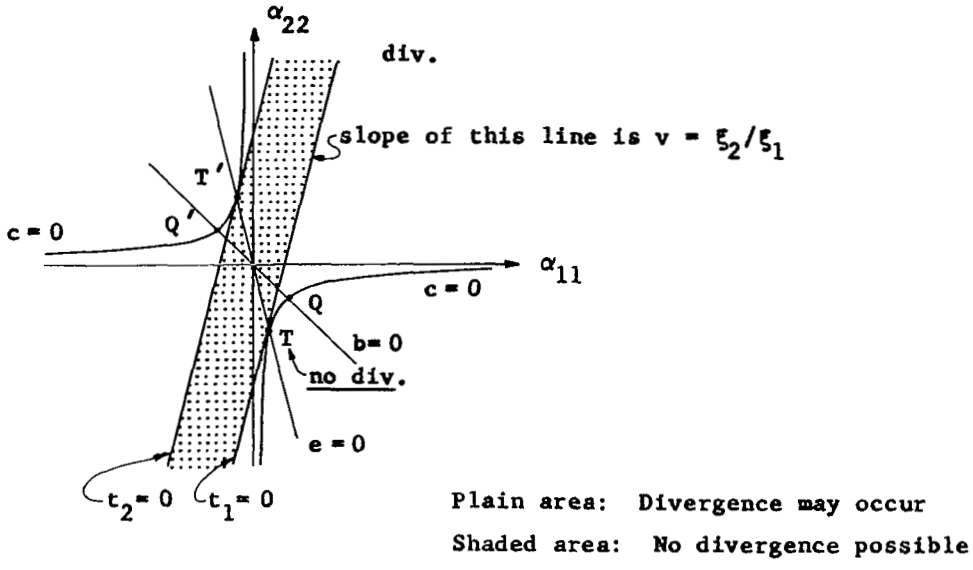

Fig. 3.9 Existence of divergence

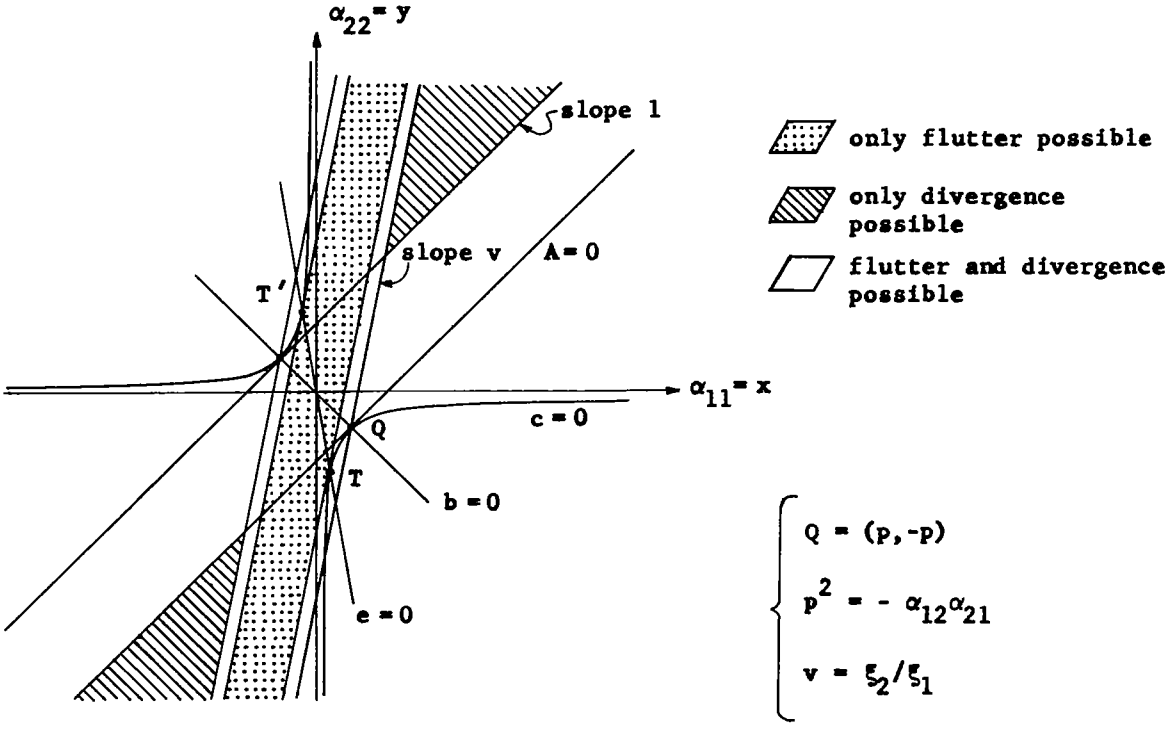

Fig. 3.10 Possibilities of flutter and divergence

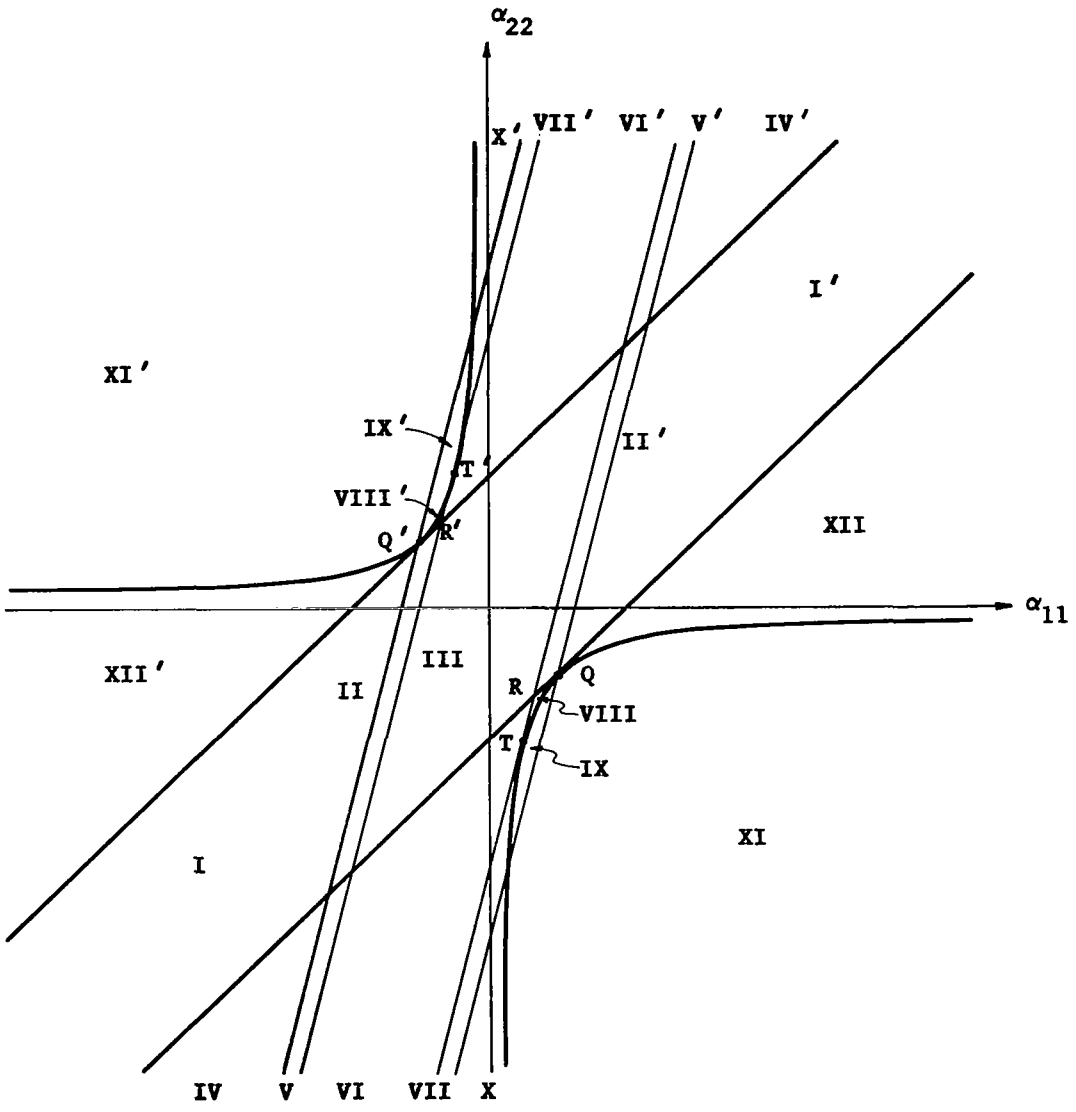

Fig. 3.11 Stability and instability areas

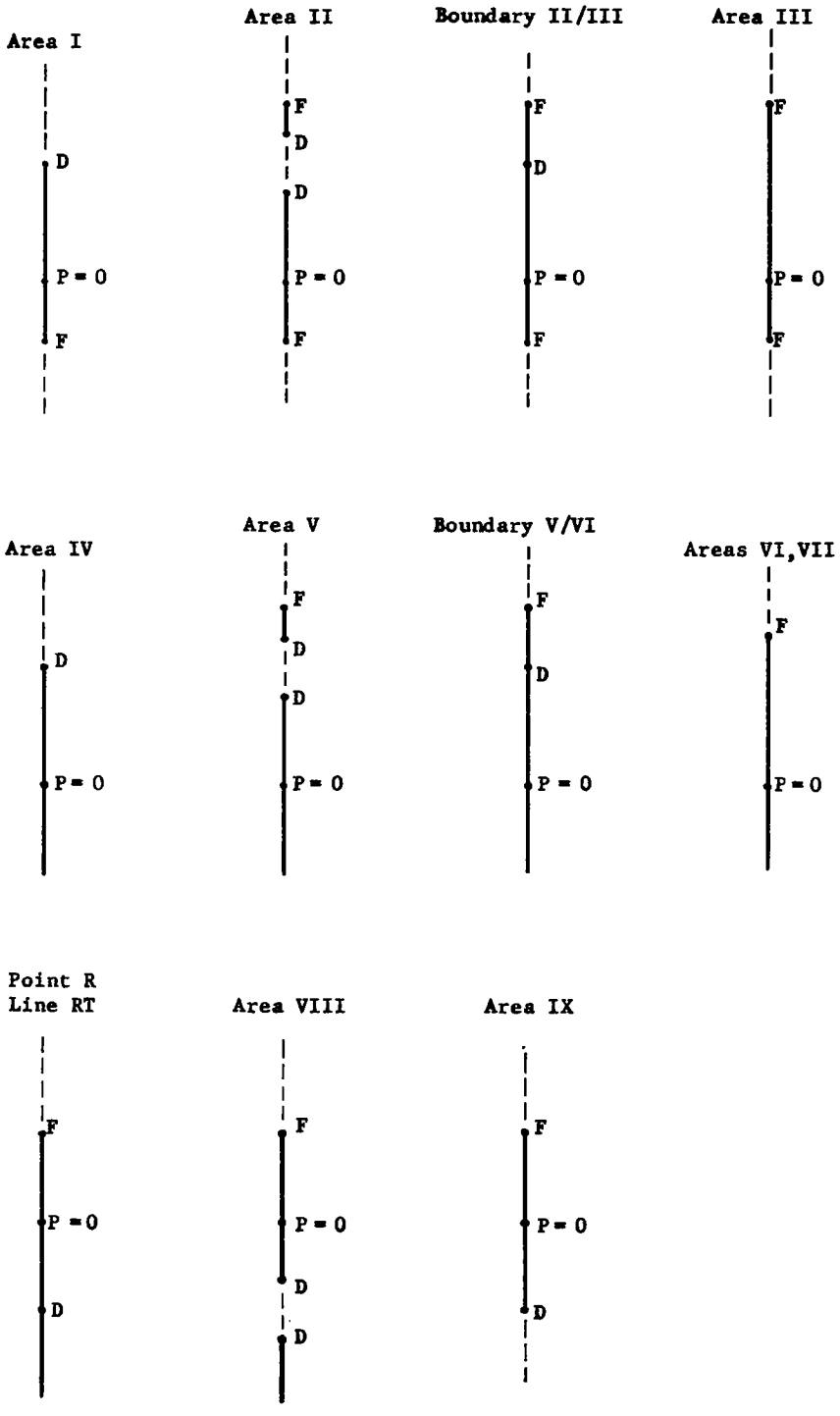

Fig. 3.12 Details of loss of stability in areas I through XII (Cont'd.)

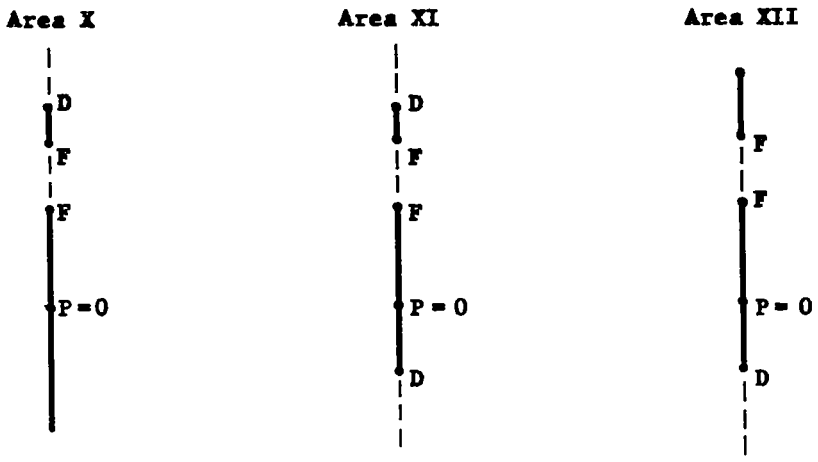

——— stability

------ instability

D indicates that stability is lost by divergence

F indicates that stability is lost by flutter

Area	I	includes	Boundary	I/II and I/XII′
"	IV	"	"	IV/V and IV/I
"	V	"	"	V/II
"	VI,VII	"	"	VI/III, VII/X, and Point T
"	VIII	"	"	VIII/XIV
"	IX	"	"	IX/XI and Point Q
"	X	"	"	X/XI
"	XII	"	"	XI/XII

Fig. 3.12 Details of loss of stability in areas I through XII (Concluded)

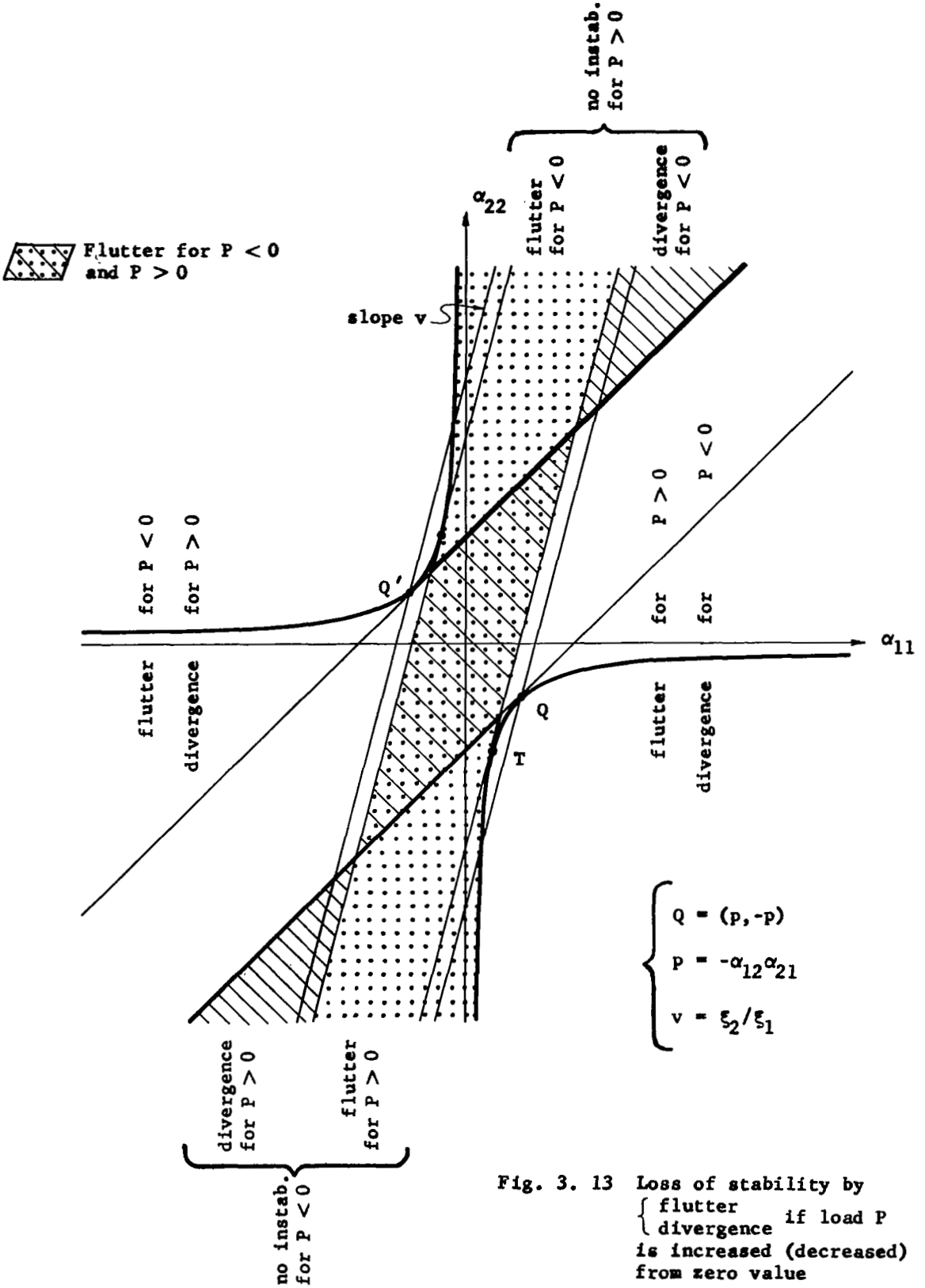

Fig. 3. 13 Loss of stability by $\begin{cases} \text{flutter} \\ \text{divergence} \end{cases}$ if load P is increased (decreased) from zero value

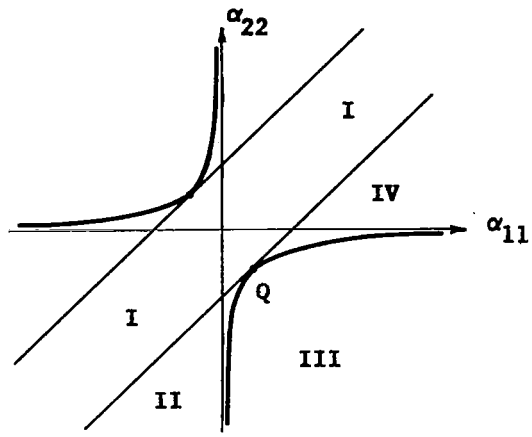

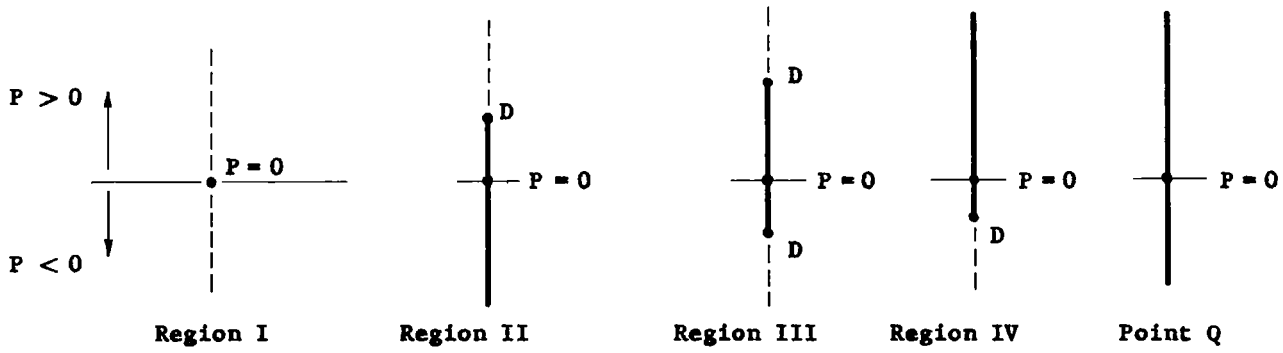

Region II includes Boundaries I/II and II/III
" IV " " III/IV and IV/I

Fig. 3.14 Loss of stability in regions I through IV

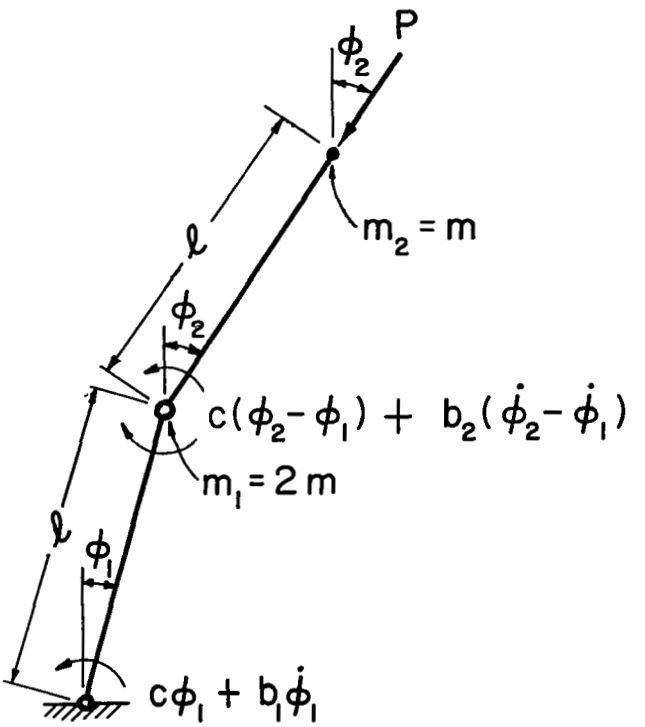

Fig. 4.1 Two-degree-of-freedom model

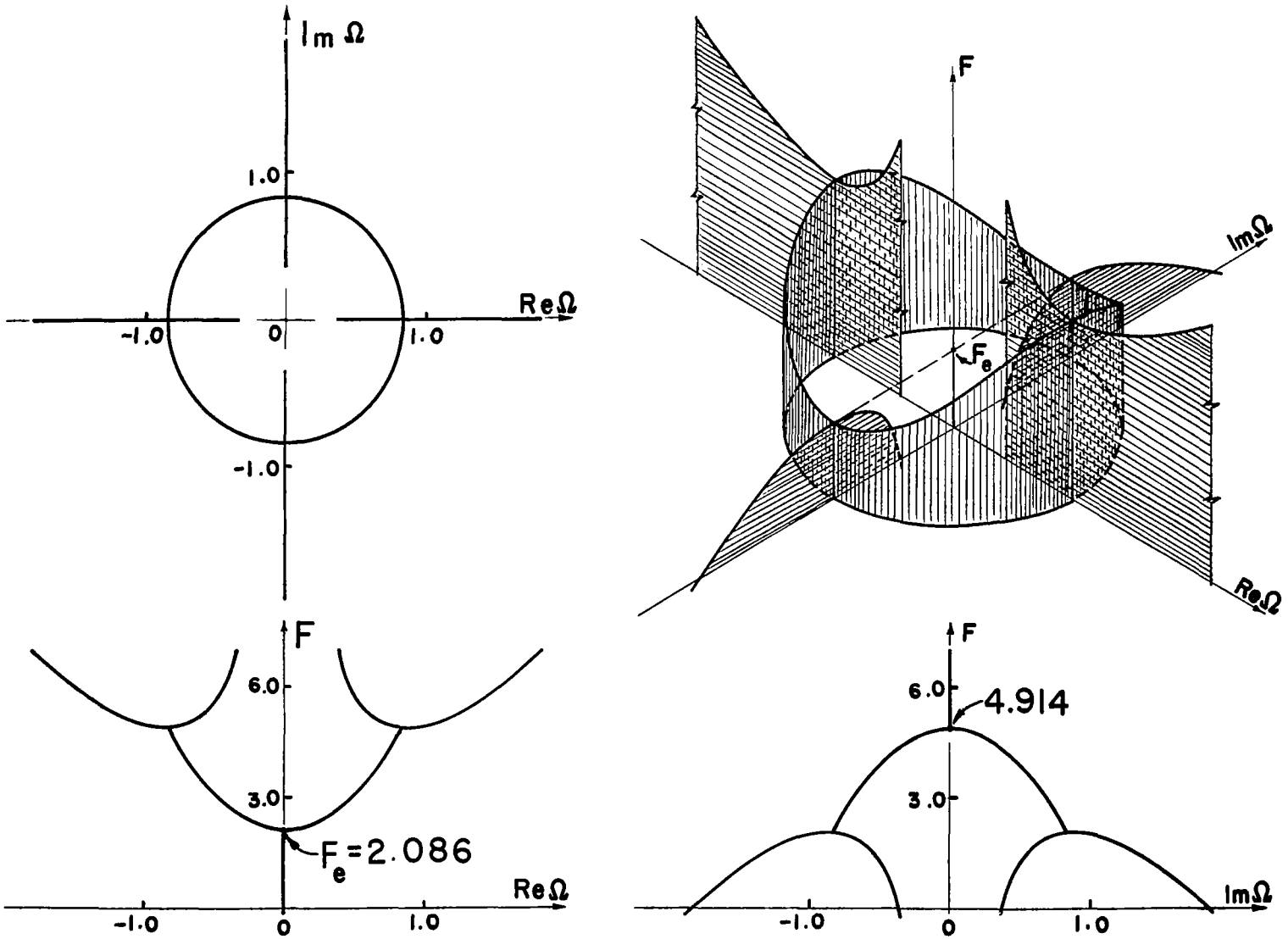

Fig. 4.2 Orthographic projections and perspective of root curves of characteristic equation with no damping

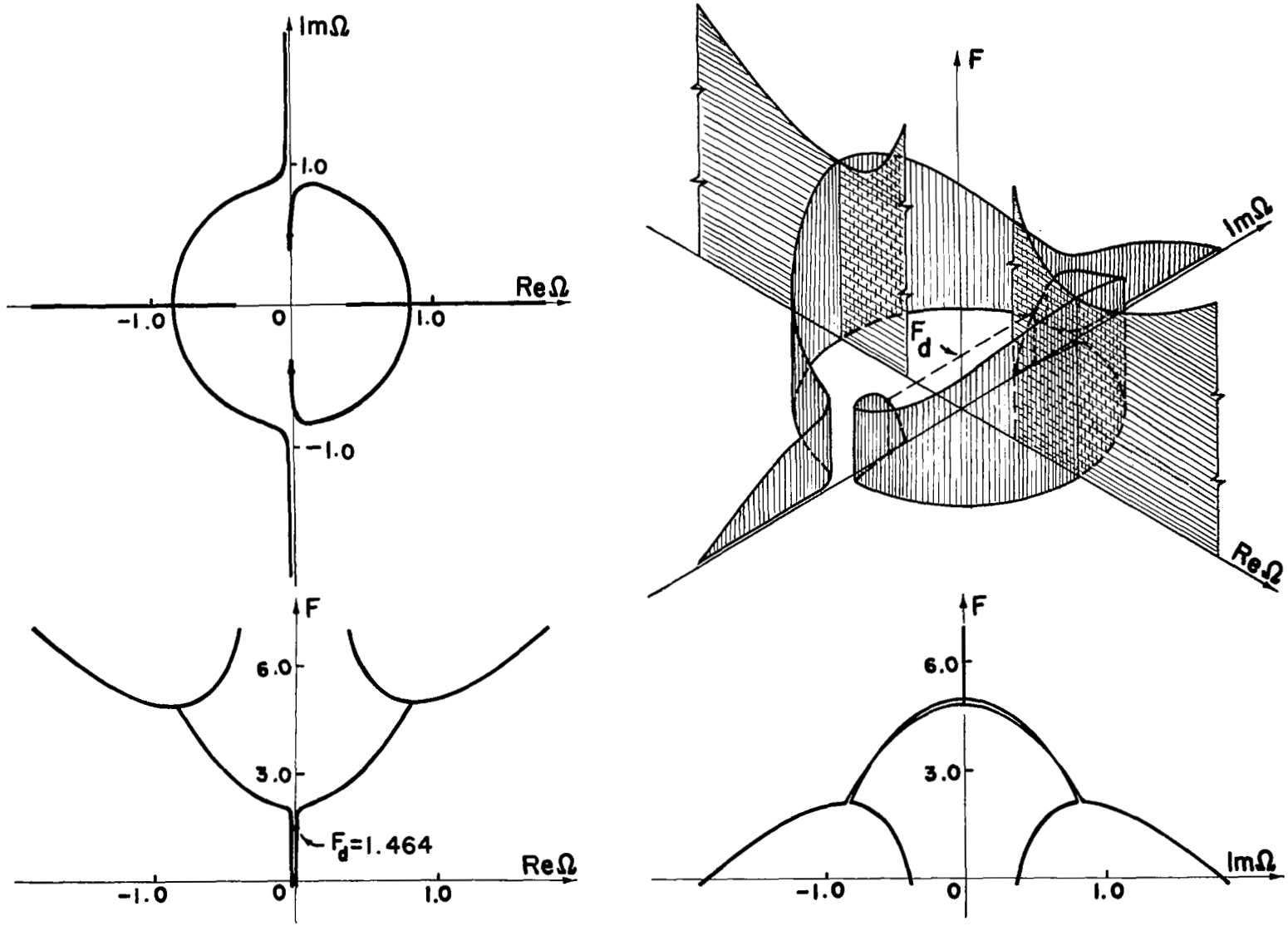

Fig. 4.3 Orthographic projections and perspective of root curves of characteristic equation with damping

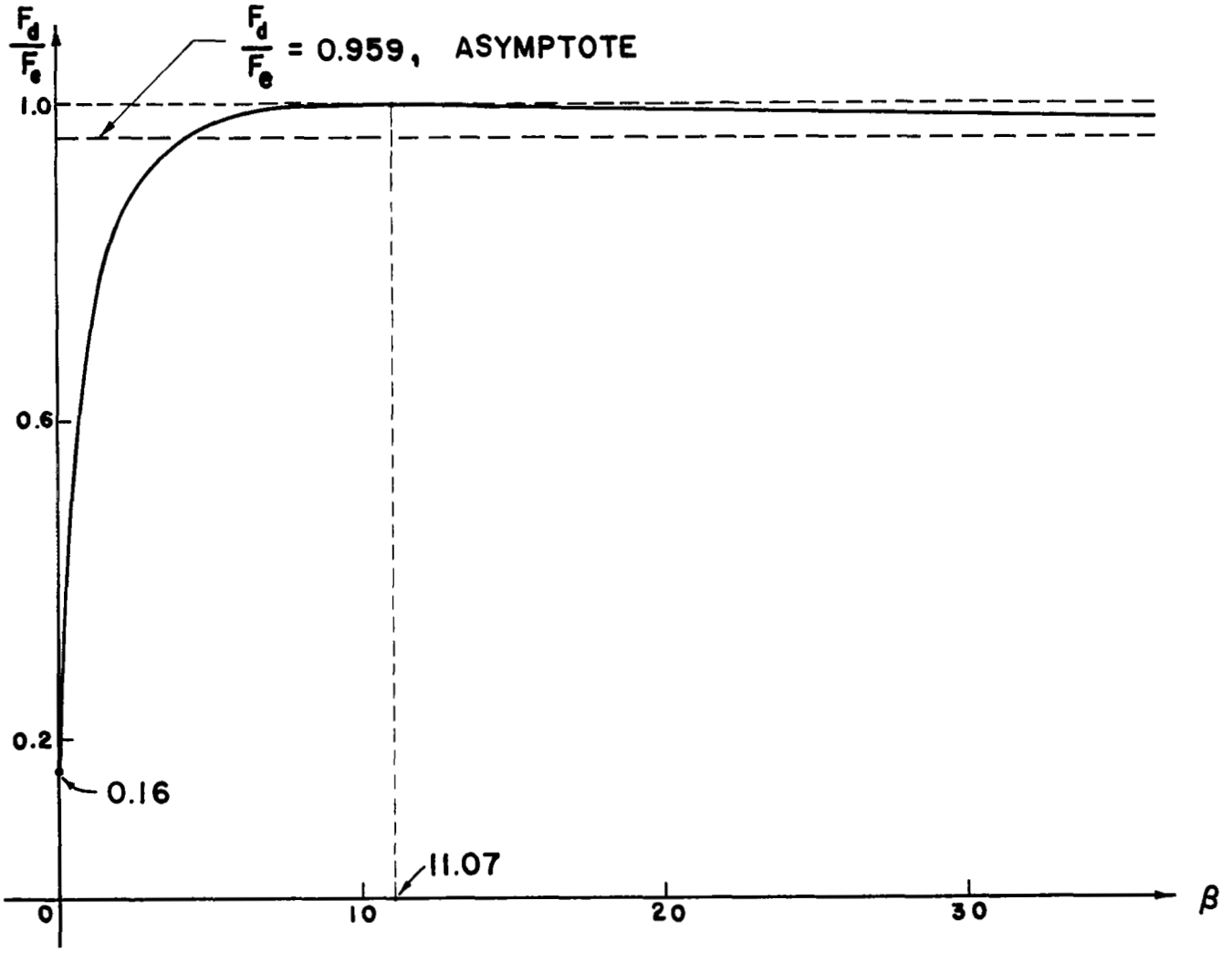

Fig. 4.4 Critical load versus ratio of damping coefficients for $B_i \ll 1$

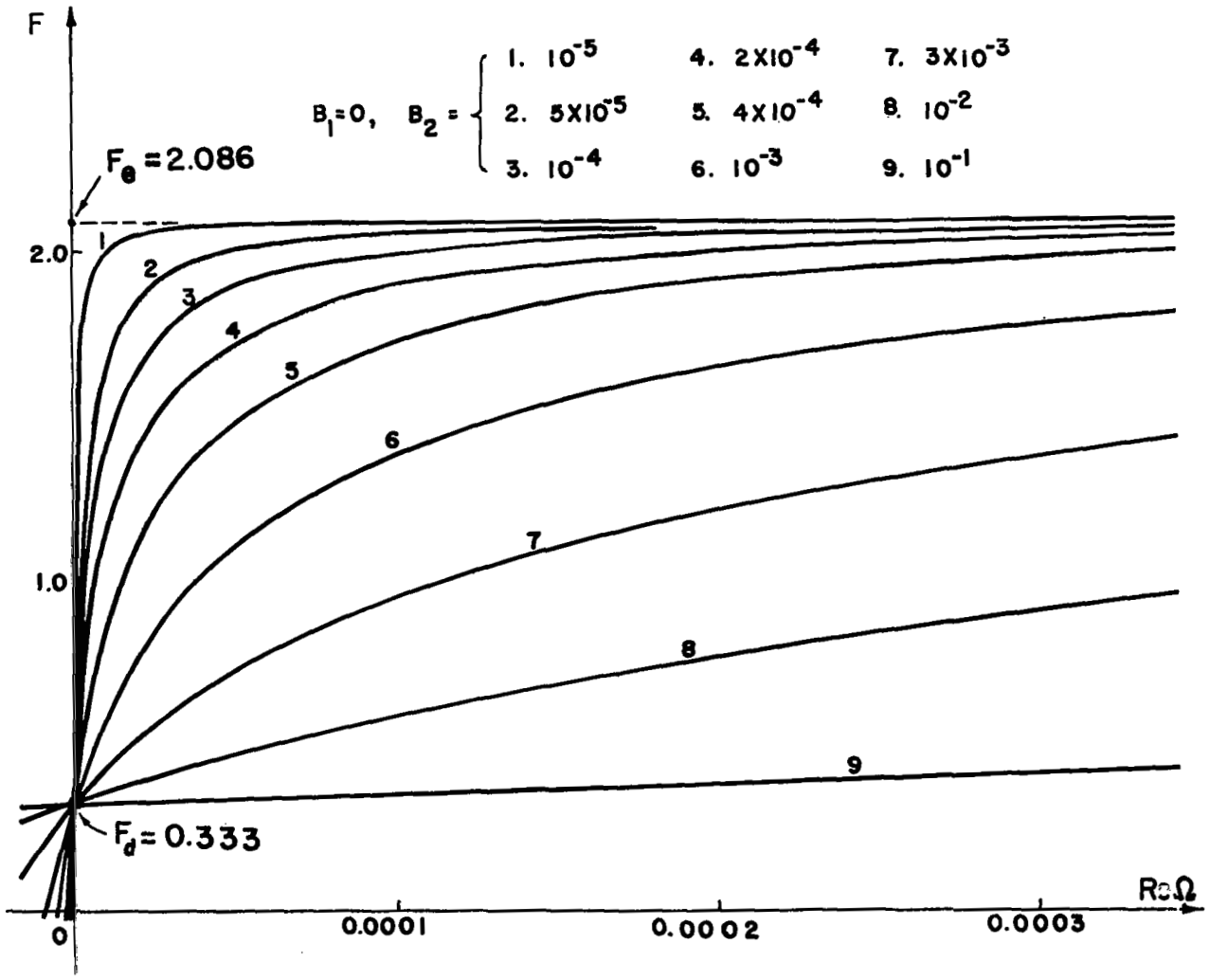

Fig. 4.5 Significance of critical load F_d as B_2 increases

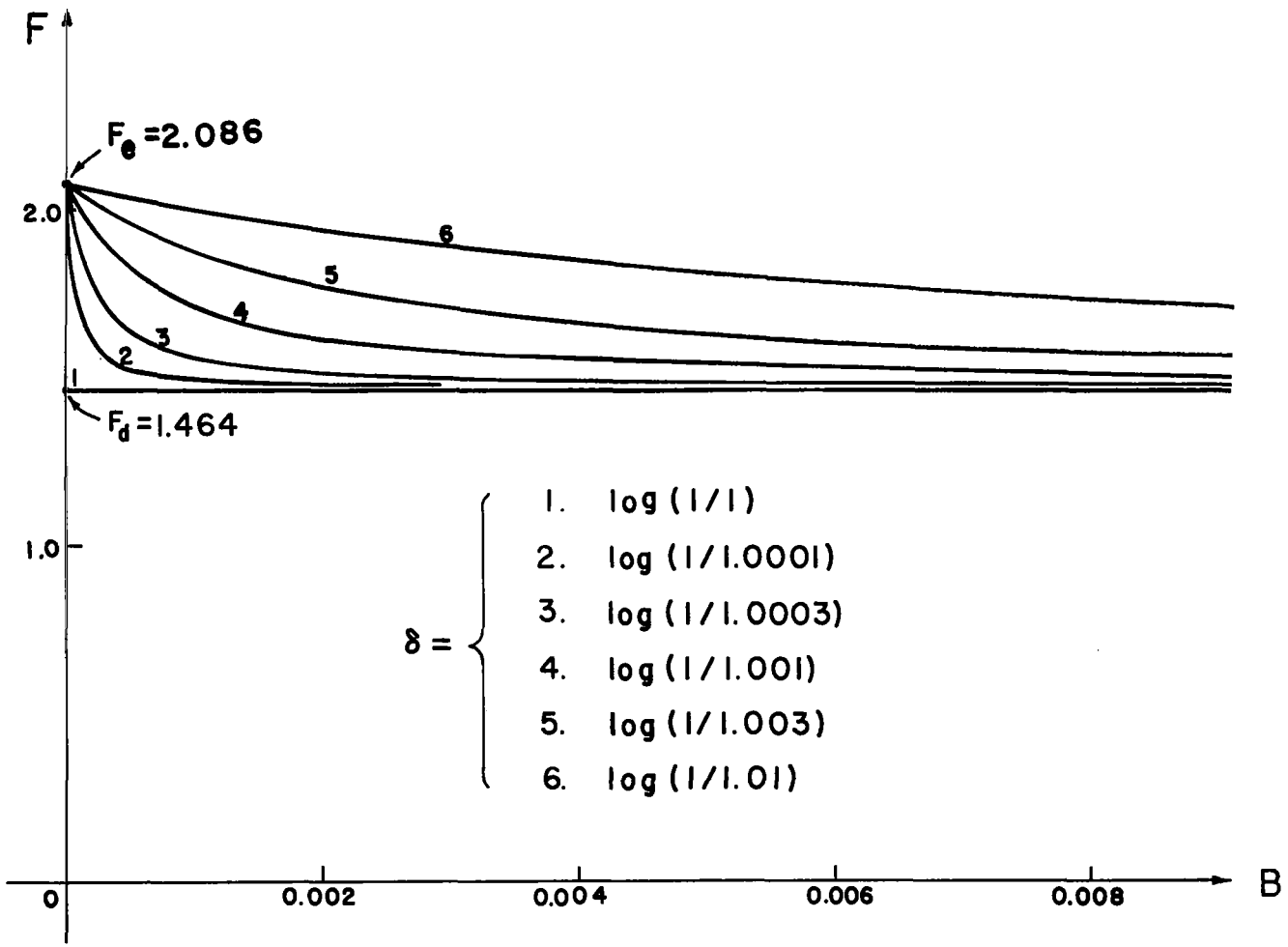

Fig. 4.6 Critical load for various degrees of instability versus small damping coefficients

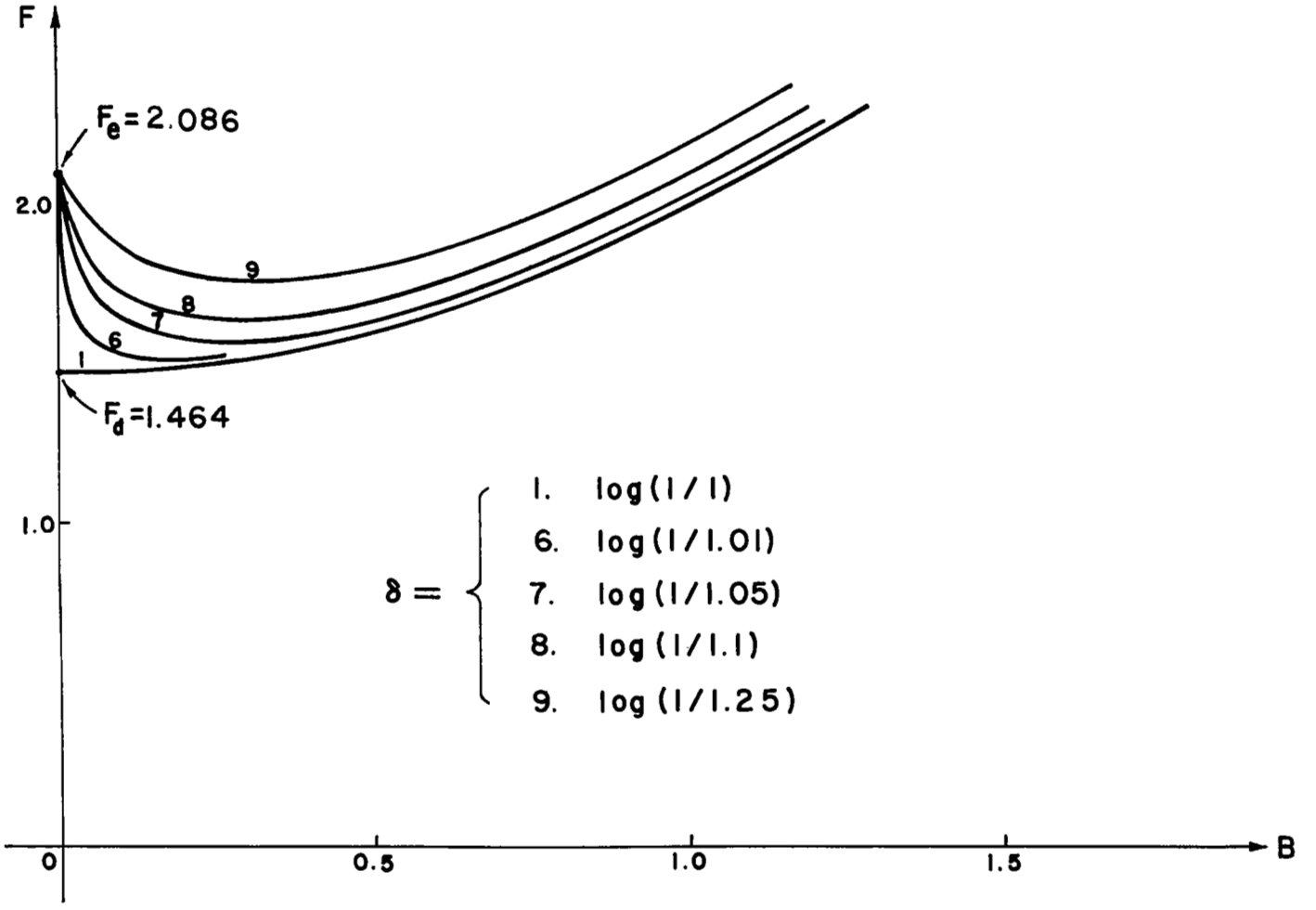

Fig. 4.7 Critical load for various degrees of instability versus large damping coefficients

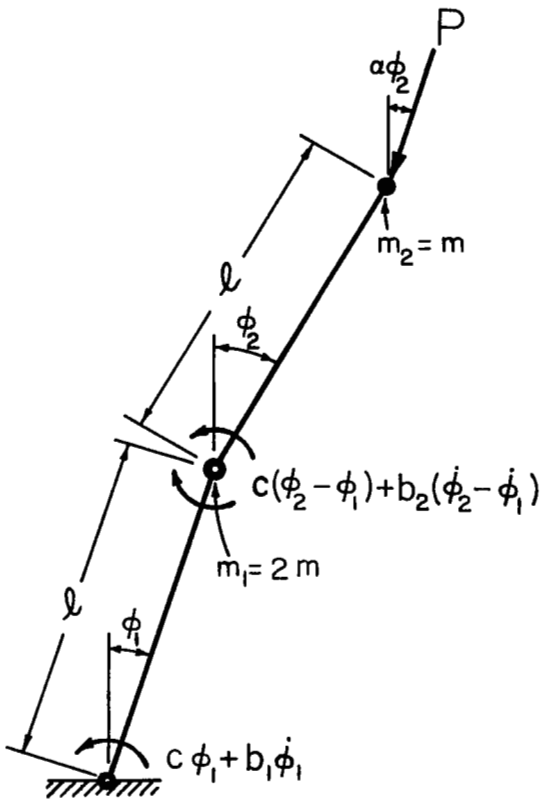

Fig. 4.8 Two-degree-of-freedom model

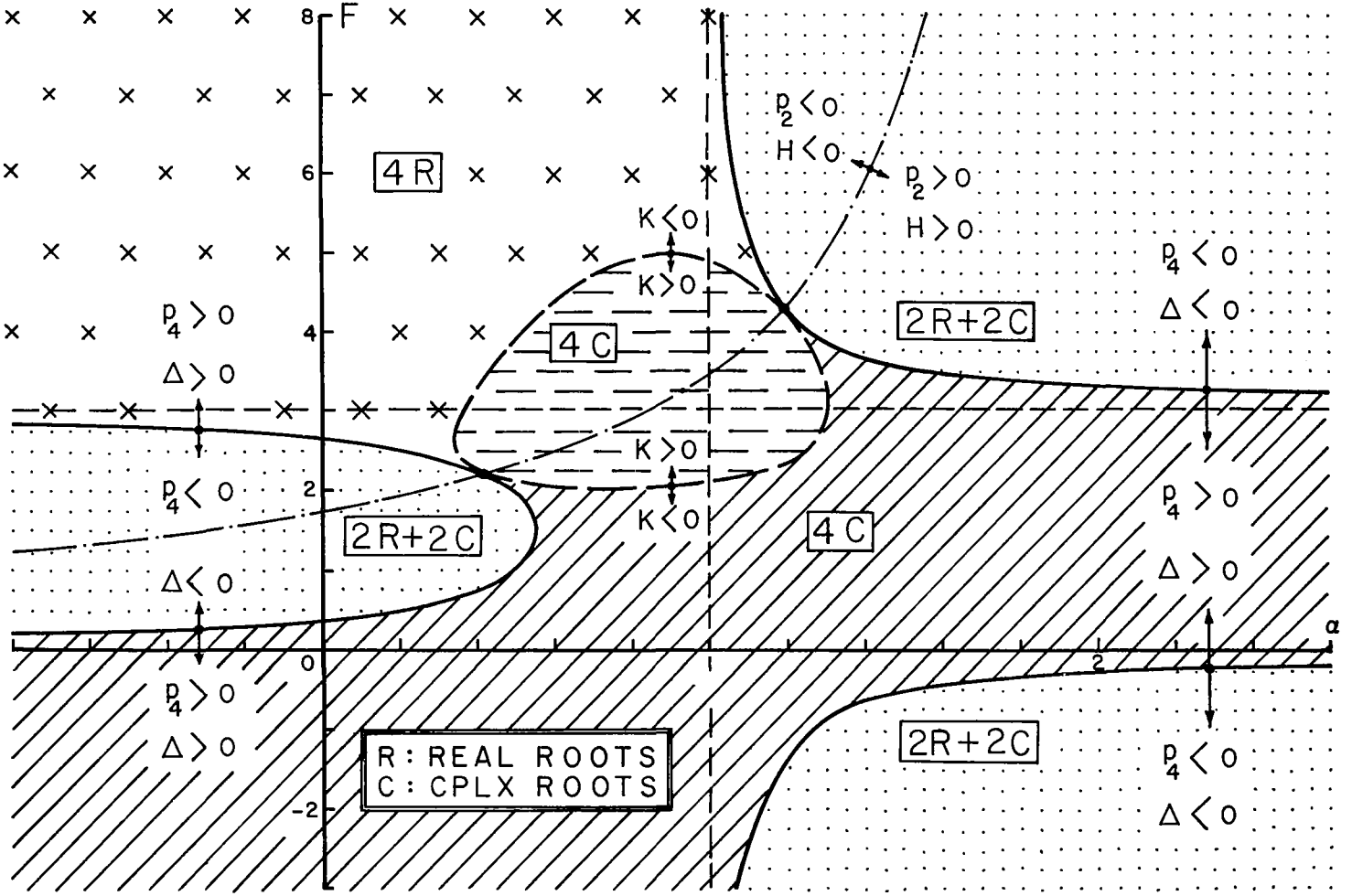

Fig. 4.9 General nature of roots of characteristic equation

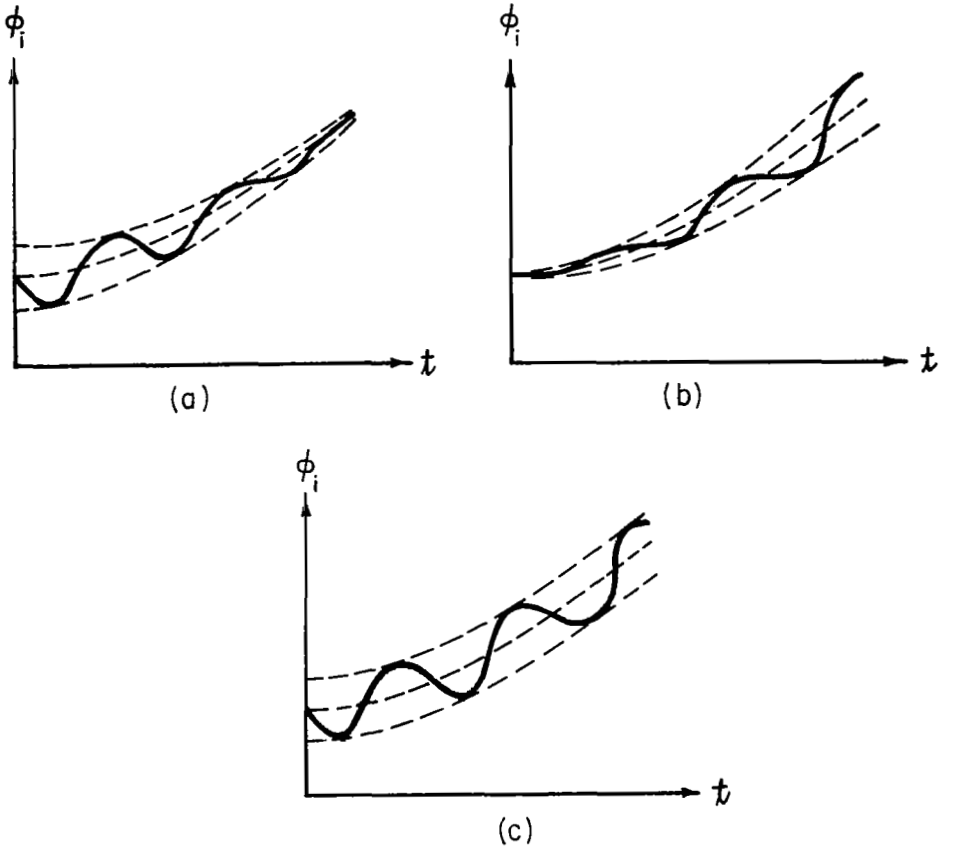

Fig. 4.10 Types of divergent motion

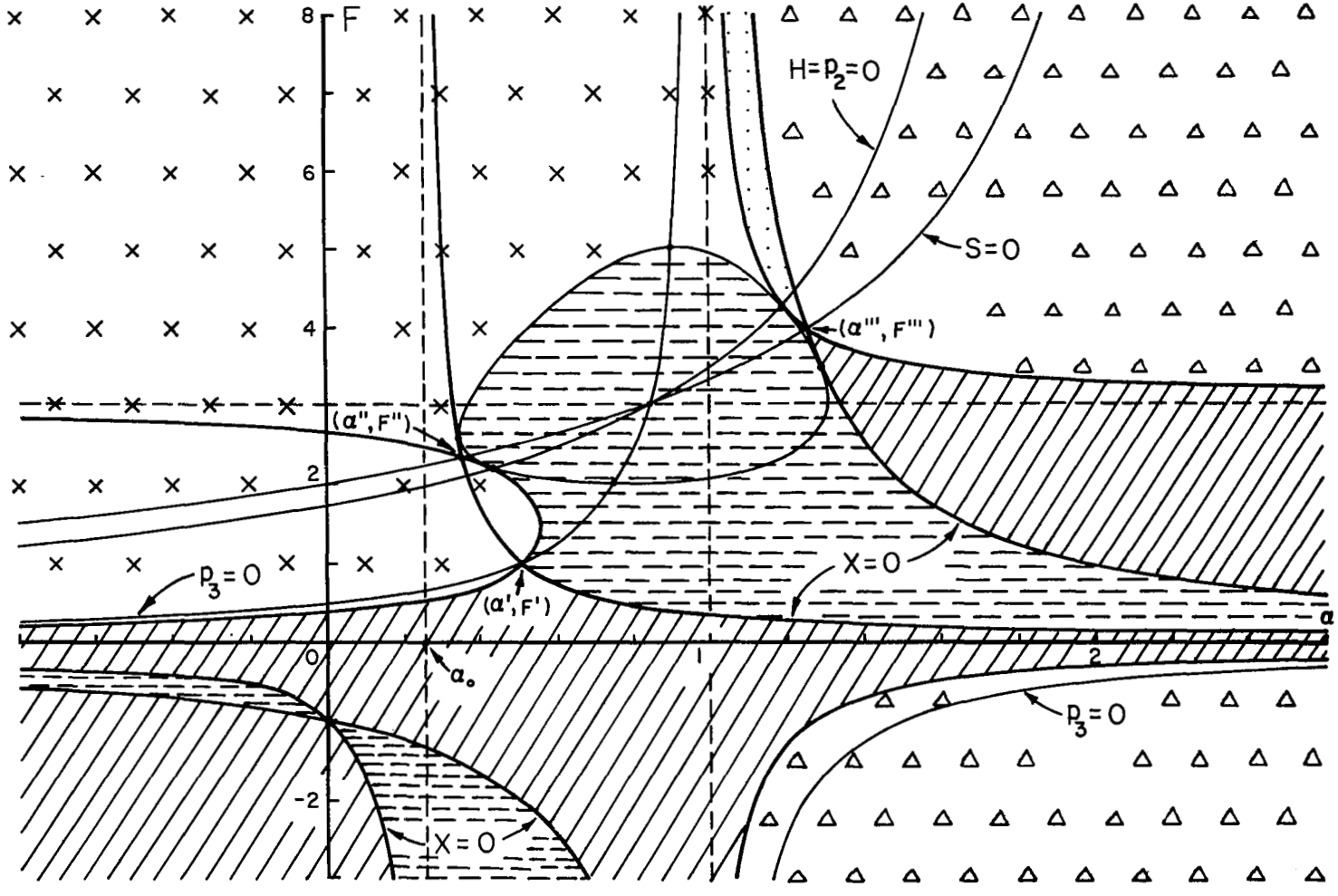

Fig. 4.11 Critical loads and instability mechanisms for β = 0

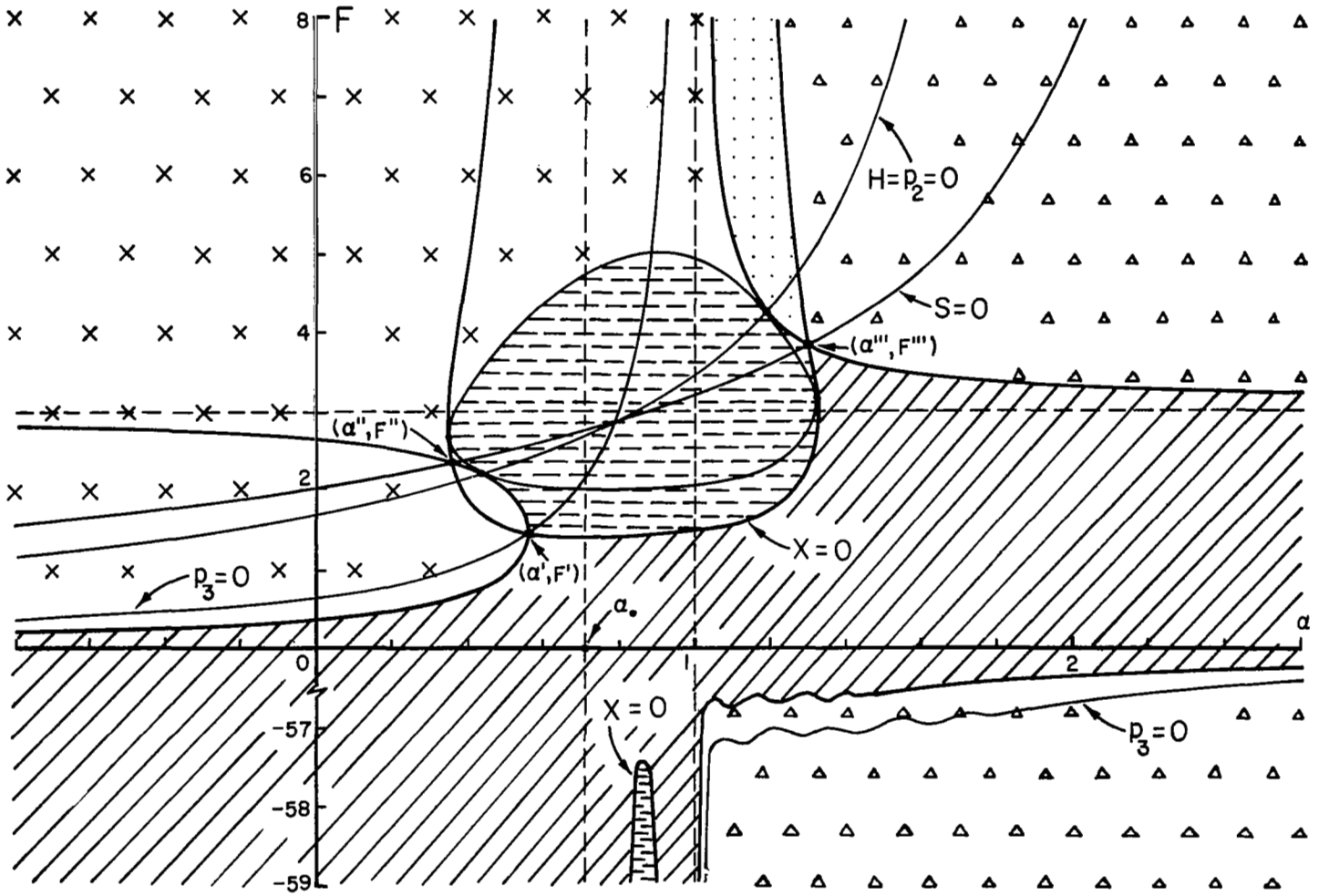

Fig. 4.12 Critical loads and instability mechanisms for β = 1

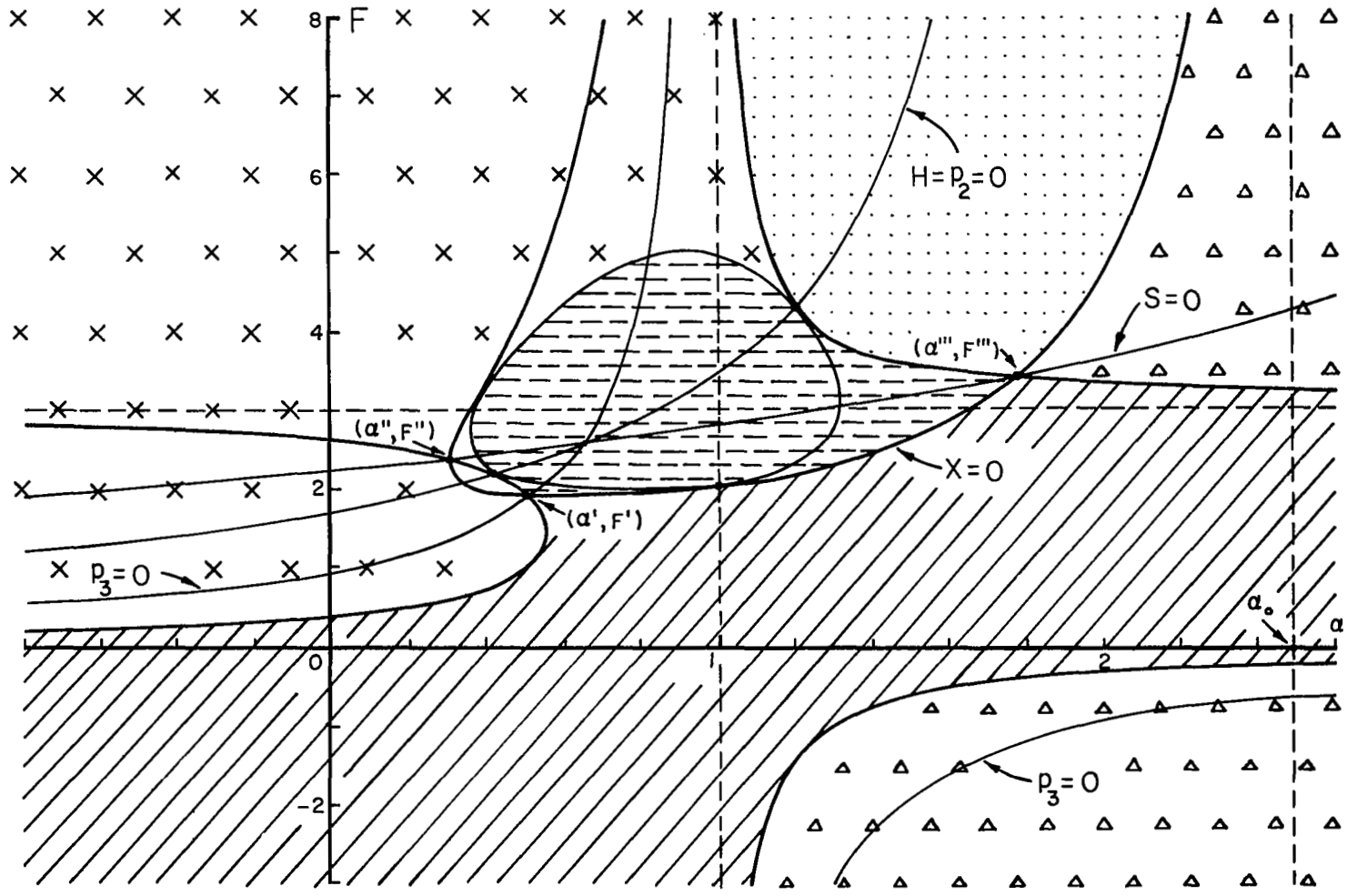

Fig. 4.13 Critical loads and instability mechanisms for β = 11.071

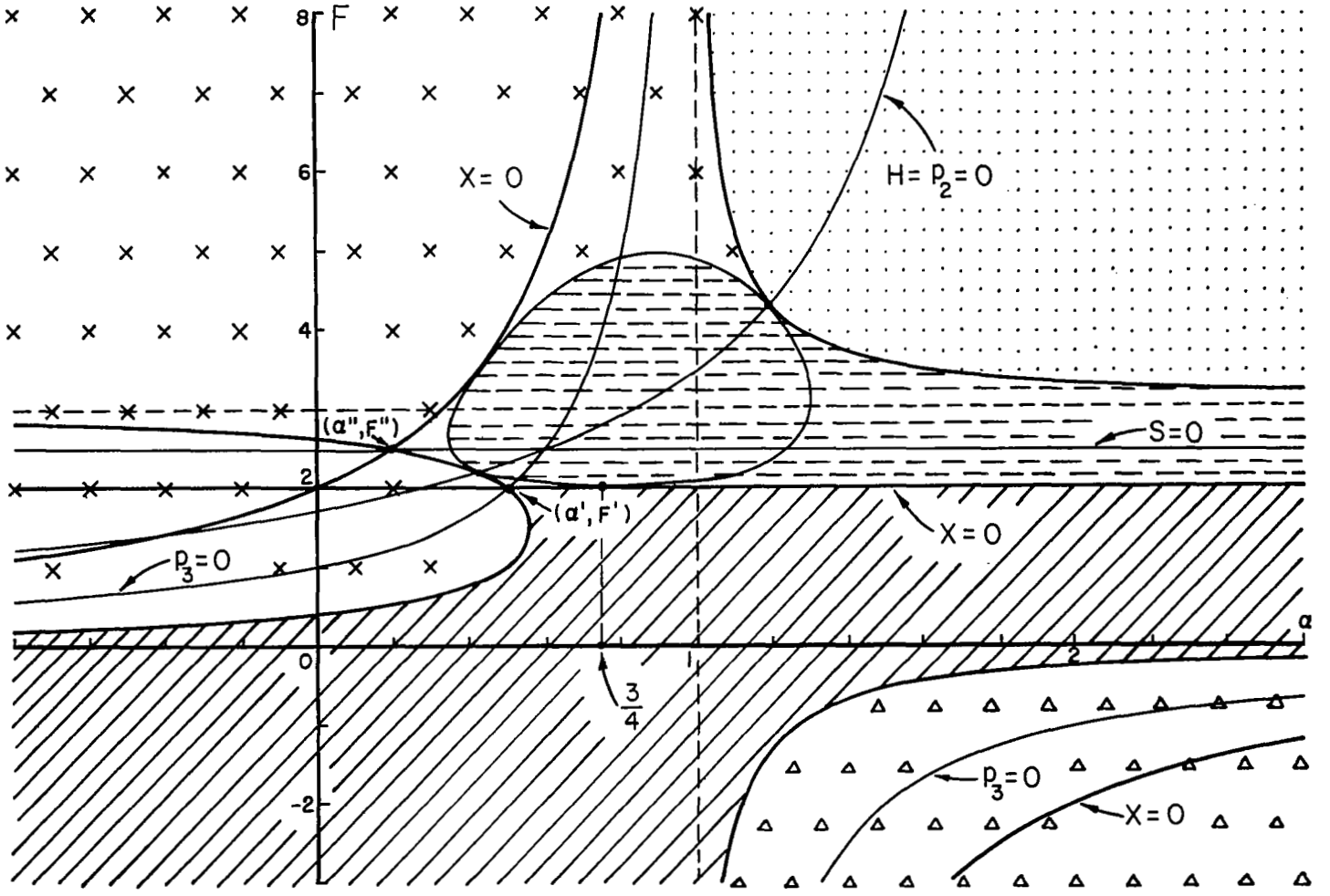

Fig. 4.14 Critical loads and instability mechanisms for $\beta = \infty$

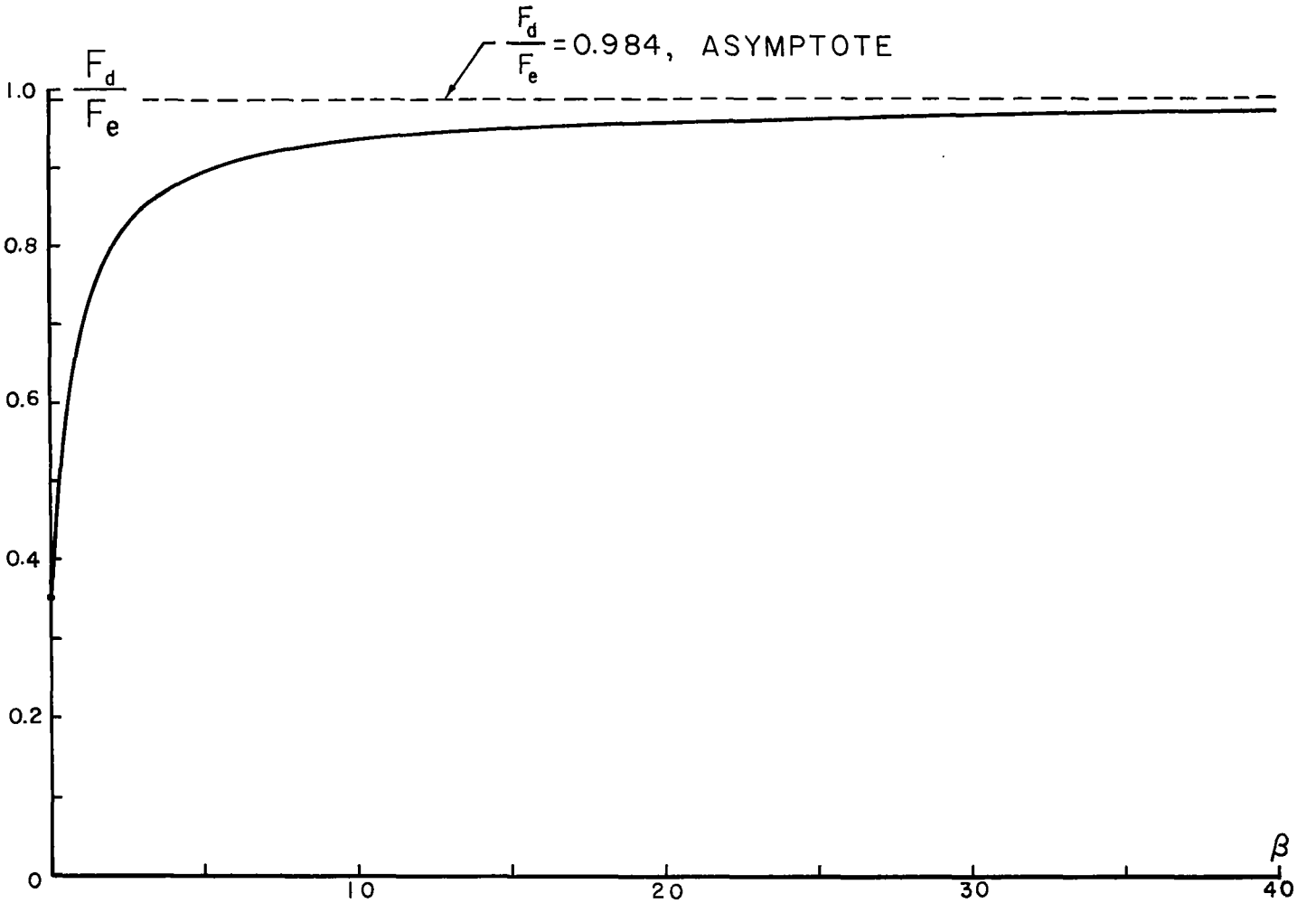

Fig. 4.15 Critical load versus ratio of damping coefficients for $\alpha = 0.6$

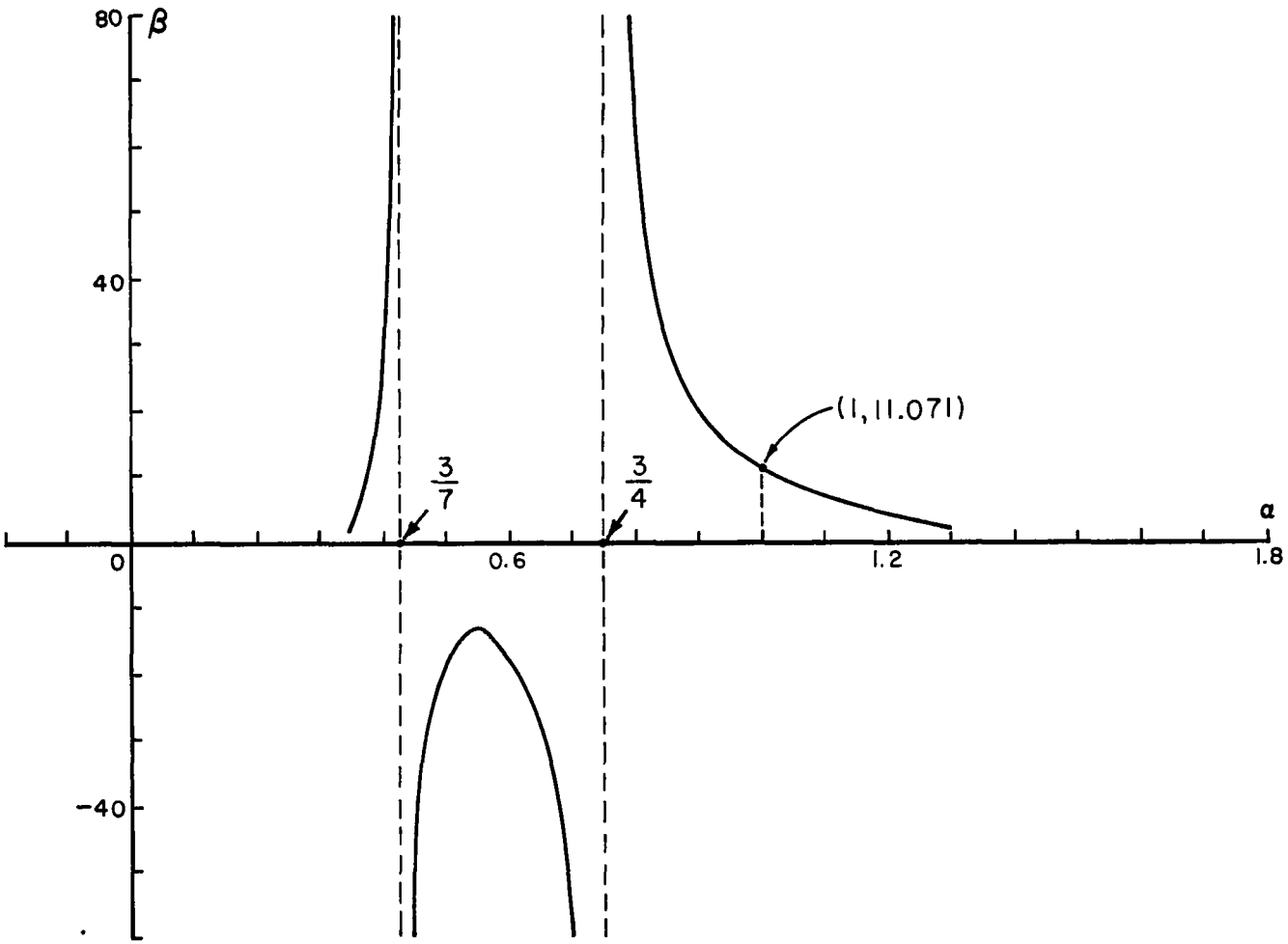

Fig. 4.16 Appropriate values of β versus values of α for complete elimination of destabilizing effect

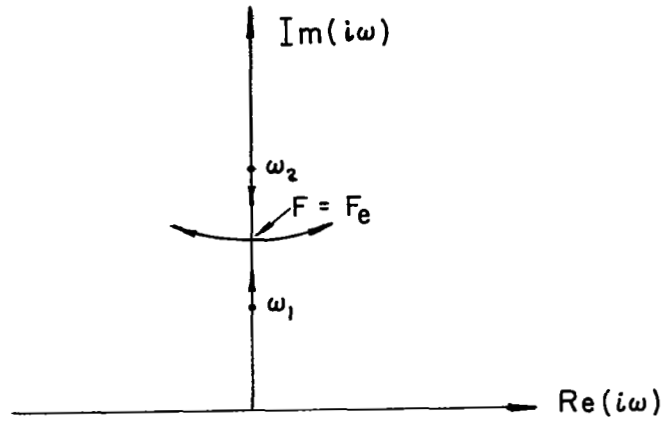

(a)

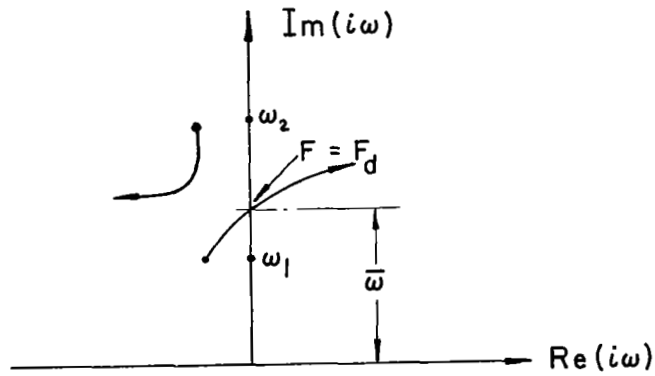

(b)

Fig. 4.17 Characteristic roots in the complex plane

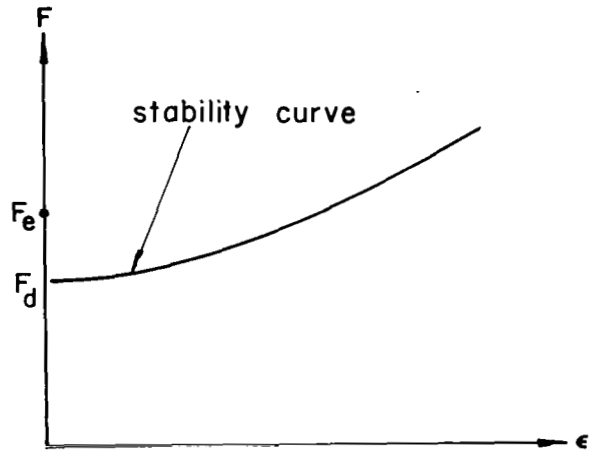

Fig. 4.18 Critical loads with and without damping

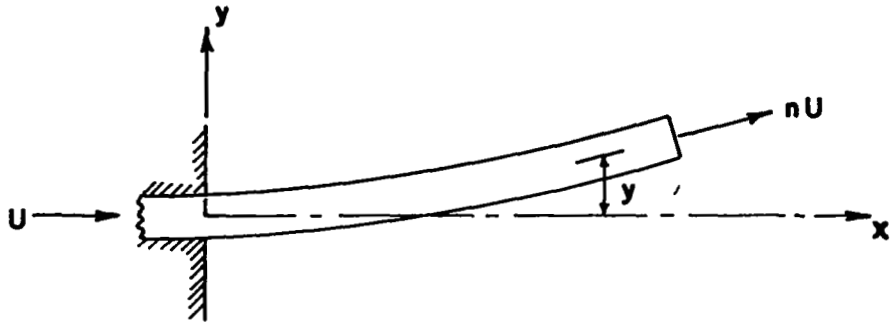

Fig. 4.19 Geometry of cantilevered pipe conveying fluid

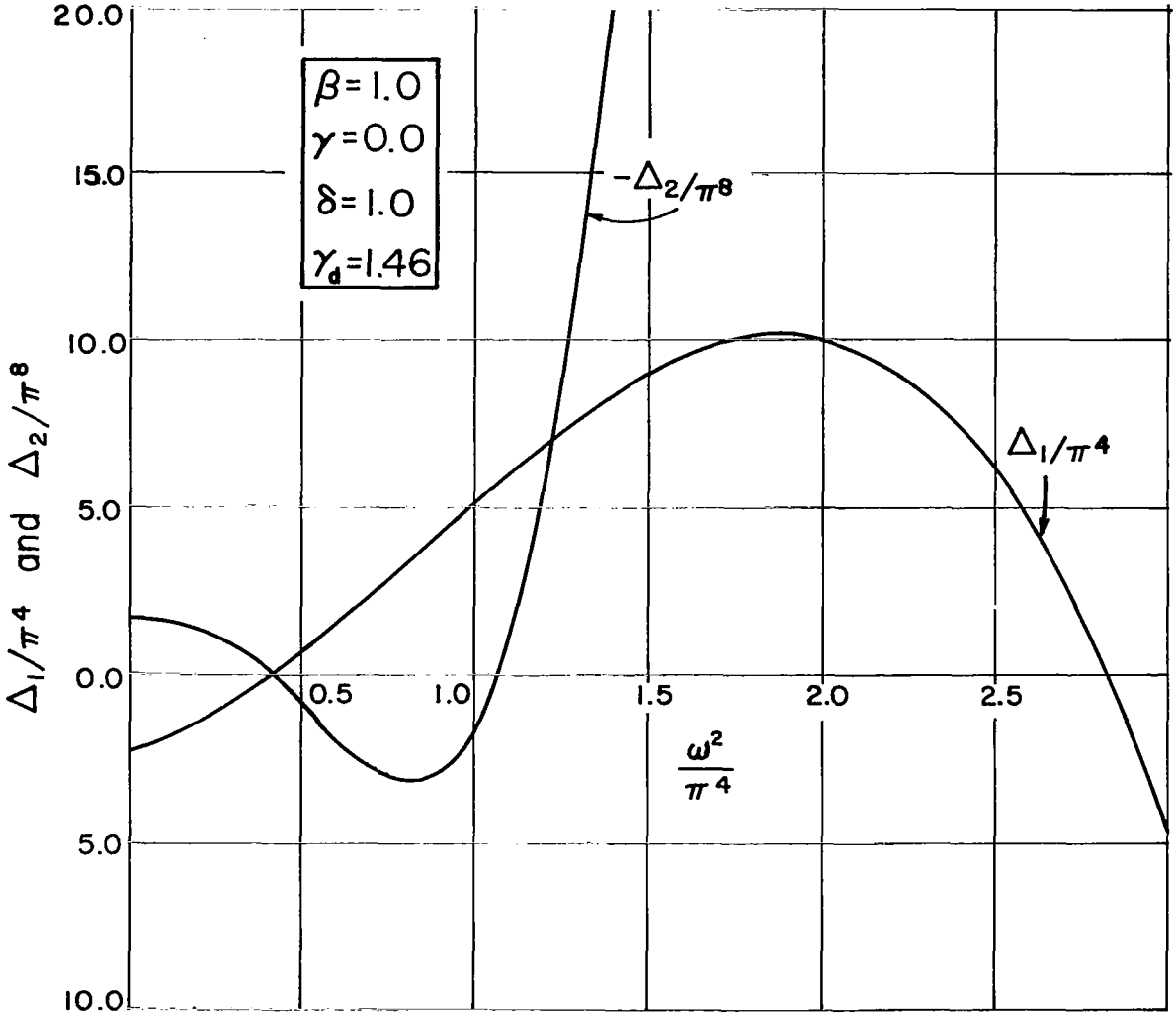

Fig. 4.20 Typical plot of frequency equation

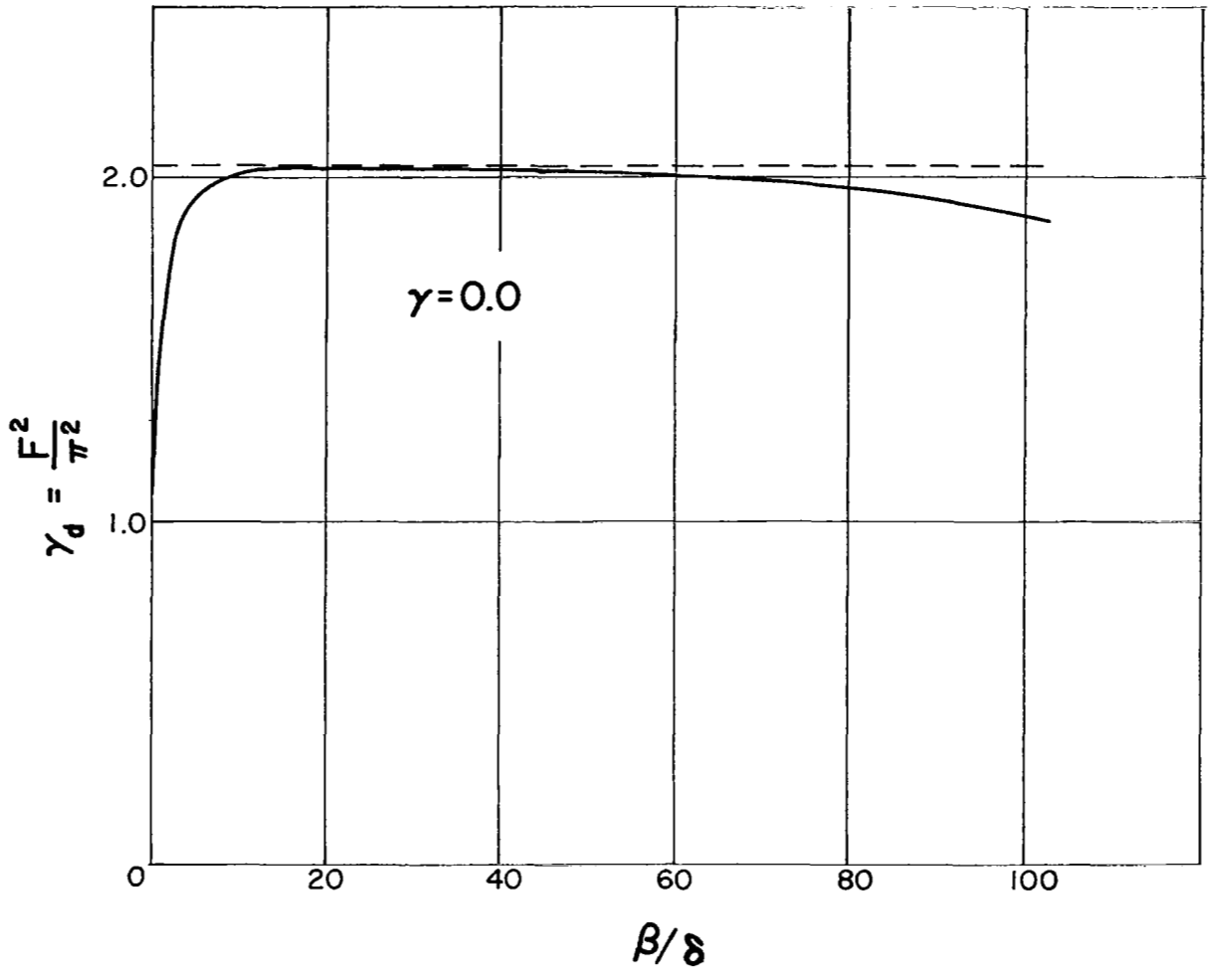

Fig. 4.21 Critical flutter parameter vs. the ratio of Coriolis force to internal damping force: zero external damping

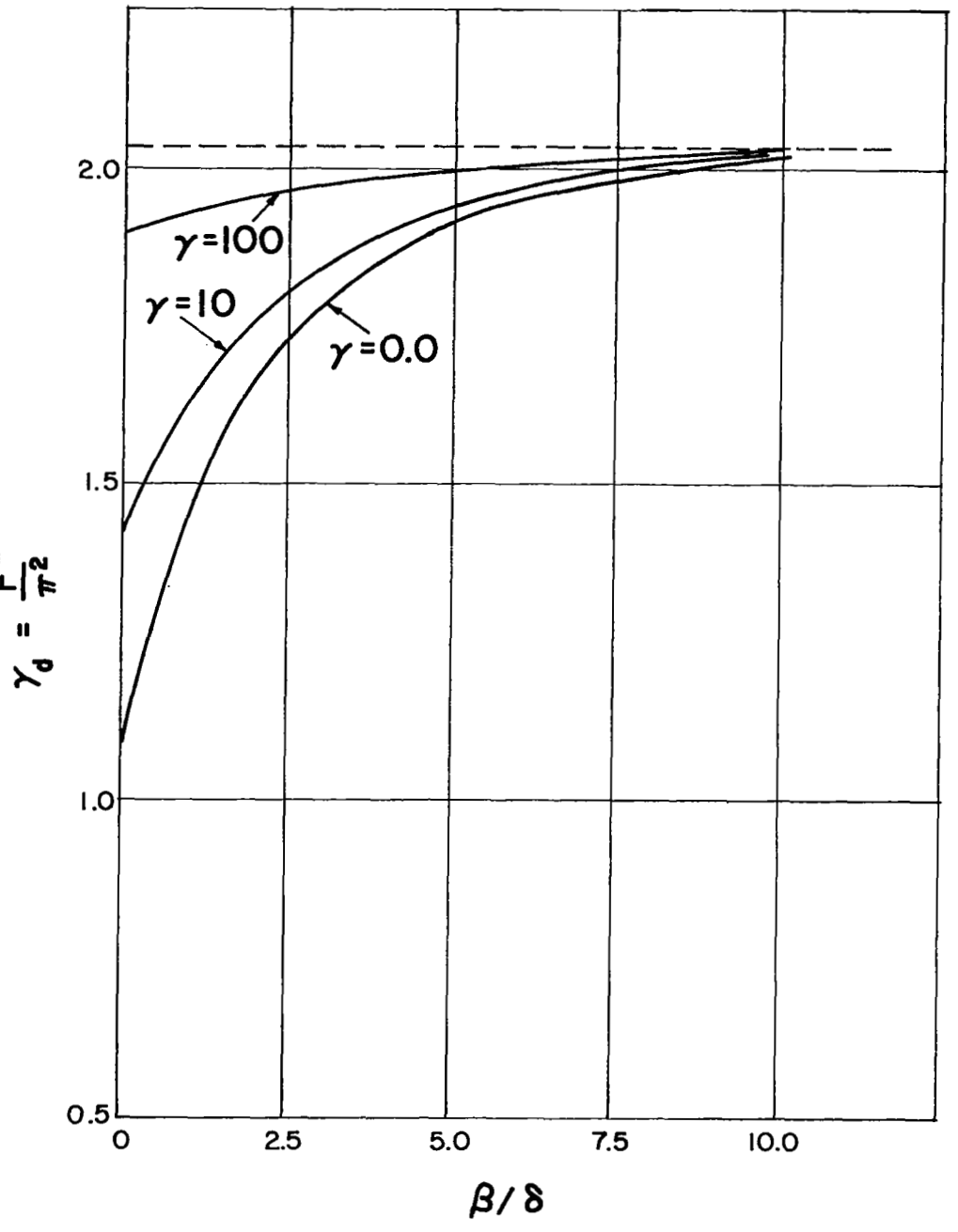

Fig. 4.22 Critical flutter parameter vs. the ratio of Coriolis force to internal damping force: external damping as indicated

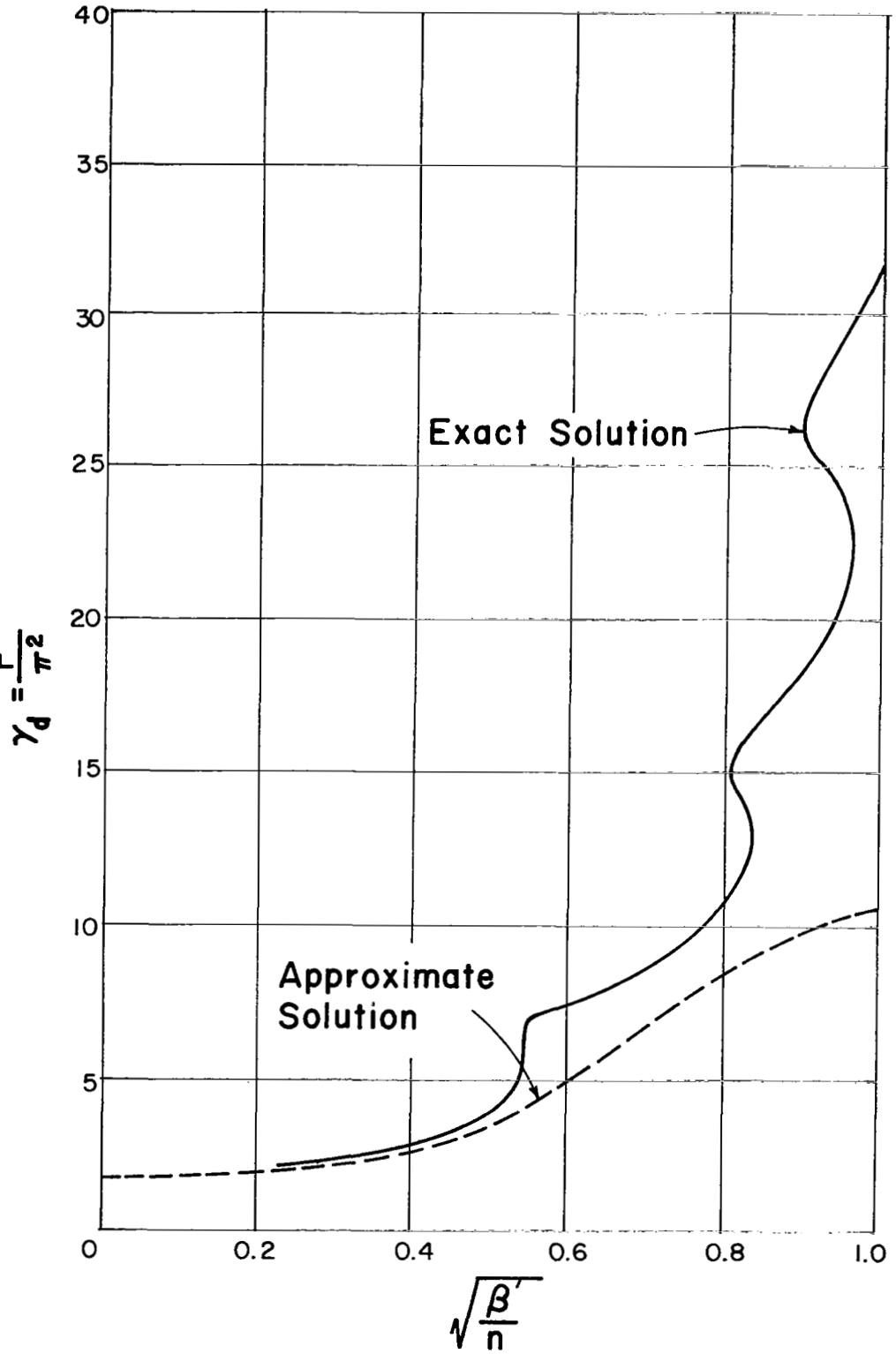

Fig. 4.23 Comparison between the exact solution and the two-term Galerkin approximation: zero external and internal damping

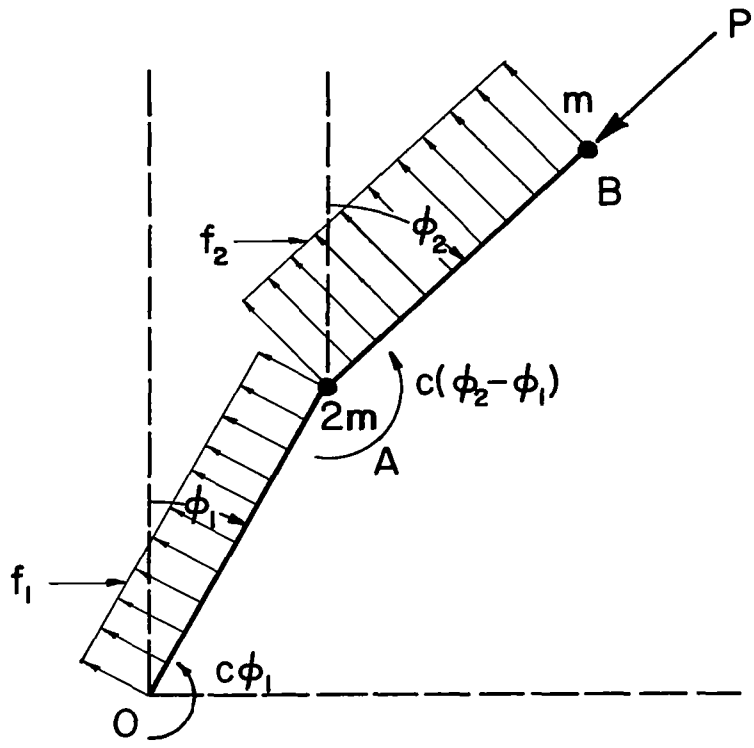

Fig. 4.24 System with two degrees of freedom

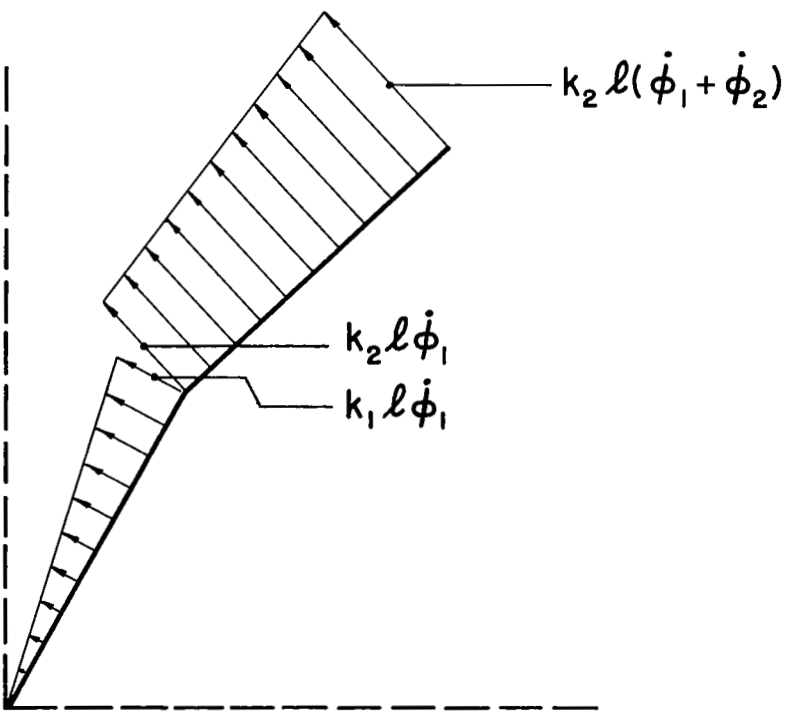

Fig. 4.25 System with distributed external damping

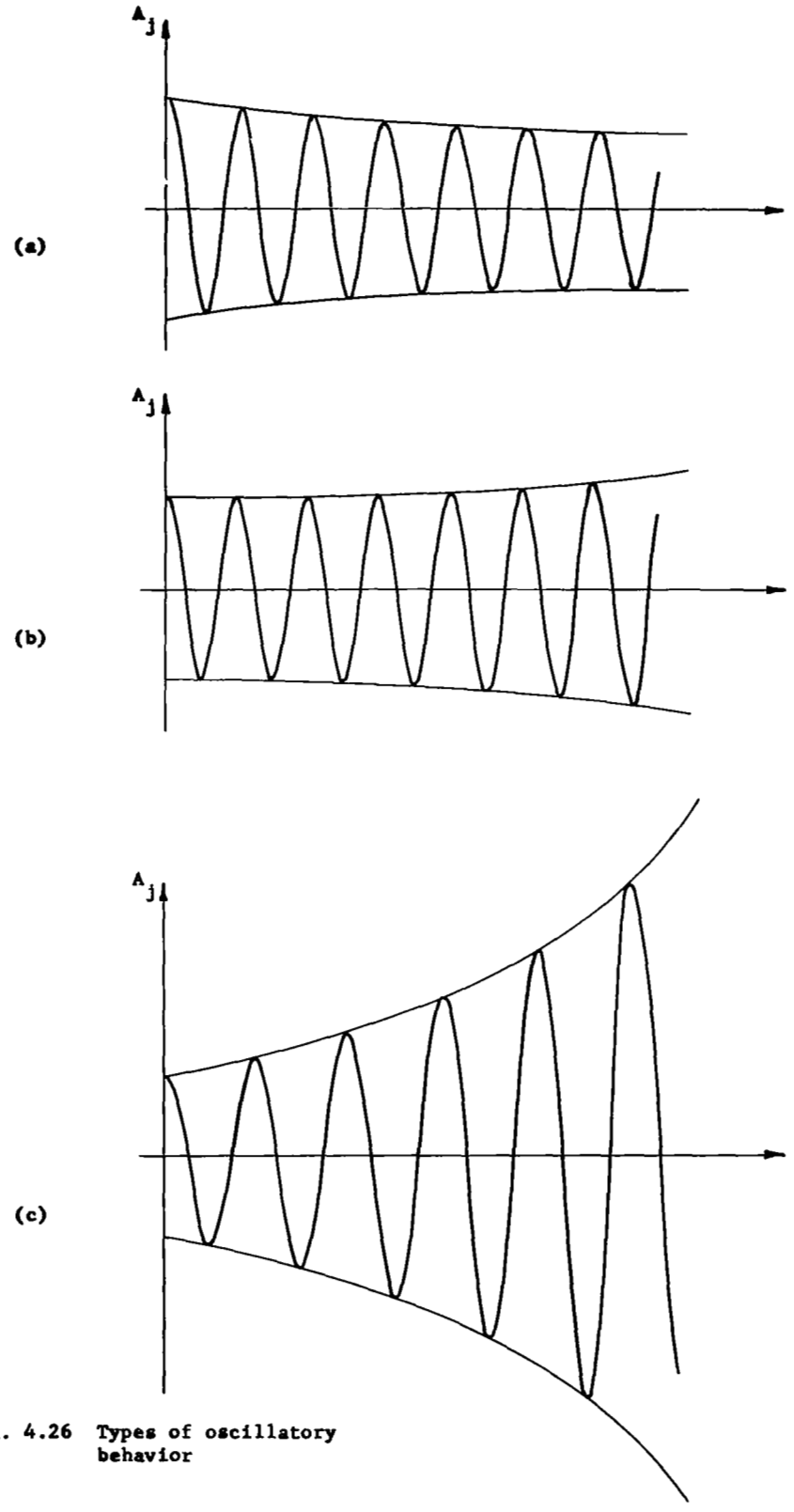

Fig. 4.26 Types of oscillatory behavior

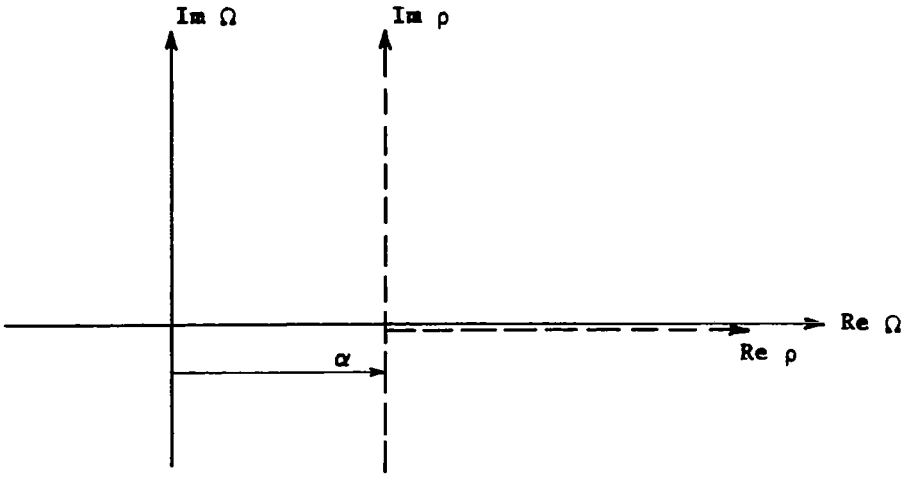

Fig. 4.27 Translation of imaginary axis in root plane

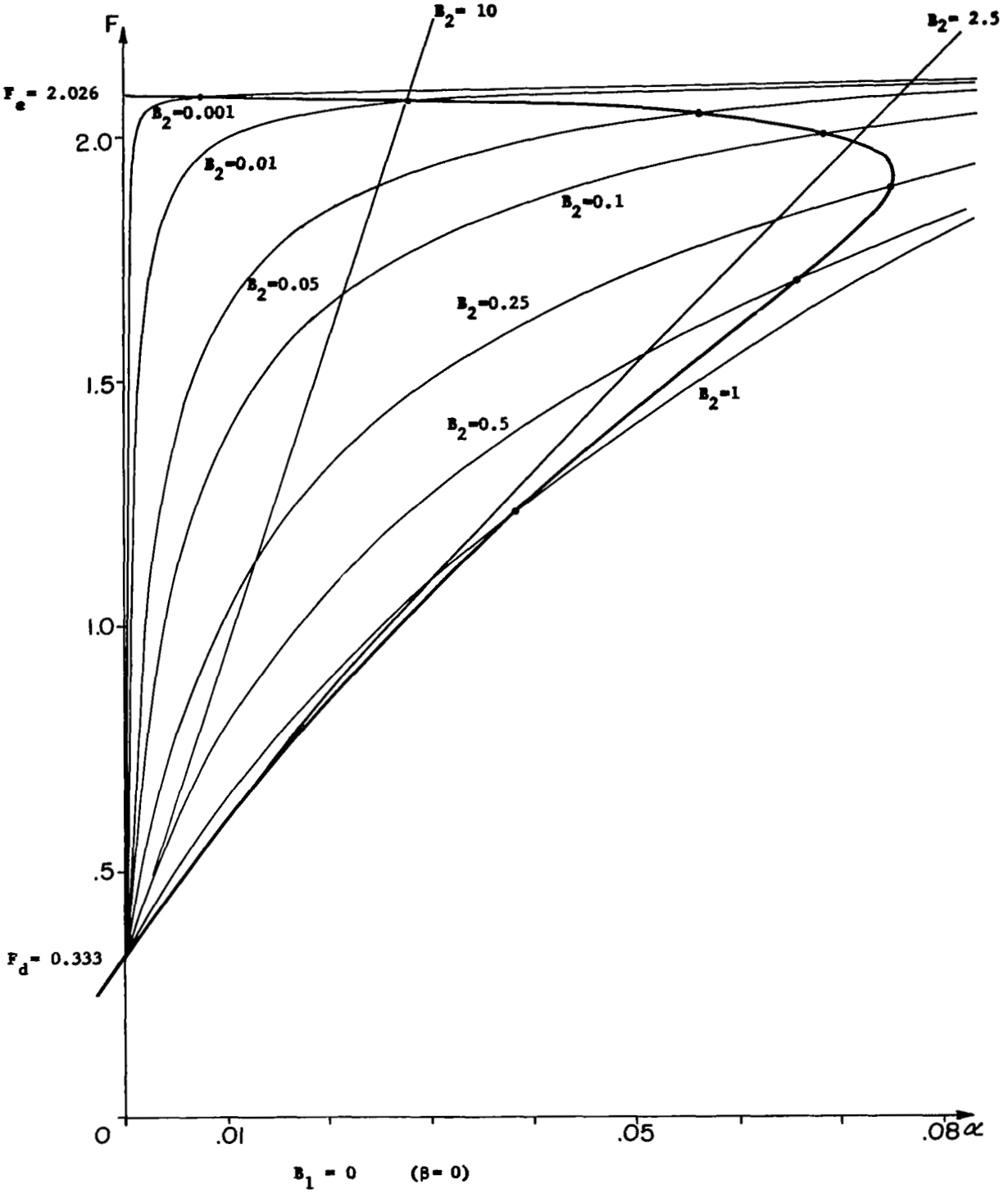

Fig. 4.28 Critical force as a function of α for various values of B_2. Thick line joins values of transition force F_t.

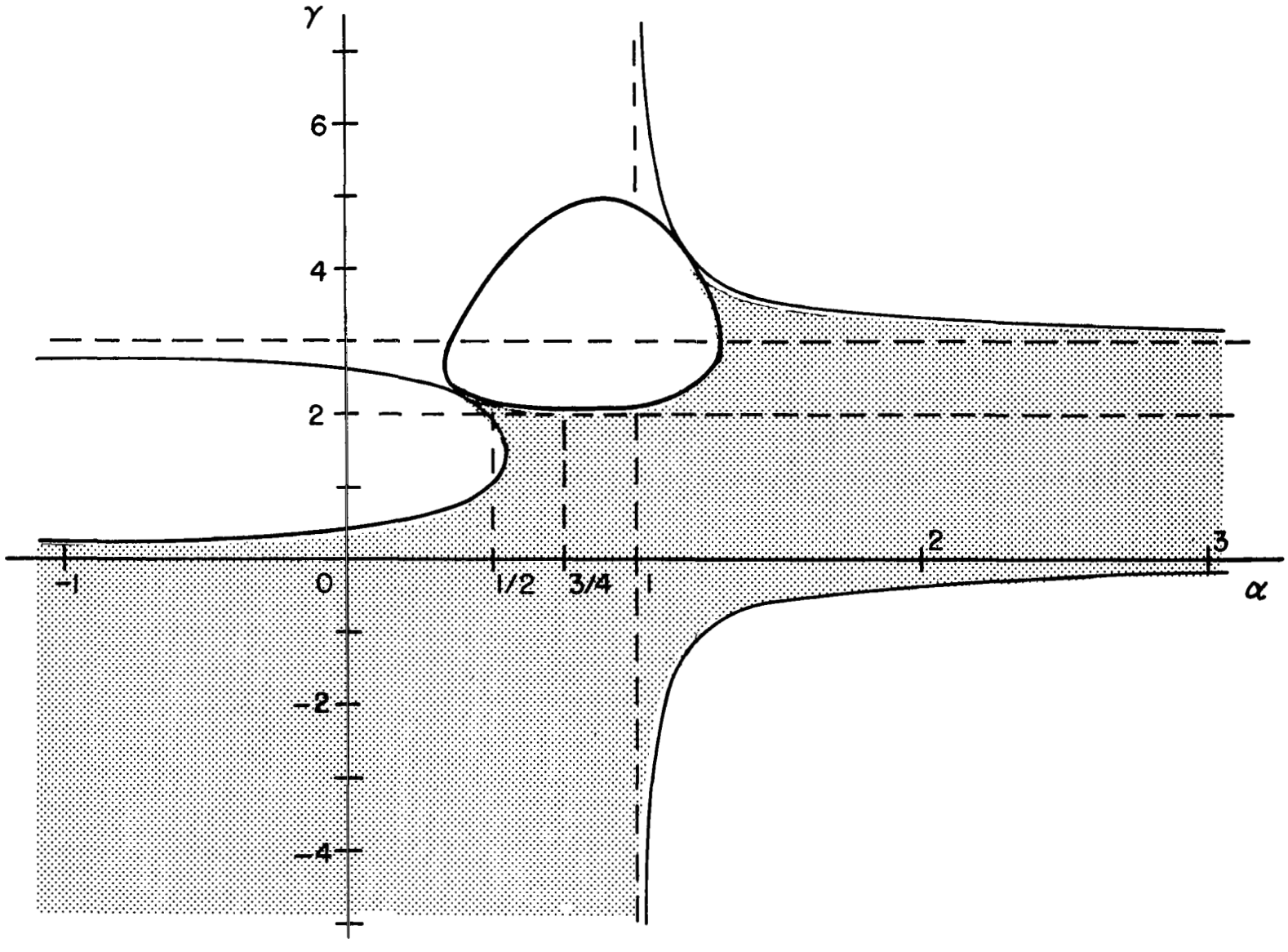

Fig. 6.1 Stability region in the parameter plane for Example 2

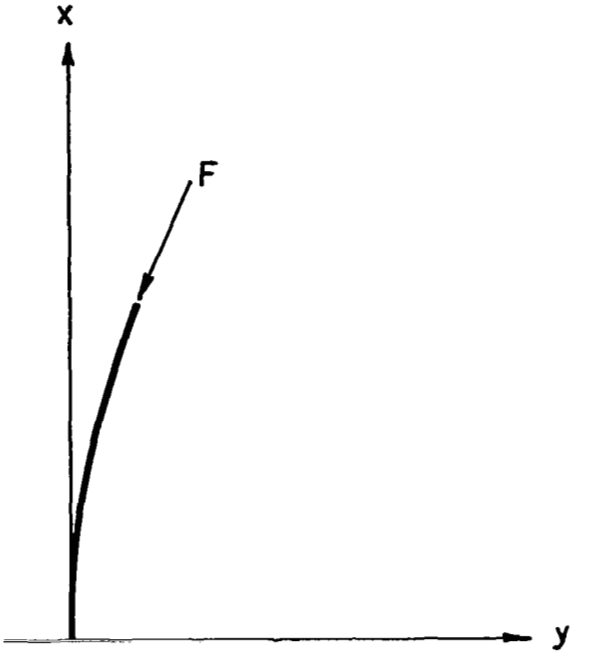

Fig. 6.2 A cantilever under a follower force (the Beck problem)

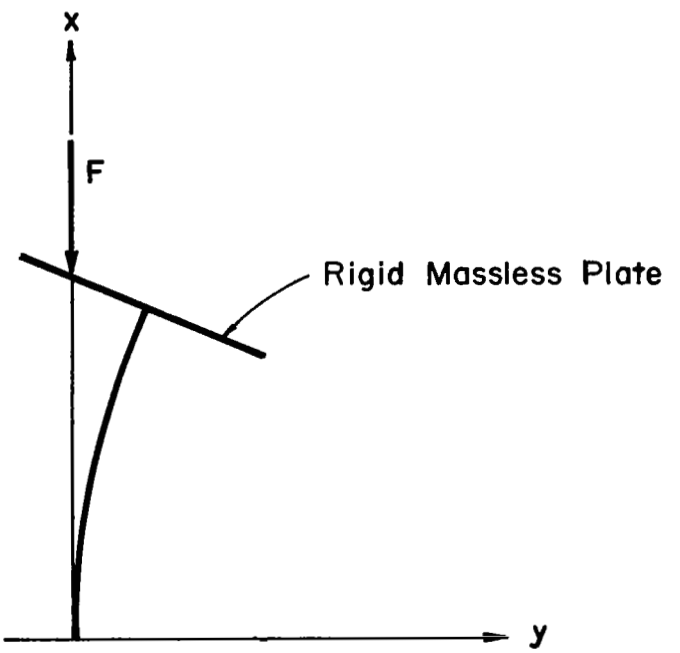

Fig. 6.3 A cantilever under a force directed along the undeformed axis (the Reut problem)

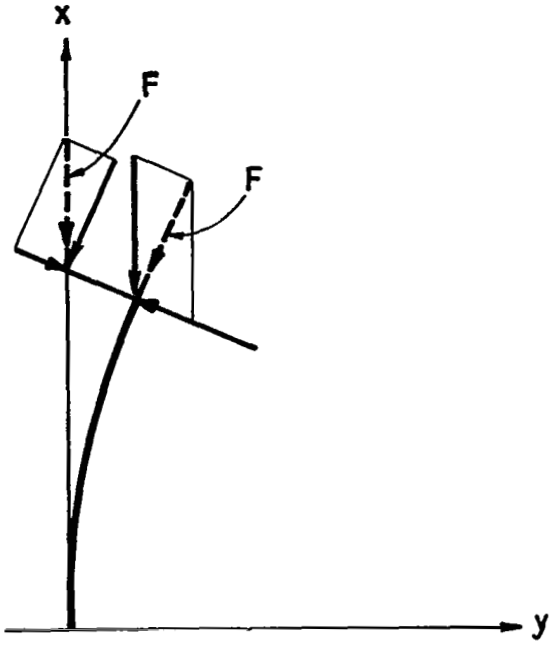

Fig. 6.4 A cantilever under both a follower force and a force directed along the undeformed axis (a conservative system)

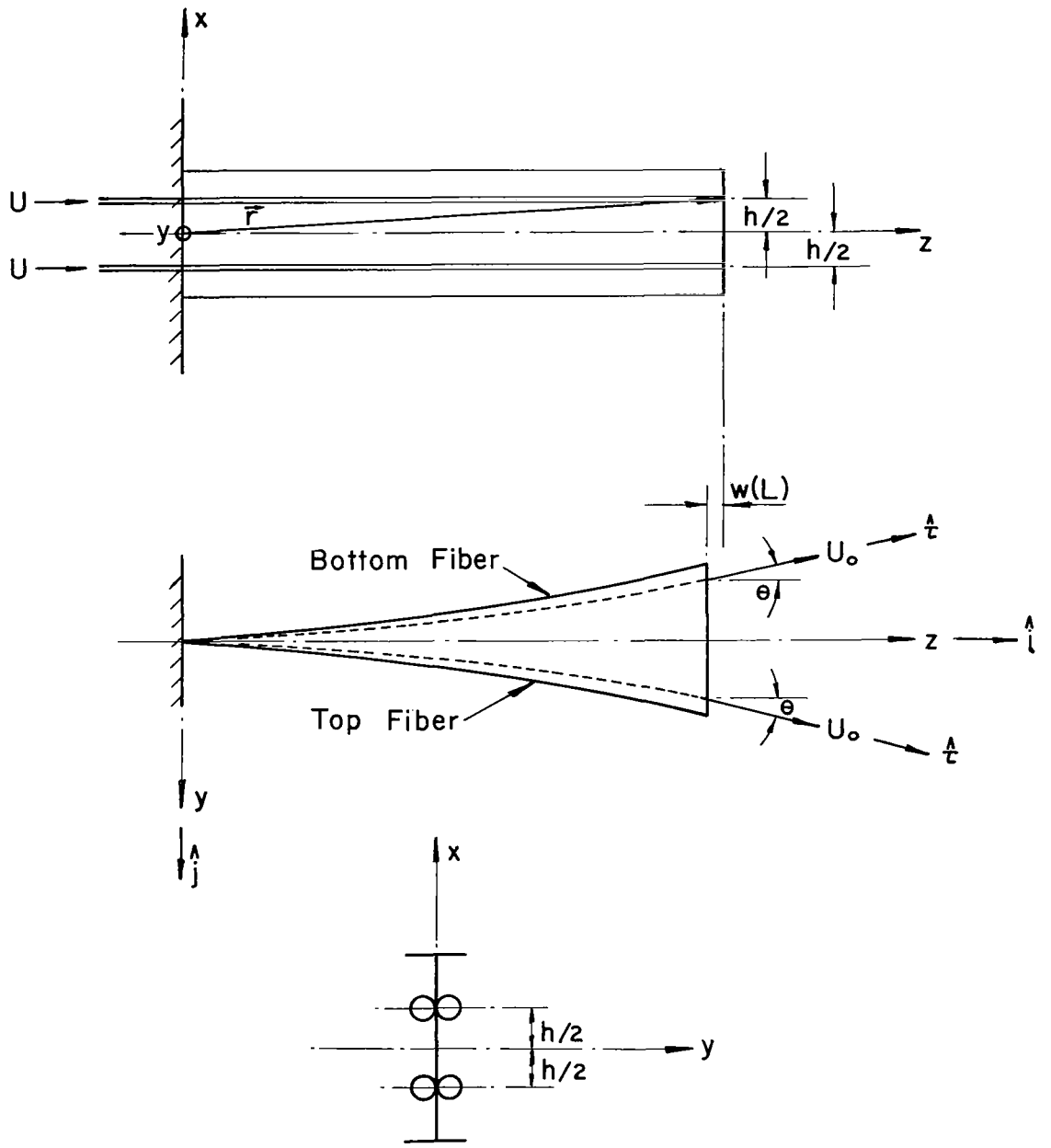

Fig. 7.1 Cantilever with two pairs of flexible pipes

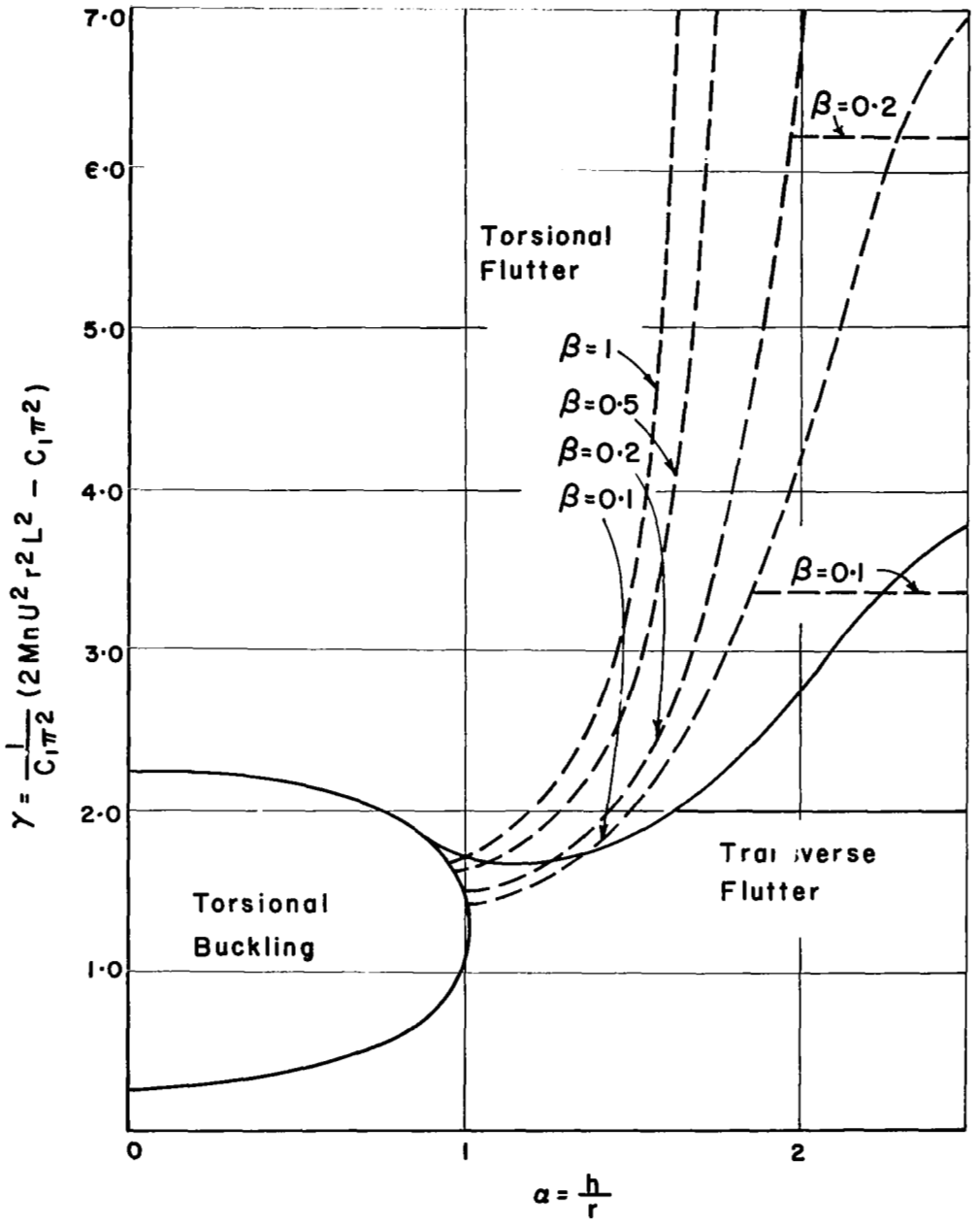

Fig. 7.2 Types of instability as a function of system geometry

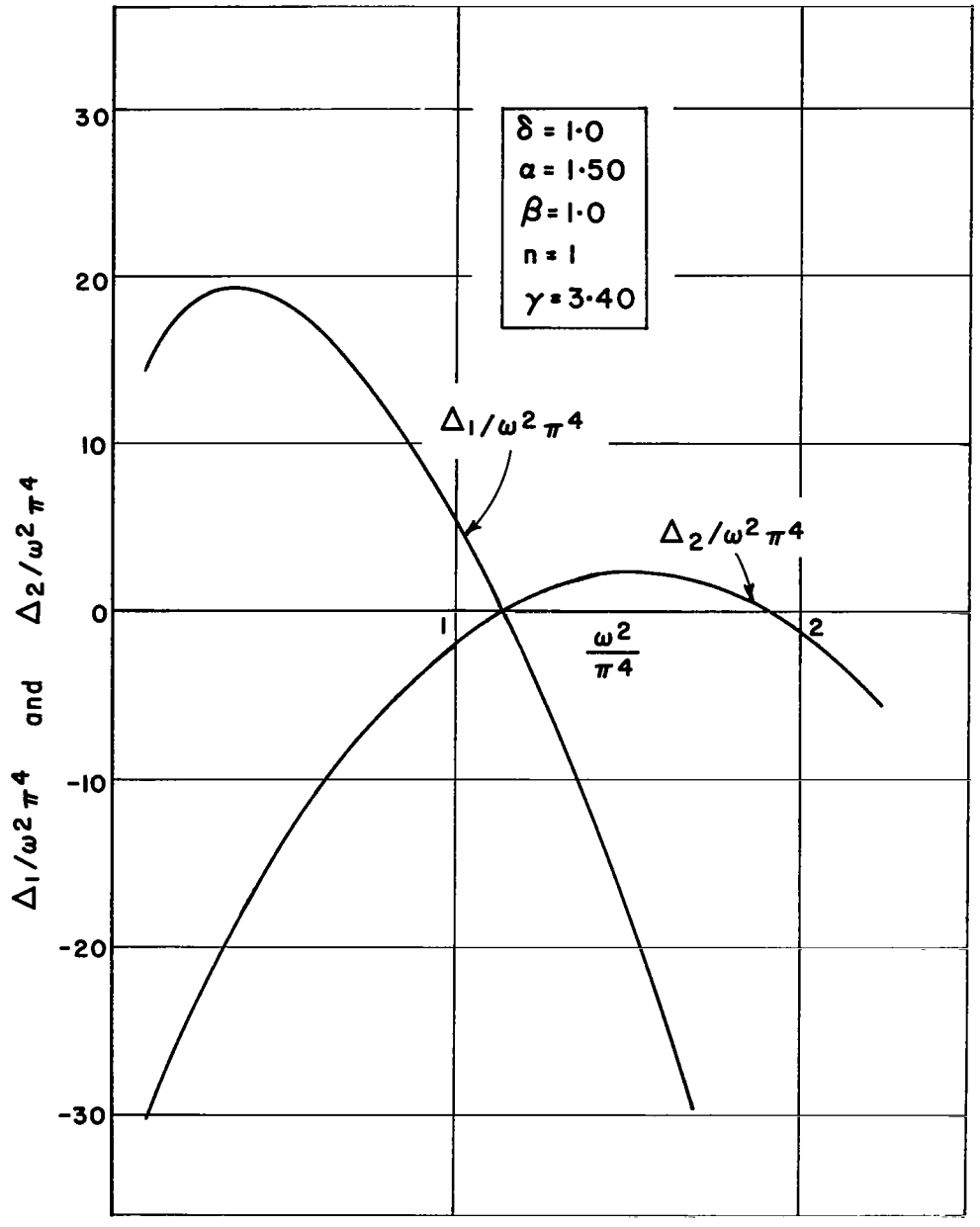

Fig. 7.3 Plots of $\Delta_1/\omega^2\pi^4$ and $\Delta_2/\omega^2\pi^4$ for $\gamma = 3{\cdot}40$

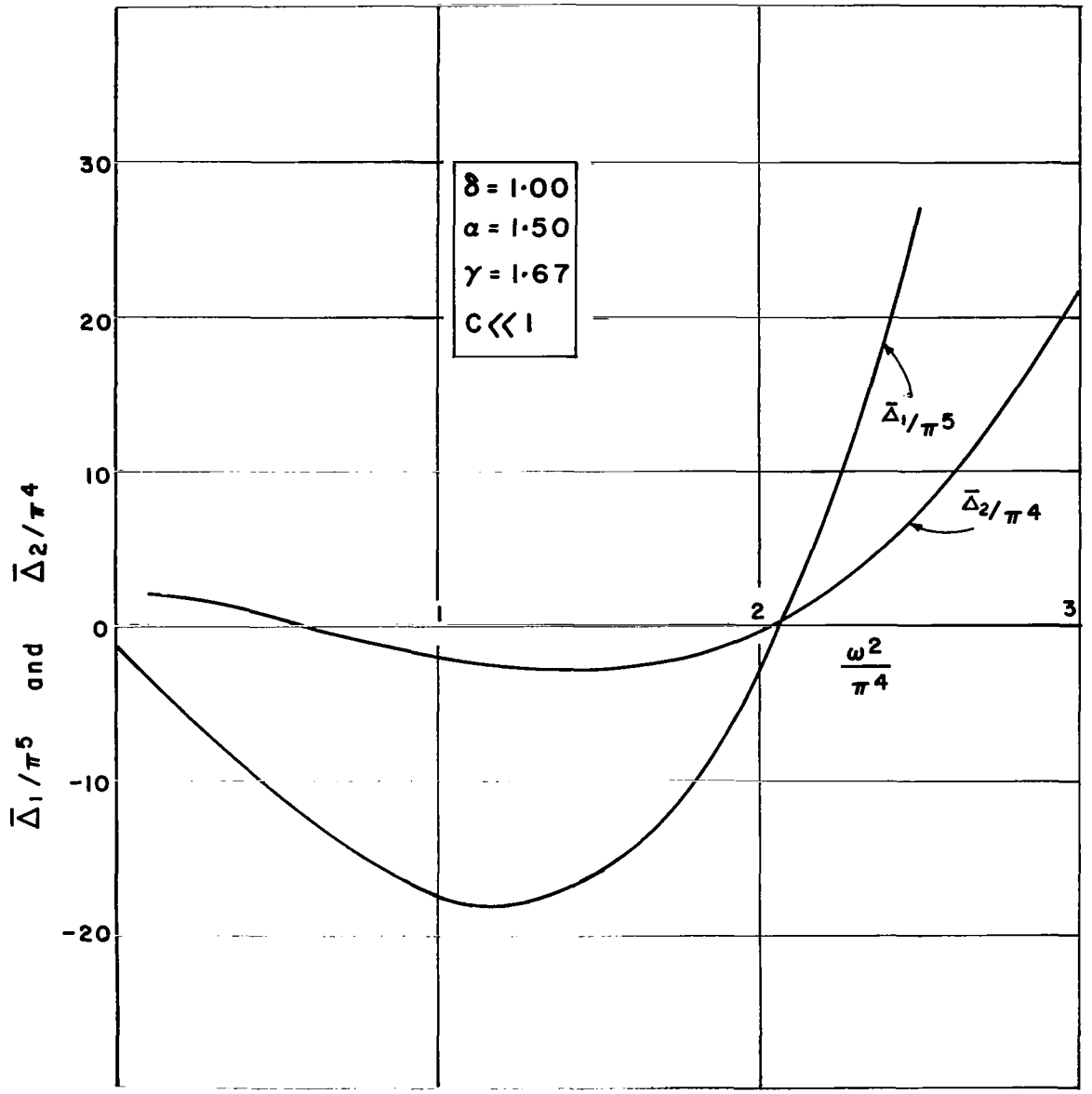

Fig. 7.4 Plots of $\bar{\Delta}_1/\pi^5$ and $\bar{\Delta}_2/\pi^4$ for $\gamma = 1{\cdot}67$

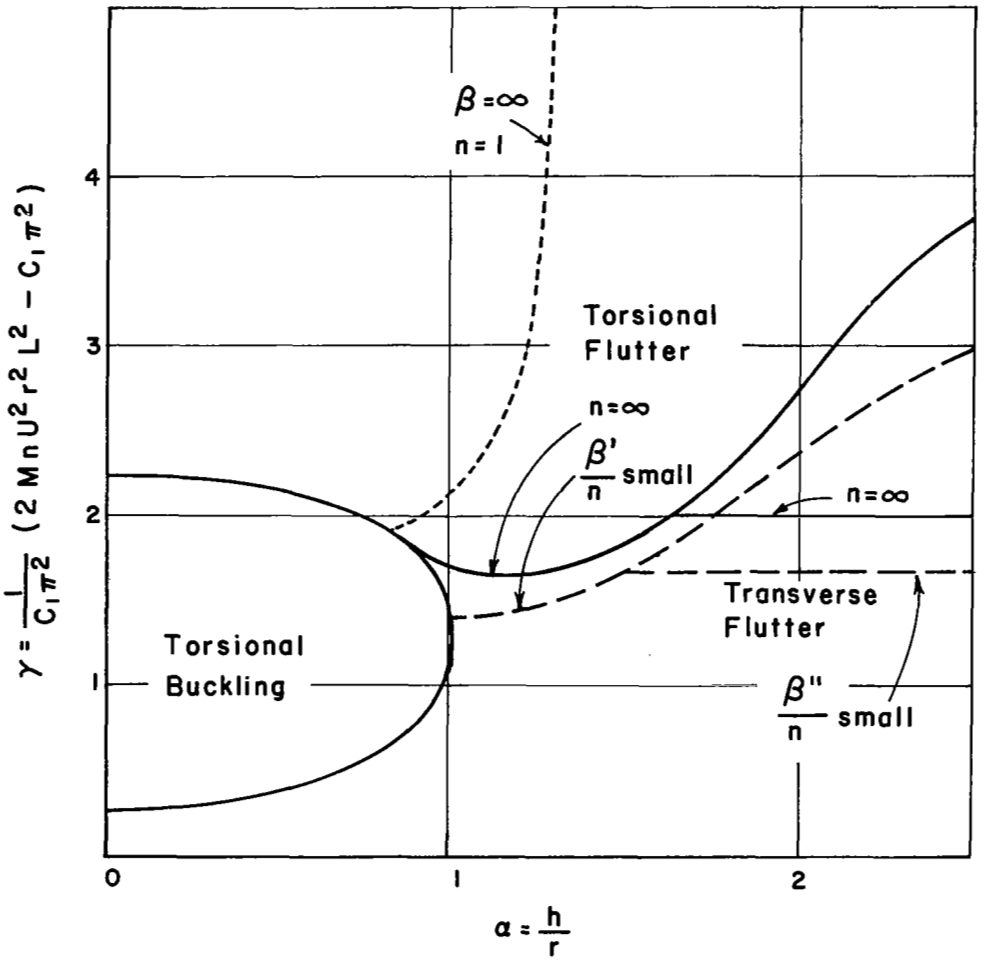

Fig. 7.5 Types of instability as a function of system geometry

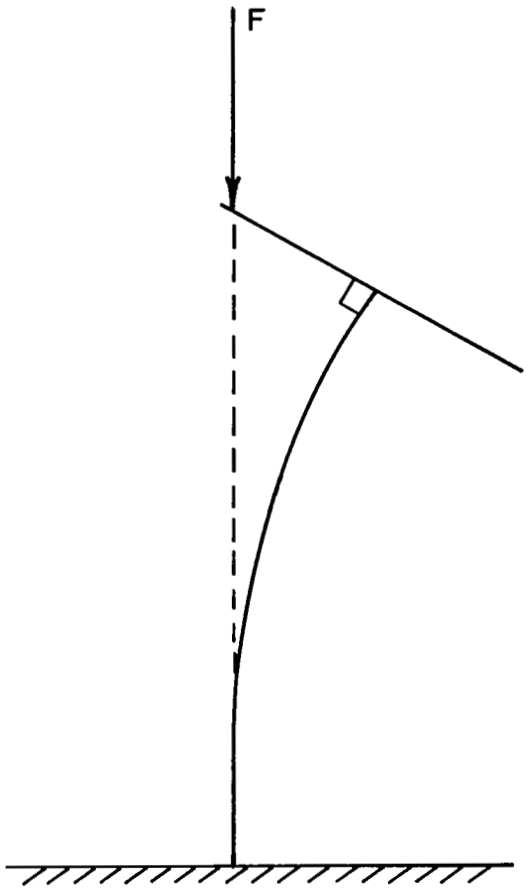

Fig. 8.1 Reut's problem

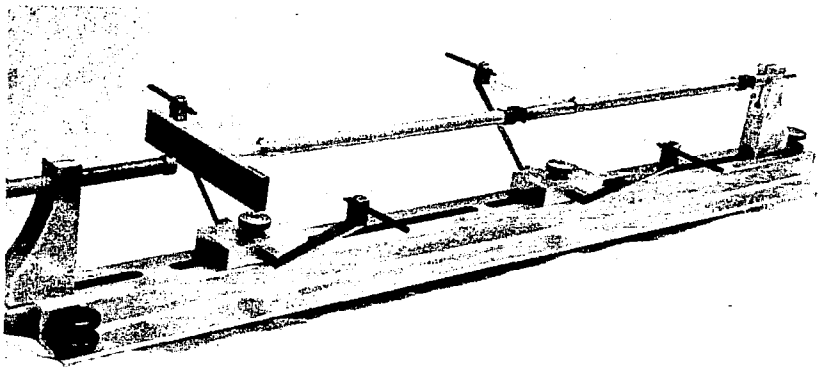

Fig. 8.2 Photograph of the model

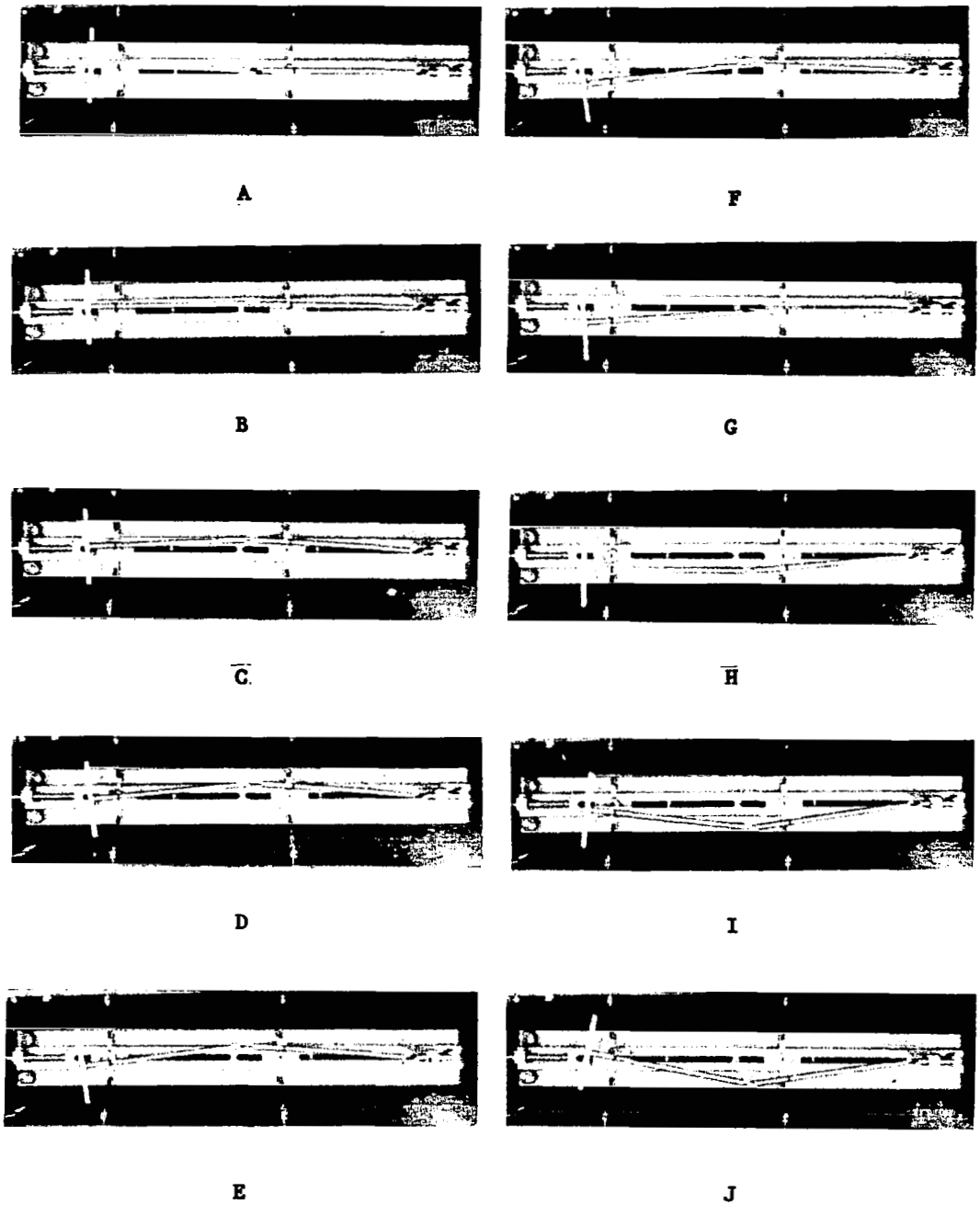

Fig. 8.3 Sequence of photographs depicting flutter

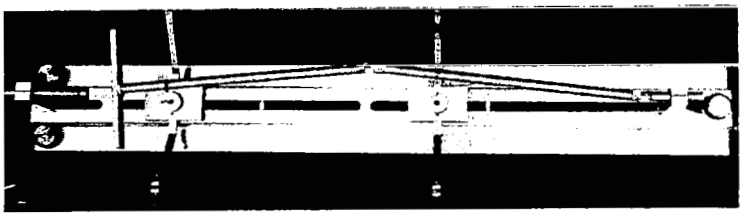

Fig. 8.4 Buckled state: Divergence

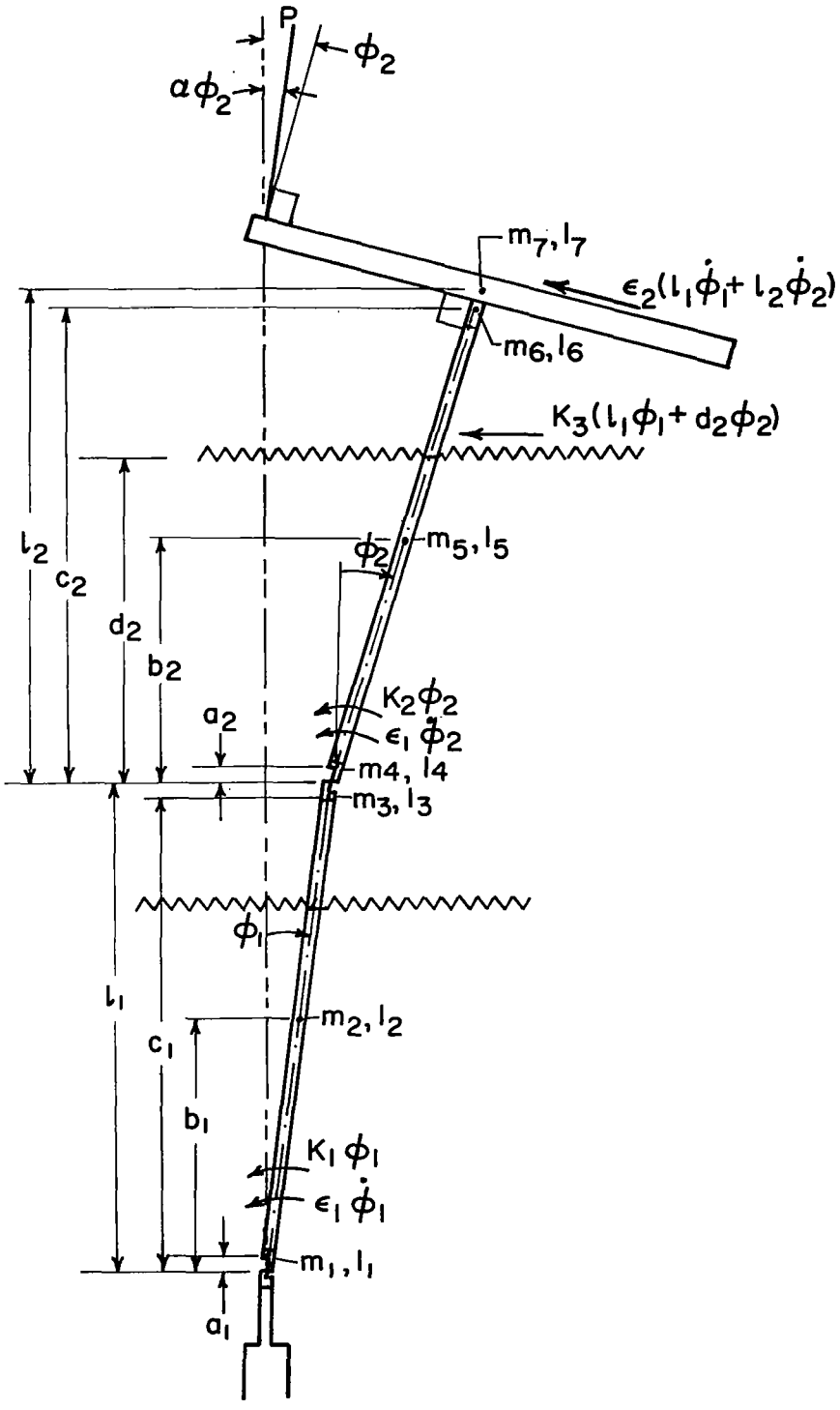

Fig. 8.5 Schematic of the model

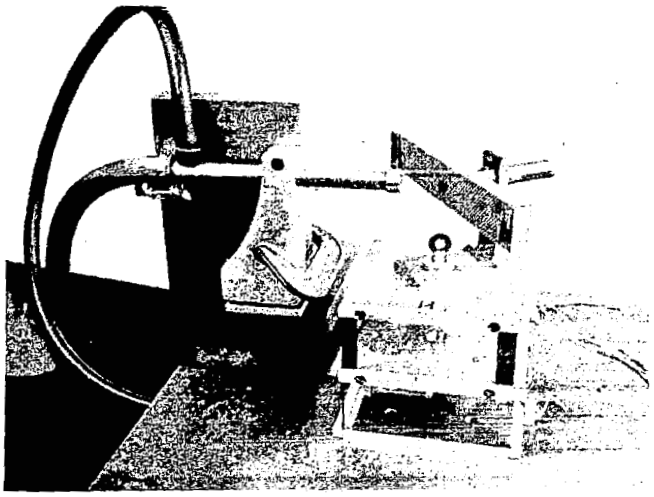

Fig. 8.6 Photograph of the calibrating system

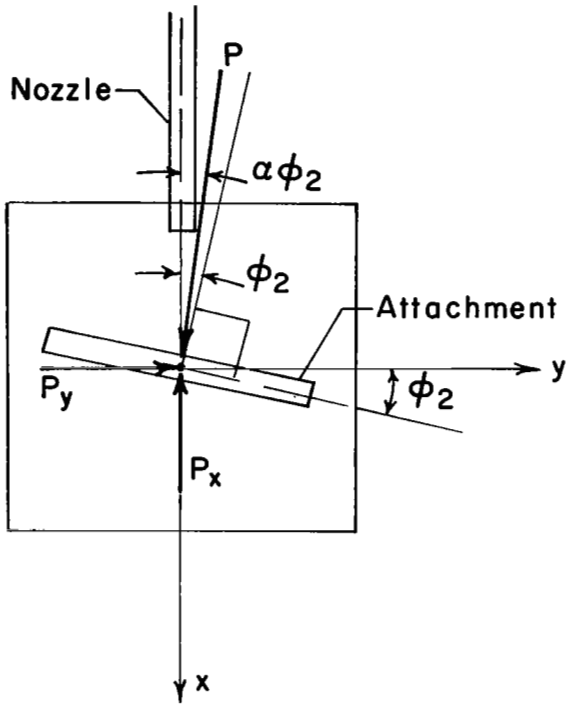

Fig. 8.7 Attachment mounted on calibrating system (top view)

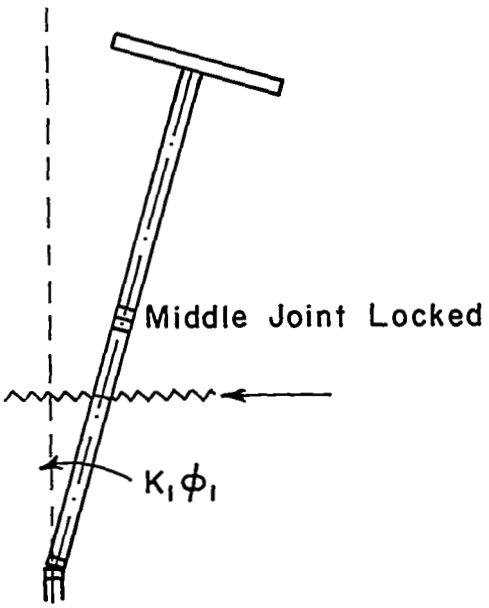

Fig. 8.8 Configuration to find K_1 by dynamic method

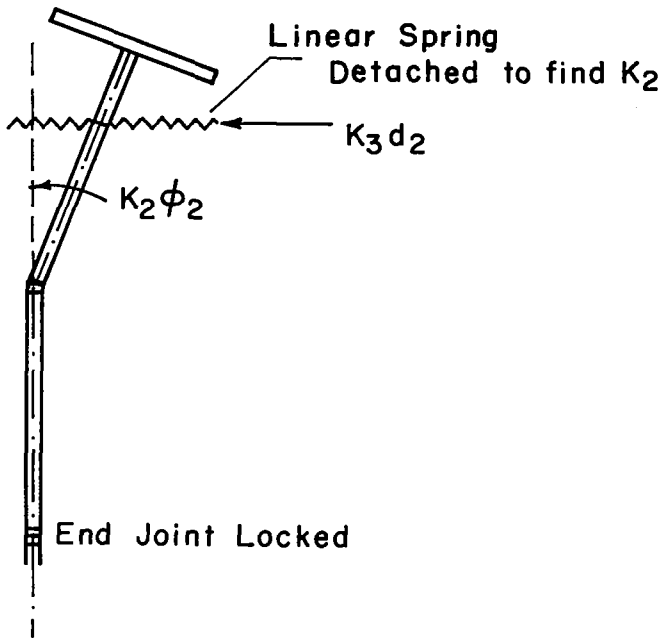

Fig. 8.9 Configuration to find K_2 and K_3 by dynamic method

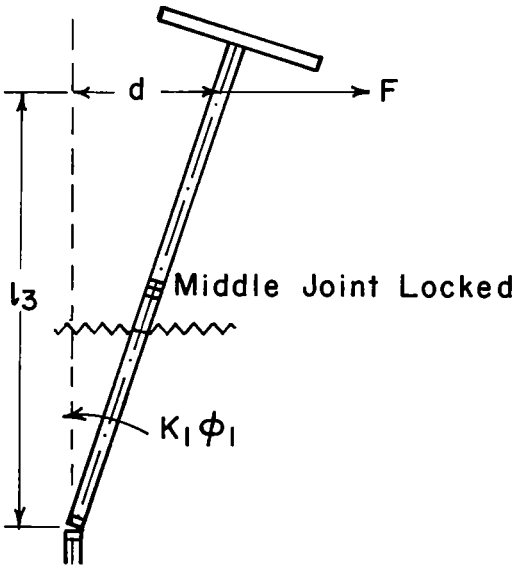

Fig. 8.10 Configuration to find K_1 by static method

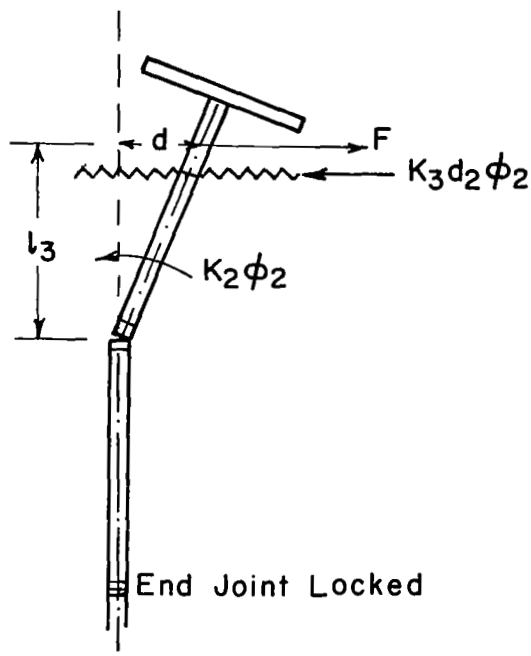

Fig. 8.11 Configuration to find K_2 and K_3 by static method

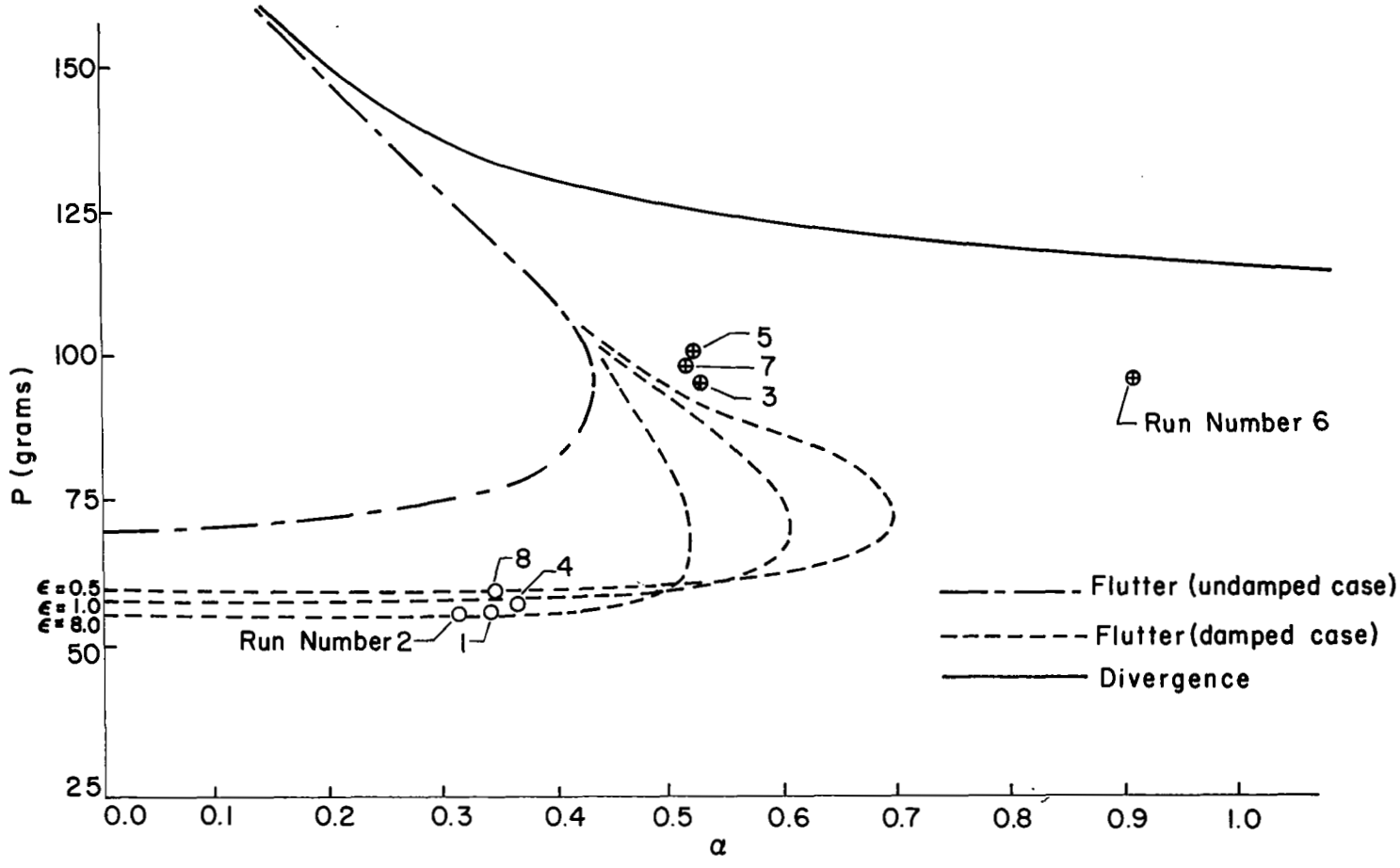

Fig. 8.12 Stability diagram - System I

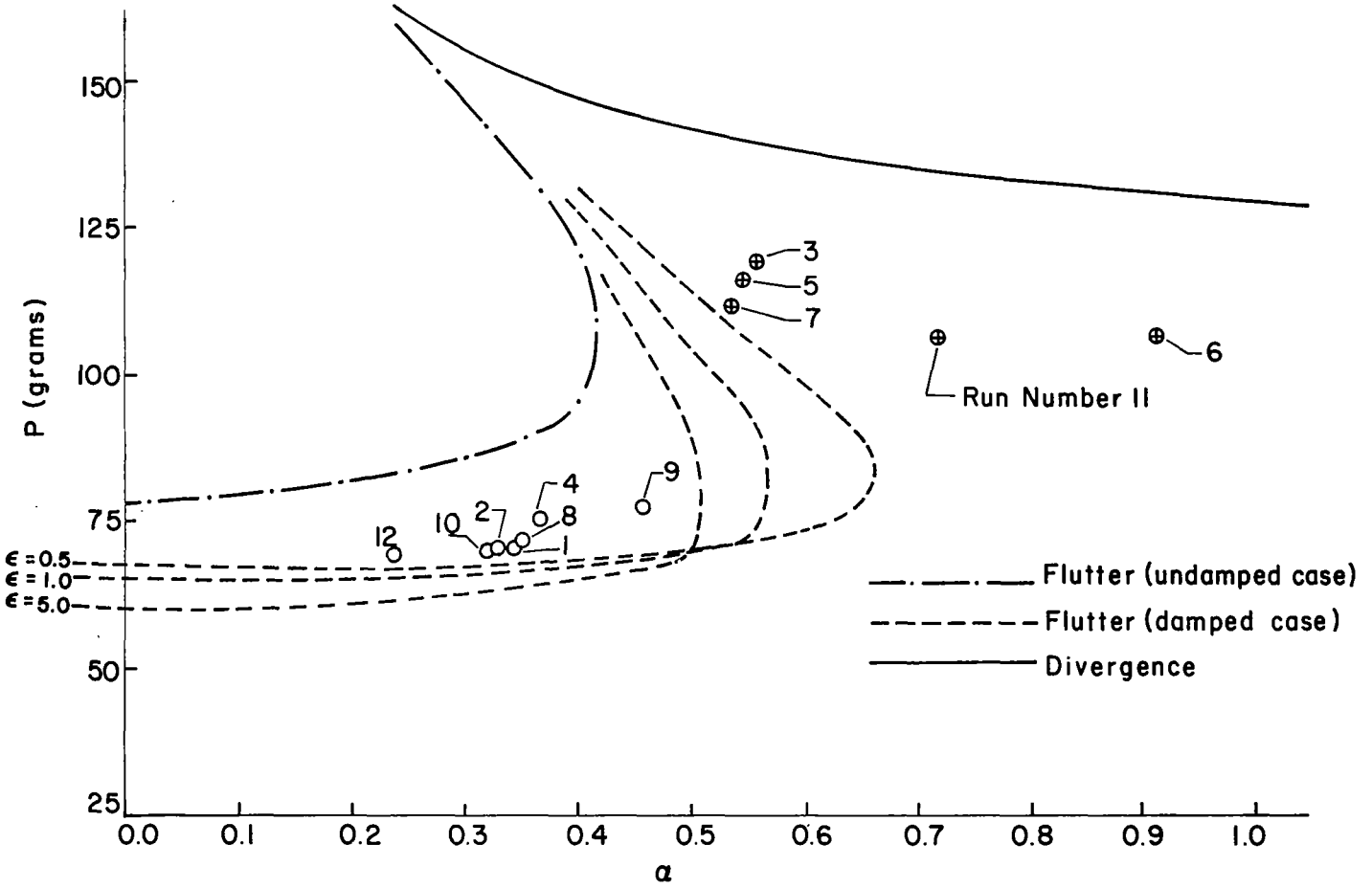

Fig. 8.13 Stability diagram - System II

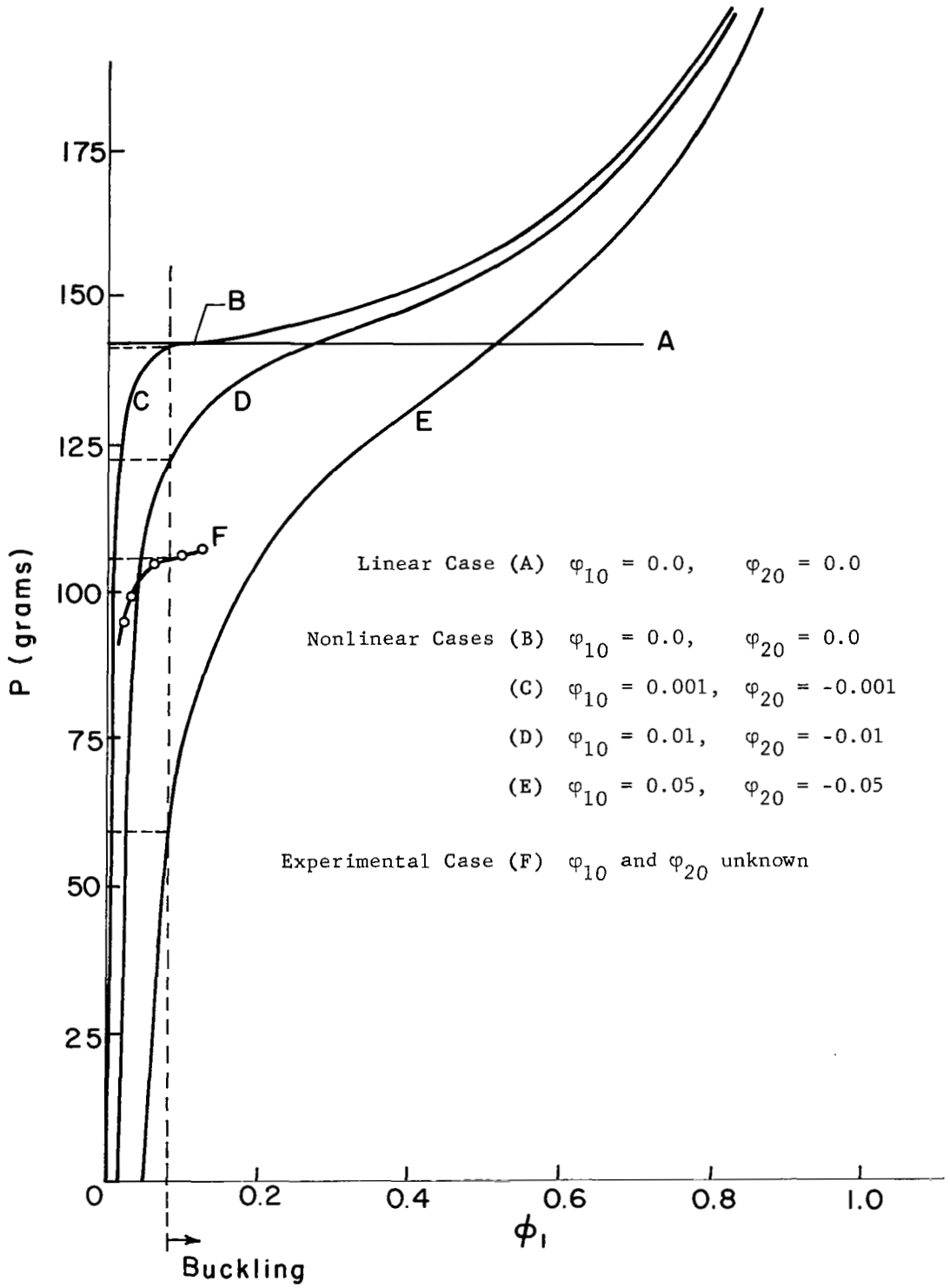

Fig. 8.14 Force versus deflection for nonlinear divergence theory with initial imperfections

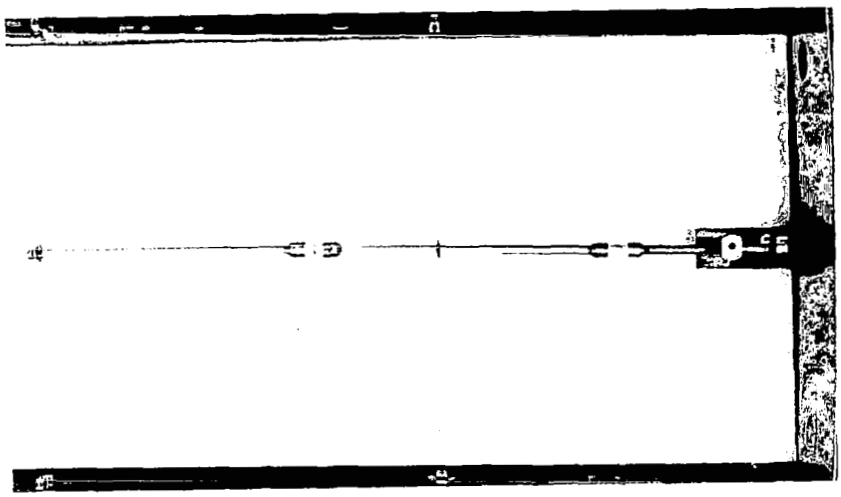

(a)

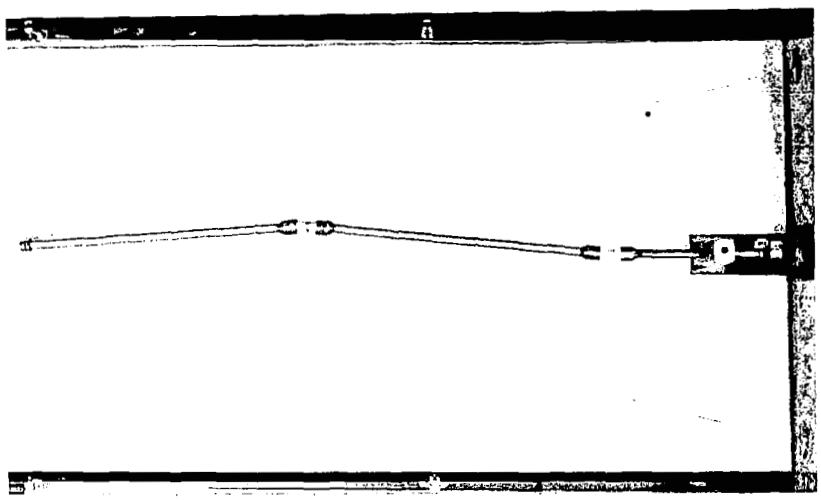

(b)

Fig. 8.15 Demonstration Model A

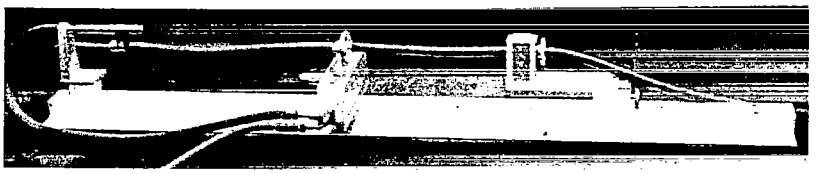

Fig. 8.16 Demonstration Model B

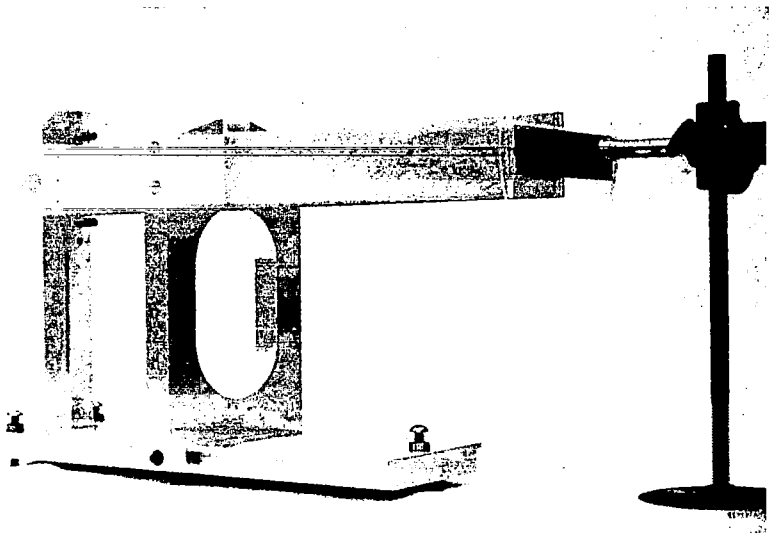

Fig. 8.17 Demonstration Model C

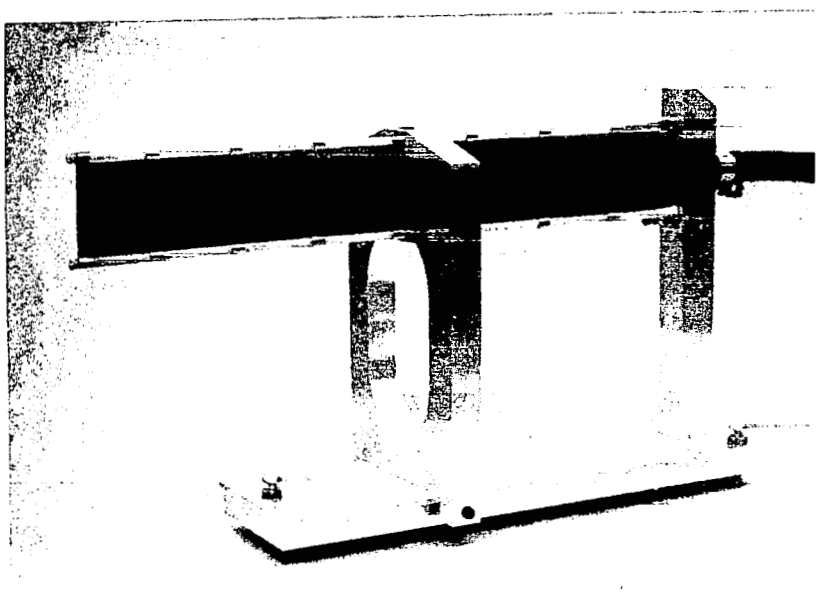

(a)

Fig. 8.18 Demonstration Model D

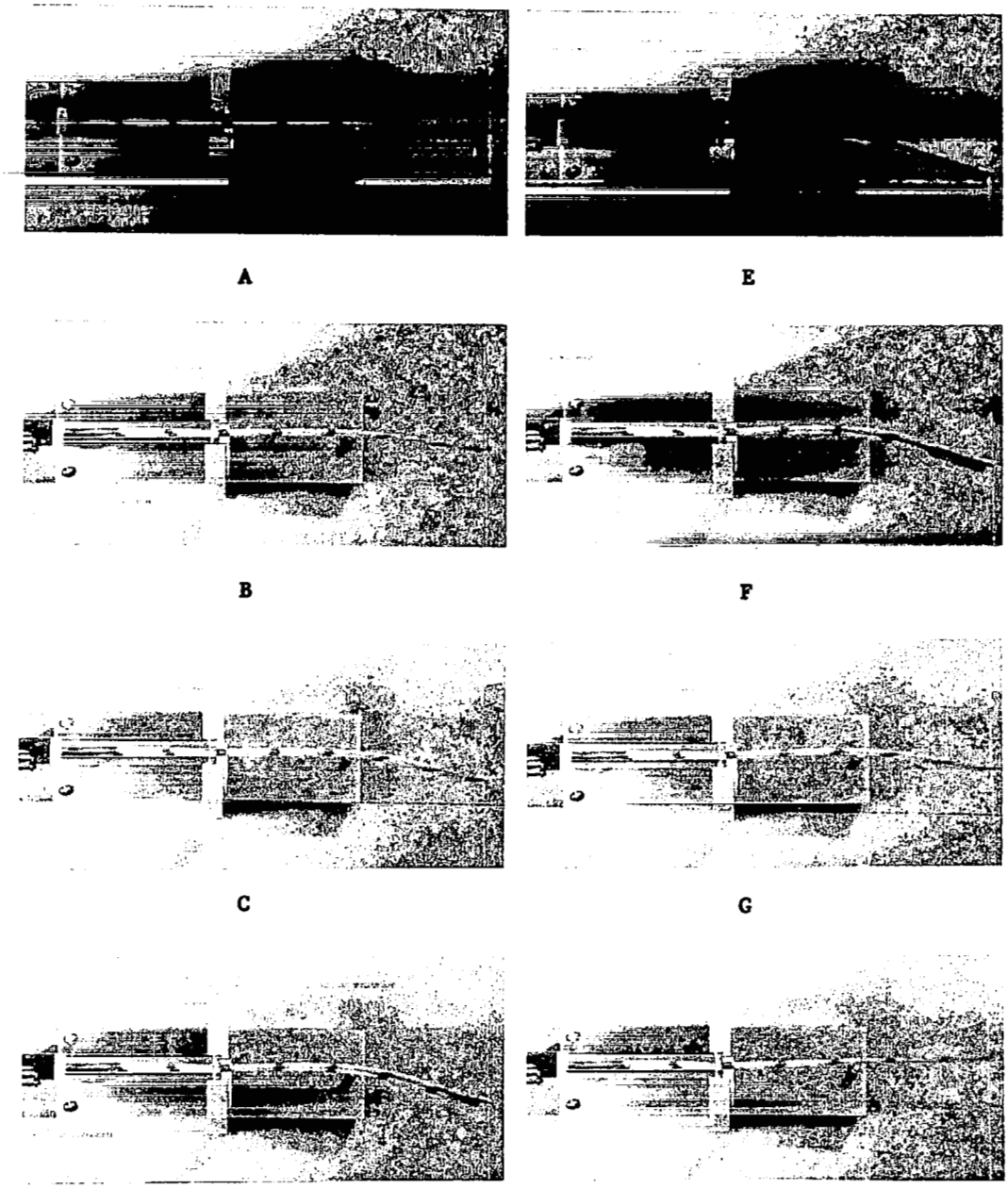

(b)

Fig. 8.18 Demonstration Model D

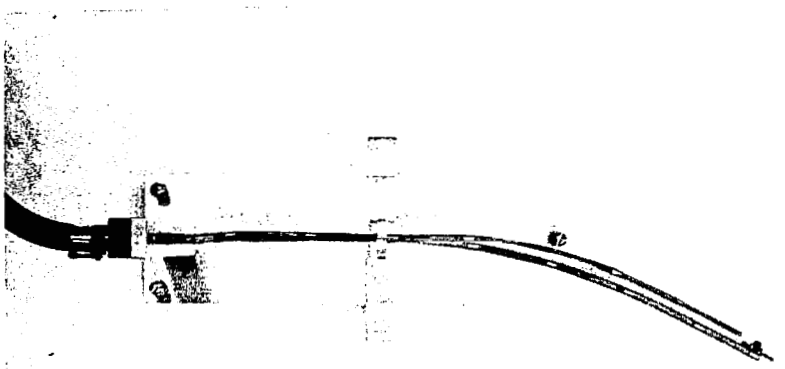

(c)

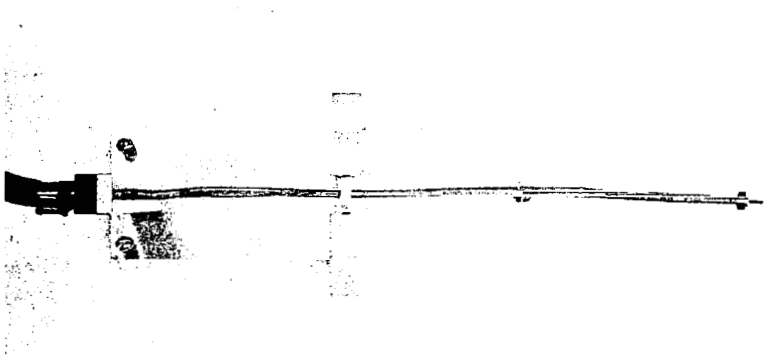

(d)

Fig. 8.18 Demonstration Model D

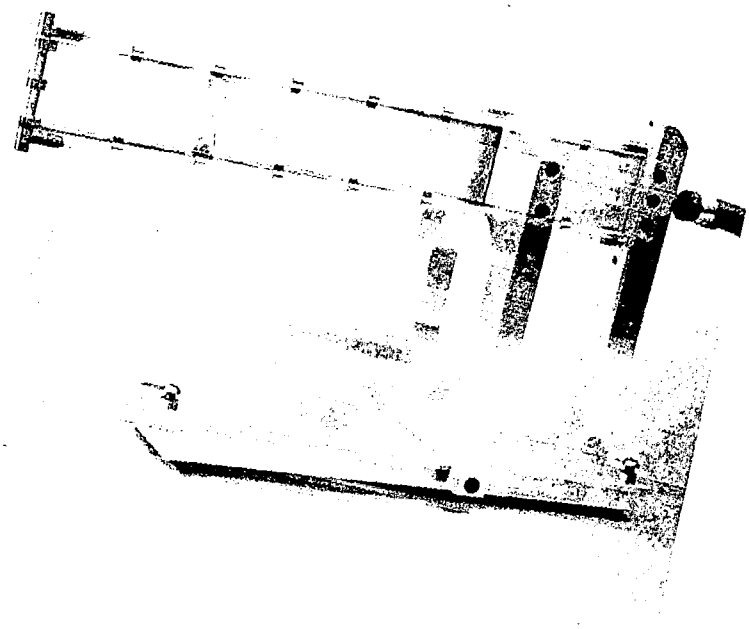

Fig. 8.19 Demonstration Model E

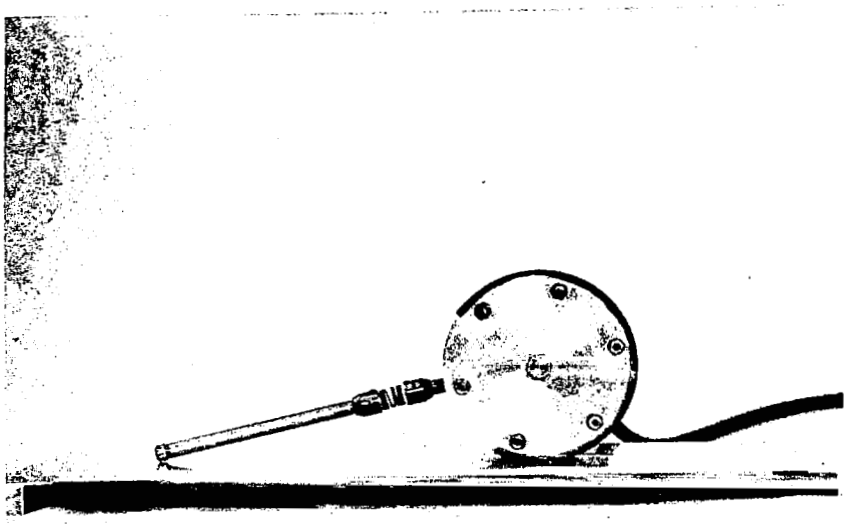

(a)

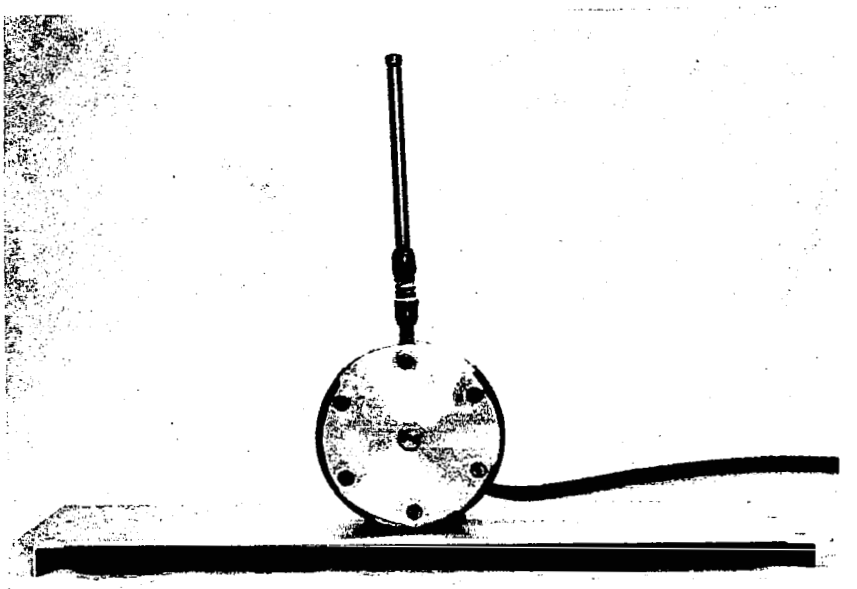

(b)

Fig. 8.20 Demonstration Model F

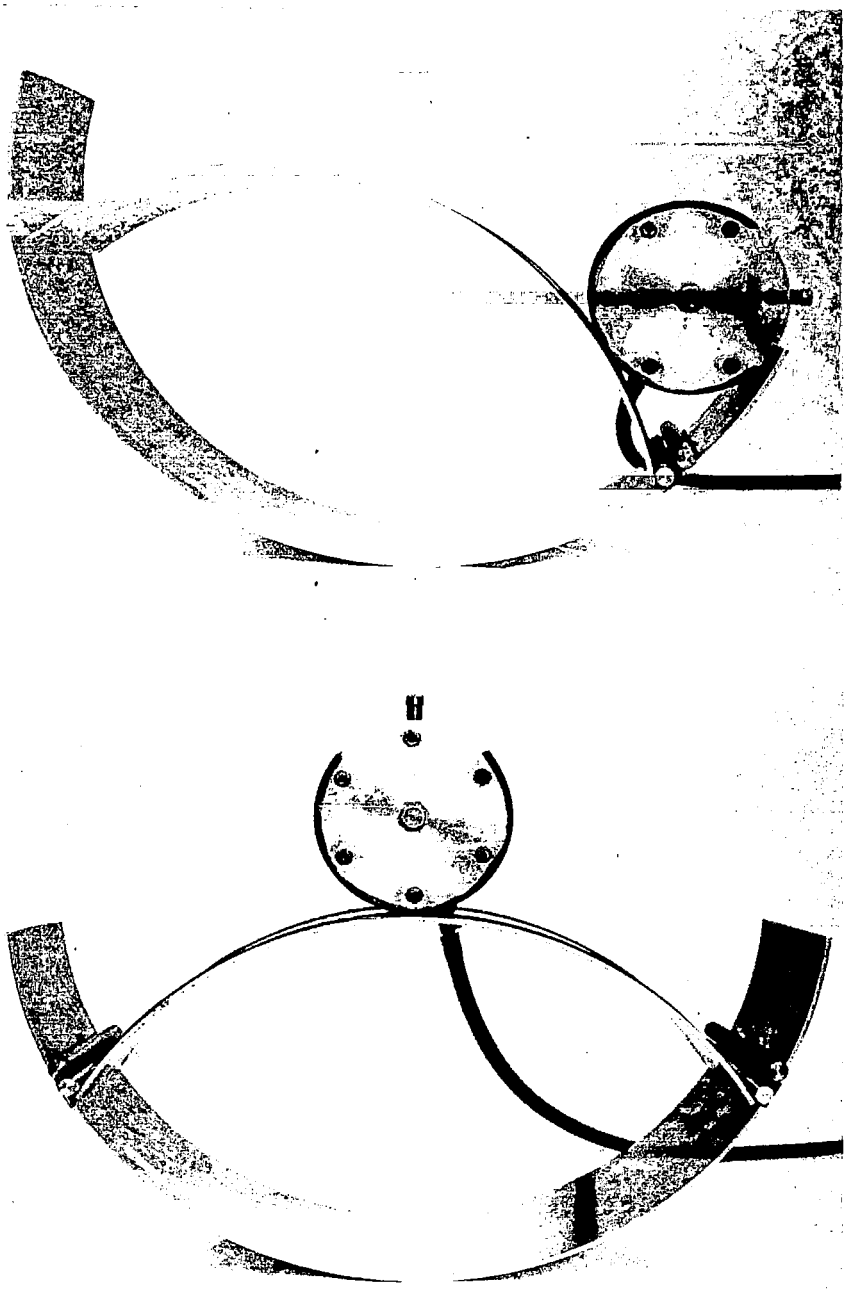

(a)

(b)

Fig. 8.21 Demonstration Model G

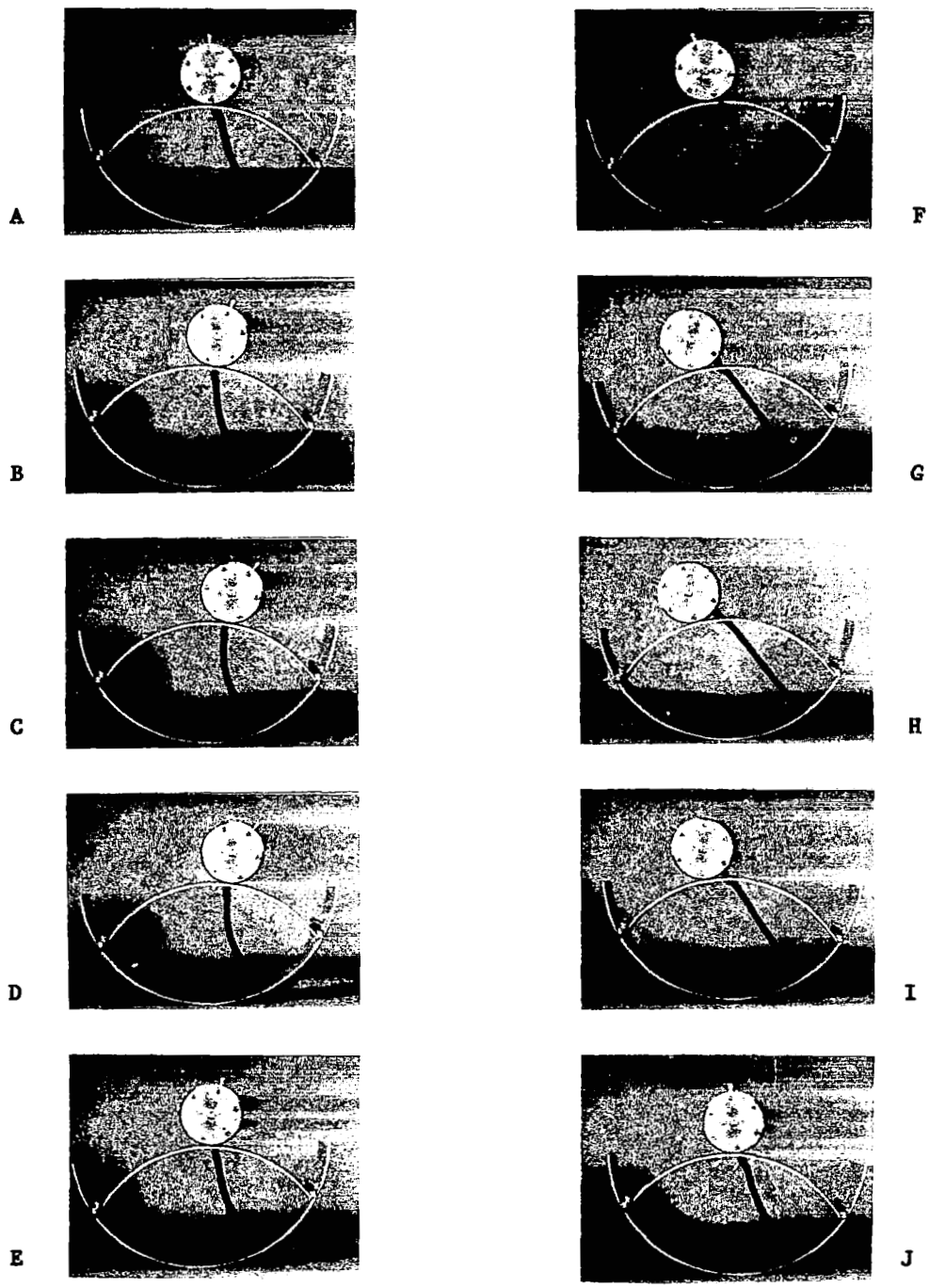

(c)

Fig. 8.21 Demonstration Model G

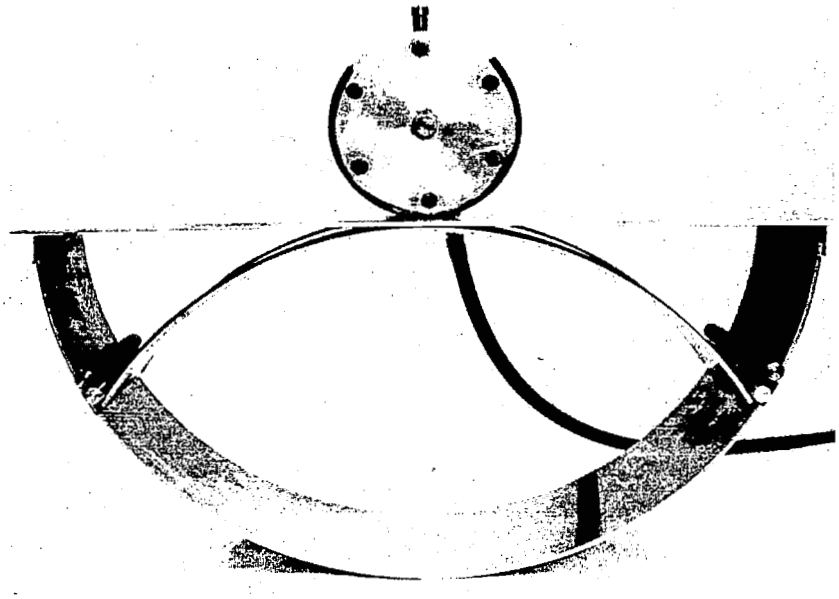

(d)

Fig. 8.21 Demonstration Model G

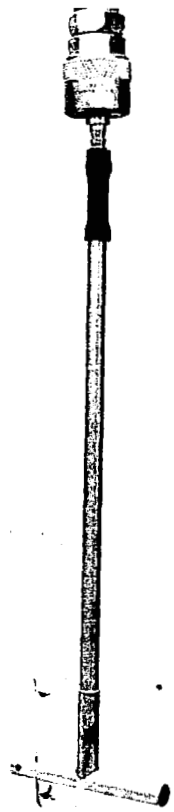

Fig. 8.22 Demonstration Model H

NASA-Langley, 1971 —— 32 CR-1782